

Mémoire

Auteur : Groulard, Antoine

Promoteur(s) : Bonfond, Bertrand

Faculté : Faculté des Sciences

Diplôme : Master en sciences spatiales, à finalité approfondie

Année académique : 2021-2022

URI/URL : <http://hdl.handle.net/2268.2/15539>

Avertissement à l'attention des usagers :

Tous les documents placés en accès ouvert sur le site le site MatheO sont protégés par le droit d'auteur. Conformément aux principes énoncés par la "Budapest Open Access Initiative"(BOAI, 2002), l'utilisateur du site peut lire, télécharger, copier, transmettre, imprimer, chercher ou faire un lien vers le texte intégral de ces documents, les disséquer pour les indexer, s'en servir de données pour un logiciel, ou s'en servir à toute autre fin légale (ou prévue par la réglementation relative au droit d'auteur). Toute utilisation du document à des fins commerciales est strictement interdite.

Par ailleurs, l'utilisateur s'engage à respecter les droits moraux de l'auteur, principalement le droit à l'intégrité de l'oeuvre et le droit de paternité et ce dans toute utilisation que l'utilisateur entreprend. Ainsi, à titre d'exemple, lorsqu'il reproduira un document par extrait ou dans son intégralité, l'utilisateur citera de manière complète les sources telles que mentionnées ci-dessus. Toute utilisation non explicitement autorisée ci-avant (telle que par exemple, la modification du document ou son résumé) nécessite l'autorisation préalable et expresse des auteurs ou de leurs ayants droit.



UNIVERSITY OF LIÈGE
FACULTY OF SCIENCES
DEPARTMENT OF ASTROPHYSICS, GEOPHYSICS AND OCEANOGRAPHY

Analysis of the dawn-dusk asymmetry in Jupiter's main auroral emission using Juno-UVS

A thesis presented for the degree of Master in Space Sciences, Research focus

Author:
Antoine Groulard

Supervisor:
Dr. Bertrand Bonfond

Evaluation committee:
Prof. Denis Grodent
Dr. Gilles Orban de Xivry
Dr. Valérie Van Grootel

Academic year 2021 – 2022

Acknowledgements

I would like to thank Bertrand Bonfond, for having given me the opportunity to work on such an interesting subject with incredible data, and for his presence when I was stuck on any problem.

I would also like to thank Bertrand Bonfond and Denis Grodent, for their invitation at the Magnetospheres of the Outer Planets meeting to present the results of this work. This has been an incredibly great first experience in a scientific meeting.

I would also like to thank my family and friends for their support during my university studies, and in particular Marie for her presence and constant trust in my capabilities, which helped me a lot, especially during the COVID period.

Finally, I would like to thank Xavier for passing on his passion for this world, without whom I probably would not have started these studies.

Contents

Acknowledgements	i
Introduction	1
1 About Jupiter	2
1.1 The planet and its moons	2
1.1.1 The fifth planet	2
1.1.2 Galilean moons	3
1.2 Plasma in the Jovian system	4
1.2.1 Elements of plasma physics	4
1.2.2 Various sources	5
1.3 Magnetosphere	7
1.4 Jupiter's aurorae	10
1.4.1 The UV lights	10
1.4.2 The main emission	11
1.4.3 The Galilean moons footprints	12
1.4.4 The polar emissions	15
1.4.5 The outer emissions	15
1.4.6 Some variabilities	16
1.4.7 The big picture	16
2 Space missions	18
2.1 Earth telescopes	18
2.2 Flyby missions	18
2.3 Galileo	19
2.4 Juno	20
2.4.1 Scientific goals	20
2.4.2 The spacecraft	21
2.4.3 Orbit	22
3 Data processing with IDL	24
3.1 create_power_profiles.pro	24
3.2 create_me_mask_bonfond.pro	27
3.3 create_me_mask_vogt.pro	27
3.4 create_me_mask_groulard_V2.pro	29
3.5 create_me_mask_groulard_vari.pro	32
3.6 measure_power_arc.pro	33
3.7 stats_dawn_dusk.pro	35
3.8 error_V2.pro	36

4	Results	37
4.1	B mask	37
4.1.1	Northern hemisphere	37
4.1.2	Southern hemisphere	39
4.2	V mask	41
4.2.1	Northern hemisphere	42
4.2.2	Southern hemisphere	43
4.3	G1 mask	45
4.3.1	Northern hemisphere	45
4.3.2	Southern hemisphere	47
4.4	G2 mask	48
4.4.1	Northern hemisphere	48
4.4.2	Southern hemisphere	52
4.5	Comparison between the masks	52
4.5.1	Comparison of the ratios	52
4.5.2	Specific considerations about the emitted power	60
4.5.3	G1 versus G2	60
4.6	Sources of uncertainties	64
5	Conclusion	68
	Appendix I: IDL routines	69
	Appendix II: Auroral maps	135
	Bibliography	178

Introduction

Since the dawn of time, polar lights have fascinated human beings. All civilizations have had their own explanation of this phenomenon. The Vikings interpreted them as the light that was reflected on the armor of the Valkyries when they led the warriors to Valhalla. The Finns thought they came from a fox running so fast through the snow that its tail made flames rising into the air. The Chinese interpreted them as the breath of dragons fighting each other. Even people as low in latitude as the Greeks and Romans had their own interpretation of these beautiful lights. Nowadays, scientists explain them by a complex chain of events linking several branches of space science.

One of the greatest discoveries of the Voyager 1 probe in 1979 is the existence of aurorae on the gas planet Jupiter. The giant planet is a great laboratory to study atmospheric and plasma physics, electromagnetism, particles and wave-particle interactions, and much more, in an extreme environment through the study of the aurorae. This subject combines a phenomenon that has fascinated people for millennia, and great scientific purposes.

The origins of the aurorae at the poles of Jupiter are not yet fully understood. In this work, a study of a part of the Jovian aurorae, called the main emission, is made to confront theoretical expectations to concrete data collected by the Juno spacecraft. To do so, a theoretical background is first introduced in Chapter 1. It consists of considerations on the Jovian system, some important plasma physics concepts, Jupiter's magnetosphere, and the aurorae. All of this is necessary to understand the objectives of this work, which become clearer at the end of the section about the main emission.

In Chapter 2, the different space missions that have flown to Jupiter are listed, with a special focus on Juno. A brief review of some important results obtained with the different spacecraft and their interests is also done at the same time.

Chapter 3 is dedicated to the detailing of the routines I wrote in the IDL programming language to convert the Juno data into usable informations. The purposes of all the routines are explained along with details on how they have been built.

Chapter 4 outlines the results obtained after the treatment done in Chapter 3. These results are discussed, including a comparison to theoretical expectations and to a similar study previously done by [Bonfond et al., 2015]. Various sources of uncertainties in the final results are also discussed.

The conclusion of this work can be found at the end of the manuscript, along with two appendices. The first one (Appendix I) contains the detailed lines of code of the routines created, and is interesting to look at when reading Chapter 3. The second one (Appendix II), is a compilation of auroral brightness maps for all Juno perijoves. This appendix provides a great visual support to the discussions made in Chapter 4.

Chapter 1

About Jupiter

1.1 The planet and its moons

1.1.1 The fifth planet

Jupiter is the largest planet of the solar system, with an equatorial radius of 71,492 km and a polar radius of 66,854 km. This difference is due to the strong centrifugal force taking place at the planet because of its fast rotation. It is also the most massive of the planets, with a mass of 1.898×10^{27} kg, or about three thousand times more than the Earth. Since Jupiter has no tangible surface, the convention is to delimit the surface by the 1 bar pressure level. This corresponds more or less to the visible surface. Indeed, the various bands that one can see on the planet come from clouds made of different ices and are due to various atmospheric processes. The lowest clouds are made of water (H_2O) starting at less than 100 km below the surface, then comes the ammonium hydrosulfide (NH_4SH) clouds, and finally the ammonia (NH_3) clouds culminating at about 20 km above the surface.

The planet interior composition is still subject to debates, but it is generally believed that a rocky core lies in the centre of the planet. [Wahl et al., 2017] estimate its mass between 6 and 25 Earth mass. This core then dissolves and mixes into the metallic hydrogen layer just above it. Metallic hydrogen is a phase of hydrogen where electrons are delocalized. It gives metallic properties to the hydrogen. Currents can then flow in this layer and these currents are taught to generate Jupiter's magnetic field by dynamo effect. Above it, a layer of helium rain in a hydrogen background is found. This layer may seem strange at first, but it explains well some Galileo and Juno data. An experiment conducted by [Brygoo et al., 2021] also showed that temperature and pressure conditions at Jupiter should create such a layer of hydrogen-helium immiscibility in its interior. Finally, a molecular hydrogen-rich layer is found at the top of Jupiter's interior. Figure 1.1 illustrates well what as just been discussed.

Jupiter's atmosphere is mostly composed of molecular hydrogen and helium. According to [Atreya et al., 2003], the atmosphere composition is $\sim 86.3\%$ of H_2 , $\sim 13.5\%$ of He. Other molecules can be found in lower abundances, the more important ones being CH_4 ($\sim 0.2\%$), H_2O , many molecules composed of carbon and hydrogen in various proportions (i.e. hydrocarbons), NH_3 , and finally H_2S . Nevertheless, those molecules can have impacts on the aurorae, as explained in Section 4.5.

A last important consideration about Jupiter is its rotation period. The visual surface of the planet cannot be used to determine its rotation period because it is made of clouds of variable velocities. This surface does not move like that of a solid body, but has a differentiated rotation. The computation of the rotation period of Jupiter is based on the rotation of its magnetic field, thought to be generated in the metallic hydrogen layer and therefore rotating with the planet

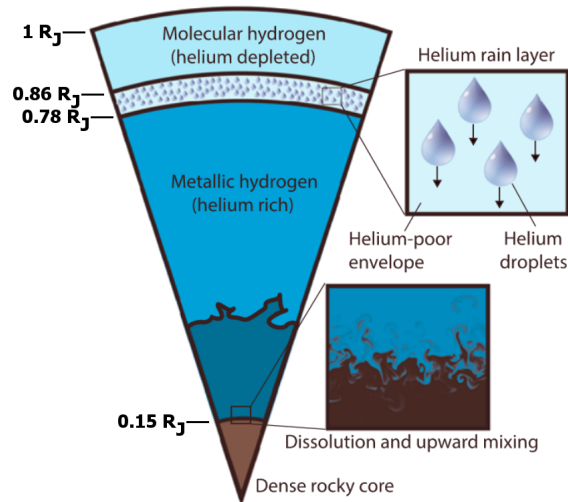


Figure 1.1: Illustration of Jupiter’s interior. The height scale is derived from Figure 3 in [Militzer et al., 2016]. Adapted from [Wahl et al., 2017].

interior. One rotation is made in 9h 55min 29s. It is convenient to define a coordinate system (named System III) that is fix with respect to this rotation to study magnetospheric processes such as the aurorae.

1.1.2 Galilean moons

Among all the 79 natural satellites of Jupiter that are known, 4 stand out for their importance in the Jovian system. Galileo Galilei discovered those 4 objects in 1610. Thus, they are often referred to as Galilean moons. During the 17th century, this discovery contributed to the emergence of the heliocentric model of the universe, and these moons are still subject to lots of scientific studies nowadays.

The first one and closest one, Io, is orbiting the planet with a semi-major axis of 421,800 km (about $5.9 R_J$), and the orbit is nearly circular. The strong volcanism of Io makes it particularly important in the process of creation of the aurorae at Jupiter. This point will be more developed in Section 1.2. The next Galilean moon is Europa, especially known for the liquid water ocean thought to lie beneath its surface that could be host to life. NASA’s upcoming mission *Europa Clipper*, scheduled for launch in 2024, will be dedicated to the study of the satellite and its ocean. This moon also has a nearly circular orbit with a semi-major axis of 671,100 km ($\sim 9.4 R_J$). Ganymede, the third Galilean moon, is the biggest satellite in the solar system, with a diameter of 5,268 km. It is even larger than Mercury and its diameter of 4,879.4 km. Ganymède will be the main target of ESA’s upcoming mission *Jupiter Icy Moons Explorer (JUICE)*. The mission will be launched in 2023 and its goal is to study the 3 icy moons Europa, Ganymede and Callisto (the 4th Galilean moon) and try to determine if life could emerge on these moons. Ganymede is also know for its intrinsic magnetic field and the aurorae it creates on the moon. The satellite orbits Jupiter at about 1,070,000 km (nearly $14.98 R_J$). Io, Europa and Ganymede are coupled by Laplace resonance. Indeed, Io has a revolution period of 1.7 days, which is half that of Europa and a quarter of that of Ganymede. The 3 satellites are thus in a 4:2:1 resonance, an important concept to explain Io’s volcanism. Finally, the last Galilean moon is Callisto. It is located at a distance of about 1,880,000 km ($\sim 26.3 R_J$) from the centre of Jupiter.

1.2 Plasma in the Jovian system

1.2.1 Elements of plasma physics

The plasma state, often considered as the 4th state of matter, is basically an ionized gas that is globally electrically neutral. It differs from the 3 usual states of matter by the absence of clear phase transition, and is characterised by a more gradual ionization of matter.

The ions and electrons constituting the plasma are electrically charged, meaning that they are influenced by magnetic fields. In a planetary environment made up of a magnetic field, such as Jupiter, the motion of the plasma will depend on the field. The basic trajectory of a charge particle in a uniform magnetic field has two components. The first one is a translation of the guiding centre of the particle along a field line, and the second is a gyration of the particle around its guiding centre. The motion of the particle is thus a helix that follows a field line. Of course, planetary magnetic fields are more complex than being uniform, what has an impact on the motion of the plasma. Some drifts in the direction perpendicular to the magnetic field may arise from curvature or gradient in the magnetic field, or the addition of a force (e.g. gravitational force).

The motion of the plasma can be even more connected to the magnetic field through what is called the Alfvén theorem, also known as the frozen flux theorem. When studying plasma physics from a fluid standpoint, a set of equations known as the magnetohydrodynamics (MHD) equations is used. By solving a system made of some of these equations, one can end up with the induction equation, which states that the modification of a magnetic field has two contributions: a diffusion term, and a transport term linked to the flow of plasma. To compare the two in a given situation, one can define a dimensionless quantity known as the magnetic Reynolds number (R_m), analogous to the usual Reynolds number derived in fluid mechanics. Two extreme cases can then be discussed. If $R_m \ll 1$, the magnetic field mostly diffuses in the medium. Conversely, if $R_m \gg 1$, the magnetic field will be mainly transported by the plasma. This is the situation we are interested in. In this case, one can easily prove that the magnetic flux crossing a surface moving with the plasma is constant. In other words, when dealing with a perfectly conducting plasma, the magnetic field and the plasma move in concert. This is what is called the Alfvén theorem. This is the case for the solar wind for example, where $R_m \sim 10^6$ (see Table 5 in [Weygand et al., 2011]).

When two field lines with opposite orientation approach each other, a phenomenon of reconnection can occur. It consists in the modification of the topology of the field lines. An illustration of the process is shown in Figure 1.2. The location where the magnetic field lines merge is called an X-line, due to the X shape of the field lines at the moment of reconnection. [Priest and Forbes, 1986] have created a general model of the reconnection process based on the flows of plasma intervening in the process. Reconnection is a process at the basis of lots of magnetospheric dynamics, including solar wind–magnetosphere interactions and magnetotail configuration.

In 1942, Swedish physicist and Nobel laureate Hannes Alfvén has suggested the existence of waves propagating in a conducting fluid placed in a magnetic field ([Alfvén, 1942]). By combining for the first time the laws of electromagnetism with those of fluid mechanics, he proved the existence of a plasma wave that is now called Alfvén wave. Development and resolution of the equation system informs us about the properties of those waves. They are ions waves propagating parallel to the ambient magnetic field. They are thought to drive accelerations of plasma particles in the Jovian magnetosphere through wave–particle interaction, and create field-aligned currents.

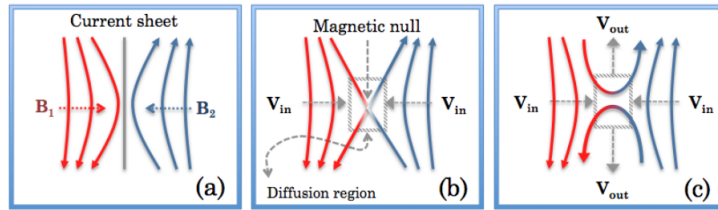


Figure 1.2: Illustration of a reconnection process. In box (a), two magnetic field lines with opposite orientations are brought close to each other. In box (b), the reconnection occurs. In box (c), the reconfigured field lines are going away from each other. From [Genestreti et al., 2012].

1.2.2 Various sources

Four sources of plasma that feeds the aurorae are discussed in this section. These are the main sources identified in the literature (e.g. [Bolton et al., 2015] ; [Bagenal and Delamere, 2011]), and those that are widely accepted by the scientific community.

The more important source of plasma in the Jovian system is by far the result of the volcanism that takes place on Io. Due to its orbital resonance with Europa and Ganymede, Io is constrained on a slightly eccentric orbit instead of a strictly circular one. Indeed, the 2 moons create a periodic force acting on Io, so that this influence is not negligible on Io's orbit around Jupiter. Even if the eccentricity of the orbit is small, the huge mass of Jupiter and the relatively small mean distance between Jupiter and Io make the moon subject to important tidal forces. Thus, the interior of Io is constantly in motion, resulting in frictional heating, called tidal heating, and melting. All this energy is released to the system through volcanism, making this satellite the most active object of the solar system. About 1 ton/s of SO_2 is ejected as neutral around Io, and half of it will be ionized through collisions or photo-ionization. This population of ions will be spherically distributed around Io, and thus create a torus of plasma around Jupiter. As the particles constituting the plasma are electrically charged, the torus will be influenced by Jupiter's magnetic field and it will thus be slightly tilted with respect to Io's orbit. Different plasma species can be found in the torus. [Thomas and Wilson, 2004] describe two different populations of ions. The first one being the cold torus, mostly made of S^+ ions located in the inner part of the torus. The outer part is mostly composed of O^+ and S^{2+} ions that forms the warm torus. S^{3+} and O^{2+} ions are also important in the composition of the torus. More recently, [Nerney et al., 2017] derived the fractional abundances (relative to the electron density) of the different ions in the centre of the torus. They found that S^{2+} and O^+ ions are the most important, with fractional abundances of $\sim 20\%$. This value drops to $\sim 5\%$ for the S^+ and S^{3+} ions, and to $\sim 3\%$ for the O^{2+} ions. The rest of the charge of the ions is carried by protons ($\sim 10\%$), SO_2^+ ($\sim 1\%$) and various minors constituents being S^{4+} , Cl^+ , Cl^{2+} and K^{2+} .

The others Galilean moons also contribute in a lesser extend to the overall population of plasma. Because the material ejected by Io and forming the Io torus cannot accumulate endlessly, a part of it expends radially to greater distances in the magnetosphere. Europa has no magnetic field, and according to [Schreier et al., 1993], sputtering of its surface by radiation belts particles and the plasma particles reaching its orbit becomes a source of water and water fragments molecules that can then be ionized. This creates a plasma torus around Europa's orbit, mainly composed of water and water fragments ions such as H_2O^+ , OH^+ , H^+ and O^+ mixed with sulfur plasma of iogenic origins. Various chemical phenomena can take place, and so less common ions like SO^+ or HS^+ can also be found in minor proportions. When the plasma flowing in Jupiter's magnetosphere reaches Ganymede, it can also interact with this moon, in a slightly different way than in the case of Europa. Ganymede has an internally driven magnetic field, that creates a small magnetosphere inside Jupiter's magnetosphere. Part of the ions from

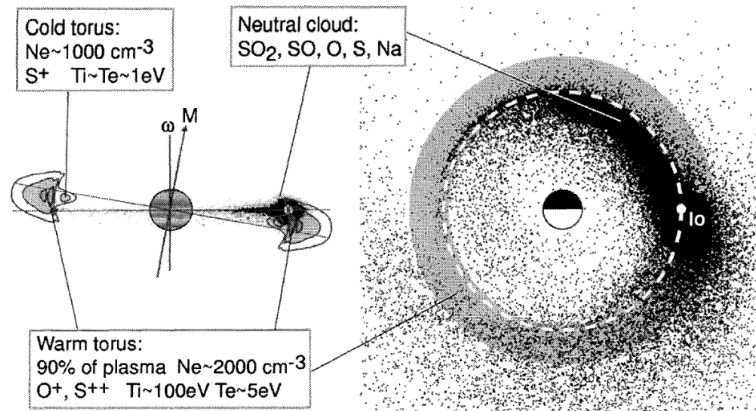


Figure 1.3: Illustration of the Io torus and the neutral cloud (left) seen edge on, and (right) from above. From [Thomas and Wilson, 2004].

the surrounding plasma can enter into Ganymede’s magnetosphere through reconnection processes, and cause sputtering on Ganymede’s surface. During the Galileo flyby, one ion species has been identified over Ganymede’s polar cap. It has first been interpreted as protons, but [Vasyliūnas and Eviatar, 2000] have found 4 major problems with this interpretation. Instead, they propose that the observed ions are O^+ , what is more plausible. Anyway, the ions still have to leave Ganymede’s magnetosphere to be injected in Jupiter’s one. This happens again via reconnection processes happening in the tail of Ganymede’s magnetosphere. Finally, ions were also detected near Callisto, but there is no evidence that these ions can leave the surrounding of the moon and be injected in Jupiter’s magnetosphere. [Gurnett et al., 2000] proposed that this plasma composes Callisto’s ionosphere and remains trapped near the moon. However, some Galileo data could be explained by the presence of a plume of plasma resulting from the interaction of the surrounding plasma and the ionosphere, that could sweep away some of the ionospheric plasma. In any case, the 3 moons Europa, Ganymede and Callisto are way less efficient sources of plasma than Io. Europa and Ganymede have ionisation rates estimated on the order of 10^{25} to 10^{26} ions/s, while the ionisation rate at Io is estimated to be on the order of 10^{28} ions/s ([Bolton et al., 2015]).

As seen in the previous section, the high atmosphere of Jupiter is mostly composed of H_2 and He. It is therefore not surprising to find H^+ , H_2^+ , H_3^+ and He^+ ions in the ionosphere. Those ions can be injected in the magnetospheric plasma through ionospheric escape. On Earth, this can be done via the Dungey cycle. Firstly proposed by [Dungey, 1961], it consists in a cycle of reconnection between the solar wind and the Earth magnetosphere at the dayside magnetopause followed by reconnection in the tail of the magnetosphere. When the magnetic field lines of the Earth reconnect with those of the solar wind and become open, a disequilibrium that can accelerate the ions away from the planet is created. On Jupiter, the existence of such a Dungey cycle is subject to debate. For example, [Cowley et al., 2003] fully integrate this mechanism in their study, while [McComas and Bagenal, 2007] reject this idea. Because only the polar field lines are concerned by this cycle, if it exists on Jupiter, it can only explain the injection of ionospheric plasma in the tail of the magnetosphere. Another mechanism that takes place in the Jovian magnetosphere, known as the Vasyliunas cycle ([Vasyliunas, 1983]), makes it possible for the ionospheric plasma to go in the middle magnetosphere, where the iogenic plasma is located. During this cycle (which will be explained in more details in the next section), reconnections also take place, creating the same kind of disequilibrium that can trigger the motion of the ionospheric plasma. [Martin et al., 2020] estimated that the ionosphere is a source of $1.3\text{--}1.8 \times 10^{28}$ ions/s. This number is close to the estimates of Io as a source. Nevertheless, the plasma

coming from the ionosphere is made of much lighter elements than the one coming from Io. Thus, this new source of plasma represents a mass flow of only 18.7–31.7 kg/s, to be compared to ~ 500 kg/s for the iogenic plasma.

Ions of typical solar origin have also been found in Jupiter’s magnetosphere (e.g. O^{6+}), providing evidence that the solar wind is also a source of plasma for the planet surrounding. Multiple hypotheses exist for the penetration of this plasma into the more powerful planetary magnetosphere of the solar system. The first one is the existence of a Dungey cycle. If it exists, solar wind could penetrate the magnetosphere when reconnection occurs on the day side. According to [Delamere and Bagenal, 2010], reconnection occurring during viscous interactions such as Kelvin-Helmholtz instabilities could be a better explanation for the presence of solar wind plasma in the magnetosphere. [Bagenal and Delamere, 2011] found that the leaking of plasma into the magnetosphere through small-scale reconnection is ~ 150 kg/s.

1.3 Magnetosphere

Jupiter’s magnetic field takes its origin in the metallic hydrogen layer. There, dynamo effects create a magnetic field one order of magnitude greater than the one created at Earth. This magnetic field is so intense that the magnetosphere that is thus created would appear as 5 times the size of the full moon if we could see it in the sky. The magnetotail even extends to the orbit of Saturn. In this section, the magnetosphere of the giant planet is reviewed, starting from the surface magnetic field up to the general shape of the magnetic field away from the planet and the electric currents systems that flow in it. All of it having repercussions on the aurorae. The general shape of the magnetosphere is illustrated in Figure 1.4 and will be developed in this section.

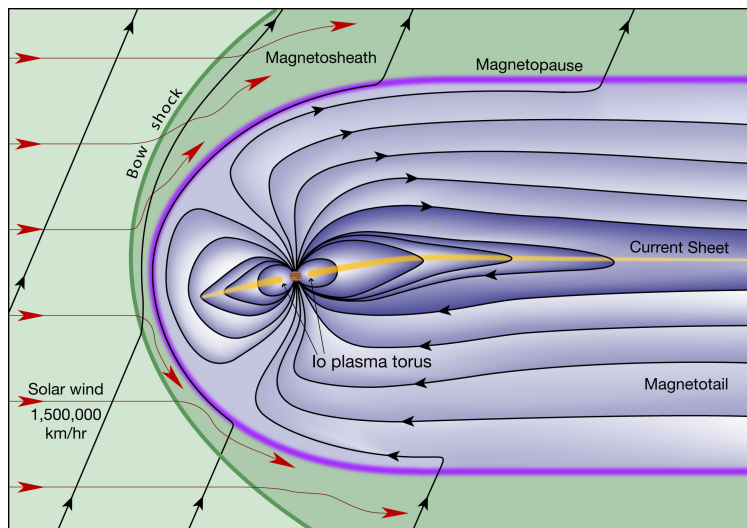


Figure 1.4: Illustration of Jupiter’s magnetosphere by F. Bagenal & S. Bartlett.

The surface field has been studied for a long time, with substantial improvements in its mapping over time. A first interesting model based on observations made with both the Hubble Space Telescope (HST) and the Infrared Telescope Facility (IRTF) in Hawaii was proposed by [Connerney et al., 1998]. According to this model, the surface magnetic field is mostly a tilted dipole. But ten years later, [Grodent et al., 2008] used more than a thousand HST images to show the existence of a magnetic anomaly in the northern hemisphere. Nowadays, this anomaly is still considered in the models. Since the arrival of Juno in 2016, more accurate data are collected,

and a region of strong magnetic field known as the Great Blue Spot has been discovered in the equator. The first magnetic field model made with Juno data known as Juno Reference Model through Perijove 9, or JRM09, has been created by [Connerney et al., 2018] and is widely used. Recently, more Juno data have been considered to create a better version of the model known as JRM33 ([Connerney et al., 2022]). The surface magnetic field map computed with this model is shown in Figure 1.5.

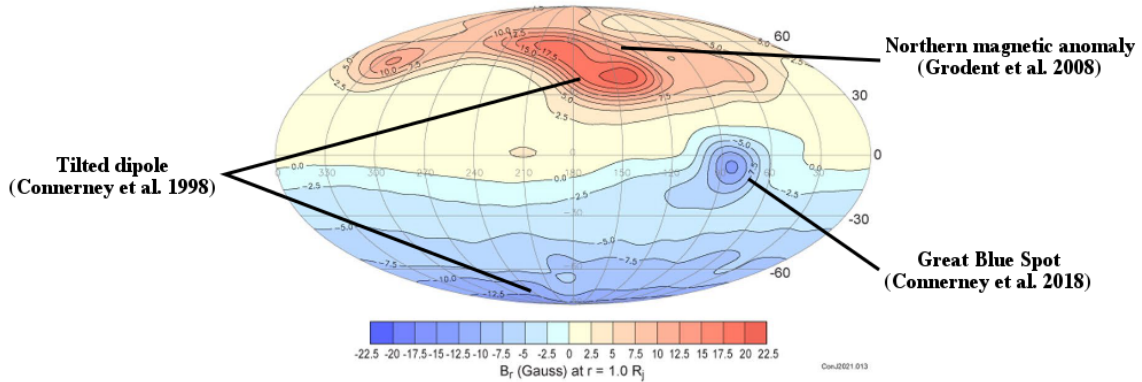


Figure 1.5: Contours of the radial magnetic field at the surface of Jupiter in Mollweide projection using the JRM33 model. Structures discovered in previous studies are labelled. Adapted from [Connerney et al., 2022].

The shape of the magnetosphere and the currents flowing in it are well synthesised by [Khurana et al., 2004]. In the inner ($<10 R_J$) and middle (10 to $40 R_J$) magnetosphere, the presence of the Io torus has a significant effect on the magnetic field. As already explained, the plasma in the torus must escape from this environment. Thus, it extends radially outward into a plasmashet (of variable shape and thickness), also called current sheet, according to a balance between the centrifugal, thermal and Lorentz forces. This plasmashet is associated to a current: the radial current. The conditions for the application of the Alfvén theorem are met in this plasma. Thus, because the plasma is frozen in the magnetic field, it bends the field lines as it flows radially outward, diverging from the classical dipolar configuration. At a point in the magnetosphere, Birkeland currents, or field aligned currents (FAC), appears, linking the external edge of the radial current to the ionosphere of Jupiter. The reasons for the appearance of these currents will be explained in detail in the next section, as they are of crucial importance to explain the auroral main emission. The current system is closed via an ionospheric current and other FAC flowing from the ionosphere to the inner edge of the radial current. This is illustrated in Figure 1.6.

A ring current associated to Jupiter's radiation belts also exist. These belts consist of high energy electrons, protons and heavy ions trapped within a few tens of Jupiter radii. The origin and evolution of those particles are not yet fully understood, but Io is known to be one of the sources ([Neron et al., 2021]). Those particles drift around Jupiter in a direction depending on their electric charge, creating a separation of the negatively and positively charged particles. A ring current is thus created around Jupiter.

According to [Khurana, 2001], similar to what is found on Earth, a partial ring current has also been found in the nightside of the plasmashet. At Jupiter, it closes by currents flowing from the ionosphere to the dusk region, and from the dawn region to the ionosphere. It forms what is called the region 2 current system on Earth, and can be called the same way for Jupiter as well, but it is also referred as the partial ring current system.

Another current system known in the magnetosphere of Jupiter is the so-called magnetopause

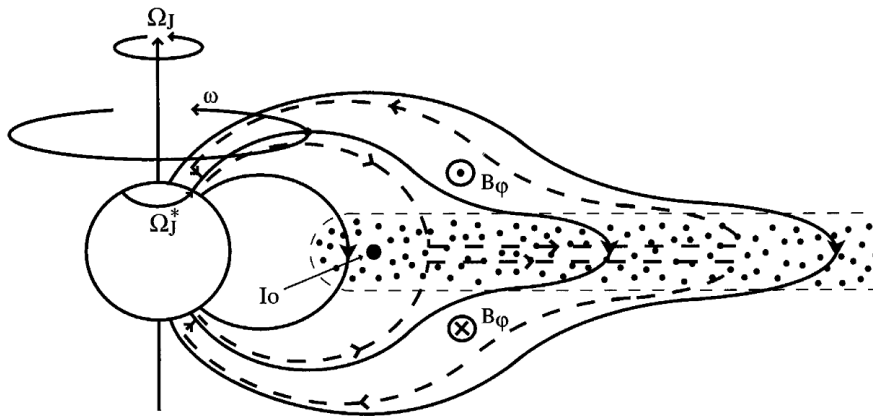


Figure 1.6: Illustration of the radial current system. The plasma constituting the plasmashield is represented by black dots. Dashed line represent the different parts of the currents. Solid lines show the magnetic field lines and how they are modified by the radial current. From [Cowley et al., 2002].

current system. A particle arriving from the solar wind into the magnetosphere will gyrate around the field lines. Since it is at the boundary between a region having a magnetic field and another without, when entering into the magnetosphere, the solar wind particles will only do half of a gyration before leaving the magnetic field region. The motion of a particle is thus a straight line before entering in the magnetosphere, followed by half of a circle when in presence of the magnetic field, and finally another straight line after leaving the magnetosphere. The semicircular trajectory in the magnetosphere is equivalent to a net motion of the charged particles in a given direction. The negatively and positively charged particles gyrating in opposite sense, the two will move in opposite directions and it will create a net current at the magnetopause, known as the Chapman-Ferraro current. This current cannot create a current loop on its own in the magnetotail because the field lines have opposite directions in the upper and lower parts of the magnetosphere. In the northern hemisphere, the field lines are leaving the planet, while they are coming to the planet in the southern hemisphere. In order to close this current system, a cross-tail current appears in the magnetic equator. This is the tail current system. The two systems are illustrated in Figure 1.7 in the case of the Earth.

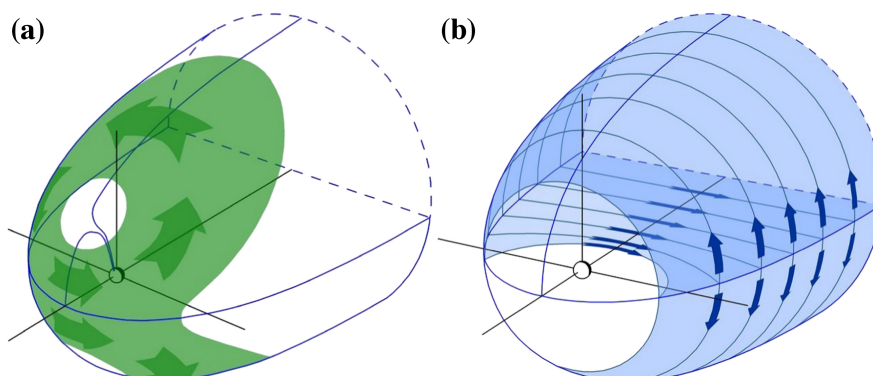


Figure 1.7: Illustration of (a) the magnetopause system (Chapman-Ferraro currents), and (b) the tail currents for the Earth. At Jupiter, the currents flow in the opposite direction because the magnetic field is in the opposite direction. Adapted from [Ganushkina et al., 2018].

1.4 Jupiter's aurorae

The general shape of the aurorae one can see at Jupiter is far from the one we are used to on Earth. Several regions can be delimited in Jupiter's aurorae, with recognizable features. Figure 1.8 shows an image of the Jovian UV aurorae with the different regions mentioned (i.e. the Galilean moons footprints, the main emission, the polar emissions and the outer emissions). In addition to these regions, considerations about the mechanisms creating the emissions and about variable structures will be addressed in this section.

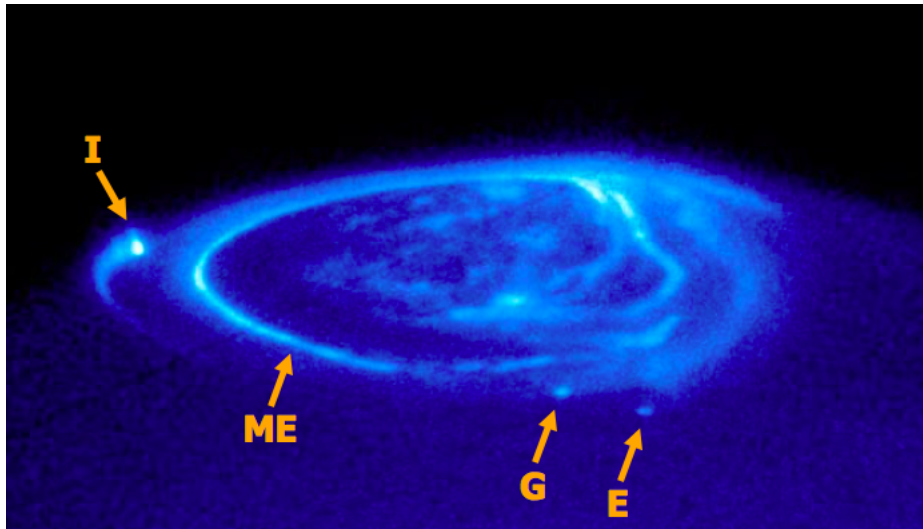


Figure 1.8: HST image of the northern UV aurorae of Jupiter by J. Clarke. Various auroral features are labelled on the image. The letter I, G and E refer to the Io, Ganymede and Europa footprints. The ME label refers to the main emission. Any aurora poleward of the main emission is part of the polar emissions, while those equatorward of the main emission are the outer emissions.

1.4.1 The UV lights

Aurorae at Jupiter have been known for a long time. When particles precipitate into the atmosphere of the planet, which is mostly made of H_2 , different reactions occur that result into auroral emissions. These mechanisms are well described by [Badman et al., 2015] and [Grodent, 2015]. At Jupiter, the most intense aurorae are by far the UV and IR ones, but X-Ray, visible and radio emissions are also present. The mechanisms of emission in the UV are relatively simple. It consists in the excitation, dissociation and ionization of atmospheric H_2 and H by collisions with the plasma electrons flowing towards Jupiter. The ionization produces secondary electrons that can also interact with the atmospheric constituents. Once excited, the H_2 molecules de-excite by emitting UV photons in the Lyman and Werner bands. In the other hand, the H atoms de-excite mostly by emitting Lyman α photons, contributing to less than 10% of the total UV emission. Any electron of energy greater than ~ 10 eV can theoretically produce a UV photon through this process. The H_2 and H photons emitted these ways can then be absorbed by atmospheric constituents (hydrocarbons, H_2 and H), what modifies the shape of the final UV spectrum. The mechanisms explained here are illustrated in Figure 1.9.

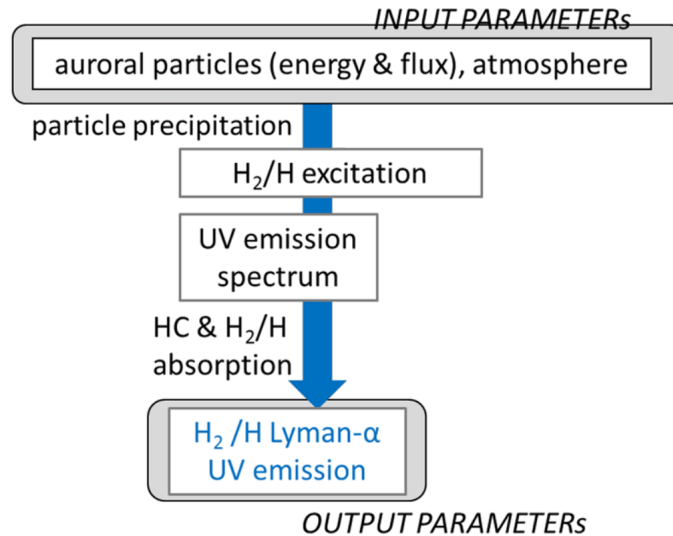


Figure 1.9: Scheme illustrating the various mechanisms leading to the UV auroral emissions. Adapted from [Badman et al., 2015].

1.4.2 The main emission

The naive and basic idea of the main emission at Jupiter is a clear permanent auroral ribbon that can be easily seen and recognized in any image of the aurorae. In reality, this main emission and the mechanisms creating it are still not fully understood. The usual explanation is based on the so-called corotation enforcement theory (CET). [Hill, 1979] and [Vasyliunas, 1983] have studied the plasma flows in the Jovian magnetosphere, what is the basis of the CET. As already explained, the plasma in the plasmashet is flowing outward. In addition to this motion, it is also rotating counterclockwise. Observations have shown that the plasma is in fact in rigid corotation with Jupiter until a the middle magnetosphere where a corotation breakdown occurs. To explain the corotation of plasma, one has to look back at the radial current system developed in Section 1.3 and to Figure 1.6. In the plasmashet, the current flows radially and a $J \times B$ force thus arises, accelerating the plasma in the direction of rotation of Jupiter. This mechanism provides momentum to ensure the corotation of the magnetospheric plasma, but this momentum cannot arise from nowhere and it must be transferred from somewhere else. According to [Cowley and Bunce, 2001], Pedersen currents flowing in the ionosphere create a $J \times B$ force in the direction opposite to the rotation of the planet. This decreases the momentum in the ionosphere, that can be transferred to the plasmashet by the radial current system coupling the ionosphere to the magnetosphere. Thus, momentum from the ionosphere is transferred to the magnetospheric plasma to ensure the corotation. As the plasma in the plasmashet goes further outward, the amount of momentum needed to ensure the corotation increases. A breakdown of the corotation occurs at a distance where the ionosphere is not able to provide enough momentum to the plasma anymore. A model created by [Vogt et al., 2011], that is used extensively in this master thesis, permits to link an auroral feature to its origin in the magnetosphere. Using this model, the main emission maps to a distance varying from $\sim 15\text{-}30 R_J$ in the dawn region to $\sim 50\text{-}60 R_J$ in the postnoon region, corresponding to the corotation breakdown distances. When the plasma stops to corotate, a lag in the rotation of the plasma appears. Because the magnetic field is frozen in the plasma, this generates a bendback of the field lines at these locations. This configuration allows the plasma to flow to the planet through FAC. Once at Jupiter, the plasma collides with the atmosphere of the planet and generates the main emission through the excitation mechanisms explained previously.

The CET explains the mechanisms at the basis of the existence of the main emission. To understand its morphology, a deeper look at the configuration of the magnetosphere is needed. A first interesting point is the difference of the magnetic field at the surface of Jupiter when comparing the two hemispheres (see Figure 1.5). The most important difference is the northern magnetic anomaly that gives a bean shape to the main emission in the northern hemisphere. In the southern hemisphere, the magnetic field is more dipolar and the main emission has an oval shape, justifying that the main emission is sometimes called the main oval. Another interesting nearly permanent feature of the main emission is the discontinuity discovered by [Radioti et al., 2008a]. This discontinuity consists in a drop in the brightness of the aurora to less than 10% of its maximum, and is located in the prenoon sector between 8:00 and 13:00 local time (LT). In this region, the plasma is nearly corotating. Thus, weaker FAC are involved, and the emission is less bright than in the other parts of the main emission.

What has been discussed here gives a good framework to try to understand what the main emission really is. Although there is no clear definition, 3 major elements seem interesting to describe the main emission:

- ◊ This is a thin region of high brightness and emitted power.
- ◊ It is due to the breakdown of corotation of the magnetospheric plasma.
- ◊ It magnetically maps to a variable distance of $\sim 30 R_J$ in the magnetosphere.

Still, the main emission at Jupiter and its definition is an active subject of debate. Most of the authors are satisfied by the idea that the CET is enough to understand the origin of the main emission (e.g. theoretically by [Cowley and Bunce, 2001]; via HST and Juno observations by [Nichols and Cowley, 2022]) but there are also evidences that a piece of the puzzle is missing. [Mauk et al., 2020] used the JEDI and JADE particles instruments onboard Juno to show the existence of 3 zones in the main emission. At low latitude is a zone of diffuse aurora. At intermediate latitude is a zone of downward electron acceleration, and at higher latitudes is a zone of bidirectional electron acceleration with upward fluxes higher than downward ones. This suggests various mechanisms to take place at the main emission. In addition, they did not find a clear boundary between the particle populations and behaviours of the main emission at high latitudes and those of the polar emission. This makes the limits of the main emission even harder to detect and define. Moreover, the main emission is often more complex than a simple arc, with sub-structures and discontinuities hard to explain with a simple theory such as the CET. [Bonfond et al., 2020] also discussed six situations where the observations contradict what is expected from the CET. One of them being the dawn-dusk brightness asymmetry detected by [Bonfond et al., 2015]. The latter study is of great importance for this thesis. Indeed, using HST data, they found that the dusk region is generally ~ 3 times brighter than the dawn one, in opposition to the theoretical expectations of the CET ([Ray et al., 2014]). To explain their results, the authors proposed that the partial ring currents could be superimposed to the corotation enforcement currents (CEC), with same direction in the dusk region and opposite direction in the dawn region. This idea is illustrated in Figure 1.10. Part of the work done in Chapters 3 and 4 of this document consists in a study similar this HST one, but with Juno data, to find if the results found at the time can be retrieved or not.

1.4.3 The Galilean moons footprints

The Galilean moons footprints are auroral spots with a tail, directly mapping to the Galilean moons location in the magnetosphere. The more easily visible one is the Io footprint (IFP), discovered for the first time in IR light by [Connerney et al., 1993]. It is the outermost footprint because the moon is the closest to Jupiter out of the four Galilean moons, thus mapping

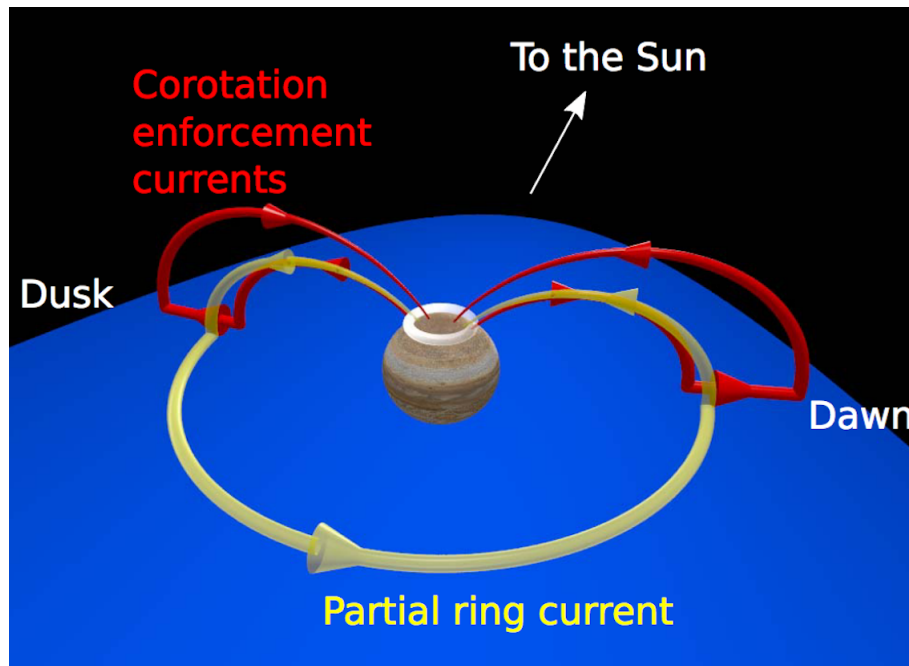


Figure 1.10: Illustration of the corotation enforcement current (CEC) and partial ring current systems to explain the dawn-dusk asymmetry. To ensure the clarity of the image, the two current systems are slightly shifted, the dusk and dawn loops are the only one represented even if the CEC are present at all local times, and only the northern hemisphere is shown. On the dusk side, the two currents flow in the same direction, increasing the intensity of the overall current. In the dawn side, the two flow in opposite direction what lowers the overall current. The result is a brighter emission at dusk when considering both of the systems. From [Bonfond et al., 2015].

to lower latitudes in the ionosphere. The origins of the IFP are well understood nowadays. [Clarke et al., 2004] explain that the Io plasma torus corotates with Jupiter, with a speed greater than Io's orbital speed by 56 km/s. Io then acts as an obstacle in the motion of the plasma torus, what generates Alfvén waves that can accelerate the plasma towards Jupiter along a magnetic field line. It is illustrated in panel (a) of Figure 1.11. This simple idea, even if incomplete, is not far from what actually happens. The tail of the IFP is not continuous but made of several spots, and [Bonfond et al., 2008] found an eventual spot before the main spot. Panel (b) of Figure 1.11 illustrates the additional mechanisms to explain those spots, that will be developed hereafter. Two processes take place at the same time. The first one is the classical Alfvén acceleration where the effects of the plasma torus are taken into account. The waves are slower in the dense plasma torus, creating a tilt in their propagation. Once at the border of the torus, the waves can either cross it and continue their journey to Jupiter or be reflected back inside the torus. The term Alfvén wing refers to the path of the Alfvén waves explained this way. When the wave arrives at the ionosphere of Jupiter, it may eventually be reflected back to the torus. The plasma accelerated by these Alfvén waves creates the Alfvén current system, flowing from the moon to Jupiter and back. The second phenomenon taking place is related to this current loop. At the Jupiter side of the loop, electrons can be accelerated. This creates trans-hemispheric electron beams (TEB) that are not affected by the plasma gradient density of the torus, and therefore are not subject to eventual reflections. TEB are thus responsible for eventual front spots as illustrated in red in the panel (b) of Figure 1.11. Since the plasma torus is tilted with respect to Io's orbit, the relative position of the different spots varies, depending on the location of Io inside the torus.

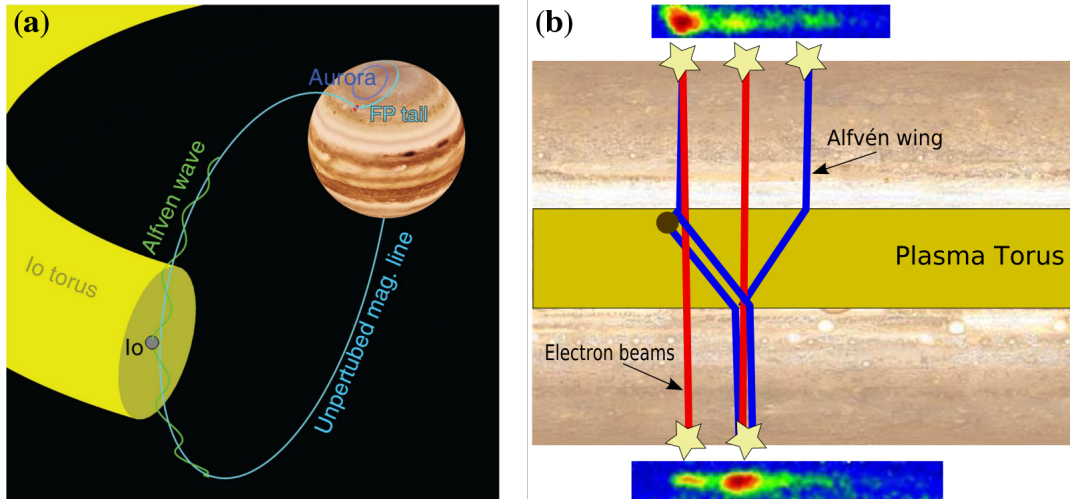


Figure 1.11: Illustration of (a) the generation of the Io footprint via the Alfvén waves acceleration of plasma traveling from Io to the ionosphere of Jupiter (adapted from [Mura et al., 2018]), and of (b) the mechanisms explaining the different spots in the IFP (from [Bonfond et al., 2008]).

The Europa footprint (EFP) is generated in the same way as the IFP. The difference being that Io is inside the main plasma torus, creating a permanent strong auroral signature while Europa torus is way less dense, creating a dimmer footprint.

The Ganymede footprint (GFP) is a little different from the first two. It is similar to the EFP in the sense that the moon is in the plasmashet environment, thus creating a weaker footprint than the IFP. The location of its orbit also makes it hard to see from time to time. Indeed, Ganymede is located at $\sim 15 R_J$, what is the lowest corotation breakdown distance computed by [Vogt et al., 2011]. The GFP is thus sometimes drawn in the main emission or in the outer emissions. But its biggest peculiarity is that the GFP is not made of a single but a double spot. It has been discovered by [Mura et al., 2018] and is attributed to the magnetosphere of Ganymede. The interaction between Ganymede and the plasma is thus not as simple as for the other moons. Alfvénic accelerations in front and behind Ganymede are made possible where Jupiter's and Ganymede's magnetospheres interact. This create 2 spots for the GFP, in contrast to the simple spot related to the moons that have no intrinsic magnetic field.

Finally, the Callisto footprint (CFP) is the most difficult to found. Being located at $\sim 26 R_J$, the moon is in the middle of the corotation breakdown area and the CFP is located in the main emission. Plus, it suffers from the same plasma density problem than the EFP and GFP. The only study claiming to have found the CFP has been made by [Bhattacharyya et al., 2018], but there is no other evidence for its existence.

The moons footprints have great scientific interests and have been used in several studies over time. Prior to the arrival of the Galileo spacecraft and long term in situ measurements, using the aurorae has been the best way to test the models of Jupiter's magnetic field. A strong argument in the model made by [Connerney et al., 1998] is its better accuracy on reproducing the IFP location. The northern magnetic anomaly discovered by [Grodent et al., 2008] has also been deduced from the surprising tracks of the Galilean moons footprints. A split of the tail has also been found in the IFP by [Mura et al., 2018], indicative of a unusual configuration of the field lines in a part of the magnetosphere. The magnetosphere model proposed by [Vogt et al., 2011] uses the GFP at its basis to accurately map the latitude of the auroral features to middle magnetosphere distances. Finally, the double spot of the GFP being due to the interaction between the magnetospheres of the planet and the moon, it also provides information about

the size of Ganymede's magnetosphere. In addition to this non-exhaustive list, one could also talk about the fundamental plasma and plasma waves processes studied through the moons footprints.

1.4.4 The polar emissions

The polar region is the area closest to the magnetic pole, and it is thought to map to the outer magnetosphere. The magnetic field lines of interest for this area are thus the closest to the magnetopause, and the solar wind may therefore play an important role in the processes. [Delamere and Bagenal, 2010] explain the origin of the polar emissions by a combination of viscous interactions at the magnetopause and the Vasyliunas cycle ([Vasyliunas, 1983]). This cycle starts on the dusk side of the magnetosphere, where the field lines begin to extend radially while rotating to the midnight sector. Then, the field lines can extend in straight lines at large magnetospheric distances on the night side, where the plasma no longer corotates with Jupiter. The plasma flowing outward stretches the field lines enough so that reconnections between the northern and southern parts of a field line can occur. This creates an X-line at a variable distance in the outer magnetosphere (above $\sim 80 R_J$, but it can occur further out), from where a plasmoid can be ejected in the tail. The other part of the field line consists of a depleted flux tube that is finally brought back to Jupiter on the dawn side.

According to [Grodent, 2015], the polar emissions are divided in 3 main regions: the active, dark and swirl regions. The active region is located just poleward the main emission, near the noon local time sector. Its location suggests that dayside reconnections are at the basis of the aurorae taking place in this region. The aurorae consist in flares, bright spots and arcs. Explosive reconnections have been proposed to be at the origin of the flares, while a Dungey cycle is thought to drive the arc structures. The dark region is a region where there is nearly no UV emission, poleward of the dawn flank of the main emission. It corresponds to the region where the empty flux tubes arrive at the end of the Vasyliunas cycle. Because these flux tubes bring only little plasma, nearly no emission is possible in this region. Finally, the swirl region is located poleward of the active and dark regions. This is a region that is thought to map to the open field lines at the poles of Jupiter. It may originate in the second part of the Dungey cycle, when returning flow comes along the field lines from the night side of the magnetosphere. The emissions in this region are transient and patchy, with turbulent and swirling motions. A more long-live quasi-Sun-aligned polar auroral filament (PAF) has also been found during several observations in this region.

1.4.5 The outer emissions

The outer emissions are located at latitudes between the main emission and the IFP. They consist in a large diffuse band surrounding the main emission. [Grodent et al., 2003] suggests that the corotation breakdown of the plasma forming the main emission do not occur abruptly but results in a gradual departure from corotation with distance. FAC could then be generated in a more extended region of the magnetosphere, generating the outer emissions. This idea is supported by several theoretical calculations made in the early 2000s. If correct, this mechanism would imply another complication in the definition of the main emission. Another possibility is the existence of wave-particle interactions that could lead to the precipitation of electrons to form the outer emissions.

1.4.6 Some variabilities

In addition to the usual aurorae depicted earlier in this section, some phenomena can occur for various reasons, creating new structures in the aurorae or modifying the usual ones. Here is a list of important phenomena that can be observed in some images of the aurorae:

- ◇ The outer emissions sometimes display hot plasma injection signatures. The cold plasma coming from the Io torus expands radially outward, but hot magnetotail plasma can have the opposite motion thus going inward in the direction to Jupiter ([Grodent, 2015]). [Mauk et al., 2002] were able to directly relate this plasma motion to a patchy corotating aurora in the outer emissions. These injection signatures are not rare events and they can be found in many auroral images.
- ◇ Midnight and polar dawn spots are recurrent spots seen every 2 to 3 days just poleward of the main emission in the dawn to midnight sector. [Radioti et al., 2008b] linked this auroral feature to the reconnection that occurs during the Vasyliunas cycle.
- ◇ A sudden global brightening coupled with a shrinking of the main emission can occur for 2 distinct reasons. The first one being the increase of the solar wind pressure. This has been discussed by [Bonfond et al., 2020]. According to MHD simulations, the main emission should dim when the solar wind pressure increases but this is not what is observed. In addition to this brightening, the main emission also shrinks closer to the pole because of the compression of the whole magnetosphere. The second reason is an increase in Io volcanism, as discussed by [Bonfond et al., 2012]. More plasma flows in the magnetosphere when it happens, obviously leading to a brightening of the main emission. There are also evidences that the increase in the plasmashet current resulting from this increase in the plasma density is able to stretch the field lines enough to contract the main emission.
- ◇ A phenomenon called dawn storms is known since 1994. It corresponds to a strong increase in the brightness and thickness of a part of the dawn sector of the main emission lasting ~ 1 to 2 hours. However, [Bonfond et al., 2021] used Juno data to have a view of the whole process and found a 5 to 10 hours chain of events ending with the historical interpretation of the dawn storm. Dawn storms have been found at different stages of evolution in about half of Juno's first 20 perijoves (PJ). Dawn storms seem to be analogous to Earth's substorms, and to be linked to tail reconnection, dipolarization and plasma injection.

1.4.7 The big picture

To summarise this complex description of the UV aurorae taking place at Jupiter, [Grodent, 2015] created an illustration that is shown here. It is actually an incomplete view of the aurorae because Juno was not yet orbiting Jupiter at the time the image was created, and no instantaneous view of the whole aurorae is possible with HST. It is also a representation of the northern hemisphere, thus including the consequences of the northern magnetic anomaly.

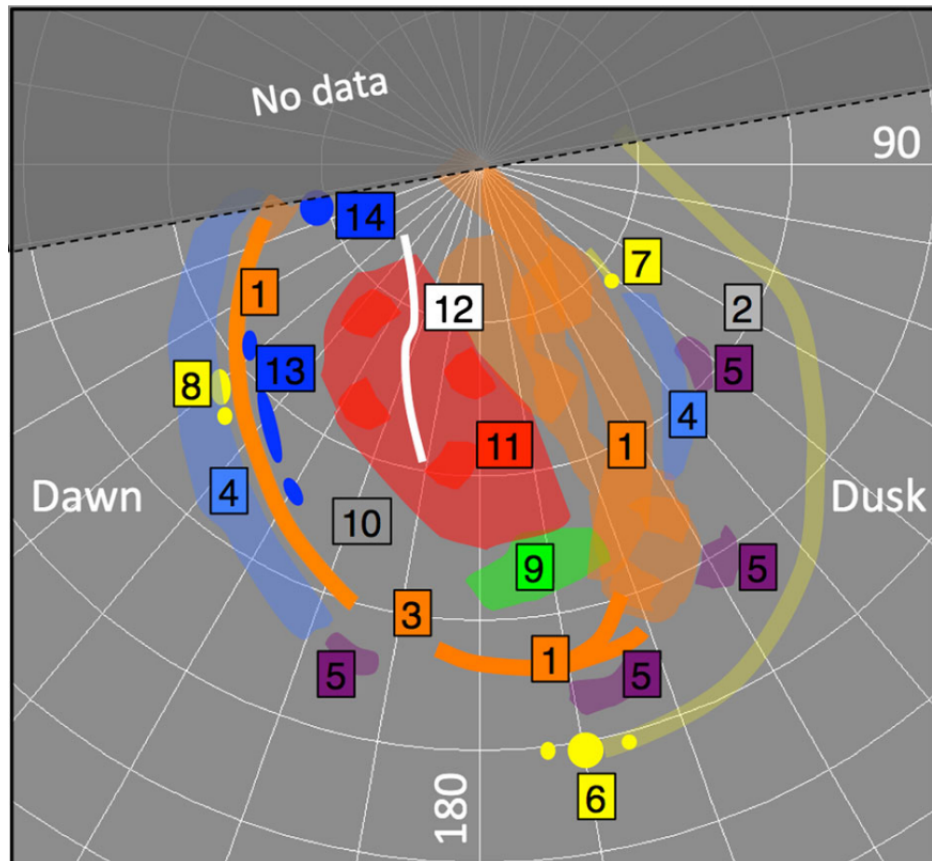


Figure 1.12: Illustration of the northern UV aurorae at Jupiter in System III coordinates. 1: Main emission composed of the diffuse region, and single or multiple arcs shape; 2: Kink due to the northern magnetic anomaly; 3: Discontinuity in the main emission; 4: Outer emissions; 5: Hot plasma injection signatures; 6: Io footprint; 7: Europa footprint; 8: Ganymede footprint; 9: Active polar region; 10: Dark polar region; 11: Swirl polar region; 12: PAF discovered in the swirl region; 13: Polar dawn spots; 14: Midnight spot. From [Grodent, 2015].

Chapter 2

Space missions

Several space missions have been launched to the outer planets and beyond. On their journey to their destinations, those spacecraft have flown over Jupiter and collected important data to better understand the biggest planet of the solar system. In this chapter, these missions and their interests are reviewed as well as some important Earth telescopes and spacecraft orbiting Jupiter.

2.1 Earth telescopes

In addition to the space missions heading towards Jupiter, Earth-based or Earth-orbiting telescopes can be used to gather data.

The IRTF is a NASA infrared telescope based at Hawaii. This is a 3.2 m telescope with a variety of instruments operating in different wavelength ranges from 0.8 to 25 μm . In the radio frequency domain, one can cite the Very Large Array (VLA). This is an array of 28 telescopes of 25 m covering an area of about 80 km in the state of New Mexico in the United States. In addition to Earth-based telescopes, HST has been orbiting the Earth at about 540 km of altitude since 1990. This space telescope operates in the near-infrared to ultraviolet domains. Of course, more telescopes can be used to observe Jupiter and this short list is not exhaustive.

These telescopes can be used alone to obtain new information about Jupiter, but their greatest interest is when they are used in complement to a space mission. This allows to obtain simultaneous observations from Earth and in situ measurements of a phenomenon. For example, [Radioti et al., 2011] used HST auroral observations and Cassini magnetic field measurements to link the polar dawn spots and inward plasma flows due to tail reconnection, supporting the idea proposed by [Radioti et al., 2008b] that the Vasyliunas cycle underlies the generation of these spots.

2.2 Flyby missions

Several missions have done a flyby of Jupiter on their way to outer targets. Due to their limited time in the Jovian system, not much data could be acquired but they are still valuable. Over the past decades, only 7 space missions have approached Jupiter to perform a flyby manoeuvre:

- ◇ The first spacecraft to reach Jupiter were Pioneer 10 and 11 in 1973 and 1974 respectively. They provided the first close-up images of Jupiter and its moons. The spacecraft also gave first measurements of Jupiter's environment.
- ◇ On their way to the edges of the solar system, Voyager 1 and 2 both did a flyby of Jupiter with 4 months interval in 1979. They provided numerous important new discoveries,

including the detections of the Great Red Spot, Jupiter’s rings, Jupiter’s aurorae on the dark side, and Io’s volcanism ([Smith et al., 1979a]; [Smith et al., 1979b]).

- ◊ Ulysses was a solar probe that has used Jupiter’s gravity to enter into polar orbit around the Sun in 1992. The magnetometer used to study the heliosphere has also been used to study Jupiter’s magnetosphere. The data acquired at that time combined with Pioneer 10 and 11 data were used to create [Connerney et al., 1998] magnetic field model discussed in Section 1.3.
- ◊ In the year 2000, the Cassini spacecraft did a 6-months flyby of Jupiter before continuing its journey to Saturn. During this flyby, the atmosphere of Jupiter has been studied, leading to a better understanding of the global structure and circulation of its clouds.
- ◊ New Horizons did a flyby of Jupiter on its way to Pluto in 2007. During the time spent at Jupiter, the spacecraft took data on its atmosphere, magnetosphere, and moons.

The data collected during these flybys are still used nowadays. They are often combined one with another, or with Galileo or Juno data to search for changes in the Jovian system over long time scales. Because of the different trajectories of all the spacecraft, the data can also be combined to have a more global view of the huge magnetosphere (e.g. [Khurana and Schwarzl, 2005] used data from Pioneer 10 and 11, Voyer 1 and 2, Ulysses and Galileo to get as complete a view as possible of the current sheet).

2.3 Galileo

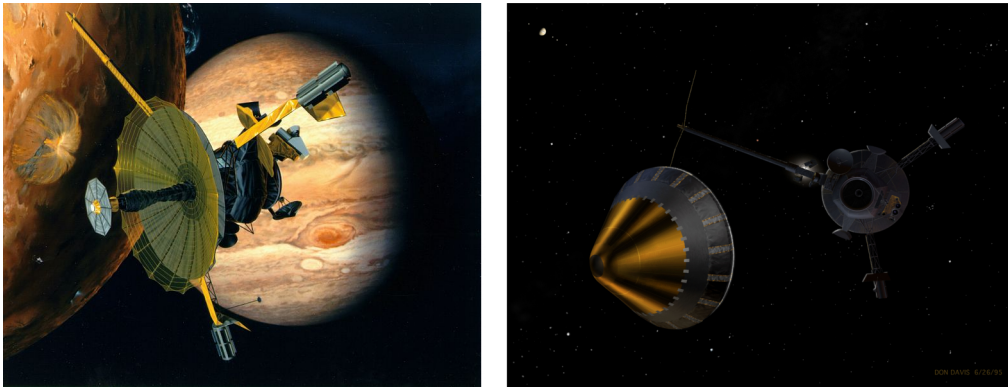


Figure 2.1: Artists views of (left) the Galileo orbiter passing close to Io and (right) the Galileo probe leaving the orbiter.

Galileo was the first spacecraft to ever orbit Jupiter. It was a NASA spacecraft made of two parts: an orbiter with 10 instruments on board and a descent probe to sample the atmosphere of the planet (see Figure 2.1). It was launched on 18th October 1989 and traveled through space for 6 years before arriving at Jupiter on 7th December 1995. During this journey, the spacecraft did a flyby of Venus, followed by one of Earth, then one of the asteroid Gaspra, before doing another flyby of Earth and leaving the system in direction of the asteroid Ida and finally reaching the giant planet ([D’Amario et al., 1992]). On its way, the spacecraft already made some interesting observations. Indeed, it found the first satellite of an asteroid when discovering Dactyl around Ida. It also did the only direct observation of a comet crashing into a planet when imaging the impact of the comet Shoemaker-Levy 9 on Jupiter.

Galileo Prime Mission lasted for 2 years from the arrival of the spacecraft in December 1995 to December 1997. This has been followed by the Galileo Europa Mission (GEM), the first extended mission, from December 1997 to December 1999. Because the spacecraft was still operating at the end of the GEM, it has been extended a second time into the Galilean Millennium Mission (GMM) from January 2000 to September 2003. In total, Galileo completed 35 orbits around Jupiter. During each orbit, the spacecraft targeted a Jovian moon to study with various scientific goals. According to [Young, 2003], the main goals of the mission were (1) to study the Jovian atmosphere in details to a depth of at least 10 bars, (2) to study the surface and interior of the 4 Galilean moons, and (3) to study the plasma physics taking place in the Jovian magnetosphere. The probe was designed to give answers to the first goal, and the orbiter to the second and third. The mission has been a huge success, and real breakthrough in our understanding of Jupiter and its moons have been made thanks to the data collected by both of the probe and the orbiter. In addition to the precisions given to already known phenomenon and structures (i.e. atmosphere, rings, moons surfaces, magnetic field, plasma physics, and many more), the Galileo spacecraft also discovered the magnetic field of Ganymede, evidences for the presence of a salty ocean beneath Europa's icy surface, and first indications of the presence of an ocean deep inside Callisto, to cite a few. During the GMM, Cassini arrived at Jupiter while Galileo was already present. This notably permitted to collect simultaneous magnetic field data from different locations during its arrival, and to see directly the effects of radiations on the Galileo spacecraft as it passed through the radiation belts.

2.4 Juno



Figure 2.2: Artist view of Juno in front of Jupiter. Credits: NASA/JPL

NASA Juno spacecraft is currently in orbit around Jupiter. It has been launch on 5th August 2011 and arrived at Jupiter on 5th July 2016. After its launch, 2 trajectory adjustment manoeuvres were performed so that it could perform a flyby of Earth flyby on 9th October 2013. After that, the spacecraft headed directly to Jupiter. The mission was supposed to end on 30th July 2021, but it has been extended until September 2025.

2.4.1 Scientific goals

[Bolton et al., 2017] did a review of the Juno mission. In their paper, they notably cite the main scientific goals of the mission:

- ◇ Determine the water abundance in the interior of Jupiter to learn whether or not a heavy element core is present at the centre of the planet. This should help in the understanding of Jupiter and the solar system formations.
- ◇ Measure the gravitational and magnetic fields of the planet to understand its inner structure and constraint the mass of its core more.
- ◇ Map the variations in atmospheric temperature, composition, dynamics and cloud opacity to depths greater than 100 bars at all latitudes. The goal being to determine the structure and dynamics of the atmosphere below the clouds.
- ◇ Improve our understanding on Jupiter's aurorae through measurements of the distribution of plasma particles and of the UV and IR emissions.

Aside from these main objectives, Juno also allows for advances in our overall understanding of the Jovian system. For example, the radiation belts and the moons are studied. As of early August 2022, 278 papers presenting results obtained via the Juno mission are referenced in any topic related to Jupiter, demonstrating the impact of Juno on our view of the planet.

2.4.2 The spacecraft

The spacecraft and its instruments are visible in Figure 2.3. It consists in a more or less cylindrical spacecraft with 3 arms, rotating on itself. Each rotation is made in 30 seconds. The 9 m-long arms are covered with solar panels to generate the energy needed by the spacecraft. The instruments onboard Juno are:

- ◇ Gravity Science (GRAV): This instrument contains the high gain antennas needed to communicate with Earth. Thanks to the Doppler effect, changes in the radio frequency informs the scientists of a change in the speed of the spacecraft on a one-minute basis. The speed of Juno being directly related to the forces applied on it, it permits to map the gravitational field of the planet.
- ◇ Magnetometer (MAG): The magnetometer is used to study the magnetic field of Jupiter and to better understand the dynamo effect in the interior of the planet.
- ◇ MicroWave Radiometer (MWR): This instrument is made of 6 antennas operating in different wavelength ranges from 1.3 to 50 cm. It is used to probe the deep interior of Jupiter and learn more about its composition and temperature profile.
- ◇ Jovian Auroral Distributions Experiment (JADE): JADE is capable to detect and characterise low-energy particles in the vicinity of the spacecraft. It can detect electrons in the energy range of 100 eV to 100 keV, and ions from 10 eV to 40 keV.
- ◇ Juno Energetic particle Detector Instrument (JEDI): The second particle instrument of Juno is dedicated to high energy particles. JEDI can detect electrons with energy varying between 20 keV and 1 MeV, and ions with energy of 15 keV to 20 MeV.
- ◇ Jovian InfraRed Auroral Mapper (JIRAM): It consists in a high-resolution IR spectrometer and imager in the 2 to 5 μm spectral range. It is used to study the aurorae and the atmosphere of Jupiter.
- ◇ UltraViolet Spectrograph (UVS): It is another imaging spectrograph on Juno, but sensitive to the extreme- and far-UV light in the spectral range 70 to 205 nm. It has a 125 km resolution and is fully dedicated to the study of the UV aurorae.

- ◊ JunoCam: It is the visible camera of Juno, used to have a view of the planet atmosphere and its dynamics.
- ◊ Waves: The Waves instrument detects radio and plasma waves in different frequency ranges. It is used to detect waves in the magnetosphere of Jupiter, that can be related to auroral signatures based on the location of Juno.



Figure 2.3: The Juno spacecraft. All the scientific instruments onboard are labelled. From [Bolton et al., 2017].

2.4.3 Orbit

Juno is placed in a highly elliptical polar orbit that brings it as close as 4200 km above the surface, and up to ~ 8 million km (or $113 R_J$) from the planet. This orbit has 2 major advantages: (1) the polar orbit allows to fly over the whole surface of the planet (see Figure 2.4), and (2) a close passage to the planet permits to pass below the radiation belts and avoid damages on the instruments and the spacecraft. The orbital plane moves from the dawn region to the dusk one, as illustrated in Figure 2.5. The inclination of the orbit also grows so that Juno crosses the equatorial plane closer to Jupiter at every orbit.

This modification of the plane of the orbits provides good measurements of the gravitational and magnetic fields from all over the planet, good views of the aurorae, measurements at all longitudes in the night part of the magnetosphere, and crossings of the equatorial plane at the moons orbit locations.

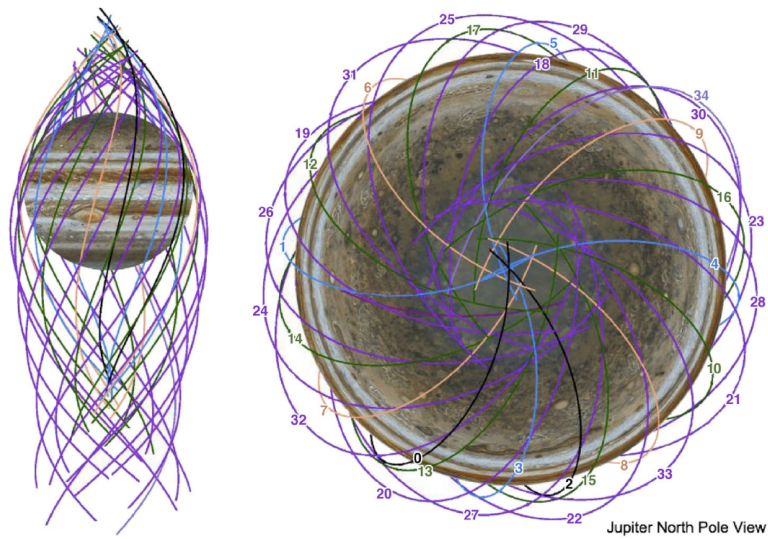


Figure 2.4: Parts of Juno orbit close to the planet for the prime mission. The black lines are perijoves where no data have been collected (PJ0 and PJ2). Successive orbits lead to a spacing of (blue) 90° , (orange) 45° , (green) 22.5° and (purple) 11.25° in longitude between the orbits, allowing for a full coverage of Jupiter. From [Bolton et al., 2017].

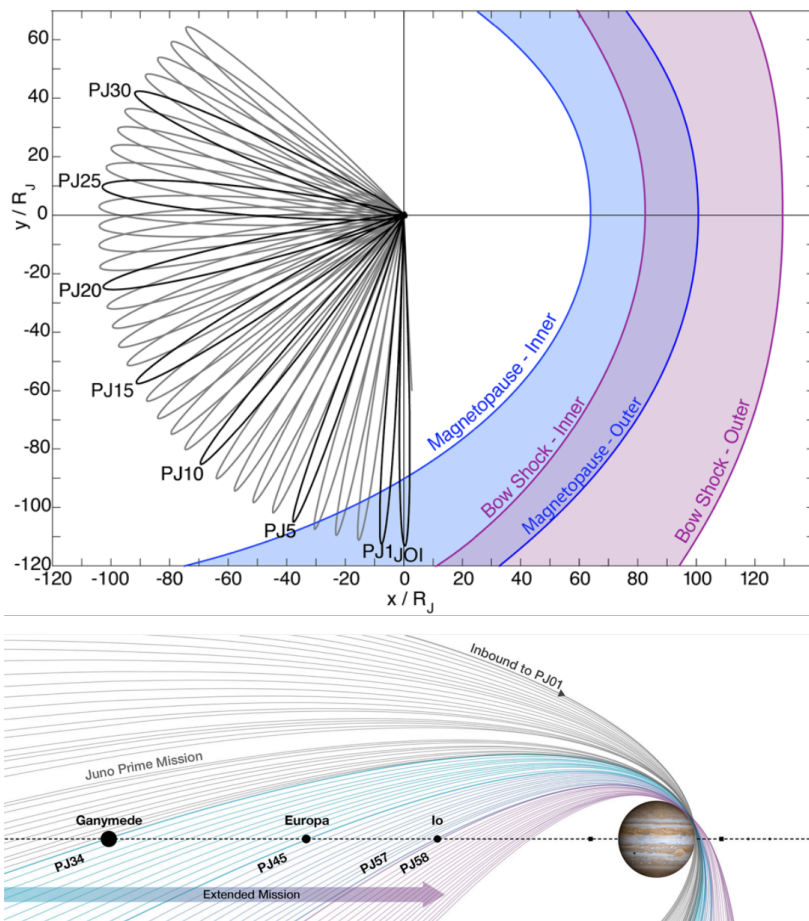


Figure 2.5: Variation of the orbital plan of the orbit of Juno (up) projected in the equatorial plane for the prime mission (from [Bolton et al., 2017]) and (down) seen perpendicularly to the orbital plane for the prime and extended missions (credits: NASA/JPL-Caltech/SwRI).

Chapter 3

Data processing with IDL

Interactive Data Language (IDL) is a proprietary language owned by the company L3Harris Geospatial. This language gives the advantage of an easy to use graphic interface, ideal for processing the data needed to visualize the auroral images created in this work.

In this chapter, the purpose and reasoning behind the creation of the routines created for this master thesis are explained. The detailed lines of code are not written here, but it may be useful to have them in parallel. One can find them in the Appendix I. In the following pages, some references to specific lines are written to know where to look in the appendix.

The goal of this master thesis was to compare the power emitted in the dusk and dawn regions of the main emission, to see if it matches the theoretical expectations supporting that the dawn region must be more powerful (e.g. [Ray et al., 2014]), or not. If not, the idea was to compare the results obtained here with those of [Bonfond et al., 2015] to see if the two studies, which are based on different data sets, yield the same conclusions. For this purpose, several steps were needed before being able to compare the emitted power in the two regions. A schematic of the different steps and the routines involved is shown in Figure 3.1.

3.1 create_power_profiles.pro

The goal of this first routine is to create brightness maps of each pole for each Juno perijove, along with the power maps corresponding. The final maps are contained in 3600×1800 elements array that can be viewed as maps in Mercator projection (i.e. cylindrical projection maps). An element of the array therefore spans one tenth of a degree in longitude and latitude. The 3600×1800 elements arrays is thus one of the basic objects used in all the routines. It is worth mentioning that the arrays I worked on are in cylindrical coordinates, but the visualization of these arrays was done through a command that changes the coordinate system to display a polar projection map in System III.

The first step of this routine consists in defining some useful quantities such as physical constants that will be used later. The ephemeris of Juno are also restored, as well as a map of the surface covered by each element of the 3600×1800 elements array. Indeed, Mercator projection tends to distort the distances. The brightness does not depend on the surface, but it is essential to know the area covered by each element of the array to compute the emitted power.

Once all these quantities in hand, it was possible to start working on the maps. Juno-UVS collects data during 30s-long spins of Juno on itself. The data collected during one rotation covers only a portion of Jupiter's surface, and adding all these fragments of map together was necessary to create a comprehensive map (see Figure 3.2). In most of the cases, the maps were built from data acquired over 100 spins. A full cover of the auroral region was not possible

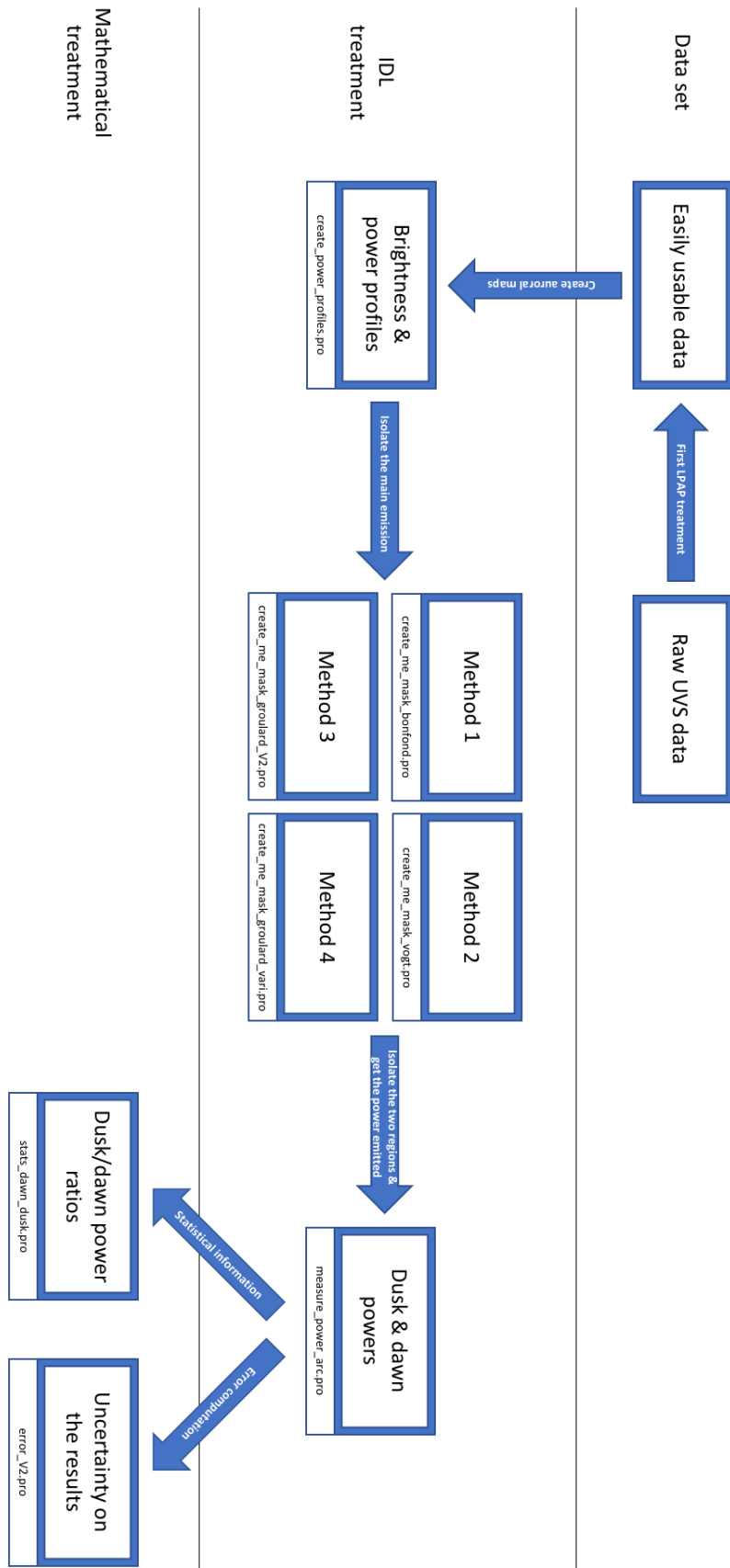


Figure 3.1: Schematic of the steps needed to compute the power emitted in the dusk and dawn regions of the main emission based on Juno data.

with less spins and adding more spins was not needed, plus it would have increased the data acquisition time and the associated error. Several parameters had to be taken into account at each rotation: the position of Juno and its viewing angle, the slit of UVS being larger at the centre than at the edges, and the side effects. As the data composing the final map are acquired on several minutes and in order to keep the dynamics of moving features (e.g. the IFP), the data from each spin were not simply added together. A variable was used to make fresher data more visible when adding the map fragments (see lines 125 and 126). It was also necessary to account for the parts of Jupiter that have been covered during multiple spins in order to not consider the same emission several times (see lines 139 to 141). At the end, two maps were created: the real brightness map that will be used in the other routines, and a fake map. The fake maps are the ones displayed in this document. Because the color panel of the graphics tool spans only a limited amount of colors, the less bright parts of the aurorae have no color attributed to them, and they appear as if no data had been collected. To have a visual idea of the area covered by UVS, the color of these regions has been set to black. The difference between the two maps is visible in Figure 3.3.

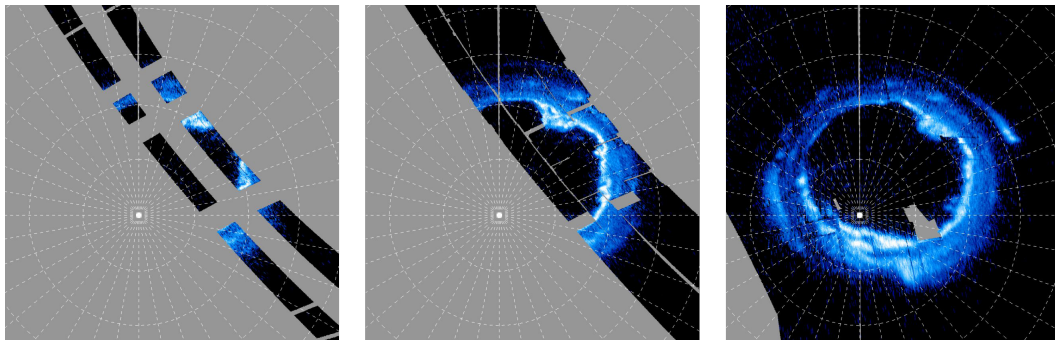


Figure 3.2: Brightness map for PJ1 in the southern hemisphere using the data collected during (left) 1, (middle) 10, and (right) 100 spins of Juno on itself.

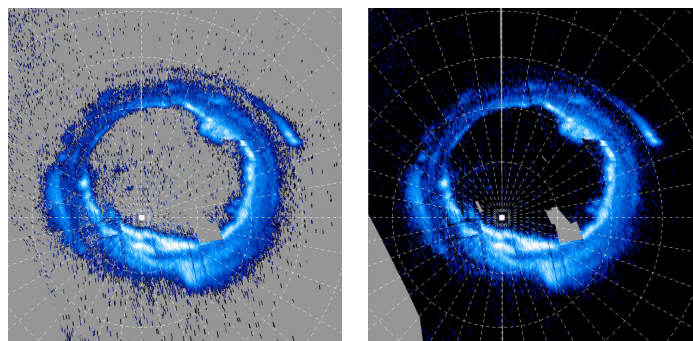


Figure 3.3: Comparison between (left) a real brightness map, and (right) a fake brightness map created to visualize the area covered by UVS.

After that, visual indications were eventually added to the map (see lines 153 to 230) to indicate the scale at the bottom of the image, the date and time of the first and last spins used, and the mean subsolar longitude.

The final step is the computation of the power map, which is easily done by converting the brightness into a power, accounting for the surface covered by each element of the brightness map array (see line 236).

3.2 `create_me_mask_bonfond.pro`

This section, as well as Sections 3.3, 3.4 and 3.5 are dedicated to the routines that permits to isolate the main emission from the other parts of the aurorae based on four different methods. In this first method, the masks (later called B masks) created to cover only the main emission are simply chosen among various masks created by Bertrand Bonfond during the 2007 HST campaign. These HST masks are made to cover the main emission, but due to its variability in size over time, all the masks have different coverages.

The routine is divided in two parts, one for each hemisphere. The first part is dedicated to the southern hemisphere. At the beginning, the HST masks are simply restored and slightly modified. Indeed, these masks are made on 3601×1800 elements arrays, so the last column has been discarded to not include a 1-element shift per line in the array. The masks are also shifted by 180° longitude, or 1800 elements, and had to be shifted back to match the auroral maps created with the previous routine. Finally, the masks had of holes at random locations for some unknown reason. These holes had to be filled in before doing any computation based on the mask (see lines 31 to 39 for the three modifications). Another problem, discovered when creating the dusk and dawn regions with a later routine, was the existence of the mask near the barycentre in a few masks. This was not supposed to happen, and the reasons for this phenomenon are still unknown. This extra feature in the mask has been easily erased by choosing the value near the barycentre to be zero (see line 59).

After that, the masks have been put on the power map to see which one covered the highest emitted power. The main emission being interpreted here as a region of high emitted power, the best fitting mask based on this criterion was chosen. The easiest way to do what was explained above is to create a loop testing each mask one after the other. Thus, at the end of the loop, the selected mask had to be restored once again (see lines 53 to 60). This newly restored mask contained the problems mentioned earlier. To cover the holes, a smoothing of the mask had to be performed. Indeed, the masks have been created in a way to be able to isolate the dusk and dawn regions in the next step. To do so, a value has been given to the elements of each degree around the barycentre of the main emission. Because of this construction method, each hole had to be filled with a different value. The easiest way to do this is by smoothing the mask, giving the holes a value close to the value of the adjacent elements. The problem with this method is that the edges of the mask will also be smoothed with the void, thus extending the mask. To prevent this from happening, a first mask taking the delimitations of the HST mask has been built, and only the elements inside these delimitations are kept in the final mask. In addition, one smoothing of the mask was not enough to have a clean mask, and 15 smoothings have been performed (see lines 73 to 89). The difference between the mask before and after the smoothing is shown in Figure 3.4. After that, some lines of code are dedicated to the making of images of the mask to conclude the first part of the routine.

The second part is dedicated to the northern hemisphere. In this case, there were no holes in the initial masks. So, the idea is the same as in the first part, but without the considerations about the holes.

3.3 `create_me_mask_vogt.pro`

The second method to create the masks is to use of the magnetosphere model created by [Vogt et al., 2011]. The masks created this way are latter called V masks.

This time again, the first half of the routine is dedicated to the southern hemisphere. Two masks are created, mapping to $30 R_J$ and $40 R_J$ in the magnetosphere. The mask covering the area with the highest emitted power is kept at the end. The routine starts with the definition

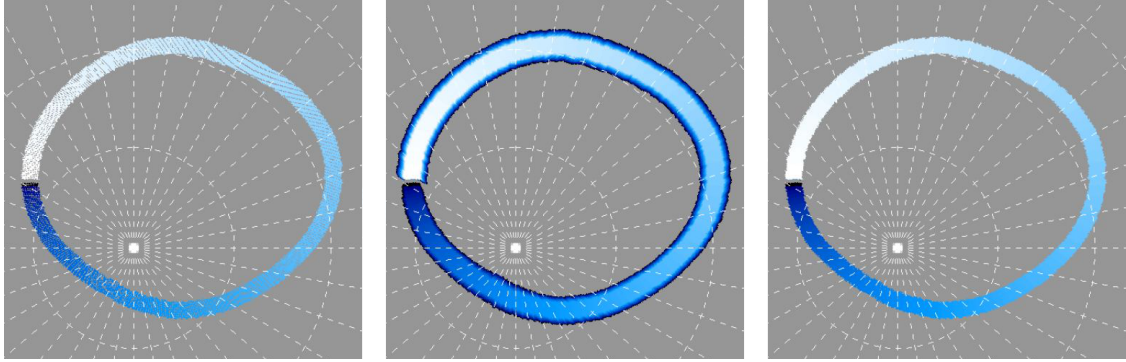


Figure 3.4: B mask for PJ1 in the southern hemisphere. On the left, the initial mask is shown with the holes in it. In the middle, the same mask after smoothing but with the extended edges do to the smoothing is displayed. Finally, on the right is an image of the final mask with the correct dimensions and no holes.

of 36 local times equally spaced. Those are directly used to obtain the longitude and latitude of the locations in the ionosphere that maps to the local times at 30 or 40 R_J in the magnetosphere (see lines 25 and 36). After that, the latitudes obtained are reorder to be interpolated over 3600 locations. This gives 3600 locations which will be the basis of the mask. This first ribbon is illustrated in the left panel of Figure 3.5. The 3600×1800 elements array containing the 3600 locations in cylindrical projection is then transformed into another array of 1024×1024 elements where the locations are in polar projection (see line 67). This polar projection is easier to manipulate in the next part of the routine.

After that, 7200 slices of the ribbon are made, one for each twentieth of a degree around the barycentre of the aurora. For each slice, the ribbon is extended to obtain the thickness desired for the final mask (see lines 72 to 76). Then, the mask is transformed back into cylindrical coordinates to match the 3600×1800 elements array usually used. Some problems may appear during this transformation (e.g. longitudes bellow 0°). After considering those problems, a value is attributed to each slice to match the aesthetics of the B mask and its advantages for selecting of the dusk and dawn regions (see lines 99 to 116). This mask is shown in the middle panel of Figure 3.5. One can see that several problems are present. First, holes appeared in the mask due to the transformation from a 1024×1024 elements array to a 3600×1800 elements array. The distortion created holes in some places. This may be an explanation for the holes in the HST masks discussed in the previous section as well, but I have not created those masks and cannot be sure of that. Then, the mask is shifted, and needs to be adjusted. Finally, the mask may also be non-zero at the barycentre for an unknown reason. The mask at the barycentre as been removed (see line 134), smoothing of the mask has been done in the same way as for the B mask (see lines 149 to 166), and the mask as been shifted (see line 174). The final mask thus obtained is visible in the right panel of Figure 3.5. Images are then created, before choosing the best mask between the ones mapping to 30 and 40 R_J in the magnetosphere. The mask covering the more emitted power is considered to cover the main emission better, and this is the one that is kept (see lines 210 to 223).

The second part of the routine refers to the northern hemisphere. The main emission in the northern hemisphere is quite different from the southern one. Here, what is important is the tilt in the dipolar field. In the northern hemisphere, this magnetic axis is so inclined that the main emission does not encompass the north pole. The function used for the interpolation works between each element of the array containing the longitudes, including between the last and first elements. This works well for the southern hemisphere, because the lowest longitude

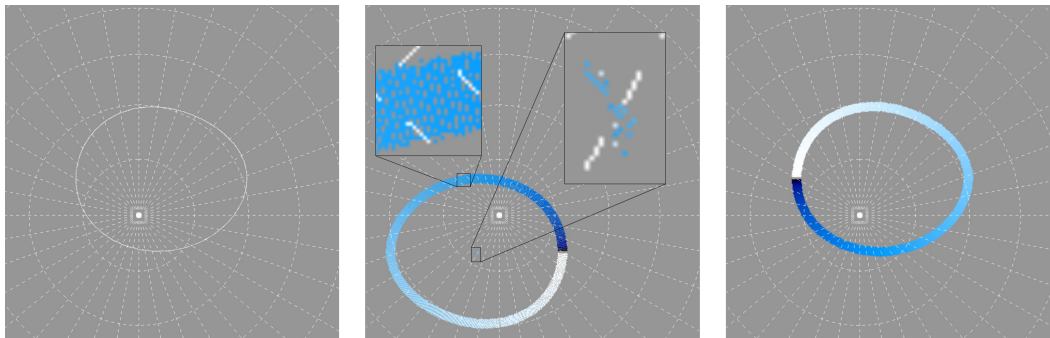


Figure 3.5: Illustration of the steps used in the creation of the V mask. On the left is the ribbon obtained when using the magnetosphere model to map the main emission. In the middle is the mask with different imperfections, and on the right is the final mask.

is close to 0° , and the highest one is close to 360° . But in the case of the northern hemisphere, the highest and lowest longitudes are not related to adjacent locations, and the interpolation does not work properly. To avoid this problem, instead of interpolating every longitude at once, it has been done through 36 smaller interpolations (see lines 266 to 280). The results of the incorrect and correct interpolation methods are shown in Figure 3.6. After that, the mask is created in the same way as for the southern hemisphere, at the exception of the smoothing that was not necessary here.

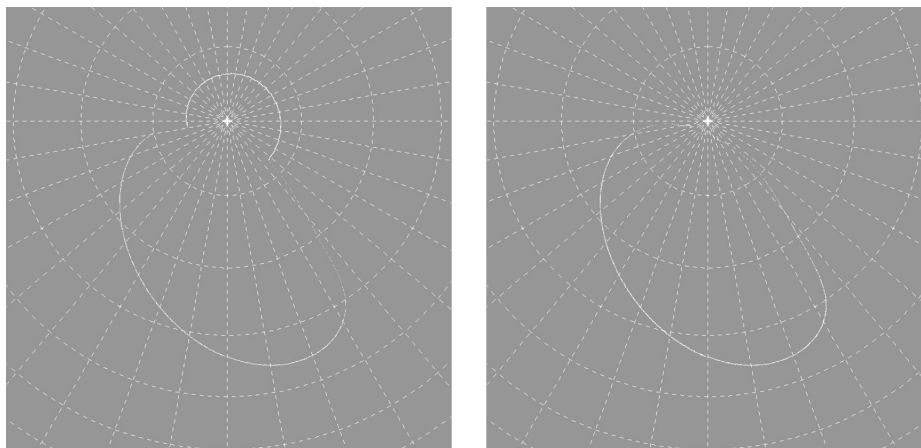


Figure 3.6: Interpolated location of the main emission using (left) the same method as in the southern hemisphere, and (right) the new fragmented method.

3.4 create_me_mask_groulard_V2.pro

The third method to create the mask consists in searching for the region of highest auroral brightness or the strongest gradient of brightness. This mask will later be referred to as the G1 mask.

Once again, the routine is separated in two parts, the first one being dedicated to the southern hemisphere. To limit the search for the main emission in a small area, and avoiding to take into account the other emissions as much as possible, this mask is based on the B mask. The basic idea is to start with the B mask, and to search for the peak of brightness in its surrounding (see line 6). Unfortunately, this did not go as well as expected. Because the B mask does not

always fit the main emission well, the main emission was sometimes far from the mask. Thus, it was necessary to allow a big divergence from this mask to found the main emission in some locations, but then the other emissions were sometimes taken into account. In this case, a small distance did not allow to found the main emission, and a larger one went into the polar or outer emissions that may be brighter than the main emission in some places. To avoid this problem, several parameters were introduced. The first one is a parameter that permits to look only outside an area around to the barycentre of the main emission, permitting to get rid of a part of the polar emissions (see line 9). The second one is a symmetry parameter. Instead of being forced to look both poleward and equatorward of the B mask, one can choose to look in both areas, only poleward, or only equatorward (see line 7). Sometimes, the B mask is just a little bit equatorward of the main emission, and only looking poleward of the mask permits to avoid taking the outer emissions into account. To go further, the B mask was not always a good starting point, and taking another HST mask coupled with the symmetry parameter could give better results (see lines 92 to 105).

After choosing the best mask and parameters, the next step was to smooth the brightness map to work on it more easily, and to have broad structures of common brightness instead of isolated elements. The first idea to do this smoothing was to simply use the *smooth* function (see lines 116 to 118). This gave a smoothed map that can be seen in the middle panel of Figure 3.7. When working on it later, this map did not appear optimal for some perijove. This idea was thus abandoned, and a new method was introduced. In this method, the idea was not much to smooth the map but to bin its elements (see lines 148 to 157). The result obtained using this method is shown in the right panel of Figure 3.7.

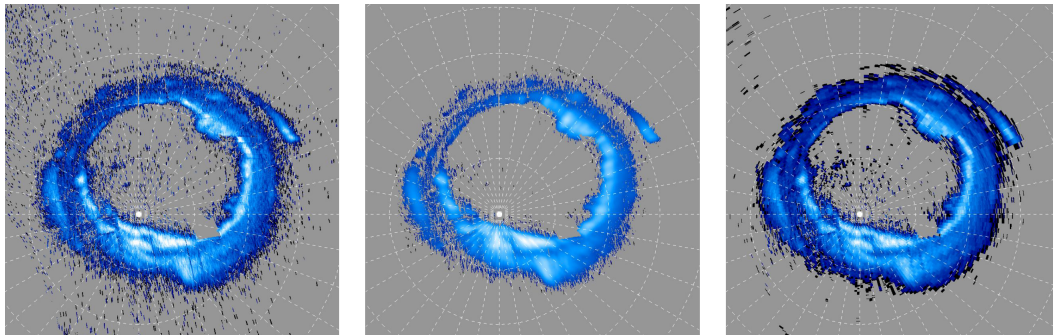


Figure 3.7: Brightness map of PJ1 in the southern hemisphere on the left, and the same map once smoothed with (middle) the IDL *smooth* function, and (right) the binning method.

Then, the arrays containing the B mask and the brightness map have been transformed into polar projections arrays and divided in 3600 slices around the barycentre of the main emission (see lines 179 to 199). For each slice, the centre of the B mask was found and the main emission was searched around this location. A threshold parameter has been created so that if the brightness is above this threshold, the routine will detect it and automatically interpret it as the main emission. If not, the highest gradient of brightness is considered to be the signature of the main emission. If there is no emission at all, the search area around the centre of the B mask is extended (see lines 210 to 232). All that has been said here is illustrated by a concrete example in Figure 3.8.

This gives 3600 points, one for each slice, where the main emission is supposed to be located. Sometimes, the main emission has an unusual shape, or there are small holes in the data. In addition, the routine does not always work perfectly and some outer emissions were taken instead of the main emission. To control it, parts of the points were manually and arbitrarily moved (see lines 239 to 277). An example is given in Figure 3.9.

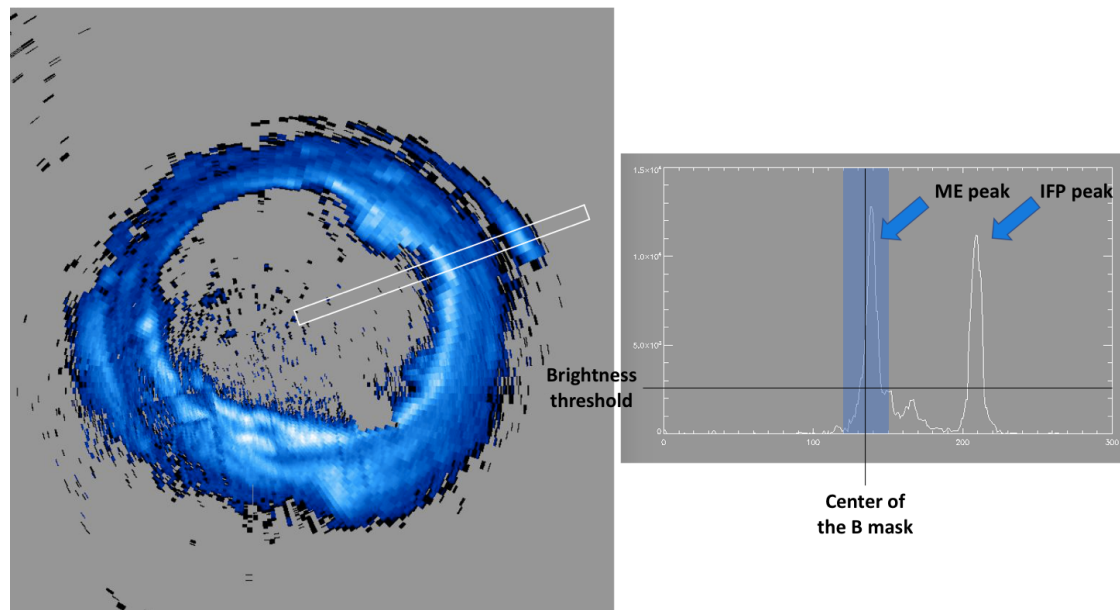


Figure 3.8: On the left is an image of the binned brightness map of PJ1 in the southern hemisphere with a slice shown in a white box. The box should be only 1 element wide but its width has been exaggerated for visual purpose. On the right is the brightness profile for this slice, with the brightness plotted as a function of the distance to the barycentre. One can see two main brightness peaks, created by the main emission (labelled "ME peak") and the IFP (labelled "IFP peak"). The centre of the B mask is also shown with a black vertical line. The brightness peak is searched in the blue area centred on the line. If the symmetry parameter was set differently, the area could extend only on the left or the right of the line. In this area, if the brightness of at least one element is higher than the brightness threshold (labelled with the black horizontal line) the routine will detect the highest brightness element as the main emission. If not, the routine detects the strongest gradient of brightness between 2 adjacent elements and takes it as the main emission. If for a reason there is no emission in the blue area, the routine will extend it and start over. In this example, the IFP peak is not considered because out of the area of concern, even if it peaks above the brightness threshold.

As said earlier, the previous steps have been done on a polar projected array of the aurorae. As it was done for the V mask, this is a 1024×1024 elements array that needs to be transformed back to the usual 3600×1800 elements array containing the cylindrical projection of the aurorae (see lines 283 to 301). After that, the 3600 points had to be smoothed and interpolated to create a solid ribbon instead of isolated points. My first idea to do this was to do a polynomial fit of the points (see lines 314 to 322). This did not fit the points well and this idea was abandoned. The second idea was to smooth the points to link them (see lines 331 to 340). This one did not work either because as expected the points were smoothed in longitude, but they were also smoothed in latitude and it shrank the ribbon. After the smoothing, the ribbon did not fit the main emission anymore. The idea that worked was the third one. It consists in fitting the points by Fourier series. To do so, a new parameter had to be added to define the number of harmonics wanted in the fit. Depending on the shape of the main emission, each perijove map needed a different amount of harmonics to fit the main emission as good as possible. The final result is shown in Figure 3.10.

Once the ribbon created, the next step was to give it a width. It was done the exact same way as for the V mask. Once the wide mask created, the holes were filled by smoothing it several

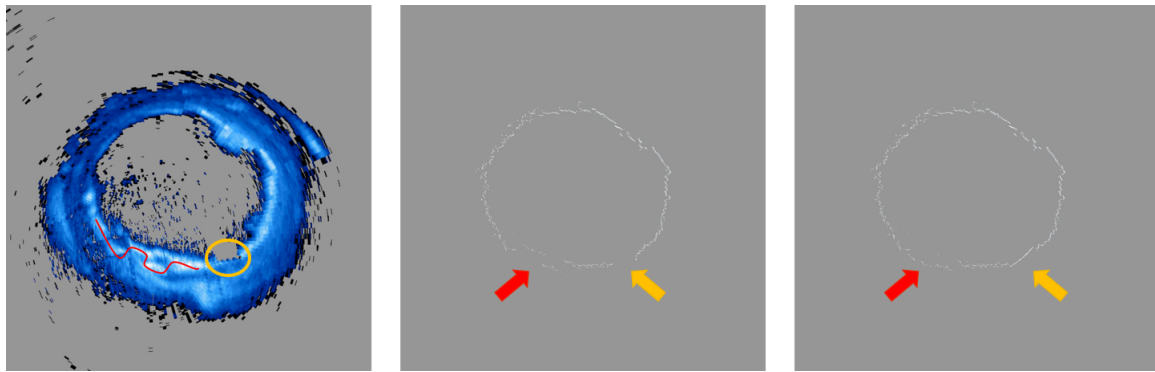


Figure 3.9: On the left is the binned map of PJ1 in the southern hemisphere with 2 remarkable structures marked. The red curve shows a part of the main emission where the shape is unusual, and the orange circle encompasses a hole in the data. In the middle panel is the main emission location as computed by the routine, with the two structures marked with arrows. Finally, the right panel is the same as the middle one, but the location of the main emission in the 2 structures have been manually adjusted.

times, as already explained in the previous sections. The first part of the routine ends with the creation of some images of the mask.

The second part is dedicated to the northern hemisphere. The first change with respect to the southern hemisphere is that the first smoothing method of the map (i.e. using the *smooth* function) was good enough and has thus been used. Another change comes from the shape of the main emission. In the southern hemisphere, the main emission has an oval shape and the variable used to get rid of the polar emissions is thus simply the radius of a circle around the barycentre of the main emission. In the northern hemisphere, the shape of the emissions does not permit such a simple parameter. A variable weight has thus been added to it depending on the longitude of interest (see line 593). Thus, the parameter now contains the variable radii of 36 arcs of circle of 10° long.

The biggest change is made to perform the Fourier fit. Because the main emission does not encompass the north pole, the Fourier fit could not be performed based on the longitude and latitude of the points. Indeed, the longitude increases before reaching a maximum and then decreases, making it unusable. The longitude has thus been replaced by the angle between an horizontal line and the line linking the point and the barycentre. The latitude has been replaced by the distance to the barycentre (see lines 852 and 853). These new coordinates can more or less be seen as the equivalent of the longitude and latitude of the point but relative to the barycentre instead of the pole.

3.5 create_me_mask_groulard_vari.pro

The 3 first masks had a constant width, fixed by an input parameter. This is not the case for this one, that is based on the G1 mask but with a variable width permitted. This is useful for some maps, when the main emission is clearly too broad for the G1 mask, or when an extended feature is not easy to clearly identify as part of the main emission. Of course, this is not always the case and this mask has not been made for every perijove. The masks created using this routine are later referred to as the G2 masks.

As always, the routine is divided into two parts, starting with the southern hemisphere. The brightness map is first binned, as it has been done for the G1 mask (see lines 80 to 89). After that, the contours of the mask are created. To do so, the arrays containing the brightness map

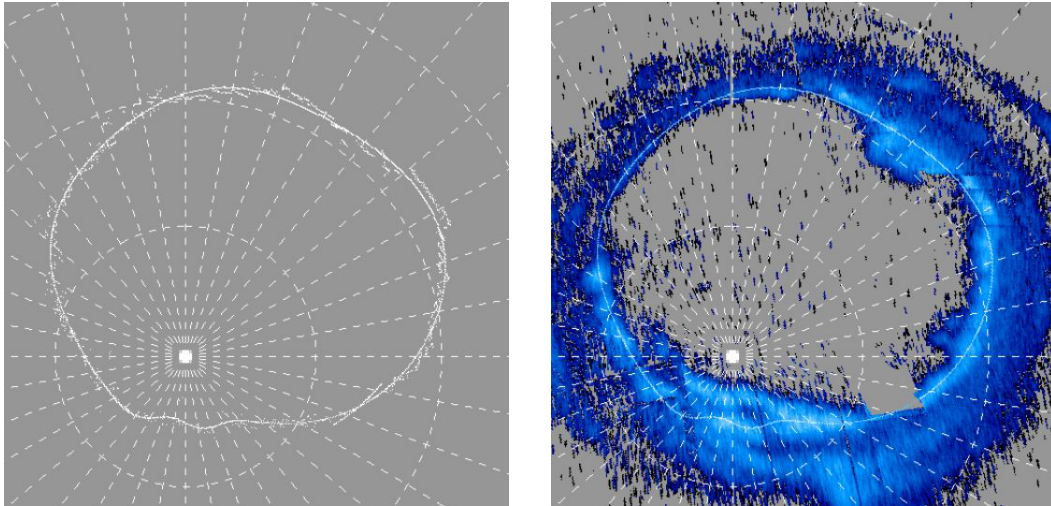


Figure 3.10: In the left panel is a polar projection of the points found with the 3600 slices of the map superimposed over the ribbon obtained when fitting the points with Fourier series. In the right panel is the same ribbon superimposed to the brightness map to show its location relative to the main emission.

and the G1 mask are transformed into arrays containing their polar projections (see lines 97 and 98). 3600 slices are then created and the main emission location is found in each of them. The limits of the G1 mask are found in each slice. If a broadening of the mask is needed, the new limits are found (see lines 139 to 150). If not, the limits of the G1 mask are kept (see lines 150 to 153). In the first case, the new limits are chosen through the use of a parameter that permits to look for high brightness regions (see line 6). All the problem is in founding the best value for this parameter so that the main emission is well covered, but the rest of the emissions are not. This problem is illustrated in Figure 3.11. If one of those regions is too wide to fit into the G1 mask, the width of the mask is modified to encompass it. The inner and outer edges of the mask of each slice are then stored in separated arrays. The next step consists is performing Fourier series fit on the inner and outer edges of the mask separately (see lines 177 to 185 and 192 to 200) to create two ribbons, before transforming it back to 3600×1800 elements arrays. 7200 slices of the ribbons are then made to create the final mask. In each slice, a value is assigned to the points located between the inner and outer ribbons in order to match the aesthetics of the previous masks. This final mask is shown in Figure 3.12.

The second part of the routine permits to create the mask in the northern hemisphere. The creation is exactly the same, at the exception of the addition of a manual modification of the edges of the mask for 2 perijoves (see lines 381 to 398).

3.6 `measure_power_arc.pro`

Now that the masks are created based on the 4 methods described in the previous sections, it is possible to found the dawn and dusk regions of the main emission and compute the power emitted in these regions. This is what this routine allows to do.

The routine starts with the use of the magnetosphere model created by [Vogt et al., 2011] to found the areas of the main emission linked to the magnetospheric plasma flowing at the local times of interest. Two different sizes of the dawn and dusk regions have been studied. The first one is the same as for the [Bonfond et al., 2015] HST study (6:00 to 8:00 LT and 16:00 to 18:00 LT) and the second one is symmetric around 6:00 LT and 18:00 LT (4:00 to 8:00

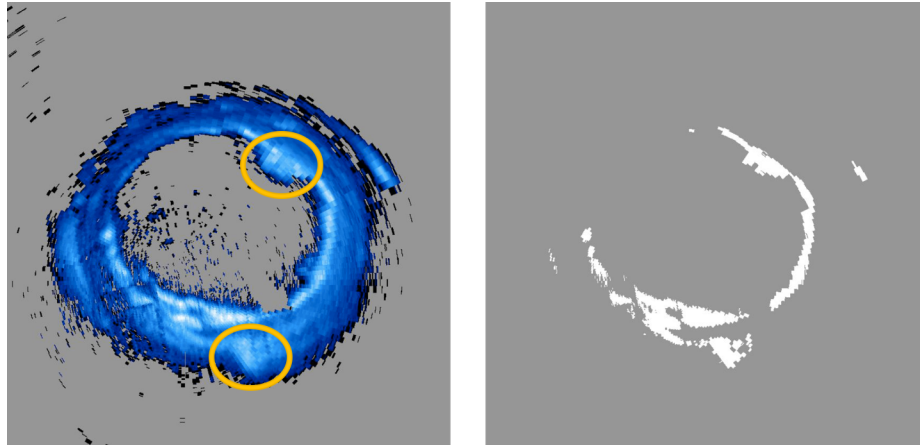


Figure 3.11: In the left panel is the binned brightness map of PJ1 in the southern hemisphere with 2 regions of same intensity labelled. The upper one is in the main emission, but the lower one is not. Thus, to cover the main emission well, the lower region as to be taken into account too. The right panel illustrates the area of the brightness map where a broadening of the mask is considered. This area is limited by a brightness threshold parameter. Due to the problem mentioned in the image of the left panel, a part of the outer emissions are taken. A combination with the parameter limiting the mask to a specified distance to the G1 mask will later permit to not consider this undesired region.

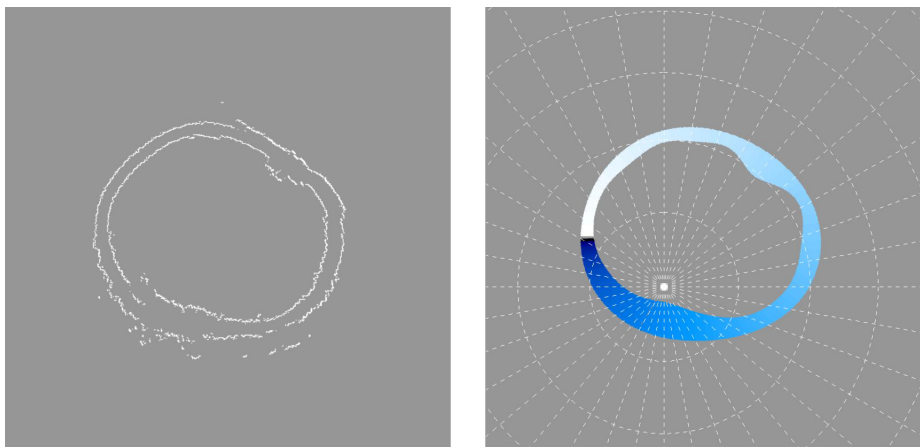


Figure 3.12: In the left panel is the inner and outer edges of the G2 mask before being smoothed through the Fourier series fits. Few imperfections arise from the threshold problem mentioned in Figure 3.11. The fits will smooth these imperfections to create the definitive limits of the mask. The final G2 mask is shown in the right panel.

LT and 16:00 to 20:00 LT). These dawn and dusk local times ranges will later be referred to as the HST sector and the symmetric sector. This model gives the longitude and latitude of an auroral location mapping to the chosen magnetospheric location (e.g. 6:00 LT at $30 R_J$ in the magnetosphere). These longitude/latitude coordinates are then transformed into an angle relative to the barycentre and a distance (see lines 51, 56, 61 and 66). What is important is the angle. It will be used to intersect the mask at the desired locations, as illustrated in Figure 3.13.

After that, the dawn and dusk regions are selected. As a reminder, the value attributed to each element of the masks depends on its position relative to the barycentre. Each slice around

the barycentre made to create the masks was attributed a value related to the angle it forms with the horizontal. Thus, it is easy to find a specific region of the mask based on its longitude and latitude now that these coordinates have been converted into an angle (see lines 208 to 212 and 224 to 228). The only problem could arise from the 360° to 0° longitude transition, creating areas that starts in higher longitudes than it ends. This possibility considered, the selection of the regions is easily done. Two masks are then created, covering both regions, and the power emitted in the areas covered by these masks are computed. These masks have small imperfections, with a few points taken when they should not be. This is probably due to the smoothing done on the masks that slightly modified the value of the elements on the edges of the mask. Anyway, this problem is not that important and it does not induce an important error, as discussed in Section 4.6.

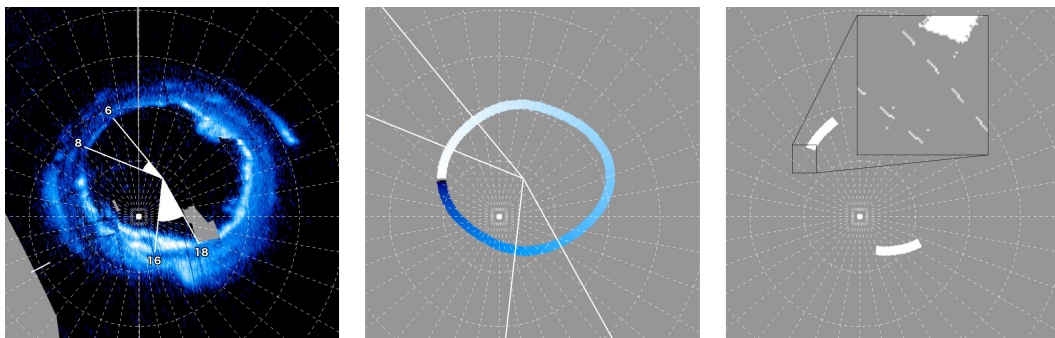


Figure 3.13: In the left panel is the brightness map of PJ1 with the locations of the 6:00, 8:00, 16:00 and 18:00 LT mapping labelled. In the middle panel are the lines linking the locations previously mentioned to the barycentre of the aurorae intersecting the B mask. In the right panel are the final dawn and dusk masks (added on a single image) based on the B mask. A part of the dawn mask is zoomed to see the small imperfections.

3.7 stats_dawn_dusk.pro

The treatment of the data collected with UVS is now done, and the only things left to do are mathematical developments. In this routine, the dusk-over-dawn ratios are computed, as well as statistical informations such as the median and standard deviation of various quantities.

The routine starts with the definition of arrays that contains the perijoves that can be used for a given mask. Indeed, some masks do not fit the main emission well and have been removed. Others arrays are then created to contain the power computed with the previous routine. The G2 mask has a separated treatment because it is not used on every map. The G1 mask can be seen as a particular case of the G2 mask when the width of the mask is constant, thus it can be used when there is no G2 mask. More lines of code must be written when treating this mask to account for this idea (see lines 84 to 94 and 103 to 113).

Now that everything is stored into the right arrays, it is time to manipulate them. All that follows is first done in the southern hemisphere, before being done in the northern hemisphere in the second part of the routine. The first quantity computed is the dusk-over-dawn ratio. This part of the routine consists in two computations: first, there is the dusk-over-dawn ratio itself. Then, depending on the value of this ratio, the perijove is classified into 1 of 3 possible scenarios. Either the dusk region is more powerful, or it is the dawn region, or they both emit the same power. The criteria to being equal has been arbitrarily fixed to a difference of less than 1% in the emitted power from the two regions (see lines 147 and 155). Once it is done for every useful

perijove, the median and standard deviation of the ratios are computed (see lines 178 to 189). The same quantities are computed for the power emitted in the dusk region (see lines 191 to 202), and in the dawn region (see lines 204 to 215).

All the informations are then printed on screen, and the routine continues with northern hemisphere considerations. This part of the routine is exactly the same as for the southern hemisphere and therefore it will not be detailed here.

3.8 error_V2.pro

This routine is made to compute the propagation of error from the count of photons hitting the detectors of UVS to the final dusk-over-dawn power ratio.

At the beginning, arrays are created to contain the perijoves that can be used, as it has been done in the previous routine. Important quantities about the mask and the emitted power are also restored. I forgot to save the dusk and dawn masks created with the routine *measure_power_arc.pro*, and they are quickly recreated here using the exact same code lines (see lines 107 to 143).

The error is then computed. This is based on [Gérard et al., 2019] computations that found 25 counts for a signal of 10kR. To found this number, they averaged the auroral brightness over a 400-km radius circle, what is also done in the brightness map. Indeed, each element of the map is computed through this same technique during the first treatment done before the creation of the routines for this thesis. So, for each element of the brightness map, one founds 25 counts per 10kR. The brightness of each element covered by the mask can thus be summed to have the total count obtained over the whole dusk or dawn region (see lines 165 and 166). The error on this count is simply given by its square root. There are hundred of thousands to millions of counts obtained from a region, and the error associated to it is then on the order of 1000 counts, or 1‰ of the total count. This brightness and error on the brightness are then converted into powers, and the error on the dusk-over-dawn ratio can finally be computed. This error is also found to be on the order of 1‰.

Chapter 4

Results

4.1 B mask

As explained in the previous chapter, the B masks are a collection of masks created by Bertrand Bonfond thanks to data collected with HST in 2007. Because of the limited time of observation during this HST campaign, only 4 masks have been created for the northern hemisphere, and 5 for the southern hemisphere. The B masks of each perijove have been chosen between these 9 masks. Due to the variability in the shape of the main emission, this restricted choice may greatly limit the accuracy of the masks.

4.1.1 Northern hemisphere

In the northern hemisphere, only 20 images have been used for the HST sector, and 18 for the symmetric sector, out of the 38 available. Different possibilities explain this selection:

- ◇ The masks did not fit the main emission at all in some parts of the dawn or dusk region, going in the polar zone where there is nearly no emission. Because of this bad match of the masks, dusk-over-dawn ratios may take extreme values (going up to 492.4 and 80.4 for PJ13 in the HST and symmetric sectors respectively).
- ◇ The location of the main emission is unclear because of its shape that is more diffused than a simple arc and holes in the map (i.e. missing data).
- ◇ Sometimes, the data collected with Juno were not enough to create a full map, and a big part of the dawn or dusk region was empty of data. In this situation, comparing the two was impossible.

Reason of exclusion	HST sector only	Symmetric sector only	Both sectors
Unsuited mask		PJ8, PJ22	PJ7, PJ13, PJ21, PJ39
Uncertain location			PJ10
Incomplete maps			PJ17, PJ18, PJ23, PJ25, PJ27, PJ28, PJ29, PJ30, PJ31, PJ33, PJ34, PJ35, PJ37

Table 4.1: Reasons of exclusion of the different perijoves.

The perijoves kept after this selection and the dusk-over-dawn ratio associated to them are illustrated in Figure 4.1. One can see that PJ3 has a high dusk-over-dawn ratio in the HST

sector. This due to a particularly dim emission in the dawn region. PJ24 also stands out in the HST sector (16.6 dusk-over-dawn ratio). The mask for this perijove is at the limit between the main emission and the polar region in the dawn part. It has been kept anyway, but the mask fits less the main emission than for the other perijoves, explaining such a big ratio. In the symmetric sector, the mask better matches the aurorae and it produces a ratio of 5.7.

4 perijoves are of particular interest. Indeed, PJ3, PJ15, PJ26 and PJ32 have a ratio below unity. The dawn region is thus brighter than the dusk one. In the case of PJ3, this is due to a bright spot that develops in the symmetric sector. It is in fact an artefact related to a dawn storm, that will be more present in the southern hemisphere. One can see in Figure 4.2 that PJ15 and PJ32 have particularly powerful dawn emissions, explaining this ratio. In the other hand, PJ26 seems to have a dusk region less powerful than usual. A deeper analysis of PJ26 consisting of looking at the map available in the Appendix II shows a total mismatch of the mask in the dusk part, and a moderate mismatch in the dawn one. This has not been seen during the selection of the perijoves, but this mask should have been removed. The other masks gave results easier to interpret for this perijove.

The mean power emitted for the HST sector is 58.3 GW and 28.1 GW in the dusk and dawn regions respectively, and it rises to 101.1 GW and 60.7 GW in the symmetric sector, which is twice the size of the HST sector. The mean dusk-over-dawn ratio is 4.9 in the HST sector and 2.9 in the symmetric one.

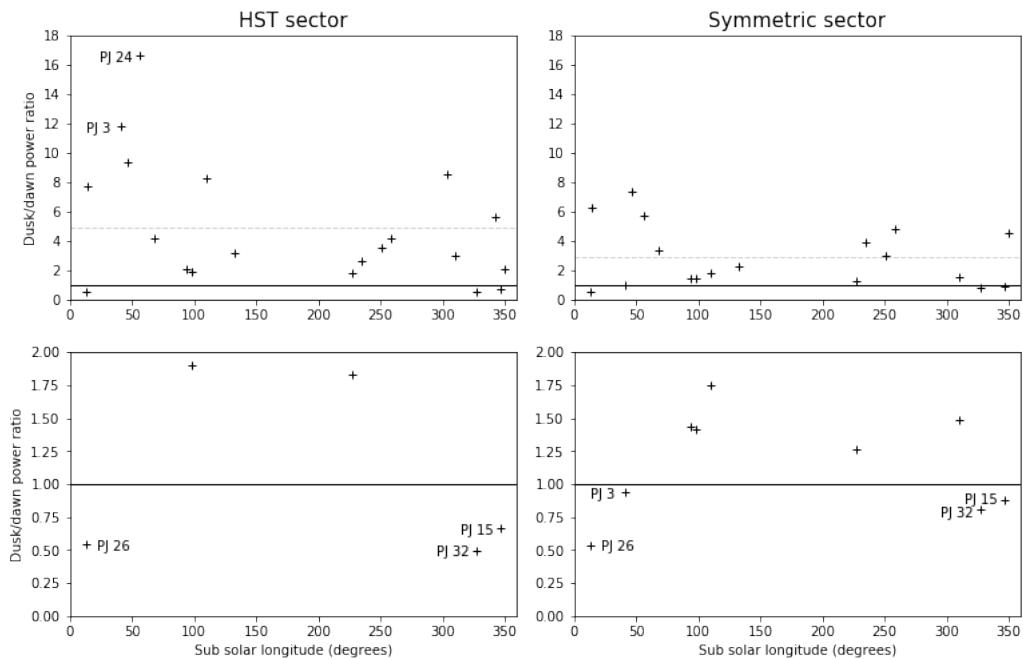


Figure 4.1: Dusk-over-dawn ratios computed using the B masks as a function of the subsolar longitude for each perijove selected in the northern hemisphere. The left plots correspond to the HST sector and the right ones to the symmetric sector. The plots in the bottom are zoomed versions of the upper ones, centred on 1. This value makes the distinction between more powerful dusk regions and more powerful dawn ones. The mean ratios are also indicated by dashed grey lines.

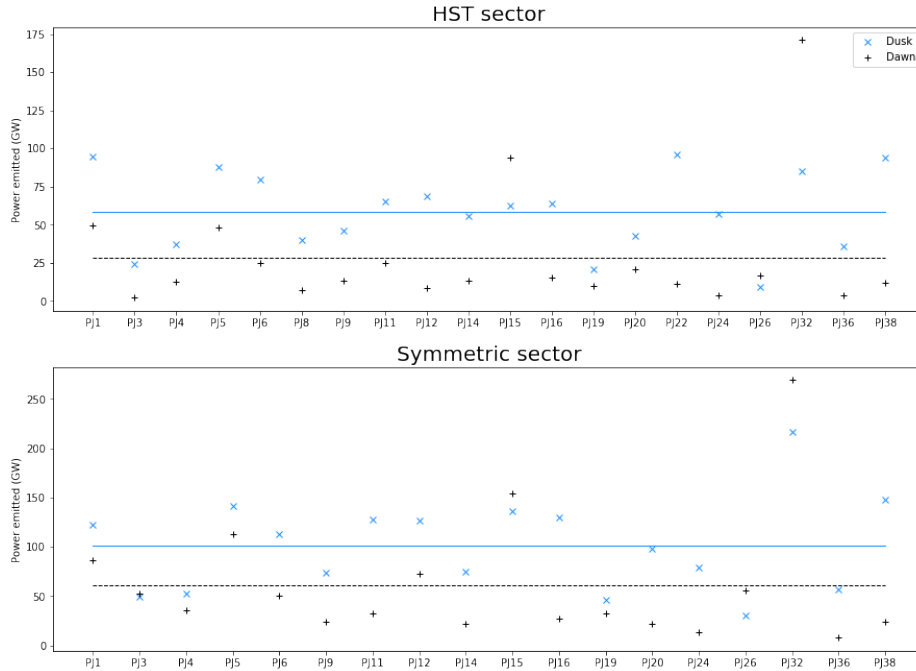


Figure 4.2: Power emitted by the dusk and dawn regions computed using the B masks in both sectors for each perijove selected in the northern hemisphere. Mean dusk and dawn power emitted are also shown with solid blue and dashed black lines respectively.

4.1.2 Southern hemisphere

In the southern hemisphere, 34 perijoves have been used for the HST sector, and 32 for the symmetric sector. The data collected in this hemisphere has permitted to create comprehensive maps for each perijove, with very limited holes. Anyway, some perijoves still had mismatches of the B mask, creating once again huge power ratios (up to 511.1 for PJ24 in the HST sector, and 93.3 for PJ7 in the symmetric sector).

Reason of exclusion	HST sector only	Symmetric sector only	Both sectors
Unsuited mask		PJ13, PJ22	PJ7, PJ24, PJ29, PJ37
Uncertain location			
Incomplete maps			

Table 4.2: Reasons of exclusion of the different perijoves.

One can see in Figure 4.3 that more perijoves are worth being discussed than in the northern hemisphere. First, PJ1, PJ5, PJ9, PJ13, PJ22, PJ36 and PJ39 all show a low power emitted in the dawn region, what increases the dusk-over-dawn ratio. Figure 4.4 shows a wide range of power emitted in the dawn region, with a lot of variability, while the power in the dusk region seems more concentrated around the mean value. Even if the power emitted in the dawn region for these perijoves seems low in comparison to the mean value, this plot and the computation of the median and the standard deviation show that it seems to be the more common value. The mean value, standard deviation and median can be found in Table 4.3. Then, PJ1 shows a drastic difference between the two sectors because of the crossing of a hole in the data in the symmetric sector. PJ13 and PJ22 are not computed in the symmetric sector because the B mask does not fit well the main emission in this sector, but a quick look at the auroral maps

of these perijoves suggests that the ratio would not be that different from the one in the HST sector. Finally, PJ23 has a powerful dawn region but the mask only goes over a part of the emission, increasing the dusk-over-dawn ratio.

Sector	Region	Mean	Standard deviation	Median
HST	Dusk	74.9	38.9	68.1
	Dawn	42.5	54.2	14.2
Symmetric	Dusk	149.2	78.3	129.3
	Dawn	98	115.3	37.1

Table 4.3: Mean power emitted, standard deviation and median power emitted for both the HST and symmetric sectors in the dusk and dawn regions, all expressed in GW.

As previously explained, there is a high variability in the power emitted in the dawn region. Thus, it is not surprising to have 8 different perijoves with a dawn region more powerful than the dusk one. The map of PJ3 has been created out of data collected between 17:55 and 18:45, and [Bonfond et al., 2021] already confirmed that a dawn storm occurred between at least 15:10 and 22:02 during this perijove. This explains the high value observed in the dawn region. In addition, the B mask does not seem to cover the dusk region well. These 2 reasons explain the low dusk-over-dawn ratio computed. PJ10, PJ15, PJ18, PJ26 and PJ32 all display a bright main emission in nearly all local times. This enhancement of the main emission can be explained by a compression of Jupiter’s magnetosphere by the solar wind, as explained in Section 1.4. Thus, the dawn region brightness rises. As shown in Figure 4.5, a dawn storm also took place during PJ32, increasing even more the brightness in the dawn region. Finally, the B masks does not cover well the dusk region for PJ20 and PJ38, lowering the ratio for both these perijoves.

The mean power emitted for the HST sector is 74.9 GW and 42.5 GW in the dusk and dawn regions respectively, and 149.2 GW and 98 GW in the symmetric sector. The mean dusk-over-dawn ratio is 5 in the HST sector and 3.8 in the symmetric one.

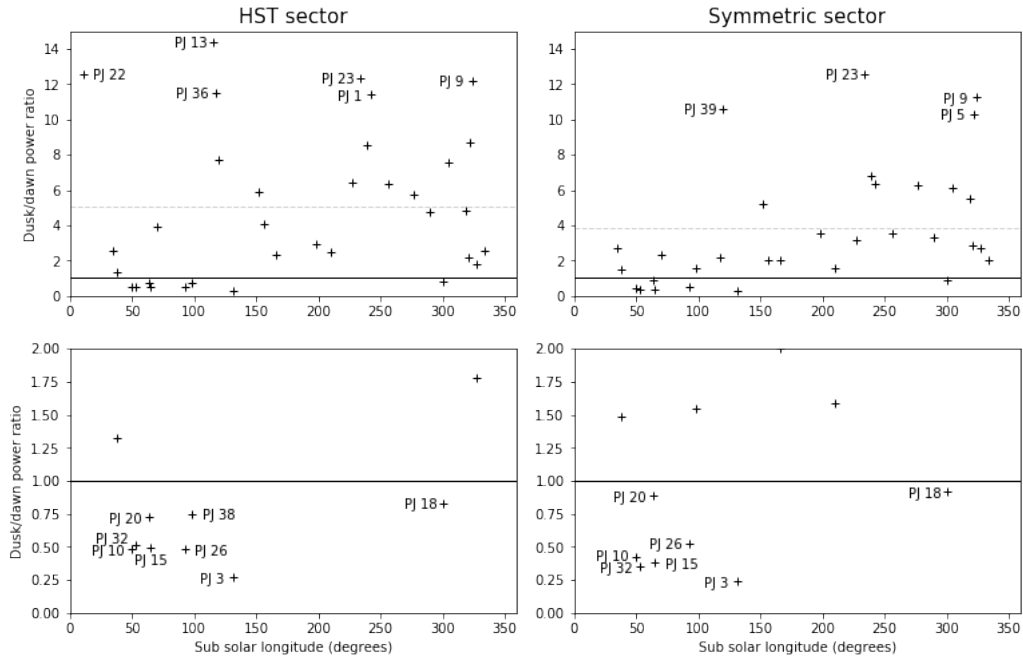


Figure 4.3: Same as figure 4.1 but in the southern hemisphere.

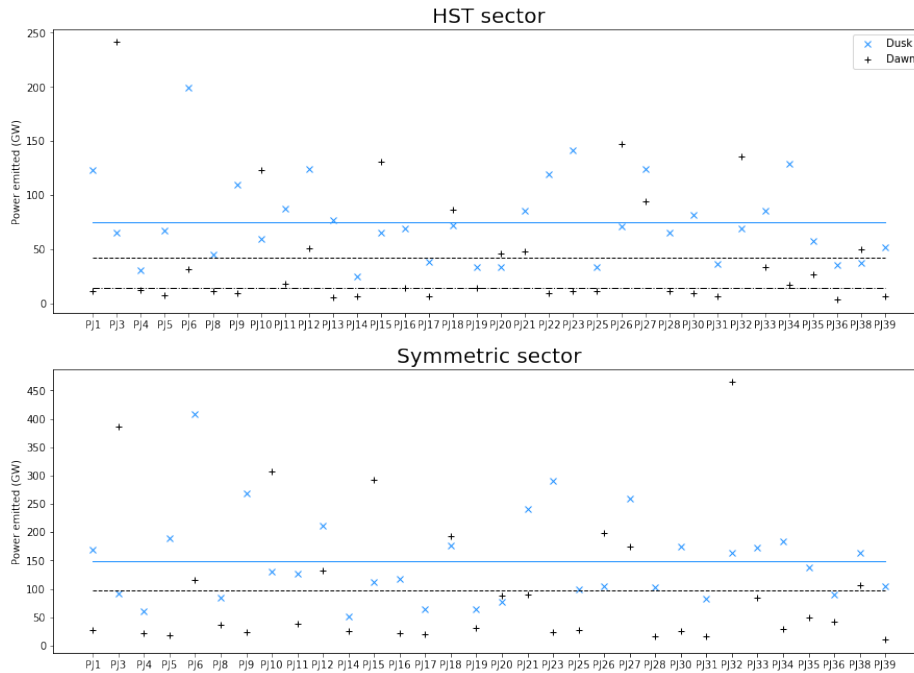


Figure 4.4: Same as Figure 4.2 but in the southern hemisphere.

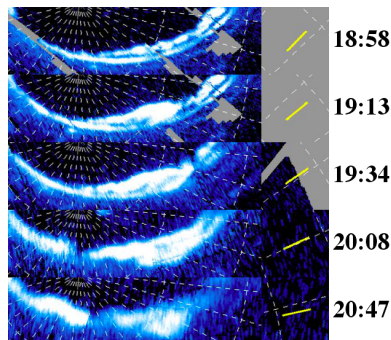


Figure 4.5: Evolution of a dawn storm during PJ32. Sunward direction is shown in yellow to facilitate the identification of the dawn region. The dusk-over-dawn ratio has been computed based on an image of the aurorae at 19:37 UT. The dawn storm had a shape close to the one visible on the image at 19:34 UT.

4.2 V mask

These masks have been created using the model of Jupiter's magnetosphere by [Vogt et al., 2011]. In their study, researchers found that the main emission maps to different distances in the magnetosphere for different local times. To create simple masks with a limited computation time, the use of a constant distance ($30R_J$ or $40R_J$) has been chosen for the masks. This can create regions where the masks do not cover the main emission well. According to the conclusions of the study, the dawn sector maps to about 15 to $30R_J$, while the post-noon region maps to about 50 to $60R_J$. One can thus anticipate that the V mask will more likely give a good cover of the dawn region than the dusk one.

4.2.1 Northern hemisphere

Out of all the perijoves, 16 were not used for this hemisphere. The 13 incomplete maps listed in the previous section are still not usable. In addition, 3 other perijoves have been withdrawn for various reasons. PJ39 covers the limit between the main emission and the polar emissions in the dusk region. PJ10 and PJ26 cover the outer emissions instead of the main emission. Thus, even if these 3 particular cases do not produce ratios reaching big values, I decided to not use them.

Reason of exclusion	HST sector only	Symmetric sector only	Both sectors
Unsuited mask			PJ10, PJ26, PJ39
Uncertain location			
Incomplete maps			PJ17, PJ18, PJ23, PJ25, PJ27, PJ28, PJ29, PJ30, PJ31, PJ33, PJ34, PJ35, PJ37

Table 4.4: Reasons of exclusion of the different perijoves.

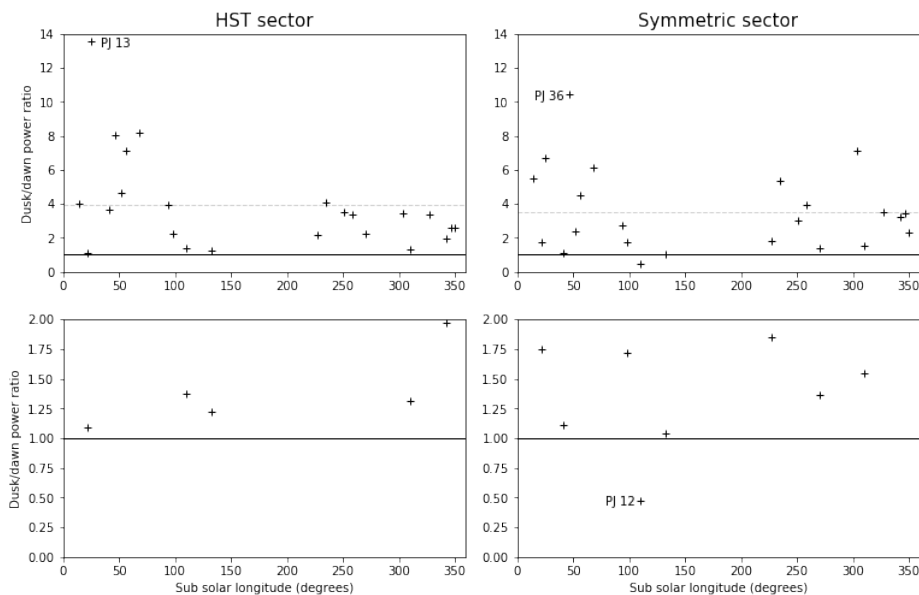


Figure 4.6: Same as Figure 4.1 but using the V masks.

Only PJ13 has a high dusk-over-dawn ratio (13.5) in the HST sector. This is due to a low emitted power in the dawn region, and a possible bad covering of the sunward edge of this region. In the symmetric sector, the dawn region is brighter and the ratio lowers to 6.7. One can see in Figure 4.7 that PJ36 does not display a particularly bright dusk emission, and an even weaker dawn one. Thus, the dusk-over-dawn ratio reaches 10.4 in the symmetric sector. The ratio is quiet high in the HST sector as well, but little holes restraint it to a value of 8.

Only 1 perijove has a more powerful dawn region, but it comes from a bad covering of the dusk region. In the HST sector, the dawn region of PJ12 is not powerful and the dusk region emits more power even if the mask covers the outer emissions instead of the main emission. The symmetric sector covers longer areas, and reaches a more powerful arc in the dawn region. Thus, the dusk-over-dawn ratio lowers to a value below 1.

In the HST sector, the mean dusk-over-dawn ratio is 3.9, and it lowers to 3.5 in the symmetric sector. The mean power emitted are 49.4 GW and 15.9 GW, and 94.4 GW and 36.4 GW in the dusk and dawn regions respectively, for the HST and symmetric sectors.

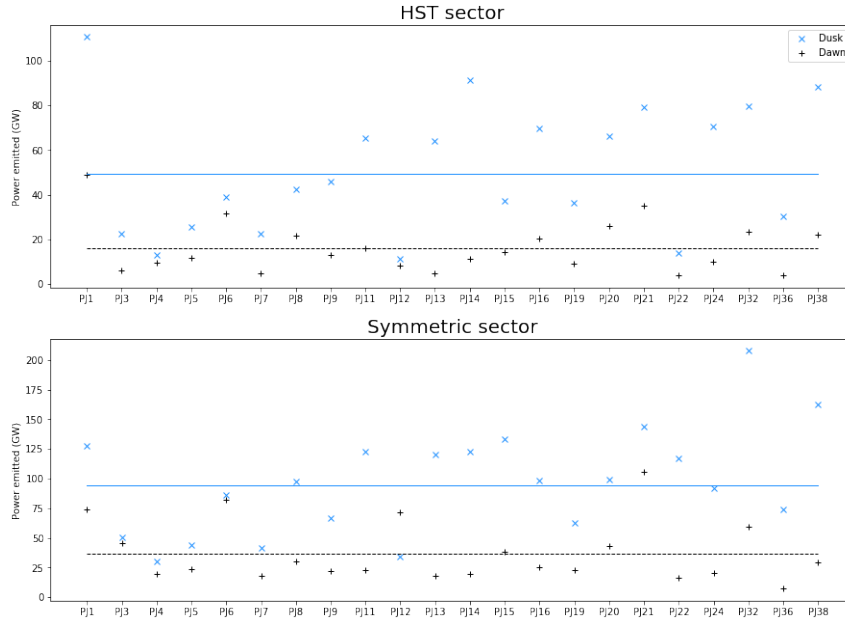


Figure 4.7: Same as Figure 4.2 but using the V masks.

4.2.2 Southern hemisphere

32 perijoves were kept for the HST sector, and 30 for the symmetric one. The perijoves that were not kept have bad covers of the mask over the dusk and dawn regions. The dusk-over-dawn ratio takes values up to 76.4 and 47 for PJ22 in the HST and symmetric sectors.

Reason of exclusion	HST sector only	Symmetric sector only	Both sectors
Unsuited mask		PJ30, PJ34	PJ16, PJ22, PJ24, PJ26, PJ27, PJ28
Uncertain location			
Incomplete maps			

Table 4.5: Reasons of exclusion of the different perijoves.

For this mask, 7 perijoves deserve to be discussed in the southern hemisphere. PJ1 has a particularly bright dusk region, with several bright patches between dusk and noon. The power emitted in the dusk region is 152.5 GW in the HST sector, and it only grows to 171.7 GW in the symmetric sector because of a hole in the map already mentioned. Thus, the ratio decreases in the symmetric sector, going from 11.3 to 9.1 because of the small increase of the emission in the dusk region. PJ9 has a bright dusk region, especially in the symmetric sector, what grows the ratio. PJ34 has also a bright dusk region, but the mask has only been used in the HST sector because of a bad cover in the dawn region of the symmetric sector. PJ13, PJ17 and PJ30 have a weak dawn emission and thus a high ratio. Finally, PJ36 has a weak dawn emission, giving a dusk-over-dawn ratio of 12.6 in the HST sector. A bad cover of the dusk region and a bright spot in the dawn region makes the ratio fall to 1.8 in the symmetric sector.

In 6 of the perijoves that were kept, the dawn region was more powerful. The appearance of dawn storms during PJ3 and PJ32 has already been discussed in Section 4.1, even if a bad cover of the V mask for PJ32 lowers the ratio in this case. The mask does not cover well the dusk region of the main emission in PJ12, PJ15, PJ18 and PJ21, and they all have a powerful dawn region, thus a low ratio.

The mean value of the ratio is shown in Figure 4.8. It is 5.2 for the HST sector, and 3.9 for the symmetric one. Figure 4.9 gives the power emitted in the different regions for each perijove, as well as the mean power emitted. 69.5 GW and 32 GW are the mean values for the dusk and dawn regions in the HST sector. These values increase to 133.3 and 76.5 in the symmetric sector.

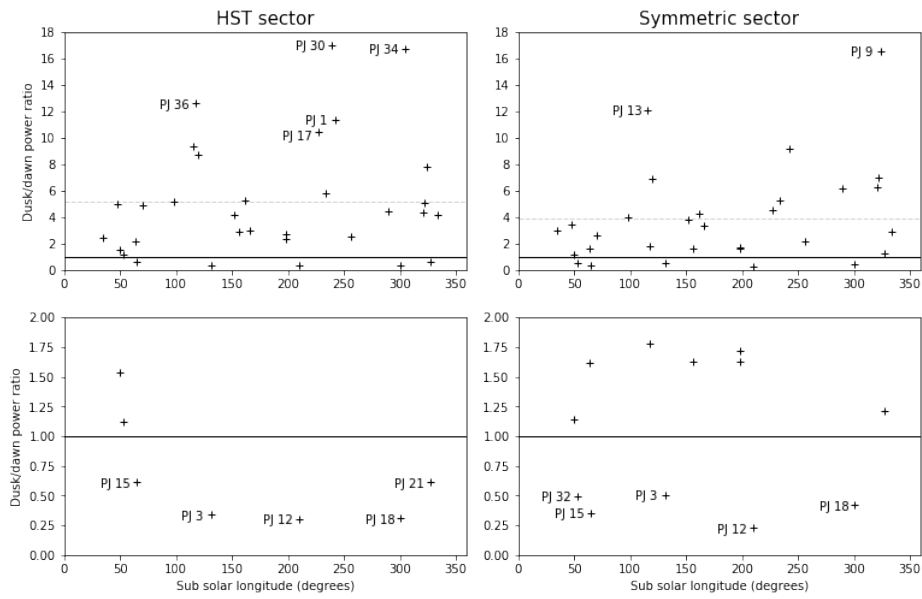


Figure 4.8: Same as Figure 4.6 but in the southern hemisphere.

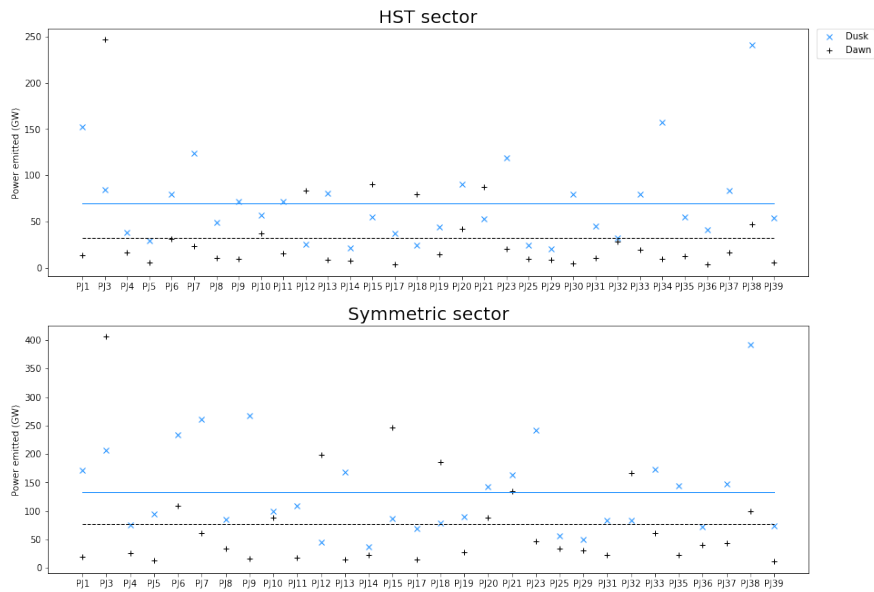


Figure 4.9: Same as Figure 4.7 but in the southern hemisphere.

4.3 G1 mask

G1 masks have been created based on a visual idea of the location of the main emission. A constant width of the masks has been kept, making it hard to cover the whole emission for some perijoves.

4.3.1 Northern hemisphere

Because of the way these masks were built, all of them at least partly covers the main emission. Thus, no mask was excluded because of a bad covering. Still, 14 masks have not been used. Those are the 13 usual incomplete maps, and PJ10 that has small holes in the map and an uncertain location of the main emission.

Reason of exclusion	HST sector only	Symmetric sector only	Both sectors
Unsuited mask			
Uncertain location			PJ10
Incomplete maps			PJ17, PJ18, PJ23, PJ25, PJ27, PJ28, PJ29, PJ30, PJ31, PJ33, PJ34, PJ35, PJ37

Table 4.6: Reasons of exclusion of the different perijoves.

PJ7 and PJ13, have a dusk-over-dawn ratio higher than 10 in the HST sector. Both of them display a particularly not powerful dawn region. This can be seen in Figure 4.11. The dawn region of PJ7 and PJ13 only produces 3.4 GW and 4.6 GW. In the symmetric sector, the power emitted by the dawn region quadruples (15.7 GW for PJ7 and 19.6 GW for PJ13), even if the sector is only twice the size of the HST one. Thus, the ratios lower from 19.5 and 14.1 to 8 and 6.5.

Here, 5 perijoves have dusk-over-dawn ratios below one. First, the symmetric sector of PJ3 covers part of the dawn storm, what lowers the ratio in this sector. Then, PJ4 has not a powerful dusk region. The dawn region is more powerful only in the symmetric sector, and the ratio only reaches 1.1 in the HST sector. PJ15 has a bright dawn region, and a more diffuse emission in the dusk region. Once again, even if the ratio is below 1 only in the HST sector, its value is as low as 1.1 in the symmetric sector. PJ26 is particularly interesting, because of the choice of location of the mask in the dusk region. When looking at the map, an arc is clearly visible in the dawn-side half of the image. But, when going to the dusk part, this arc vanishes and a small region of no emission appears. The bright emission in the dusk region thus seems to be polar emissions, with no clear trace of the main emission in that region. This is hard to tell if the outer edge of this supposed polar emission could be the main emission or not, because some patches look aligned like if it was the main emission. A visual support of this discussion can be found in Figure 4.12. Finally, the lack of data makes it hard to say if the dawn storm identified in the southern hemisphere during PJ32 was already present when Juno passed over the northern hemisphere. In both sectors, the dawn region is abnormally powerful, but the map is not enough refreshed over time to see the dynamics of the main emission. The high emitted power in the dawn region is linked to the global brightening of the main emission, but a dawn storm could enhance this brightening in that region.

The mean ratio is 5.2 in the HST sector and 3.5 in the symmetric one. The mean power emitted are 71 GW and 30.3 GW for the dusk and dawn regions in the HST sector, and 135.4 GW and 66.6 GW in the symmetric sector.

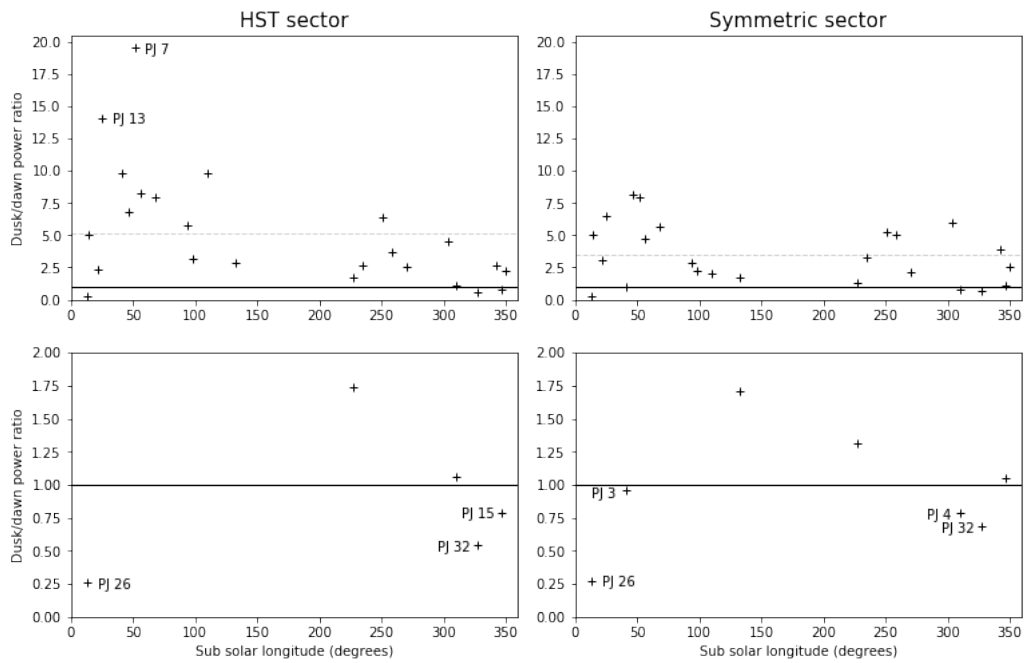


Figure 4.10: Same as Figure 4.1 but using the G1 masks.

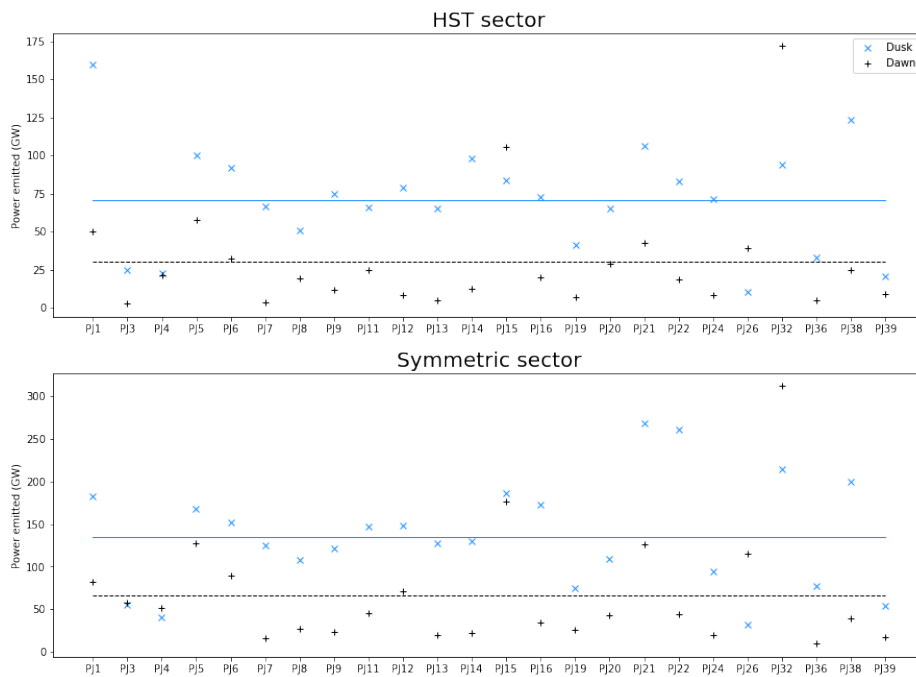


Figure 4.11: Same as Figure 4.2 but using the G1 masks.

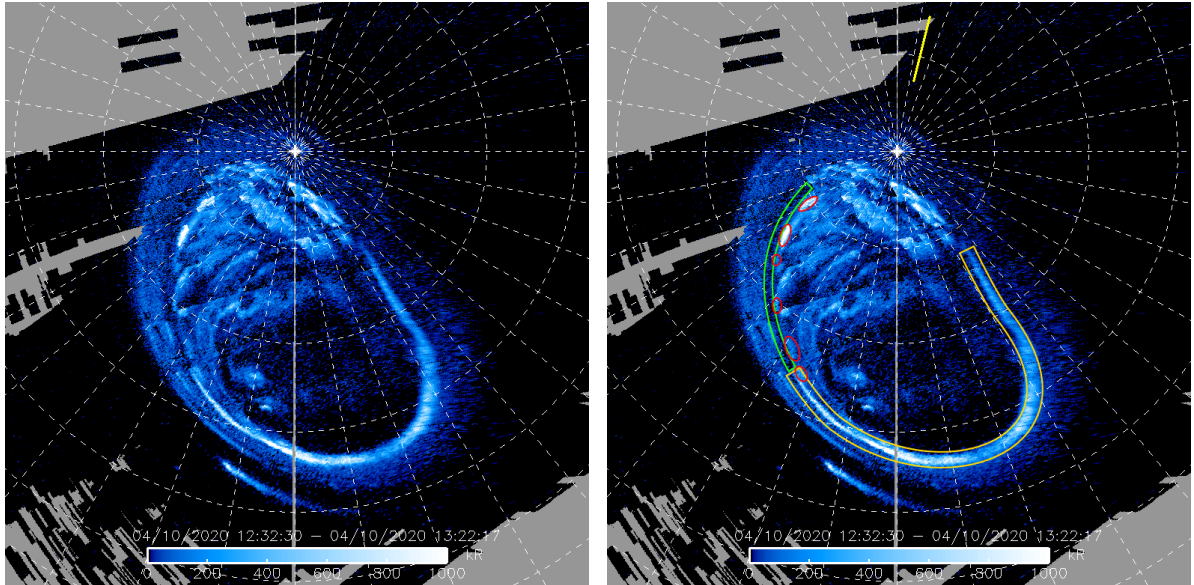


Figure 4.12: (left) Polar projection of PJ26 in the northern hemisphere. (right) The same image with the sunward direction labelled in yellow. The main emission in the dawn part of the image is in the yellow box. The region without any emission is in the green box, and patches that could be the main emission are circled in red.

4.3.2 Southern hemisphere

All perijoves were used in both of the sectors for these masks. Between the 38 perijoves, a few have big ratios. The first one is PJ1, which has already been discussed during the study of the B and V masks. A bright dusk region grows the ratio, but a hole in the symmetric sector prevent it to stand out. PJ5 and PJ9 have also been discussed in the previous sections. They both show a low power emitted in the dawn region, and PJ9 also have a bright dusk region. Finally, PJ29 has a really dim dawn region, emitting only 5.6 GW in the HST sector.

On the other hand, 5 perijoves have a dusk-over-dawn ratio below 1 in both of the sectors. There is PJ3 and PJ32 where dawn storms have been identified. PJ10, PJ15 and PJ26 all show a global brightening of the main emission, as already explained in Section 4.1.

For these masks, the mean ratio are 5.2 and 4 in the HST and symmetric sectors respectively. One can see in Figure 4.14 that the mean power emitted in the dusk and dawn regions are 106.8 GW and 47.5 GW in the HST sector, and it reaches 200 GW and 105.8 GW in the symmetric sector.

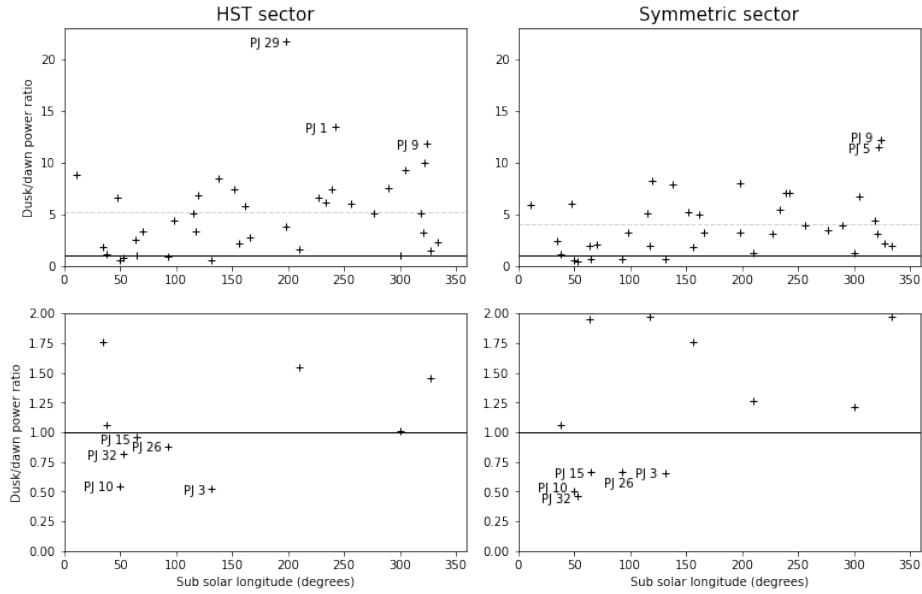


Figure 4.13: Same as Figure 4.10 but in the southern hemisphere.

4.4 G2 mask

The G2 masks are based on the G1 masks with variable width. They have been created as an alternative to the G1 masks when the coverage by these masks were not perfect. Thus, not all perijoves have a G2 mask. In fact, 3 main reasons justify the use of a broaden mask:

- ◇ The main emission seems to fork into multiple arcs. This configuration is often correlated to a diffuse main emission. An illustration of this case is shown in the panel a) of Figure 4.15.
- ◇ The main emission is broader than the G1 mask at some locations, and a broader mask is needed to accurately cover the emission. This can be due to broad patches or parallel arcs. An illustration of this case is shown in the panel b) of Figure 4.15.
- ◇ The main emission is not closed on itself, in which case the G1 mask made a transition between the 2 parts of the arc but did not cover it all. An illustration of this case is shown in the panel c) of Figure 4.15.

The G2 mask is a generalisation of the G1 mask, where the width is variable. Following this idea, the G1 masks can be seen as a particular case of the G2 masks and therefore, in the following discussion, they are used for the perijoves where a G2 mask was not needed.

4.4.1 Northern hemisphere

This time, 24 perijoves have been used in the HST sector for this hemisphere, and 25 in the symmetric sector. The perijoves excluded are the usual ones (i.e. those with missing data), and PJ10 in the HST sector. For this last perijove in the symmetric sector, the variable width of the G2 mask makes it possible to cover the whole area where the location of the main emission is not clear. Thus, PJ10 has been used in this sector, but it may cover too much of the Jovian aurorae, covering a part of the outer or polar emissions as well. There was still too much uncertainty on the location of the main emission in the HST sector and it has been decided to not use this perijove in this sector.

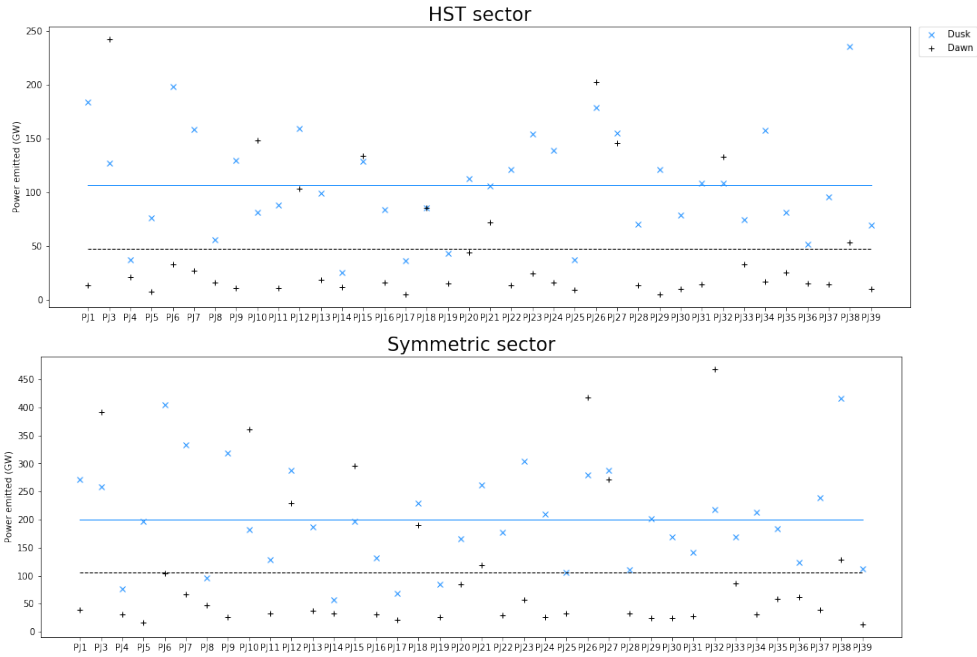


Figure 4.14: Same as Figure 4.11 but in the southern hemisphere.

Reason of exclusion	HST sector only	Symmetric sector only	Both sectors
Unsuited mask			
Uncertain location	PJ10		
Incomplete maps			PJ17, PJ18, PJ23, PJ25, PJ27, PJ28, PJ29, PJ30, PJ31, PJ33, PJ34, PJ35, PJ37

Table 4.7: Reasons of exclusion of the different perijoves.

One can see in Figure 4.16 that 4 perijoves have a worth discussing dusk-over-dawn ratio in the HST sector. But only 3 of them have been changed by the G2 masks. First, there is PJ12 that has a broad dusk region in the HST sector in order to cover the 2 parallel arcs present in that location. This large dusk region coupled with a weak power emitted in the dawn region justifies a ratio of 10.4 for this perijove. PJ13 has been barely modified by the G2 mask in the dusk and dawn regions. The dim dawn emission still gives a high ratio of 10.8. Finally, PJ19 has a broad dusk region covered and a thin dawn one. The presence of multiple arcs in the dusk region and only a small power emitted in the dawn region gives a ratio of 11.5.

PJ15 in the HST sector and PJ10 in the symmetric sector both display dawn regions more powerful than dusk ones. PJ10 displays a powerful dawn region (see Figure 4.17) and a broad dusk region is not enough to balance it, leading to a dusk-over-dawn ratio of 0.51. The incomplete map and the lack of refresh of the dawn region makes it hard to say if a dawn storm occurred during this perijove or not. But [Bonfond et al., 2021] did not notice a dawn storm for this particular perijove, and an analyse of the southern hemisphere data favours the idea of a global brightening of the main emission, coupled with a disturbed dusk region. In the northern hemisphere, because the map is not complete in that disturbed region, the ratio is lowered. But even with a comprehensive map and a good cover of the dusk region, a ratio close to 1 could be expected. PJ15 is in the case of a main emission that does not close on itself. Thus, a broad

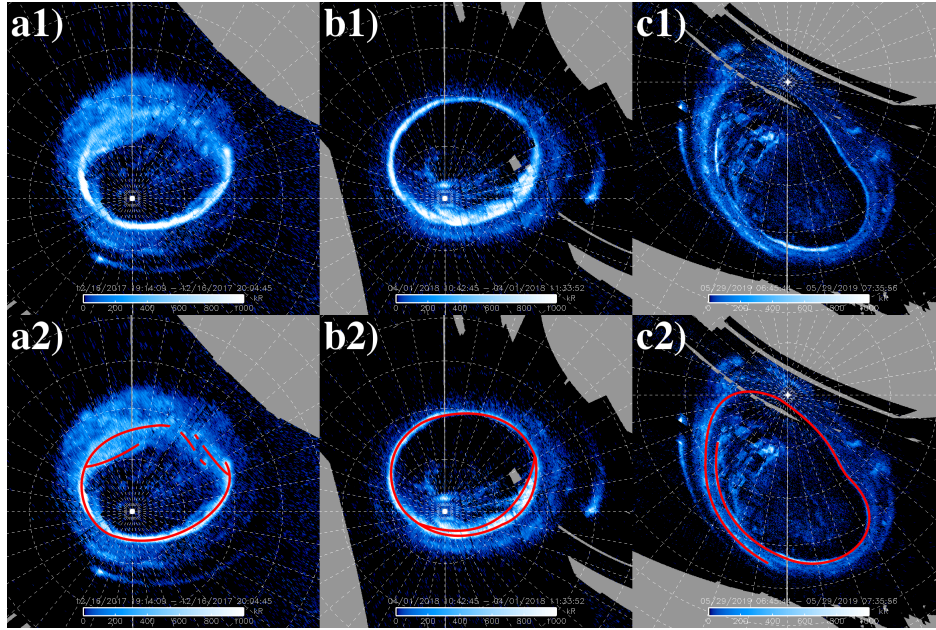


Figure 4.15: Illustration of the reason of use of the G2 mask with polar projections of different perijoves on top of the image, and the same images with the main emission labelled in the bottom. **a)** PJ10 – south. The main arc forks into multiple arcs. **b)** PJ12 – south. The main emission is broader than the G1 mask. **c)** PJ20 – north. The main arc is not closed on itself.

mask covers the 18:00 to 20:00 LT region. Still, in the HST sector, the mask is thin in the dusk region and the dawn region is powerful, lowering the ratio.

The mean dusk-over-dawn ratio is 5.4 in the HST sector and 3.6 in the symmetric one. The mean power emitted in the dusk region is 75.3 GW and 149.1 GW for the HST and symmetric sectors respectively. In the dawn region, the mean values are 30.8 GW and 82 GW. It is interesting to notice that the symmetric sector is twice the size of the HST sector, but the symmetric sector is ~ 2.5 times more powerful than the HST sector in the dawn region. This could be due to the variable width of the G2 mask. A generally thin HST sector and broad symmetric one may cause a difference in the quantity of plasma injected in the aurorae that is considered, and thus on the mean emitted power computed.

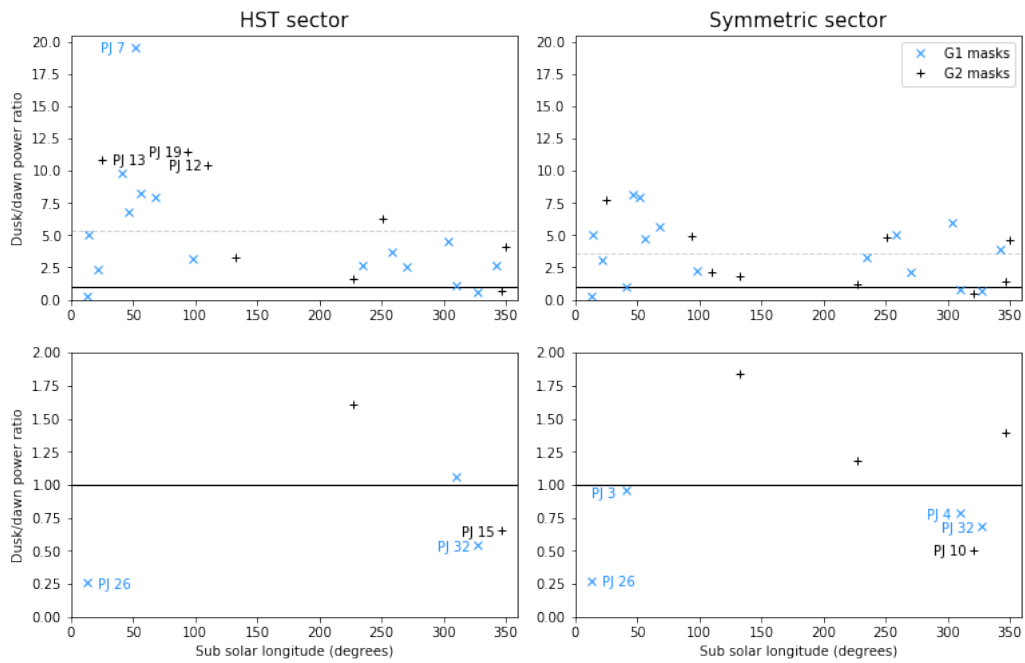


Figure 4.16: Same as Figure 4.1 but using the G2 masks.

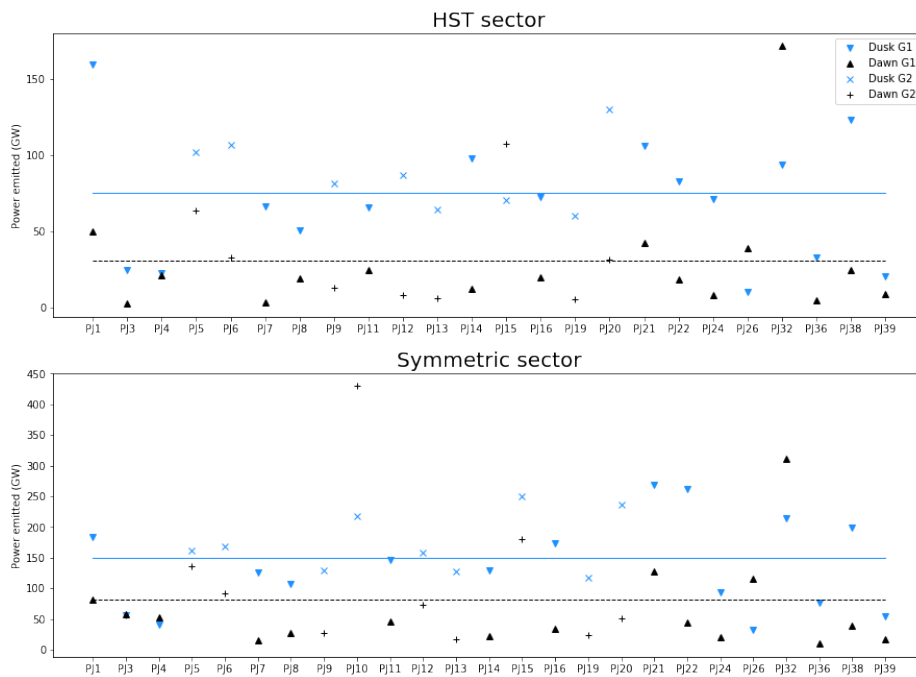


Figure 4.17: Same as Figure 4.2 but using the G2 masks.

4.4.2 Southern hemisphere

Between the 38 perijoves used, 6 stand out by their high ratio, including PJ9 that has not been modified by the G2 mask. As already explained, PJ1 has a bright dusk region but a hole is present in the symmetric sector. The broad dusk region in the HST sector grows even more the ratio. PJ5 has also been discussed in the previous sections, and a broadening of the diffuse dusk region in the HST sector makes it have a big dusk-over-dawn ratio in this sector. The dawn region of PJ25 only emits 10.4 GW in the HST sector and the broad dusk emission is fully covered by the mask. Thus, a high ratio is found for this perijove. In the symmetric sector, the dawn region is more powerful, and the ratio lowers. PJ29 has already been discussed in Section 4.3, and the broadening of the mask in the dusk region grows the ratio. Finally, PJ31 displays two bright patches in the dusk region. In the HST sector, the dawn region emits 12.2 GW and the dusk one emits 137.1 GW. In the symmetric sector, the dawn region more or less doubles to 25.6 GW, but a highly powerful patch raises the dusk emission to 348.3 GW, what raises the ratio to 13.6 in that sector.

The 3 perijoves having a dusk-over-dawn ratio lower than one are PJ3, PJ26 and PJ32. Once again, dawn storms are known in PJ3 and PJ32, explaining this low ratio. PJ26 has not been modified by the G2 mask, and has been discussed in the previous section.

The mean ratio are 6.4 and 5 in the HST and symmetric sectors. The mean power emitted are 135.1 GW and 256 GW in the dusk region, and 51.7 GW and 114.6 GW in the dawn region for the HST and symmetric sectors respectively.

4.5 Comparison between the masks

4.5.1 Comparison of the ratios

Figures 4.20, 4.21, 4.22 and 4.23 display comparisons between the different masks in the two sectors of the two hemispheres. Some pieces of information can be easily seen on these images.

First, [Bonfond et al., 2015] have found the dusk-over-dawn ratio to be ~ 3 using HST data. Here, we found a value of ~ 4.8 in the northern hemisphere and ~ 5.4 in the southern hemisphere using Juno data. The detailed values can be found in Table 4.8. The differences in the values of the 2 hemisphere can be explained by the lack of data in the northern hemisphere. Indeed, there are 9 ratios above 10 in the northern hemisphere, and 20 in the southern hemisphere. Out of those 20 big ratios, 8 are computed on perijoves that could not be computed in the northern hemisphere because data are missing. The 8 ratios that could not be computed in the northern hemisphere notably include PJ29 that takes the extreme values of 21.7 and 31.1. Of course, there are also ratios that have a dawn region more powerful in the southern hemisphere that were not usable in the northern hemisphere. 9 ratios are below unity in the northern hemisphere and 21 in the southern, but only 2 of those 21 ratios were not computed in the northern hemisphere. Furthermore, the lowest ratio is 0.26 (PJ26 in the northern hemisphere for the G1 and G2 masks), which represent a dawn region about 4 times more powerful than the dusk one, while the high ratios are all above 10, or a dusk region at least 10 times more powerful than the dawn one. Thus, even if there is the same number of high ratios than low ones (9 and 9 for the northern hemisphere, and 20 and 21 in the southern hemisphere), the high ratios have a much more important impact on the mean value.

Still, any of the values obtained with Juno is in agreement with the one found with HST. This could come from the color ratio chosen for the HST study. During that survey, they used the ACS F115LP filter. One can see in Figure 4.24 that this filter peaks in an absorbed part of the spectrum, which means that they had to count for this absorption. This is done through a color ratio. The idea of the color ratio is to attribute a number to quantify the quantity of absorption

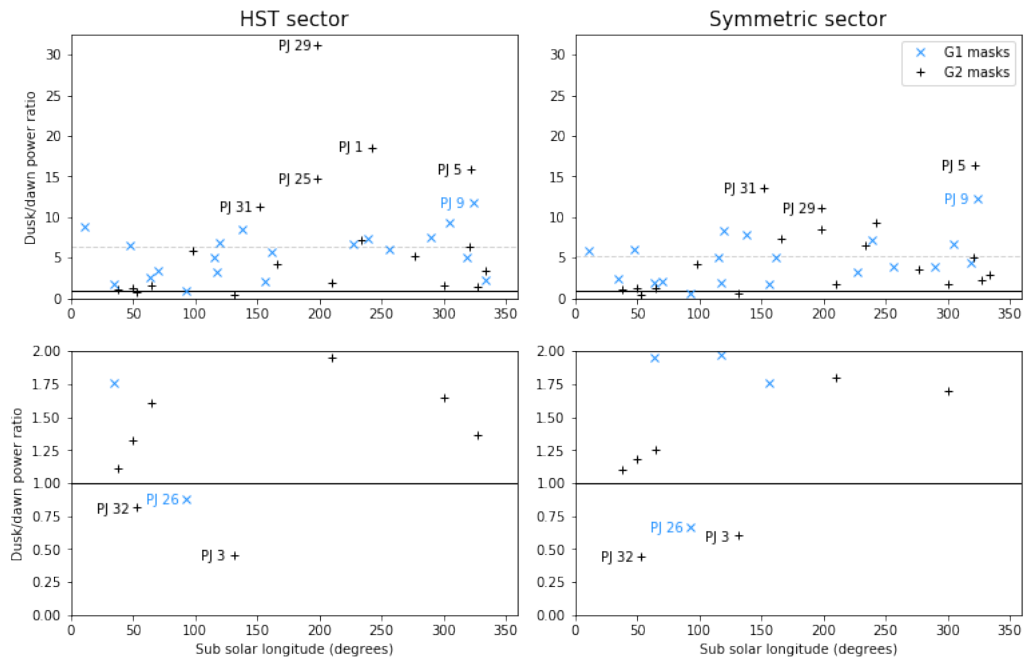


Figure 4.18: Same as Figure 4.16 but using in the southern hemisphere.

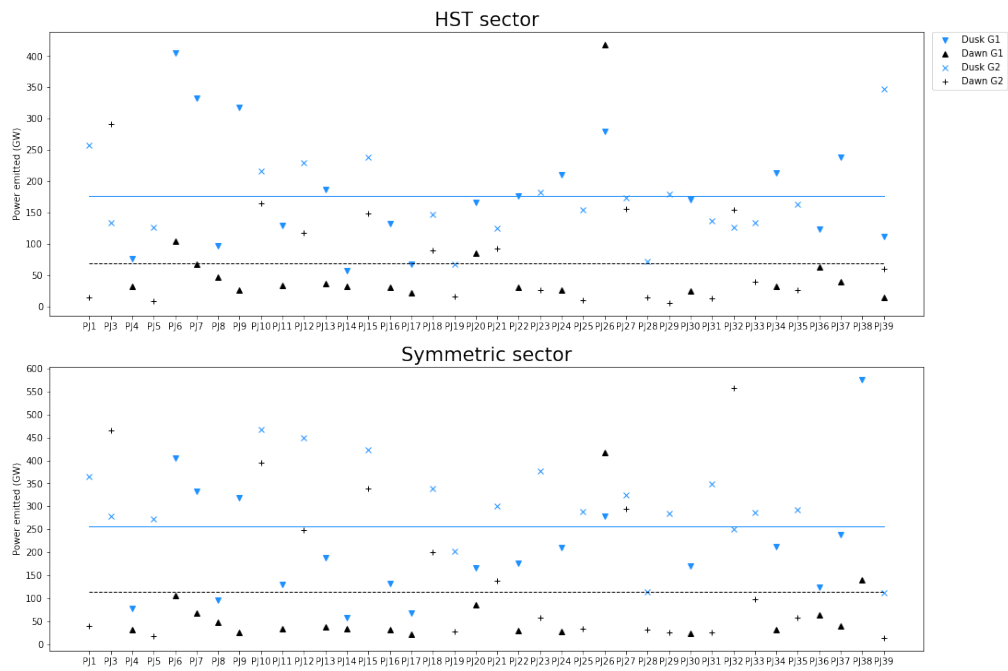


Figure 4.19: Same as Figure 4.17 but in the southern hemisphere.

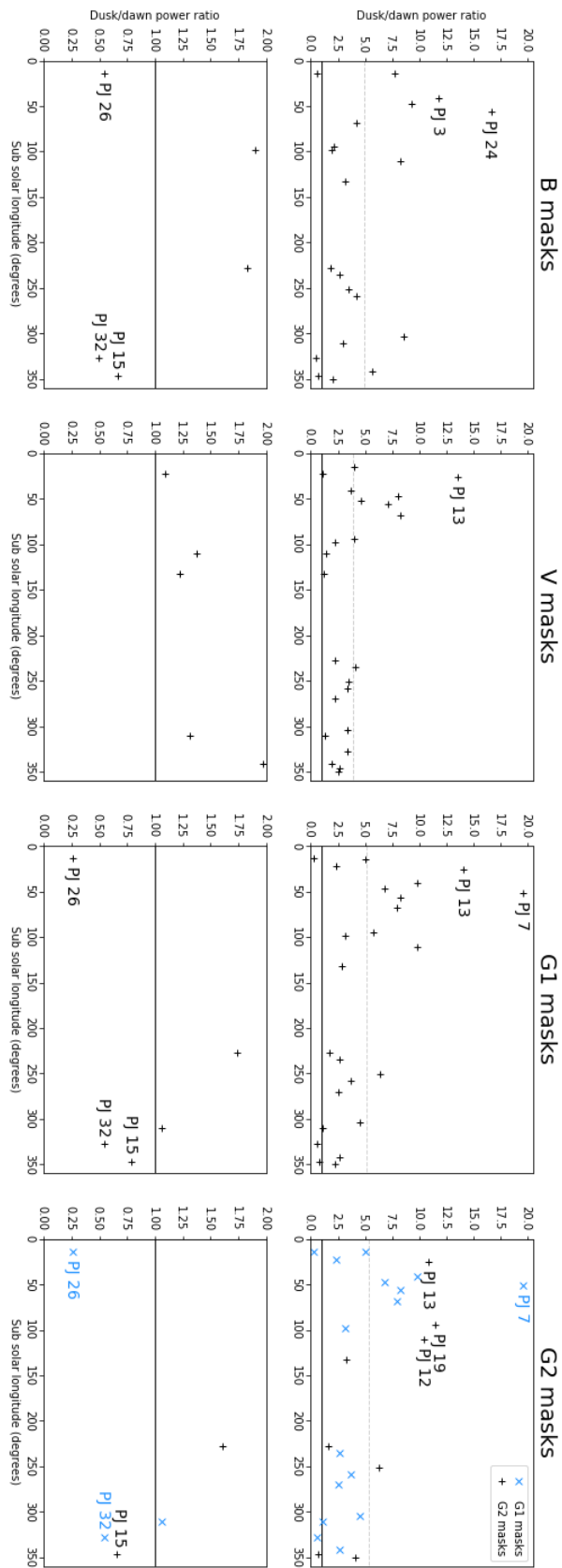


Figure 4.20: Dusk-over-dawn power ratio as a function of subsolar longitude for the different masks in the HST sector of the northern hemisphere.

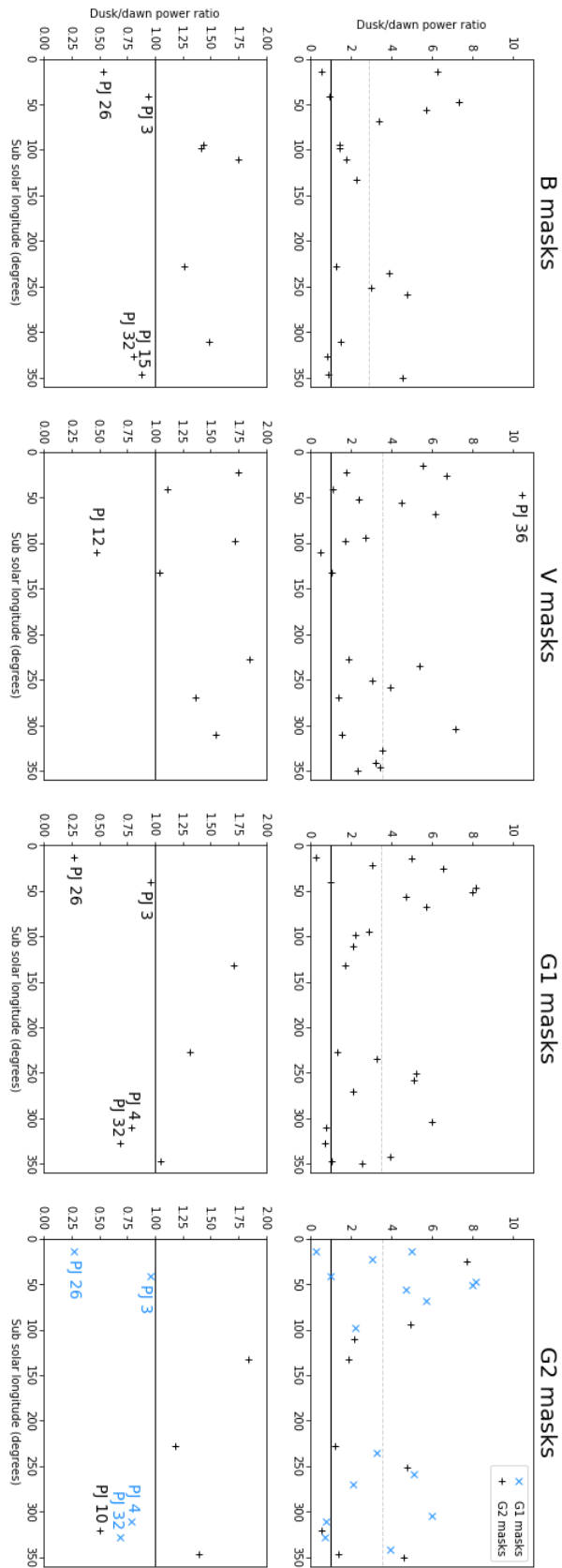


Figure 4.22: Dusk-over-dawn power ratio as a function of subsolar longitude for the different masks in the symmetric sector of the northern hemisphere.

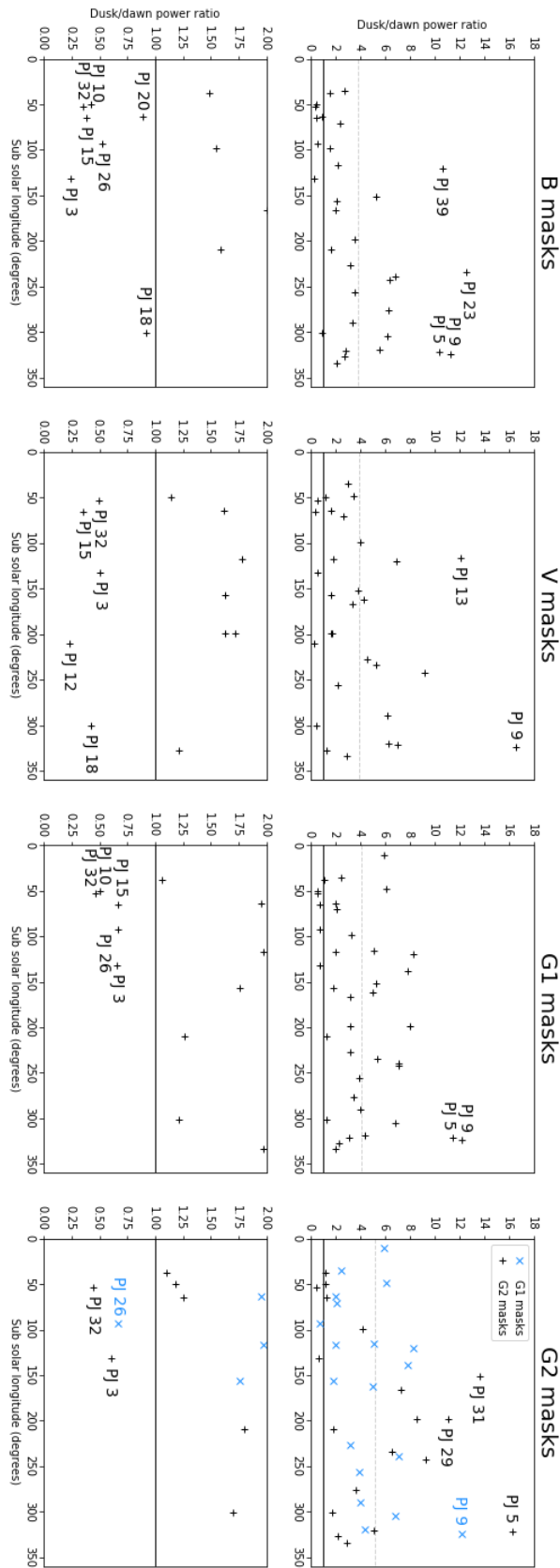


Figure 4.23: Dusk-over-dawn power ratio as a function of subsolar longitude for the different masks in the symmetric sector of the southern hemisphere.

Sector	Hemisphere	B masks	V masks	G1 masks	G2 masks	Mean
HST	North	4.904 ± 0.005	3.904 ± 0.003	5.190 ± 0.005	5.397 ± 0.005	4.849 ± 0.002
	South	5.047 ± 0.002	5.153 ± 0.002	5.183 ± 0.002	6.397 ± 0.002	5.445 ± 0.001
Symmetric	North	2.868 ± 0.002	3.529 ± 0.002	3.465 ± 0.001	3.561 ± 0.001	3.356 ± 0.001
	South	3.802 ± 0.001	3.860 ± 0.001	4.037 ± 0.001	4.963 ± 0.001	4.166 ± 0.001

Table 4.8: Mean dusk-over-dawn ratios for the 4 masks used and mean value of the 4 ratios, for the 2 sectors in both hemispheres.

of a location. Formally, it is done by taking the ratio of photons in a non-absorbed part of the spectrum and photons in an absorbed part of the spectrum coming from that location. They chose the color ratio to be constant and equal to 2.5 for the whole aurora. [Gérard et al., 2016] have shown that electrons responsible for the main emission more or less follows the Knight linear approximation. This means that FAC will be more easily sustained if the electrons have a high energy. Thus, brighter regions of the main emission correspond to locations where the electrons have a high energy and can go deep in the atmosphere of Jupiter where methane can absorb the emitted photons. This implies a high color ratio for bright regions. Because the color ratio was assumed to be 2.5 during the HST study, the power emitted in the region of higher color ratios has been underestimated. This is the dusk region that is often more powerful and brighter, and higher color ratios correspond to this regions. So, most of the dusk-over-dawn ratios have been underestimated during that study. The data collected with Juno that were used during this master thesis are not concerned by such a consideration about the color ratio because the filter used here covers a part of the spectrum where there is no absorption. So, the ratios computed here are not affected by this error, while [Bonfond et al., 2015] ratios are globally underestimated.

Then, the mean values of the ratios are globally lower in the symmetric sector than in the HST one. Several reasons may at least partly explain this difference. A first idea that could contribute to few isolated cases but could not explain the general trend at all comes from the creation of the map themselves. The refreshment (or the absence of refreshment) of the data in some locations can induce a displacement of maximum one hour of local time in the locations of the different regions. The reasons for this error will be more developed in the next section. The discontinuity in the main emission discovered by [Radioti et al., 2008a] and already discussed in Chapter 1 can be located between 8:00 and 13:00 LT. Thus, a displacement of one hour in this discontinuity may bring it in the 7:00 to 8:00 LT zone. Up to half of the dawn region of the HST sector may thus show a really low power emitted, what grows the dusk-over-dawn ratio. Another reason to explain some of the lower ratios in the symmetric sector is the presence of dawn storms. According to [Bonfond et al., 2021], an element of this process is the brightening of the post-midnight region that slowly expands to the dawn region. If the auroral map is created with data collected during this expansion phase, the bright region may be located in the symmetric sector but not in the HST sector yet. So, the symmetric sector covers a patch of bright dawn emission that is not covered by the HST sector, what lowers the dusk-over-dawn ratio of the symmetric sector. This is the case for PJ6 in the southern hemisphere for example, that is well documented because discussed in Figure 2 of the study made by [Bonfond et al., 2021]. The

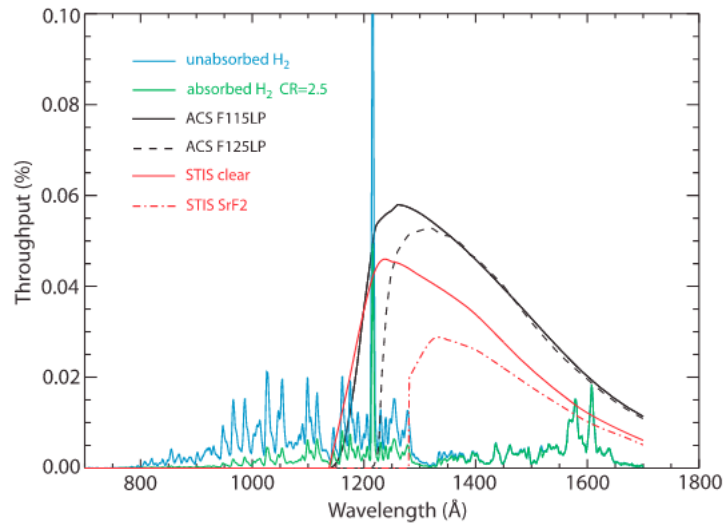


Figure 4.24: Total system throughput for different filters available on HST. Spectra of unabsorbed H_2 and absorbed H_2 with a color ratio of 2.5 are shown in blue and green respectively. From [Gustin et al., 2012].

map created during this master thesis is located just between 2 of the images present in the study, and the expansion of the arc that enters in the symmetric sector can be identified. A last and more general idea to explain the lower ratios in the symmetric sector is simply the fact that the sector is bigger and the chances to cover a relatively bright spot grows. If this bright spot is in the dusk region, the impact is generally weak because it is already a bright part of the aurorae. The dawn region often display at low emitted power, so even a not so bright spot of a few tenth of gigawatt can have a huge impact on the dusk-over-dawn ratio.

A third easily visible point is the absence of dependence of the dusk-over-dawn ratio to the subsolar longitude. There is no obvious reason for such a dependence but there is also no obvious reason for no dependence. Despite the various techniques used to create the masks, none of the plots of the ratio as a function of the subsolar longitude show this dependence. One can thus assert that the ratio is independent of the subsolar longitude.

Finally, there are some high or low ratios that appear multiple times when using different masks on the same perijove. In the high ratios, we have PJ1, PJ5, PJ9, PJ13, PJ29 and PJ36. They appear 4, 4, 7, 5, 3 and 3 times respectively. These are the only perijoves showing a high ratio in more than 2 cases, thus appearing with at least 2 different masks. All these perijoves have been discussed in the previous sections, and the ratio essentially comes from powerful dusk regions or dim emission in the dawn region. The more interesting ratios are the ones below unity. In those cases, different phenomenon can take place. The perijoves concerned by a low ratio are PJ3, PJ10, PJ12, PJ15, PJ18, PJ26 and PJ32. This is the case 11, 5, 3, 10, 4, 12 and 12 times respectively. PJ3 and PJ32 have already been discussed a lot, and a dawn storm is clearly responsible for the low ratios for these perijoves. PJ26 has also been discussed, with a surprisingly vanishing main emission in the dusk region. Then, there are PJ10, PJ12, PJ15 and PJ18 that all seem to result from the same phenomenon. A global brightening of the main emission, as well as a contracted main emission are visible for these perijoves. As explained in Section 1.4, these 2 characteristics are found when the solar wind compresses Jupiter's magnetosphere or when the volcanism from Io increases. In addition, some polar dawn spots can also increase the power emitted in the dawn region when covered by the mask. This can be seen for PJ15 in Figure 4.25.

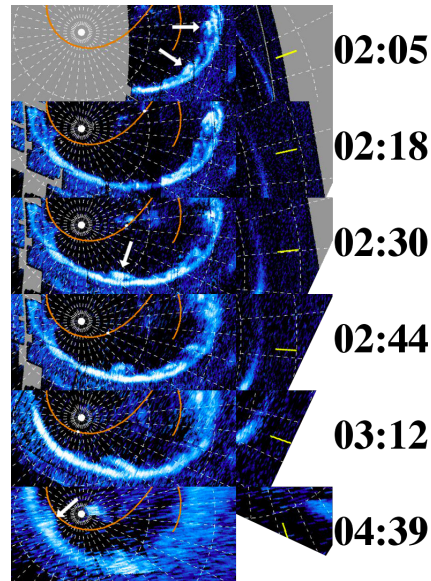


Figure 4.25: Evolution of polar dawn spots during PJ15. The spots are highlighted by white arrows, and their dynamics can be followed over time.

4.5.2 Specific considerations about the emitted power

An interesting point as been when in Section 4.1 when looking at Figure 4.4 showing the power emitted in the southern hemisphere. In this plot, a clear low value of the dawn region can be seen, whereas the emission in the dusk region seems more variable. Figures 4.26 and 4.27 are based on the same idea, but with all the masks displayed at once. This time again, a low value seems to emerge in the dawn region, this is obvious in the southern hemisphere but it is also visible in the northern hemisphere. This can be seen by computing the median and standard variation of the set of data in complement to the mean emitted power. This is what has been done in Tables 4.9 and 4.10 for the northern and southern hemispheres. One can see in these tables that the dusk region always have a median emitted power close to the mean value. The standard deviation is also about half of the mean value, or at least considerably smaller. So, no matter the mask used, the power emitted by the dusk region is always spread more or less equitably around a mean value. In the dawn region, thinks are different. The median power emitted is about one third to two thirds of the mean value, with a standard deviation being about the value of the mean power emitted. This indicates a way less balanced power emitted as a function of the perijove studied. Two populations exists here and are visible in the plots. The first one is not much powerful, and is the more common. The second one is much more powerful but rarer. This is what has been discussed all along this chapter. The dawn region seems to be less powerful than the dusk one, with some transient events such has dawn storms that can boost the power emitted by the dawn region during a limited time.

4.5.3 G1 versus G2

The G2 masks permit to cover bigger areas than the G1 masks. It can be interesting to see what impact that broadening has on the dusk-over-dawn ratios. Figures 4.28 and 4.29 shows a comparison of the ratios computed with both masks for the perijoves for which a G2 mask has been created. In the northern hemisphere, the ratios of PJ5, PJ6, PJ9, PJ10, PJ12 and PJ15 are barely modified, and the G2 mask has been created to cover broad areas of the main emission that are not in the dusk or dawn regions. These perijoves are not that interesting for

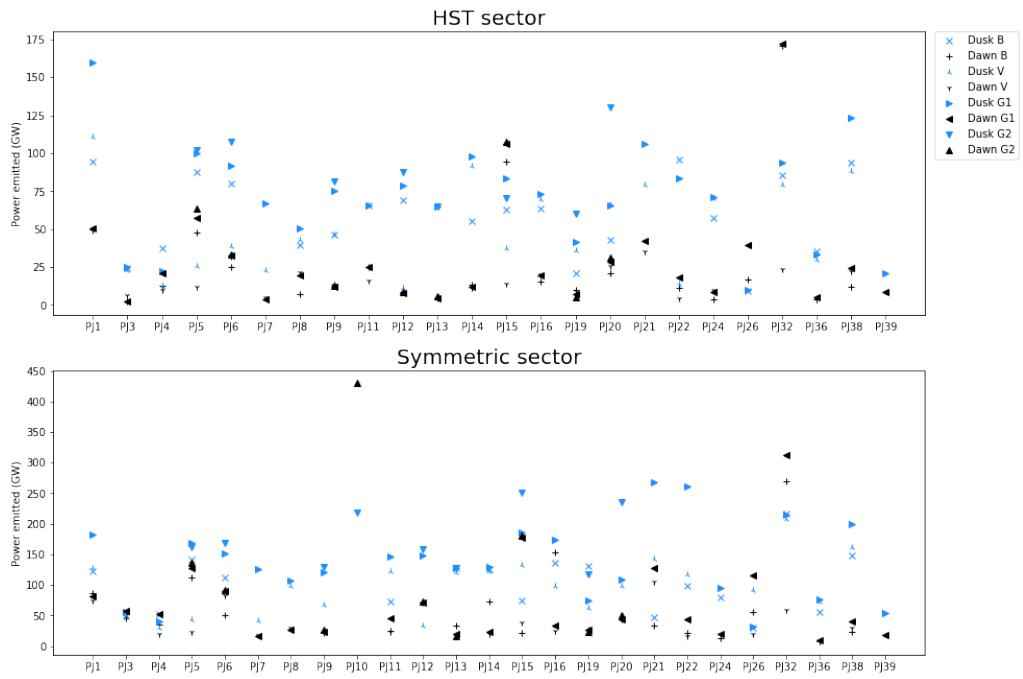


Figure 4.26: Dusk and dawn power emitted as computed with the 4 different masks for each perijove in the northern hemisphere.

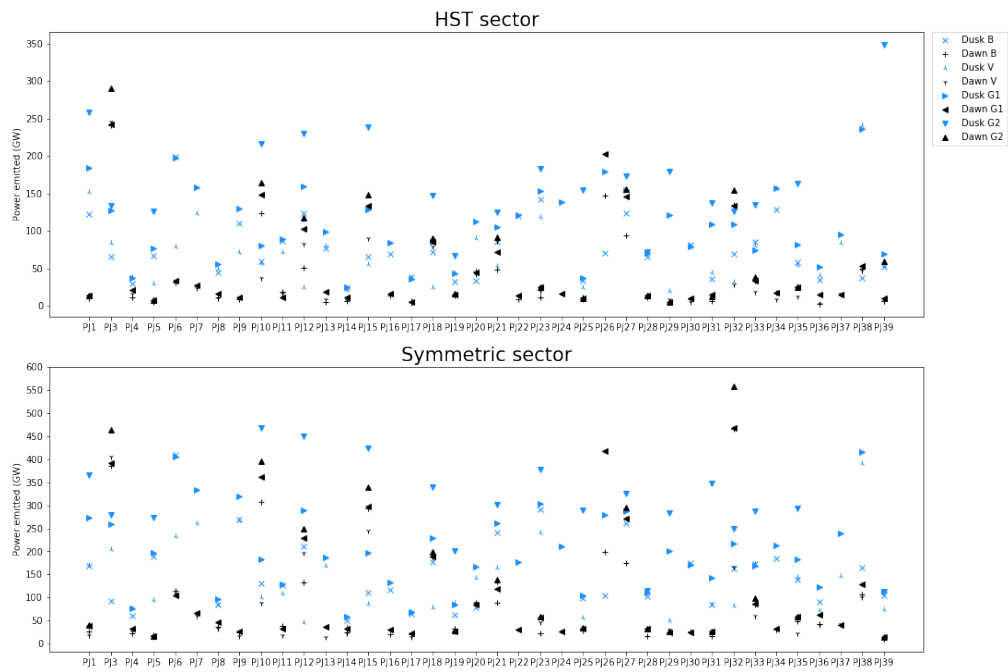


Figure 4.27: Same as Figure 4.26 but in the southern hemisphere.

Mask	Sector	Region	Mean	Standard deviation	Median
B	HST	Dusk	58.3	25.4	60
		Dawn	28.1	38.9	13.2
	Symmetric	Dusk	101.1	46.1	105.1
		Dawn	60.7	62.3	34
V	HST	Dusk	49.4	28.6	42.6
		Dawn	15.9	11.1	11.7
	Symmetric	Dusk	94.4	44.6	97.7
		Dawn	36.4	24.8	23.9
G1	HST	Dusk	71	34.3	72
		Dawn	30.3	37.1	19.7
	Symmetric	Dusk	135.4	62.9	128.7
		Dawn	66.6	66.4	43.5
G2	HST	Dusk	75.3	36.4	72
		Dawn	30.8	37.4	19.7
	Symmetric	Dusk	149.1	67.7	147.1
		Dawn	82	96.7	45.2

Table 4.9: Mean power emitted, standard deviation and median power emitted for both the HST and symmetric sectors in the dusk and dawn regions for the four different masks in the northern hemisphere, all expressed in GW.

Mask	Sector	Region	Mean	Standard deviation	Median
B	HST	Dusk	74.9	38.9	68.1
		Dawn	42.5	54.2	14.2
	Symmetric	Dusk	149.2	78.3	129.3
		Dawn	98	115.3	37.1
V	HST	Dusk	69.5	46.7	55
		Dawn	32	46	15.5
	Symmetric	Dusk	133.3	80.8	97.6
		Dawn	76.5	87	37
G1	HST	Dusk	106.8	48.8	102.3
		Dawn	47.48	58.4	16.9
	Symmetric	Dusk	200.1	87.8	192.2
		Dawn	105.8	125.1	39
G2	HST	Dusk	135.1	66.8	131.5
		Dawn	51.7	66.1	17
	Symmetric	Dusk	256.2	120.8	275.9
		Dawn	114.6	141.8	39.5

Table 4.10: Same as Table 4.9 but in the southern hemisphere.

this comparison. The ratios of PJ13, PJ19 and PJ20 have a more distinguishable variation. First, the dusk region in PJ13 is not impacted by the variation of width of the mask. The dawn region however is much more modified. The G2 mask is broader than the G1 mask at 4:00 LT, then shrinks and becomes thinner at 6:00 LT, before becoming broader again at 8:00 LT. The variation in the width makes the power decrease in the HST sector, and increase in the symmetric one. This variation of width is not due to the emission in the dawn region itself, but to the main emission that is not closed on itself in the pre-noon region. Thus, the variation of ratio has no real interest here. In the auroral map of PJ19, the main emission is hard to found in the dusk region. It seems to be made of various parallel arcs, and the G2 mask is thus broader than the G1 one in the dusk region. The mask in the dawn region also shrinks to ensure a better cover of other parts of the main emission out of this region. The combination of these two variations grows the ratio computed with the G2 mask in both sectors. Finally, the mask is not modified in the dawn region of PJ20, but is way broader in the dusk region. Indeed, in the dusk region, the main emission is not closed on itself and the mask has to be broad to cover the two parts of the arc.

In the southern hemisphere, PJ21, PJ27 and PJ28 have small variations in the width of the masks in the dusk and dawn regions, and the ratios do not vary a lot. These perijoves are not interesting here. PJ1 has a broadening of the noonward edge of the dusk region to cover the main emission that has an unusual shape in the post-noon region. This grows the ratio in both sectors. The G2 mask computed for PJ3 is interesting because it broadens both the dusk and dawn regions. It results in ratios that are not much modified. PJ5 and PJ33 have a diffuse main emission in the post-noon region, and the mask is thus broader in the dusk region to cover it well. The width is not modified in the dawn region, what grows the ratios. PJ10 displays the same kind of diffuse main emission, but extended to the dusk region and, in a more moderated way, to the dawn region. The mask is thus broader in both regions, but more significantly in the dusk one, what grows the ratio in both sector. In PJ12, the mask is slightly broader in the dusk region and there is a small increase in the ratios. A broadening of the mask was needed for PJ15 in the dusk region to cover the diffuse main emission. To ensure a smooth mask, the dawn region of the mask is also broaden and thus covers some polar dawn spots that should not be covered. Thus, the ratios does not change much. The main emission is once again more complex than a simple arc in the dusk region of PJ18. A broadening of the mask was needed in that region, but the more powerful part of the emission was already covered by the G1 mask and this broadening has a minor impact on the ratios. In PJ19 and PJ31, the main emission is also diffuse in the dusk region, and the broadening of the mask increases the ratios, especially the one in the symmetric sector. In the dusk region of PJ23, the main emission seems to fork in 2 places. It is hard to know if it really is the main emission that has an unusual shape, or if the additional arcs come from independent processes. Anyway, the whole structure has been covered by the G2 mask and their is a small increase in the ratios. The main emission is again diffuse in the dusk region of PJ25, and the covering of the whole emission grows the ratios. PJ29 is comparable to PJ23, but with only one additional arc, located in the post-noon region. The mask is still broader in the dusk region to cover it well. Thus, the ratio grows in both sectors, but especially in the symmetric one. PJ32 is interesting because of the dawn storm already discussed. Here, a broader mask is needed in the dawn region to cover the dawn storm that broadens the main emission. But this dawn storm happened during a global brightening of the main emission, coupled with a disturbed shape in the noon to dusk region. A broader mask is also needed in this region, and so the ratios do not change even if the dusk and dawn regions are both better covered. During PJ35, the dusk region of the main emission has an unusual shape in the HST sector. The arc of the main emission seems to fork into 2 similar parallel arcs composed of a bright spot before coming back together. Contrary to the G1 mask that can cover

only 1 arc, the G2 covers both and the ratios increase. Finally, the main emission is once again more diffused and less well defined in the dusk region of PJ38. The G2 mask is thus broader in this region, and there is an increase in the ratios.

What comes out of this detailed analysis of the 2 masks is that all relevant modification of the ratio consists in an increase of this one. The dusk region, and more generally the noon-to-dusk region, seems to be broader than the dawn one, what suggests that more phenomena take place in the part of Jupiter's magnetosphere connected to this region. A decrease of the ratio could take place during a dawn storm but unfortunately, the only dawn storm that could be studied was embedded in other phenomena, and its consequences could not be analysed separately.

4.6 Sources of uncertainties

Several sources of uncertainties are listed and discussed in this section. The first one being the systematic error. It has been discussed by [G erard et al., 2019]. According to their study, the effective area of UVS has a 16% uncertainty. Another systematic error comes from the conversion of brightness into the total unabsorbed H₂ emission in the bands of interest of UVS (i.e. Lyman and Werner bands). They found a value of 10 kR of Lyman and Werner bands emission for a 1 mW/m² electron precipitation with a 12% uncertainty. The random error is also discussed in this paper. The shot noise, which is associated to the number of photons hitting the detector, has been computed. They found that one count per pixel on the detector is produced by 10 kR of H₂ emission. Using a value of 25 pixels to cover the whole region over which the brightness is averaged, one finds 25 counts produced by 10 kR of emission. When counting events like so, an uncertainty equal to the square root of the count exists. Thus, for a 10 kR brightness, one has 25±5 counts, and for a 1000 kR brightness, this value grows to 2500±50 counts. This idea has been integrated in the IDL routine *error_V2.pro*, that can be found in Appendix I and has been discussed in Section 3.8, that computes the uncertainty on the dusk-over-dawn power ratio based on the brightness maps displayed in Appendix II. As an example, the results for the B mask in the HST sector are the following. For PJ1, 8,792,470±2965 (i.e. an error of 0.3‰) counts in the dusk region, and 406,141±637 (i.e. an error of 1.6‰) counts in the dawn region are found. This translates into 122.75±0.04 GW and 10.78±0.02 GW of emitted power in the dusk and dawn regions respectively. This gives a ratio of 11.39±0.02. Similar values are obtained for the other perijoves, and the mean ratio can thus be computed. A value of 5.0474±0.0018 is found. The uncertainties for all the different masks are the one written in Table 4.8. What can be seen in this table are errors up to 0.005 on ratio on the order of ~5. This only represents a maximum error of ~1‰. This error is thus negligible.

The creation of the masks also introduced an error. As explained in Section 3.6, the masks covering the dawn and dusk regions contain a few elements that should not be taken into account. In PJ1, the mask created on the dawn region based on the B mask for the HST sector contains 4181 elements, out of which 5 should not be taken. This only represents an error of ~1.2‰, what is negligible. This error is of the same order for all the masks created.

Another source of uncertainties comes from the way the auroral maps were created. Indeed, The data collected with Juno are made while it does successive spins on itself, each of one lasting for 30 seconds. Most of the maps are composed of data collected during 100 spins to have enough data to create comprehensive maps. The few exceptions are in the northern hemisphere when Juno did not collect data during at least 100 spins before going to the southern hemisphere (e.g. PJ29 – north). This means that most of the maps are build with data collected during 50 minutes. This may not seem much, but accounting for the fact that Jupiter rotates on itself in a bit less than 10 hours, the data are collected during a twelfth of the rotation time of the planet. There is thus a rotation of 30° between the first data collected and the last ones. To compute

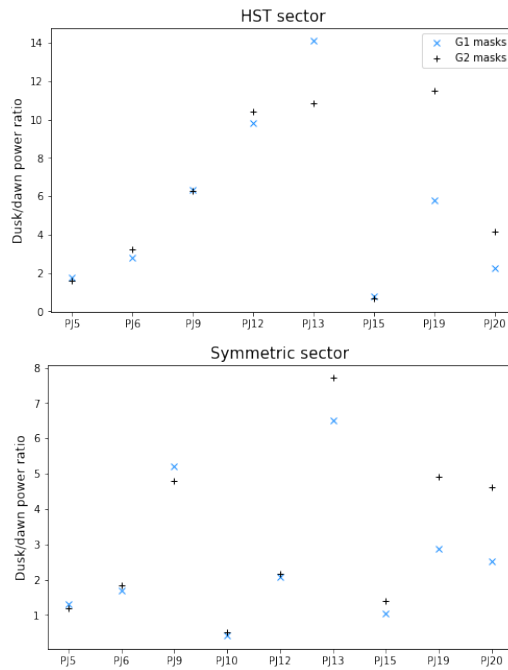


Figure 4.28: Dusk-over-dawn ratio computed with the G1 and G2 masks for the perijoves that required the creation of a G2 mask in the northern hemisphere.

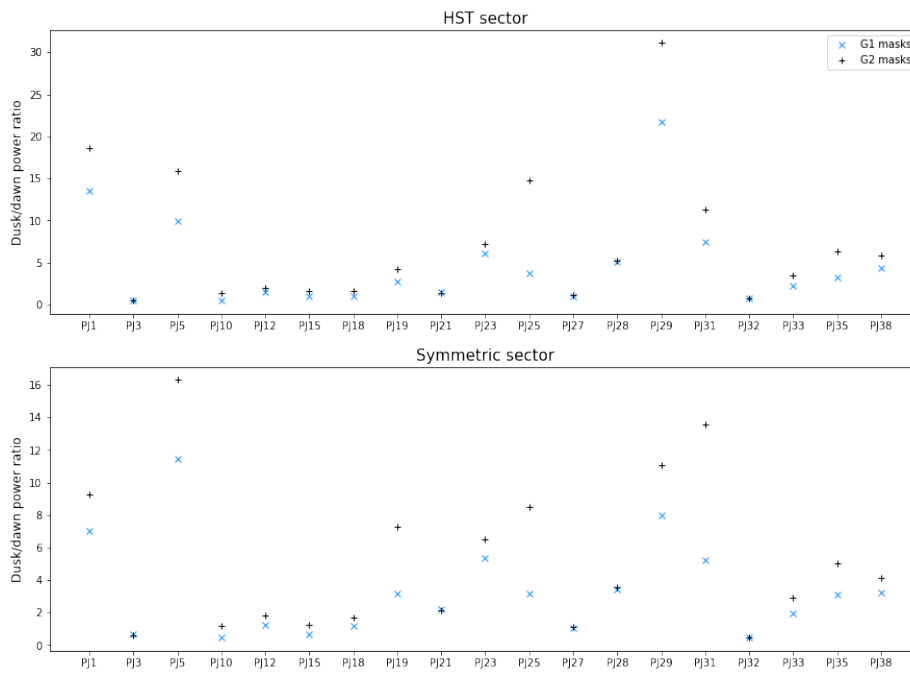


Figure 4.29: Same as Figure 4.28 but in the southern hemisphere.

the location of the dusk and dawn regions, a unique subsolar longitude had to be used. The mean longitude of the 50 minutes has naturally been chosen. This means that the instantaneous location of the dusk and dawn regions of a set of data constituting a part of the map may not correspond to the dusk and dawn regions computed. The error on this location is restricted by collection time of the data, i.e. 25 minutes before and after the time of mean subsolar longitude. In other words, a lag of maximum 15° (i.e. 1 hour of local time) in the locations of the dusk and dawn regions may exist. On average, this error cancels out and certainly have minor impacts on the conclusions of this work but it can have important effects on specific perijoves (e.g. the displacement of the discontinuity region in the HST sector explained in the previous section).

Then, a first selection bias arises again from the creation of the map. The 200 spins needed to create the final maps of the 2 hemispheres are arbitrarily chosen through a set of data composed of about 700 to 1,200 spins for each perijove. Thus, a typical time of about 2×4 hours of data is available for each perijove and only 50 minutes are used to create each map. During the 4 hours interval in each hemisphere, the dynamics of the aurorae can change the emitted power quite a lot. Dawn storms may appear or disappear, having an impact on the dusk-over-dawn ratio computed. This is easily illustrated in Figure 4.5 of Section 4.1, showing the dawn storm that occurred during PJ32. In this image, the emitted power varies a lot in a 2 hours interval. During the creation of the maps, the selection of data has been made without any conscious consideration for this bias. The data have been chosen based on 2 criteria, without any consideration on the dynamics of the aurorae. The first one is the wish of having a comprehensive map, with as few holes as possible. The second one is the quality of data constituting the maps. Juno's distance to Jupiter and viewing angle varying along its orbit, UVS resolution varies as well. An illustration based on maps created on different data acquired during the same perijove is shown in Figure 4.30. Those 2 criteria restraint a lot the time interval of usable data, what also lowers the chances of an important variation of the emitted power in a location between various possible maps, even if it does not totally prevent it to happen. Anyway, the variation of the power emitted on different maps, and thus of possible dusk-over-dawn ratios, for a perijove is not conscientiously chosen, and the impact of this effect is minor on the general trend of the ratios.

Finally, a second selection bias comes from the exclusion of the different perijoves when studying the various masks. Exclusions of maps happened for several reasons:

- ◇ A bad cover of the dusk and dawn regions by the mask. In this case, 3 different situations happened. First, the mask clearly covered a region where there is no emission in the polar zone, increasing the dusk-over-dawn ratio to high values. In this case, the exclusion is justified by the simple fact that a zone of absence of emission does not match any definition of the main emission. Then, there are maps where the dusk or dawn region is not complete because of holes. In this case, the choice of excluding the map is harder to justify. It has been made on visual considerations, depending on the size of the holes and the brightness of the locations around the holes to evaluate the impact they may have on the ratio. If this impact was considered not significant, the data were kept in the study. Otherwise, the map was excluded. The exclusions of perijoves based on this discussion is arbitrary, and may not be suitable for everyone. Finally, when the mask does not cover the idea we have of the main emission (i.e. the well defined oval or bean shape of high emission) but goes in the equatorward region, the masks were kept. This may seem strange, but it is based on the idea that the G masks are created to suit the visual idea we have of the main emission. If all the masks that does not cover it well were excluded, there would be no point in creating the B and V masks. In fact, the idea of creating different masks based on different methods makes the results more robust. The masks were all made to test different ideas of what the main emission is (i.e. the search for high emitted power

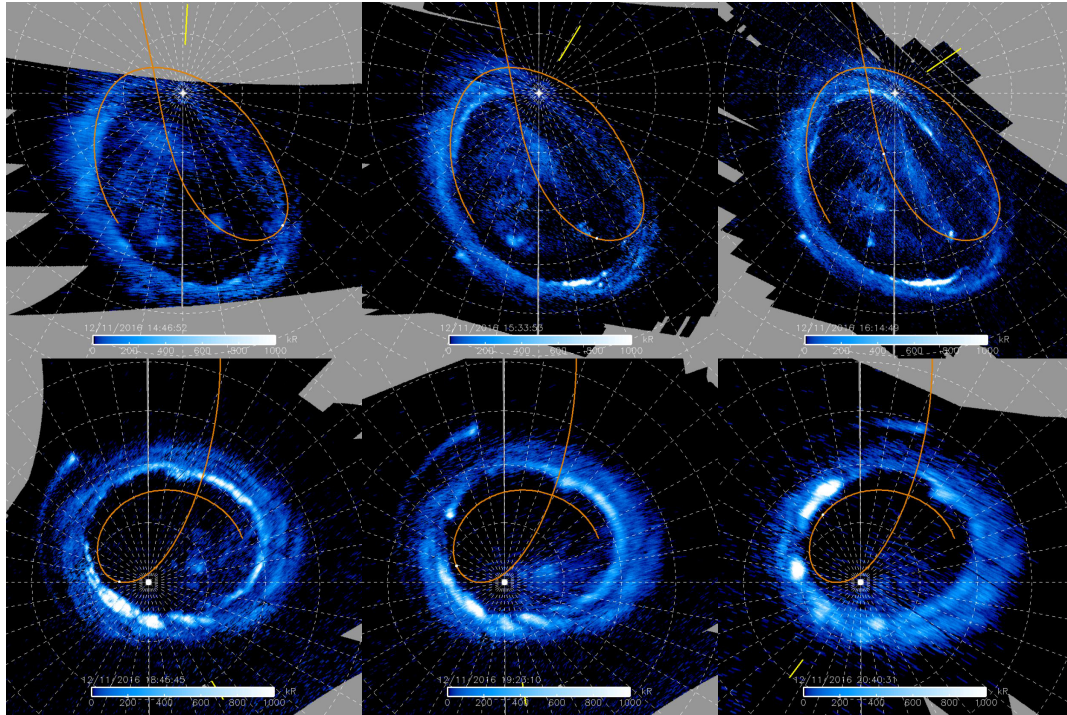


Figure 4.30: 6 auroral maps created with different data acquired during the same perijove. The time of collection of the last data used for each map is written in the middle bottom of the map, varying from 14:47 to 16:15 UT in the northern hemisphere, and from 18:46 to 20:41 UT in the southern hemisphere. Juno’s orbit is shown with an orange curve, as well as its position along this trajectory with a white dot. The resolution increases in the northern hemisphere as Juno comes closer to the planet, and then decreases as it goes away from it in the southern hemisphere.

based on HST data through the B masks, the idea of a corotation breakdown through the V masks, and a restricted and a broad visual interpretations based on Juno data through the G1 and G2 masks). It would not be interesting to rule out some masks based on ideas that were tested by the other masks.

- ◊ In the northern hemisphere, PJ10 has been excluded in most of the cases because of the uncertain location of the main emission. In this case, the data constituting the map were not easy to interpret. There are holes in the data, and the dusk part of the aurorae is hard to analyse. To have the more chances to include the main emission in the mask, the choice of using only the G2 mask, that could encompass broader areas, has been made. Even this mask has only been kept in the symmetric sector to minimise the impact of the holes. The B, V and G1 masks have not been excluded based on the definition of the main emission they are related to, but on the question if it even makes sense to look for the main emission on this set of data knowing the curious shape it seems to have and the presence of holes. Once again, this choice is arbitrary but I had to choose between using data that could more probably give false results than in the majority of the perijoves, or not using them. Anyway, this only concerns one perijove and should not modify the conclusions.
- ◊ Some holes were big enough to cover several hours in local times. In this case, their were no data at all to use in the study, and the exclusion of those maps came naturally.

Chapter 5

Conclusion

Using UVS, the UV spectro-imager onboard Juno, the main emission of Jupiter's aurorae has been studied thanks to data collected during the 39 first perijoves. No data has been collected during PJ2, and it was not always possible to use the data collected during the other perijoves, especially in the northern hemisphere. Due to the lack of good definition of the main emission, it has been decided to identify it in 4 different ways. All of them gave similar results and led to the same conclusions.

Because of the variable shape of the aurorae over time, the IDL routines created during this thesis have been made to isolate the main emission case-by-case. The power emitted has been computed in the dawn and dusk regions of this part of the Jovian aurorae. The dusk-over-dawn ratios computed out of it inform us of a dusk region ~ 4.8 and ~ 5.4 times more powerful than the dawn one in the small (HST) sector (6:00 to 8:00 LT and 16:00 to 18:00 LT) for the northern and southern hemispheres respectively. These ratios go down to ~ 3.4 and ~ 4.2 in the big (symmetric) sector (4:00 to 8:00 LT and 16:00 to 20:00 LT). The uncertainty on these results has also been computed and turn out to be negligible. The more important uncertainties come from selection biases and integration time considerations, that are supposed to cancel out when performing a statistical study as it has been done here.

These results are in adequation with a similar study done by [\[Bonfond et al., 2015\]](#) using HST data, but not with theoretical expectations from the CET. The results obtained here thus go in the sense of the need for a more complete understanding of the mechanisms at the basis of the auroral main emission, and an incorporation of these mechanisms in MHD simulations.

Others relevant discoveries have been done during this work. The absence of dependency of the ratio on the subsolar longitude indicates that the orientation of Jupiter relative to the Sun has no influence on the power repartition in the main emission. The differences in the variability of the emitted power from the dawn and dusk regions over the perijoves suggests different mechanisms to take place on both sides. In another vein, a dawn storm has been found during PJ32, what could be interesting for future studies of this phenomenon.

Finally, even if this study already gave good results, it would be interesting to complete it with the remaining perijoves at the end of the Juno mission to have more data, thus more statistically robust results. The brightness maps and main emission masks created during this thesis can also be used to perform similar studies in other regions. A noon-midnight study would be particularly interesting. Indeed, HST cannot see the midnight region and such a comparison has never been done. An even more complete study could consist in dividing the whole main emission in several adjacent regions to search for the variation of emitted power with local time. This may be used to test the hypothesis that the dawn-dusk asymmetry studied here is due to the partial ring current system.

Appendix I: IDL routines

In this appendix, one can find the different routines created during this master thesis. The routines are destined to be an extra support to the understanding of Chapter 3. Most of the procedures used in the lines of code are implanted in the IDL language and are explained in details at <https://www.l3harrisgeospatial.com/docs/routines-1.html> if needed. Still, a few have been created by independent people such as the LPAP or myself. These procedures are listed hereunder.

List of procedures

- ◇ **bpglobe:** Displays a polar projection of the specified array.
- ◇ **dgtv:** Displays a cylindrical projection of the specified array.
- ◇ **latlon2angle_AG:** Takes the longitude and latitude of a given location in entry and returns its angle and distance to the barycentre of the main emission.
- ◇ **mapping_function2019:** Applies the [Vogt et al., 2011] magnetosphere model to link locations in the magnetosphere and in the ionosphere. Several parameters can be set. Here, it has always been done in a way that the function takes the location in the magnetosphere in entry, and returns the location in the ionosphere, using the JRM09 magnetic field model.
- ◇ **projpol:** Takes an array in cylindrical coordinates in entry and returns an array that is a polar projection of the initial array.

latlon2angle_AG.pro

```
1 function latlon2angle_AG, lat, lon, dista=dista
2   ; lat = latitude of the location to be converted.
3   ; lon = longitude of the location to be converted.
4   ; dista = distance to be computed.
5
6   if lat gt 0 then begin ;North
7     lat_bary=73.9340
8     lon_bary=185.670
9
10
11     yb=750.*cos((lat_bary)*!dtor)*(cos((lon_bary)*!dtor))+750.
12     xb=750.*cos((lat_bary)*!dtor)*(sin((lon_bary)*!dtor))+750.
13
14     yp=750.*cos((lat)*!dtor)*(cos((lon)*!dtor))+750.
15     xp=750.*cos((lat)*!dtor)*(sin((lon)*!dtor))+750.
16
17     angle_i=(atan((yp-yb)/(xp-xb))/!dtor+(180.*(xp lt xb)))
18     if (xp eq xb) then angle_i=90.*((yp gt yb)*2.-1.)
19
20     dista=norm([xp-xb,yp-yb])
21
22
23   endif else begin ;South
24     lat_bary=-81.9309
25     lon_bary=31.9209
26
27
28     yb=750.*cos((-lat_bary)*!dtor)*(cos((180.+lon_bary)*!dtor))+750.
29     xb=750.*cos((-lat_bary)*!dtor)*(sin((180.+lon_bary)*!dtor))+750.
30
31     yp=750.*cos((-lat)*!dtor)*(cos((180.+lon)*!dtor))+750.
32     xp=750.*cos((-lat)*!dtor)*(sin((180.+lon)*!dtor))+750.
33
34     angle_i=(atan((yp-yb)/(xp-xb))/!dtor)+(180.*(xp lt xb))
35     if (xp eq xb) then angle_i=90.*((yp gt yb)*2.-1.)
36     dista=norm([xp-xb,yp-yb])
37   endelse
38
39   if angle_i lt 0 then angle_i=angle_i+360.
40   if angle_i gt 360 then angle_i=angle_i-360.
41
42   a=[angle_i,dista]
43
44   return, a
45 end
```

create_power_profiles.pro

```

1 pro create_power_profiles, pj, st=st, cosi=cosi, n_im=n_im, rerun=rerun
2 ; pj = perijove number.
3 ; st = first spin to use.
4 ; cosi = taking into account the correction for Juno's viewing angle. 1 or 0 in
   entry.
5 ; n_im = number of spins to use.
6 ; rerun = use of a map already created. 1 or 0 in entry.
7
8
9 ;-----
10 ; Definition of various quantities
11 ;-----
12
13 str_st=strcompress(string(st), /re)
14 str_n_im=strcompress(string(n_im), /re)
15
16 pondvect=1./(2.^findgen(n_im))
17
18 path1='/LPAP/HST/redu/juno/'+pj+'/ephem/'
19
20 if n_elements(st) eq 0 then st=0
21 if n_elements(rerun) eq 0 then rerun=0
22 if n_elements(n_im) eq 0 then n_im=20
23 if n_elements(cosi) eq 0 then cosi=0
24
25 if cosi eq 1 then begin
26     cosi_str='_cos'
27 endif else begin
28     cosi_str=''
29 endelse
30
31 loadct,1, file='/home/LPAP/groulard/Memoire/colors_blwh01.tbl'
32 altitude='400' ; km
33
34 convert_nabs_to_totalH2=4.4 ; or 4.1
35
36 threshold_bri=1000
37
38 c=299792458.
39 h=6.63e-34
40 mean_wl=1240.97
41 mean_energy=1.65590e-18
42
43
44 ;-----
45 ; restore the surface map and the ephemerides
46 ;-----
47
48 restore, '/LPAP/HST/work/bonfond/Fichiers_de_reference/surface_vect.idl'
49 surf_mat=rebin(transpose(surface_vect),3600,1800) ; in km^2
50
51 restore, '/LPAP/HST/work/bonfond/brightness_stat/all_aurora_mask.idl'
52 implan_all_aurora=implem_all_aurora(0:3599,*)
53
54 restore, path1+pj+'_ephem03.idl'
55
56 print, ephem_orb(st).lat_ssc
57

```

APPENDIX I. IDL ROUTINES

```

58  nelm_orb=n_elements(ephem_orb)
59  measured_total_power=fltarr(nelm_orb)
60
61
62  ;-----
63  ; Use a map already built, or build a new one
64  ;-----
65
66  implan_clean=fltarr(3600,1800) ; will contain the final brightness map
67  implan_mask_uni=fltarr(3600,1800)
68
69  filename='/home/LPAP/groulard/juno/'+pj+'/auroral_power_02.idl'
70
71  if file_test(filename) and rerun eq 0 then begin
72      restore, filename
73  endif else begin
74
75      for j=st,st+n_im-1 do begin ; each j works on a different spin
76          implan_tot=fltarr(3600,1800)
77          implan_mask=fltarr(3600,1800)
78
79          rootname=ephem_orb(j).rootname
80          count=ephem_orb(j).count
81          count_mask=count
82
83          ind_ephem=j
84
85          ; Check if data exist for spin j
86          print, '/LPAP/HST/redu/juno/'+pj+'/reduced_data/'+rootname+count+'_'+
altitude+'_map'+cosi_str+'03.idl', string(file_test('/LPAP/HST/redu/juno/'+
pj+'/reduced_data/'+rootname+count+'_'+altitude+'_map'+cosi_str+'03.idl'))
87          print, '/LPAP/HST/redu/juno/'+pj+'/reduced_data/'+rootname+count_mask+'_'+
altitude+'_slit_map02.idl', string(file_test('/LPAP/HST/redu/juno/'+pj+'/
reduced_data/'+rootname+count_mask+'_'+altitude+'_slit_map02.idl'))
88
89          if file_test('/LPAP/HST/redu/juno/'+pj+'/reduced_data/'+rootname+count+'_'+
+altitude+'_map'+cosi_str+'03.idl') and file_test('/LPAP/HST/redu/juno/'+pj+
'/reduced_data/'+rootname+count_mask+'_'+altitude+'_slit_map02.idl') then
begin
90              restore, '/LPAP/HST/redu/juno/'+pj+'/reduced_data/'+rootname+count+'_'+
altitude+'_map'+cosi_str+'03.idl'
91              restore, '/LPAP/HST/redu/juno/'+pj+'/reduced_data/'+rootname+count_mask+
'_'+altitude+'_slit_map02.idl'
92
93              if cosi eq 1 then begin
94                  map_nabs=map_nabs_cos ; map_nabs = map without absorption
95              endif
96
97              ; Correcting for side effects
98              ind_wide=where(map_wide_slit eq 1 or map_wide_slit eq 5)
99              mask_wide=map_wide_slit*0.
100             mask_wide(ind_wide)=1
101             if ephem_orb(j).dist_jup_center gt 4 then mask_wide=erode(smooth(
mask_wide,3) gt 0, fltarr(7,7)+1.) else begin
102                 if ephem_orb(j).dist_jup_center gt 2.5 then mask_wide=erode(smooth(
mask_wide,3) gt 0, fltarr(5,5)+1.) else begin
103                     mask_wide=erode(smooth(mask_wide,3) gt 0, fltarr(3,3)+1.)
104                 endelse
105             endelse
106
107

```

APPENDIX I. IDL ROUTINES

```

108      ;-----
109      ; Centering of the map
110      ;-----
111
112      mup=(map_nabs*mask_wide*convert_nabs_to_totalH2)>0
113      mop=shift(mup,1800)
114      mop=rotate(mop,5)
115
116      implan_tot(*,*)=mop
117      implan_mask(*,*)=rotate(shift(mask_wide,1800),5)
118  endif
119
120
121      ;-----
122      ; Add the partial map of each spin accounting for the temporal shift
123      ;-----
124
125      implan_clean=implean_clean+implean_tot(*,*)*pondvect(st+n_im-j-1)
126      implan_mask_uni=implean_mask_uni+implean_mask(*,*)*pondvect(st+n_im-j-1)
127
128      count=string(fix(st+n_im),/re)
129      if count lt 10 then count='0'+count
130      if count lt 100 then count='0'+count
131      if count lt 1000 then count='0'+count
132  endfor
133
134
135      ;-----
136      ; Correcting for the surfaces covered during several spins
137      ;-----
138
139      ind_cl=where(implean_mask_uni ne 0)
140      implan_clean(ind_cl)=implean_clean(ind_cl)/implean_mask_uni(ind_cl)
141      implan_clean_visu=implean_clean
142
143
144      ;-----
145      ; Visual effect to see black pixels where data were acquired but the aurora
146      ; is not bright enough to appear on the final map. ! Only used to create
147      ; visual maps but not to work on them !
148      ;-----
149
150      inde=where(implean_clean_visu le threshold_bri/255. and implan_mask_uni ne 0)
151      implan_clean_visu(inde)=threshold_bri/255.
152  endelse
153
154      ;-----
155      ; Shows the final brightness map
156      ;-----
157
158      threshold=threshold_bri
159
160      ; Use implan_clean to have the "real" map and implan_clean_visu to have the
161      ; map with black pixels.
162      bpglobe,90-180.*(ephem_orb(j).lat_ssc lt 0.),0.,180.*(ephem_orb(j).lat_ssc lt
163      0.),rotate(implean_clean_visu,5.*(ephem_orb(j).lat_ssc lt 0.)),res,/grid,/
164      horizon,/linscl, min=0., max=threshold, londel=10, latdel=10, glinestyle=2
165
166      if ephem_orb(st).lat_ssc gt 0. then begin ; North
167      pos_x=428

```

APPENDIX I. IDL ROUTINES

```

164     pos_y=200
165 endif else begin ; South
166     pos_x=503
167     pos_y=490
168 endelse
169
170 ; Adds the color in the scale.
171 for m=0,400 do plots, (pos_x+650/2.-200.+m)*[1,1],[0,20]+pos_y, color=m
    /400.*255,/device
172 plots, (pos_x+650/2.)+[-200.,200],pos_y*[1,1],thick=3,color=255,/device
173 plots, (pos_x+650/2.)+[-200.,200],pos_y+20*[1,1],thick=3,color=255,/device
174 plots, (pos_x+650/2.)+[-200.,-200],[0,20]+pos_y,thick=3,color=255,/device
175 plots, (pos_x+650/2.)+[200.,200],[0,20]+pos_y,thick=3,color=255,/device
176 plots, (pos_x+650/2.)+[-200.,-200]+1.*400./5.,[0,5]+pos_y,thick=2,color=255,/
    device
177 plots, (pos_x+650/2.)+[-200.,-200]+2.*400./5.,[0,5]+pos_y,thick=2,color=255,/
    device
178 plots, (pos_x+650/2.)+[-200.,-200]+3.*400./5.,[0,5]+pos_y,thick=2,color=255,/
    device
179 plots, (pos_x+650/2.)+[-200.,-200]+4.*400./5.,[0,5]+pos_y,thick=2,color=255,/
    device
180 plots, (pos_x+650/2.)+[-200.,-200]+5.*400./5.,[0,5]+pos_y,thick=2,color=255,/
    device
181
182 ; Adds the numbers in the scale.
183 xyouts, (pos_x+650/2.)-200+0.*400./5.,-20+pos_y,'0',color=255,/device, ali
    =0.5, charsize=2
184 xyouts, (pos_x+650/2.)-200+1.*400./5.,-20+pos_y,strcompress(string(fix(
    threshold/5.)),/re),color=255,/device, ali=0.5, charsize=2
185 xyouts, (pos_x+650/2.)-200+2.*400./5.,-20+pos_y,strcompress(string(fix(
    threshold/5.*2)),/re),color=255,/device, ali=0.5, charsize=2
186 xyouts, (pos_x+650/2.)-200+3.*400./5.,-20+pos_y,strcompress(string(fix(
    threshold/5.*3)),/re),color=255,/device, ali=0.5, charsize=2
187 xyouts, (pos_x+650/2.)-200+4.*400./5.,-20+pos_y,strcompress(string(fix(
    threshold/5.*4)),/re),color=255,/device, ali=0.5, charsize=2
188 xyouts, (pos_x+650/2.)-200+5.*400./5.,-20+pos_y,strcompress(string(fix(
    threshold)),/re),color=255,/device, ali=0.5, charsize=2
189
190 xyouts, (pos_x+650/2.)-200+5.*400./5.+25,-20+pos_y+25,'kR',color=255,/device,
    ali=0, charsize=2;
191
192 ; Adds the date and time of first and last spin used.
193 etcm=ephem_orb(st).date+' - '+ephem_orb(st+n_im).date
194 xyouts, (pos_x+650/2.)-220,pos_y+30,etcm,color=255,/device, ali=0, charsize=2
195
196 if 1 eq 0 then begin
197 ; Adds the mean subsolar longitude.
198 restore, '/LPAP/HST/work/bonfond/Fichiers_de_reference/ifp_fit_s10b.idl'
199 lon_ifp_fit_s=lon_ifp_fit
200 lat_ifp_fit_s=lat_ifp_fit
201 restore, '/LPAP/HST/work/bonfond/Fichiers_de_reference/ifp_fit_n10b.idl'
202 lon_ifp_fit_n=lon_ifp_fit
203 lat_ifp_fit_n=lat_ifp_fit
204
205 if ephem_orb(st).lat_ssc gt 0. then begin ; North
206     lat_ifp_fit=lat_ifp_fit_n
207     lon_ifp_fit=lon_ifp_fit_n
208     ind_neg=where(lon_ifp_fit lt 0 and findgen(n_elements(lon_ifp_fit)) gt 3000)
209 if ind_neg(0) ne -1 then lon_ifp_fit(ind_neg)=lon_ifp_fit(ind_neg)+360.
210 endif else begin ; South
211     lat_ifp_fit=lat_ifp_fit_s

```


APPENDIX I. IDL ROUTINES

```

212     lon_ifp_fit=lon_ifp_fit_s
213     ind_neg=where(lon_ifp_fit_s lt 10 and findgen(n_elements(lon_ifp_fit_s)) gt
214     2500)
215     if ind_neg(0) ne -1 then lon_ifp_fit(ind_neg)=lon_ifp_fit(ind_neg)+360.
216     endelse
217
218     lat_st=interpol(lat_ifp_fit,lon_ifp_fit,ephem_orb(st).lon_sun)
219     lat_fin=interpol(lat_ifp_fit,lon_ifp_fit,ephem_orb(st+n_im).lon_sun)
220     lat_sun=(lat_st+lat_fin)/2
221
222     lon_st=ephem_orb(st).lon_sun
223     lon_fin=ephem_orb(st+n_im).lon_sun
224     if lon_fin lt lon_st then lon_fin = lon_fin+360.
225     lon_sun=(lon_st+lon_fin)/2
226     if lon_sun ge 360. then lon_sun = lon_sun - 360.
227
228     loadct,4
229     if ephem_orb(st).lat_ssc gt 0. then oplot, 180-lon_sun*[1,1], [lat_sun(0)+3,
230     lat_sun(0)-4], thick=3 else $
231     oplot, 180+lon_sun*[1,1], [lat_sun(0)+3,lat_sun(0)+7], thick=3
232     endif
233
234     ;-----
235     ; Create the power map
236     ;-----
237
238     power_map=mean_energy*implan_clean*1.e13*surf_mat*1.e6
239
240     measured_total_power=total(power_map*implan_all_aurora)
241
242     ;-----
243     ; Export the brightness map as a png file and save some variables to be reused
244     ; in other routines
245     ;-----
246
247     if ephem_orb(st).lat_ssc gt 0. then begin ; North
248     x_photo=363
249     y_photo=170
250     hemi='N'
251     endif else begin ; South
252     x_photo=438
253     y_photo=460
254     hemi='S'
255     endelse
256
257     photo=tvrd(x_photo,y_photo,780,780,true=1)
258     tvlct, r,g,b,/get
259     fnameout='/home/LPAP/groulard/'+str_st+'_'+str_n_im+'.png'
260     write_png, fnameout, photo, r, g, b
261     save, filename='/home/LPAP/groulard/juno/'+pj+'/auroral_power_'+pj+'_'+hemi+'.
262     idl', measured_total_power, st, n_im, implan_clean, implan_clean_visu,
263     lat_sun, lon_sun, power_map
264
265 end

```

create_me_mask_bonfond.pro

```

1 pro create_me_mask_bonfond, pj, hemi
2   ; pj = perijove number. 'PJ#' in entry.
3   ; hemi = hemisphere. 'N' or 'S' in entry.
4
5 ;for k=1, 39 do begin ; automatically do all of the 39 PJ
6 ;   pj='PJ'+strcompress(k,/re)
7 ;   print, pj
8 ;if k ne 2 then begin
9   restore, '/home/LPAP/groulard/juno/'+pj+'/auroral_power_'+pj+'_'+hemi+'.idl'
10  loadct,1, file='/home/LPAP/groulard/Memoire/colors_blwh01.tbl'
11  restore, '/LPAP/HST/redu/juno/'+pj+'/ephem/'+pj+'_ephem03.idl'
12
13  if hemi eq 'S' then begin
14
15      lon_lat_bary=[31.9209,-81.9309]
16
17      x_photo=438
18      y_photo=460
19
20
21      ;-----
22      ; Find the best fitting mask
23      ;-----
24
25      month=['February', 'March', 'April', 'May', 'June']
26      power=fltarr(5)
27
28      for i=0, 4 do begin
29          masque_month=fltarr(3600,1800)
30          restore, '/LPAP/HST/work/bonfond/local_time_zones/oval_bands_'+month(i)+'
_S_15_a01.idl'
31          implan_me_area=implan_me_area(0:3599,*)
32          implan_me_area(where(implan_me_area ne 0))=1.
33          implan_me_area=shift(implan_me_area,1800,0)
34
35          for j=0, 3599 do begin
36              ind_max=max(where(implan_me_area(j,*) ne 0))
37              ind_min=min(where(implan_me_area(j,*) ne 0))
38              masque_month(j,ind_min:ind_max)=1
39          endfor
40
41          mask_month_on=implan_clean_visu
42          mask_month_on(where(masque_month eq 1))=1000.
43
44          bpglobe,90-180.*(ephem_orb(st).lat_ssc lt 0.),0.,180.*(ephem_orb(st).
lat_ssc lt 0.),rotate(mask_month_on,5.*(ephem_orb(st).lat_ssc lt 0.)),res,/
grid,/horizon,/linscl, min=0., max=1000., londel=10, latdel=10, glinestyle=2
45          photo=tvrd(x_photo,y_photo,780,780,true=1)
46          tvlct, r,g,b,/get
47          fnameout='/home/LPAP/groulard/juno/'+pj+'/'+'_'+pj+'_mask_'+month(i)+'_'+hemi+
'.png'
48          write_png, fnameout, photo, r, g, b
49
50          power(i)=total(power_map*masque_month)
51      endfor
52
53      power_max=min(where(power eq max(power)))
54      month_used=month(power_max)

```

APPENDIX I. IDL ROUTINES

```

55  print, month_used
56
57  restore, '/LPAP/HST/work/bonfond/local_time_zones/oval_bands_'+month(
power_max)+'_S_15_a01.idl'
58  masque_me=implan_me_area(0:3599,*)
59  masque_me(3600-lon_lat_bary(0)*10.-150.:3600-lon_lat_bary(0)*10.+150.,
lon_lat_bary(1)*10.+875.:lon_lat_bary(1)*10.+925.)=0. ; Takes out the mask
near the barycentre that is not always 0 for an unknown reason.
60  masque_me=shift(masque_me,1800,0)
61
62  bpglobe,90-180.*(lat_sun lt 0.),0.,180.*(lat_sun lt 0.),rotate(masque_me
,5.*(lat_sun lt 0.)),res,/grid,/horizon,/linscl, min=0., max=7200, londel=10
, latdel=10, glinestyle=2
63  photo=tvrd(x_photo,y_photo,780,780,true=1)
64  tvlct, r,g,b,/get
65  fnameout='/home/LPAP/groulard/juno/'+pj+'/' +pj+'_masque_me_b_'+hemi+'.png'
66  write_png,fnameout,photo,r,g,b
67
68
69  ;-----
70  ; Do 15 smoothing of the mask to cover the holes in the mask
71  ;-----
72
73  ind=fltarr(3600,1800)
74  masque=fltarr(3600,1800) ; Array that will be used to be sure that the mask
does not extend during the smoothings.
75
76  for i=0, 3599 do begin
77      ind_max=max(where(masque_me(i,*) ne 0))
78      ind_min=min(where(masque_me(i,*) ne 0))
79      masque(i,ind_min:ind_max)=1
80  endfor
81
82  masque_me_smooth=masque_me
83  ind=where(masque_me ne 0)
84  for i=0, 14 do begin
85      masque_me_smooth=smooth(masque_me_smooth,2)
86      masque_me_smooth(ind)=masque_me(ind)
87  endfor
88  masque_me=masque_me_smooth
89  masque_me=masque_me*masque
90
91
92  ;-----
93  ; Images
94  ;-----
95
96  if 1 eq 0 then begin
97  dgtv,  congrid(masque_me,720,360)
98  photo=tvrd(0,0,720,360,true=1)
99  tvlct, r,g,b,/get
100  fnameout='/home/LPAP/groulard/juno/'+pj+'/' +pj+'_dgtv_'+hemi+'.png'
101  write_png,fnameout,photo,r,g,b
102  endif
103
104  mask_on=implan_clean_visu
105  ind=where(masque_me ne 0)
106  mask_on(ind)=1000
107  bpglobe,90-180.*(lat_sun lt 0.),0.,180.*(lat_sun lt 0.),rotate(mask_on,5.*(
lat_sun lt 0.)),res,/grid,/horizon,/linscl, min=0., max=1000, londel=10,
latdel=10, glinestyle=2

```

APPENDIX I. IDL ROUTINES

```

108
109   photo=tvrd(x_photo,y_photo,780,780,true=1)
110   tvlct, r,g,b,/get
111   fnameout='/home/LPAP/groulard/juno/'+pj+'/' +pj+'_mask_on_b_'+hemi+'.png'
112   write_png,fnameout,photo,r,g,b
113
114   if 1 eq 0 then begin
115     bpglobe,90-180.*(lat_sun lt 0.),0.,180.*(lat_sun lt 0.),rotate(masque_me
,5.*(lat_sun lt 0.)),res,/grid,/horizon,/linscl, min=0., max=7200, londel=10
, latdel=10, glinestyle=2
116     photo=tvrd(x_photo,y_photo,780,780,true=1)
117     tvlct, r,g,b,/get
118     fnameout='/home/LPAP/groulard/juno/'+pj+'/' +pj+'_mask_moi2_'+hemi+'.png'
119     write_png,fnameout,photo,r,g,b
120     endif
121
122   endif
123
124
125 ; -----
126 ; |                               North                               |
127 ; -----
128
129   if hemi eq 'N' then begin
130
131     lon_lat_bary=[185.670,73.9340]
132
133     x_photo=363
134     y_photo=170
135
136
137     ; -----
138     ; Find the best fitting mask
139     ; -----
140
141     month=['February', 'March', 'May', 'June']
142     power=fltarr(4)
143
144     for i=0, 3 do begin
145       masque_month=fltarr(3600,1800)
146       restore, '/LPAP/HST/work/bonfond/local_time_zones/oval_bands_'+month(i)+'
_N_15_a01.idl'
147       implan_me_area=implan_me_area(0:3599,*)
148       masque_month(where(implan_me_area ne 0))=1.
149       mask_month_on=implan_clean_visu
150       mask_month_on(where(masque_month eq 1))=1000.
151
152       bpglobe,90-180.*(ephem_orb(st).lat_ssc lt 0.),0.,180.*(ephem_orb(st).
lat_ssc lt 0.),rotate(mask_month_on,5.*(ephem_orb(st).lat_ssc lt 0.)),res,/
grid,/horizon,/linscl, min=0., max=1000., londel=10, latdel=10, glinestyle=2
153       photo=tvrd(x_photo,y_photo,780,780,true=1)
154       tvlct, r,g,b,/get
155       fnameout='/home/LPAP/groulard/juno/'+pj+'/' +pj+'_mask_'+month(i)+'_' +hemi+
'.png'
156       write_png,fnameout,photo,r,g,b
157
158       power(i)=total(power_map*masque_month)
159     endfor
160
161     power_max=min(where(power eq max(power)))
162     month_used=month(power_max)

```

APPENDIX I. IDL ROUTINES

```

163   print, month_used
164
165   restore, '/LPAP/HST/work/bonfond/local_time_zones/oval_bands_'+month(
power_max)+'_N_15_a01.idl'
166   masque_me=implan_me_area(0:3599,*)
167   masque_me=shift(masque_me,1800,0)
168   masque_me(3600-lon_lat_bary(0)*10.-100.:3600-lon_lat_bary(0)*10.+100.,
lon_lat_bary(1)*10.+875.:lon_lat_bary(1)*10.+925.)=0.
169   masque_me=shift(masque_me,1800,0)
170
171
172   ;-----
173   ; Images
174   ;-----
175
176   bpglobe,90-180.*(lat_sun lt 0.),0.,180.*(lat_sun lt 0.),rotate(masque_me
,5.*(lat_sun lt 0.)),res,/grid,/horizon,/linscl, min=0., max=7200, londel=10
, latdel=10, glinestyle=2
177   photo=tvrd(x_photo,y_photo,780,780,true=1)
178   tvlct, r,g,b,/get
179   fnameout='/home/LPAP/groulard/juno/'+pj+'/' +pj+'_masque_me_b_'+hemi+'.png'
180   write_png,fnameout,photo,r,g,b
181
182
183   if 1 eq 0 then begin
184   dgtv,   congrid(masque_me,720,360)
185   photo=tvrd(0,0,720,360,true=1)
186   tvlct, r,g,b,/get
187   fnameout='/home/LPAP/groulard/juno/'+pj+'/' +pj+'_dgtv_'+hemi+'.png'
188   write_png,fnameout,photo,r,g,b
189   endif
190
191   mask_on=implan_clean_visu
192   ind=where(masque_me ne 0)
193   mask_on(ind)=1000
194   bpglobe,90-180.*(lat_sun lt 0.),0.,180.*(lat_sun lt 0.),rotate(mask_on,5.*(
lat_sun lt 0.)),res,/grid,/horizon,/linscl, min=0., max=1000, londel=10,
latdel=10, glinestyle=2
195   photo=tvrd(x_photo,y_photo,780,780,true=1)
196   tvlct, r,g,b,/get
197   fnameout='/home/LPAP/groulard/juno/'+pj+'/' +pj+'_mask_on_b_'+hemi+'.png'
198   write_png,fnameout,photo,r,g,b
199
200   if 1 eq 0 then begin
201   bpglobe,90-180.*(lat_sun lt 0.),0.,180.*(lat_sun lt 0.),rotate(masque_me
,5.*(lat_sun lt 0.)),res,/grid,/horizon,/linscl, min=0., max=7200, londel=10
, latdel=10, glinestyle=2
202   photo=tvrd(x_photo,y_photo,780,780,true=1)
203   tvlct, r,g,b,/get
204   fnameout='/home/LPAP/groulard/juno/'+pj+'/' +pj+'_mask_moi2_'+hemi+'.png'
205   write_png,fnameout,photo,r,g,b
206   endif
207
208   endif
209
210   save, filename='/home/LPAP/groulard/juno/'+pj+'/' +pj+'_masque_b_'+pj+'_'+hemi+'.idl',
masque_me, month_used
211 ;endif
212 ;endfor
213
214 end

```

create_me_mask_vogt.pro

```

1 pro create_me_mask_vogt, pj, hemi, thickness_me
2 ; pj = perijove number. 'PJ#' in entry.
3 ; hemi = hemisphere. 'N' or 'S' in entry.
4 ; thickness_me = thickness of the mask covering the main emission.
5
6 ;for l=1, 39 do begin ; automatically do all of the 39 PJ
7 ; pj='PJ'+strcompress(l,/re)
8 ; print, pj
9 ;if l ne 2 then begin
10
11 restore, '/home/LPAP/groulard/juno/'+pj+'/auroral_power_'+pj+'_'+hemi+'.idl'
12 loadct,1, file='/home/LPAP/groulard/Memoire/colors_blwh01.tbl'
13 restore, '/LPAP/HST/redu/juno/'+pj+'/ephem/'+pj+'_ephem03.idl'
14
15 if hemi eq 'S' then begin
16
17     pos_bary_s=[474.,451.]
18     lon_lat_bary=[31.9209,-81.9309]
19
20     x_photo=438
21     y_photo=460
22
23     hemi_str='south'
24
25     local = [0.33, 1., 1.66, 2.33, 3., 3.66, 4.33, 5., 5.66, 6.33, 7., 7.66,
26             8.33, 9., 9.66, 10.33, 11., 11.66, 12.33, 13., 13.66, 14.33, 15., 15.66, 16
27             .33, 17., 17.66, 18.33, 19., 19.66, 20.33, 21., 21.66, 22.33, 23., 23.66]
28     lon=fltarr(36)
29     lat=fltarr(36)
30
31     dista=[30.,40.]
32
33     for k=0,1 do begin
34         distance=dista(k)
35
36         ; Find the longitude and latitude of the ionospheric location mapping to
37         ; the local time and distance in the magnetosphere specified.
38         for i=0, 35 do begin
39             pos = mapping_function2019('mag_to_ion_'+hemi_str, lon_sun, distance,
40             local(i), 'jrm09')
41             lon(35-i)=pos(1)
42             lat(35-i)=pos(0)
43         endfor
44
45         ; Order the 36 longitude found.
46         ind=where(lon eq min(lon))
47         lon=shift(lon, -ind)
48         lat=shift(lat, -ind)
49
50         ; Interpolate the latitude on the 360 degrees
51         me_lon=findgen(3600)/10.
52         me_lat=interpol([lat,lat,lat],[lon-360.,lon,lon+360],me_lon)
53
54         me=fltarr(3600,1800)
55         me(3600.-me_lon*10.,me_lat*10.+900.)=1000.
56         me=shift(me,1800.,0)
57
58         me_visu=implan_clean_visu

```

APPENDIX I. IDL ROUTINES

```

55     me_visu(where(me eq 1000.))=1000.
56
57     bpglobe,90-180.*(ephem_orb(st).lat_ssc lt 0.),0.,180.*(ephem_orb(st).
lat_ssc lt 0.),rotate(me_visu,5.*(ephem_orb(st).lat_ssc lt 0.)),res,/grid,/
horizon,/linscl, min=0., max=1000., londel=10, latdel=10, glinestyle=2
58
59     implan_south_area=fltarr(3600,1800)
60     masque_me=fltarr(3600,1800)
61
62
63     ;-----
64     ; Create the mask based on 7200 slices in the interpolated locations
65     ;-----
66
67     oval_manual=PROJPOL(smooth(me,3) gt 0,512,512,0,-90,0)
68     for i=0,7200-1 do begin
69
70         if i mod 500 eq 0 then print, i
71
72         imrotov=rot(oval_manual,i*0.05,1,pos_bary_s(0),pos_bary_s(1),/pivot) gt
0
73
74         indx=where(imrotov(pos_bary_s(0):pos_bary_s(0)+250,pos_bary_s(1)) eq 1)
75         indx=indx(floor(n_elements(indx)/2.))
76         indx2=indx+indgen(thickness_me)-floor(thickness_me/2)
77
78         pos_max=indx2
79
80
81         ;-----
82         ; Transforms the location of the slice of the mask in the polar
coordinates into the cylindrical coordinates
83         ;-----
84
85         xp=pos_bary_s(0)+pos_max*cos(i*0.05/180.*!pi)
86         yp=pos_bary_s(1)+pos_max*sin(i*0.05/180.*!pi)
87
88         fi=atan((xp-512.)/((yp-512.)*1.))
89         teta=acos(((yp-512.)/512.)*(1./cos(fi)))
90         ind=where(teta gt !pi/2.)
91         if ind(0) ne -1 then teta(ind)=!pi-teta(ind)
92         if ind(0) ne -1 then fi(ind)=!pi+fi(ind)
93
94         oval_south_area_lon=-(-180.+fi*180./!pi)
95         oval_south_area_lat=-teta*180./!pi
96
97         steps=20
98
99         order=sort(oval_south_area_lon)
100        oval_south_area_lon2=interpol(oval_south_area_lon(order),findgen(
n_elements(oval_south_area_lon)),findgen((n_elements(oval_south_area_lon)-1)
*steps)/steps)
101        oval_south_area_lat2=interpol(oval_south_area_lat(order),findgen(
n_elements(oval_south_area_lat)),findgen((n_elements(oval_south_area_lat)-1)
*steps)/steps)
102
103        indi=where(oval_south_area_lon2 lt 0)
104        if indi(0) ne -1 then oval_south_area_lon2(indi)=oval_south_area_lon2(
indi)+360.
105        indi=where(oval_south_area_lon2 gt 360)
106        if indi(0) ne -1 then oval_south_area_lon2(indi)=oval_south_area_lon2(

```


APPENDIX I. IDL ROUTINES

```

indi)-360.
107     indi=where(oval_south_area_lon lt 0)
108     if indi(0) ne -1 then oval_south_area_lon(indi)=oval_south_area_lon(
indi)+360.
109     indi=where(oval_south_area_lon gt 360)
110     if indi(0) ne -1 then oval_south_area_lon(indi)=oval_south_area_lon(
indi)-360.
111
112     indi=where(oval_south_area_lon2 gt min(oval_south_area_lon) and
oval_south_area_lon2 lt max(oval_south_area_lon))
113     oval_south_area_lon2=oval_south_area_lon2(indi)
114     oval_south_area_lat2=oval_south_area_lat2(indi)
115
116     implan_south_area(round(oval_south_area_lon*10.),round(
oval_south_area_lat*10+900.))=1.+i
117     endfor
118
119
120     ;-----
121     ; Images
122     ;-----
123
124     masque_me=implan_south_area
125
126     if 1 eq 0 then begin
127     bpglobe,90-180.*(lat_sun lt 0.),0.,180.*(lat_sun lt 0.),rotate(
implan_south_area,5.*(lat_sun lt 0.)),res,/grid,/horizon,/linscl, min=0.,
max=1000, londel=10, latdel=10, glinestyle=2
128     photo=tvrd(x_photo,y_photo,780,780,true=1)
129     tvlct,r,g,b,/get
130     fnameout='/home/LPAP/groulard/juno/'+pj+'/' +pj+'_implan_south_area_'+hemi+
'.png'
131     write_png,fnameout,photo,r,g,b
132     endif
133
134     masque_me(3600-lon_lat_bary(0)*10.-150.:3600-lon_lat_bary(0)*10.+150.,
lon_lat_bary(1)*10.+875.:lon_lat_bary(1)*10.+925.)=0. ; Takes out the mask
near the barycentre that is not always 0 for an unknown reason.
135
136     if 1 eq 0 then begin
137     bpglobe,90-180.*(lat_sun lt 0.),0.,180.*(lat_sun lt 0.),rotate(masque_me
,5.*(lat_sun lt 0.)),res,/grid,/horizon,/linscl, min=0., max=1000, londel=10
, latdel=10, glinestyle=2
138     photo=tvrd(x_photo,y_photo,780,780,true=1)
139     tvlct,r,g,b,/get
140     fnameout='/home/LPAP/groulard/juno/'+pj+'/' +pj+'_me_area_'+hemi+'.png'
141     write_png,fnameout,photo,r,g,b
142     endif
143
144
145     ;-----
146     ; Do 15 smoothing of the mask to cover the holes in the mask
147     ;-----
148
149     ind=fltarr(3600,1800)
150     masque=fltarr(3600,1800) ; Array that will be used to be sure that the
mask does not extend during the smoothings.
151
152     for i=0, 3599 do begin
153     ind_max=max(where(masque_me(i,*) ne 0))
154     ind_min=min(where(masque_me(i,*) ne 0))

```

APPENDIX I. IDL ROUTINES

```

155     masque(i,ind_min:ind_max)=1
156   endfor
157
158   masque_me_smooth=masque_me
159   ind=where(masque_me ne 0)
160   for i=0, 14 do begin
161     masque_me_smooth=smooth(masque_me_smooth,2)
162     masque_me_smooth(ind)=masque_me(ind)
163   endfor
164
165   masque_me=masque_me_smooth
166   masque_me=masque_me*masque
167
168
169   ;-----
170   ; Images
171   ;-----
172
173   if 1 eq 0 then begin
174     masque_me=shift(masque_me,1800,0)
175     dgtv,  congrid(masque_me,720,360)
176
177     photo=tvrd(0,0,720,360,true=1)
178     tvlct, r,g,b,/get
179     fnameout='/home/LPAP/groulard/juno/'+pj+'/' +pj+'_dgtv_'+hemi+'.png'
180     write_png,fnameout,photo,r,g,b
181
182     mask_on=implan_clean_visu
183     ind=where(masque_me ne 0)
184     mask_on(ind)=1000
185     bpglobe,90-180.*(lat_sun lt 0.),0.,180.*(lat_sun lt 0.),rotate(mask_on
,5.*(lat_sun lt 0.)),res,/grid,/horizon,/linscl, min=0., max=1000, londe1=10
, latdel=10, glinestyle=2
186
187     photo=tvrd(x_photo,y_photo,780,780,true=1)
188     tvlct, r,g,b,/get
189     fnameout='/home/LPAP/groulard/juno/'+pj+'/' +pj+'_mask_on_moi_'+hemi+'.png'
190     write_png,fnameout,photo,r,g,b
191
192     bpglobe,90-180.*(lat_sun lt 0.),0.,180.*(lat_sun lt 0.),rotate(masque_me
,5.*(lat_sun lt 0.)),res,/grid,/horizon,/linscl, min=0., max=7200, londe1=10
, latdel=10, glinestyle=2
193
194     photo=tvrd(x_photo,y_photo,780,780,true=1)
195     tvlct, r,g,b,/get
196     fnameout='/home/LPAP/groulard/juno/'+pj+'/' +pj+'_mask_moi2_'+hemi+'.png'
197     write_png,fnameout,photo,r,g,b
198   endif
199
200   if k eq 0 then masque_30=masque_me
201   if k eq 1 then masque_40=masque_me
202
203   endfor
204
205
206   ;-----
207   ; Find the best fit between the 30 R_J and 40 R_J mask
208   ;-----
209
210   masque_30_test=fltarr(3600,1800)
211   masque_30_test(where(masque_30 ne 0))=1.

```

APPENDIX I. IDL ROUTINES

```

212 masque_40_test=fltarr(3600,1800)
213 masque_40_test(where(masque_40 ne 0))=1.
214
215 if total(power_map*masque_30_test) gt total(power_map*masque_40_test) then
begin
216     print, 30
217     masque_me=masque_30
218     distance=30.
219 endif else begin
220     print, 40
221     masque_me=masque_40
222     distance=40.
223 endelse
224
225 endif
226
227
228 ; -----
229 ; |                               |
230 ; -----
231
232 if hemi eq 'N' then begin
233
234     pos_bary_n=[498.,371.]
235     lon_lat_bary=[185.670,73.9340]
236
237     x_photo=363
238     y_photo=170
239
240     hemi_str='north'
241
242     local = [0.33, 1., 1.66, 2.33, 3., 3.66, 4.33, 5., 5.66, 6.33, 7., 7.66,
8.33, 9., 9.66, 10.33, 11., 11.66, 12.33, 13., 13.66, 14.33, 15., 15.66, 16
.33, 17., 17.66, 18.33, 19., 19.66, 20.33, 21., 21.66, 22.33, 23., 23.66]
243     lon=fltarr(36)
244     lat=fltarr(36)
245
246     dista=[30.,40.]
247
248     for k=0,1 do begin
249         distance=dista(k)
250
251         ; Find the longitude and latitude of the ionospheric location mapping to
the local time and distance in the magnetosphere specified.
252         for i=0, 35 do begin
253             pos = mapping_function2019('mag_to_ion_'+hemi_str, lon_sun, distance,
local(i), 'jrm09')
254             lon(35-i)=pos(1)
255             lat(35-i)=pos(0)
256         endfor
257
258         ; Order the 36 longitude found.
259         ind=where(lon eq min(lon))
260         lon=shift(lon, -ind)
261         lat=shift(lat, -ind)
262
263         ; Interpolate the latitude on the 360 degrees
264         me=fltarr(3600,1800)
265
266         for j=0, 35 do begin
267             me_lon1=findgen(201)/200.

```

APPENDIX I. IDL ROUTINES

```

268     if j eq 35 then begin
269         me_lon2=lon(0)-lon(j)
270         me_lon3=me_lon1*me_lon2
271         me_lon=lon(j)+me_lon3
272         me_lat=interpol([lat(0),lat(j)], [lon(0),lon(j)], me_lon)
273     endif else begin
274         me_lon2=lon(j+1)-lon(j)
275         me_lon3=me_lon1*me_lon2
276         me_lon=lon(j)+me_lon3
277         me_lat=interpol([lat(j+1),lat(j)], [lon(j+1),lon(j)], me_lon)
278     endelse
279     me(3600.-me_lon*10., me_lat*10.+900.)=1000.
280 endfor
281
282 me=shift(me, 1800., 0)
283
284
285 ;-----
286 ; Images
287 ;-----
288
289 me_visu=implan_clean_visu
290 me_visu(where(me eq 1000.))=1000.
291
292 bpglobe, 90-180.*(ephem_orb(st).lat_ssc lt 0.), 0., 180.*(ephem_orb(st).
lat_ssc lt 0.), rotate(me_visu, 5.*(ephem_orb(st).lat_ssc lt 0.)), res, /grid, /
horizon, /linscl, min=0., max=1000., londel=10, latdel=10, glinestyle=2
293
294 photo=tvrd(x_photo, y_photo, 780, 780, true=1)
295 tvlct, r, g, b, /get
296 fnameout='/home/LPAP/groulard/juno/'+pj+'/' +pj+'_me_centre_'+hemi+'.png'
297 write_png, fnameout, photo, r, g, b
298
299 oval2=smooth(me, 6)
300 ind2=where(oval2 ne 0)
301
302 implan_oval2=implan_clean_visu
303 implan_oval2(ind2)=1000.
304
305 bpglobe, 90-180.*(ephem_orb(st).lat_ssc lt 0.), 0., 180.*(ephem_orb(st).
lat_ssc lt 0.), rotate(implan_oval2, 5.*(ephem_orb(st).lat_ssc lt 0.)), res, /
grid, /horizon, /linscl, min=0., max=1000., londel=10, latdel=10, glinestyle=2
306
307 photo=tvrd(x_photo, y_photo, 780, 780, true=1)
308 tvlct, r, g, b, /get
309 fnameout='/home/LPAP/groulard/juno/'+pj+'/' +pj+'_me_centre_'+hemi+'.png'
310 write_png, fnameout, photo, r, g, b
311
312
313 ;-----
314 ; Create the mask based on 7200 slices in the interpolated locations
315 ;-----
316
317 implan_north_area=fltarr(3600, 1800)
318 masque_me=fltarr(3600, 1800)
319
320 oval_manual=PROJPOL(smooth(me, 6) gt 0, 512, 512, !pi, -90, 90)
321
322 for i=0, 7200-1 do begin
323
324     if i mod 500 eq 0 then print, i

```

APPENDIX I. IDL ROUTINES

```

325     imrotov=rot(oval_manual,i*0.05,1,pos_bary_n(0),pos_bary_n(1),/pivot) gt
0
326
327     indx=where(imrotov(pos_bary_n(0):pos_bary_n(0)+400,pos_bary_n(1)) eq 1)
328     indx=indx(floor(n_elements(indx)/2.))
329     indx2=indx+indgen(thickness_me)-floor(thickness_me/2)-1
330
331     pos_max=indx2
332
333
334     ;-----
335     ; Transforms the location of the slice of the mask in the polar
coordinates into the cylindrical coordinates
336     ;-----
337
338     xp=pos_bary_n(0)+pos_max*cos(i*0.05/180.*!pi)
339     yp=pos_bary_n(1)+pos_max*sin(i*0.05/180.*!pi)
340
341     fi=atan((xp-512.)/((yp-512.)*1.))
342     teta=acos(((yp-512.)/512.)*(1./cos(fi)))
343     ind=where(teta gt !pi/2.)
344     if ind(0) ne -1 then teta(ind)=!pi-teta(ind)
345     if ind(0) ne -1 then fi(ind)=!pi+fi(ind)
346
347     oval_north_area_lon=-(-180.+fi*180./!pi)
348     oval_north_area_lat=teta*180./!pi
349
350     steps=20
351
352     order=sort(oval_north_area_lon)
353     oval_north_area_lon2=interpol(oval_north_area_lon(order),findgen(
n_elements(oval_north_area_lon)),findgen((n_elements(oval_north_area_lon)-1)
*steps)/steps)
354     oval_north_area_lat2=interpol(oval_north_area_lat(order),findgen(
n_elements(oval_north_area_lat)),findgen((n_elements(oval_north_area_lat)-1)
*steps)/steps)
355
356     indi=where(oval_north_area_lon2 lt 0)
357     if indi(0) ne -1 then oval_north_area_lon2(indi)=oval_north_area_lon2(
indi)+360.
358     indi=where(oval_north_area_lon2 gt 360)
359     if indi(0) ne -1 then oval_north_area_lon2(indi)=oval_north_area_lon2(
indi)-360.
360     indi=where(oval_north_area_lon lt 0)
361     if indi(0) ne -1 then oval_north_area_lon(indi)=oval_north_area_lon(
indi)+360.
362     indi=where(oval_north_area_lon gt 360)
363     if indi(0) ne -1 then oval_north_area_lon(indi)=oval_north_area_lon(
indi)-360.
364
365     indi=where(oval_north_area_lon2 gt min(oval_north_area_lon) and
oval_north_area_lon2 lt max(oval_north_area_lon))
366     oval_north_area_lon2=oval_north_area_lon2(indi)
367     oval_north_area_lat2=oval_north_area_lat2(indi)
368
369     implan_north_area(round(oval_north_area_lon2*10.),round(
oval_north_area_lat2*10.+900.))=1.+i
370     endfor
371
372     masque_me=shift(implan_north_area,1800,0)
373

```

APPENDIX I. IDL ROUTINES

```

374
375 ; -----
376 ; Images
377 ; -----
378
379     if 1 eq 0 then begin
380         bpglobe,90-180.*(lat_sun lt 0.),0.,180.*(lat_sun lt 0.),rotate(
implan_north_area,5.*(lat_sun lt 0.)),res,/grid,/horizon,/linscl, min=0.,
max=1000, londel=10, latdel=10, glinestyle=2
381         photo=tvrd(x_photo,y_photo,780,780,true=1)
382         tvlct, r,g,b,/get
383         fnameout='/home/LPAP/groulard/juno/'+pj+'/' +pj+'_implan_north_area_'+hemi+
'.png'
384         write_png,fnameout,photo,r,g,b
385
386         masque_me(3600-lon_lat_bary(0)*10.-100.:3600-lon_lat_bary(0)*10.+100.,
lon_lat_bary(1)*10.+875.:lon_lat_bary(1)*10.+925.)=0.
387         masque_me=shift(masque_me,1800,0)
388
389         bpglobe,90-180.*(lat_sun lt 0.),0.,180.*(lat_sun lt 0.),rotate(masque_me
,5.*(lat_sun lt 0.)),res,/grid,/horizon,/linscl, min=0., max=1000, londel=10
, latdel=10, glinestyle=2
390         photo=tvrd(x_photo,y_photo,780,780,true=1)
391         tvlct, r,g,b,/get
392         fnameout='/home/LPAP/groulard/juno/'+pj+'/' +pj+'_me_area_'+hemi+'.png'
393         write_png,fnameout,photo,r,g,b
394
395         dgtv,   congriid(masque_me,720,360)
396
397         photo=tvrd(0,0,720,360,true=1)
398         tvlct, r,g,b,/get
399         fnameout='/home/LPAP/groulard/juno/'+pj+'/' +pj+'_dgtv_'+hemi+'.png'
400         write_png,fnameout,photo,r,g,b
401
402         mask_on=implan_clean_visu
403         ind=where(masque_me ne 0)
404         mask_on(ind)=1000
405         bpglobe,90-180.*(lat_sun lt 0.),0.,180.*(lat_sun lt 0.),rotate(mask_on
,5.*(lat_sun lt 0.)),res,/grid,/horizon,/linscl, min=0., max=1000, londel=10
, latdel=10, glinestyle=2
406
407         photo=tvrd(x_photo,y_photo,780,780,true=1)
408         tvlct, r,g,b,/get
409         fnameout='/home/LPAP/groulard/juno/'+pj+'/' +pj+'_mask_on_moi_'+hemi+'.png'
410         write_png,fnameout,photo,r,g,b
411
412         bpglobe,90-180.*(lat_sun lt 0.),0.,180.*(lat_sun lt 0.),rotate(masque_me
,5.*(lat_sun lt 0.)),res,/grid,/horizon,/linscl, min=0., max=7200, londel=10
, latdel=10, glinestyle=2
413
414         photo=tvrd(x_photo,y_photo,780,780,true=1)
415         tvlct, r,g,b,/get
416         fnameout='/home/LPAP/groulard/juno/'+pj+'/' +pj+'_mask_moi2_'+hemi+'.png'
417         write_png,fnameout,photo,r,g,b
418         endif
419
420         if k eq 0 then masque_30=masque_me
421         if k eq 1 then masque_40=masque_me
422
423     endfor
424

```

APPENDIX I. IDL ROUTINES

```
425
426 ; -----
427 ; Find the best fit between the 30 R_J and 40 R_J mask
428 ; -----
429
430 masque_30_test=fltarr(3600,1800)
431 masque_30_test(where(masque_30 ne 0))=1.
432 masque_40_test=fltarr(3600,1800)
433 masque_40_test(where(masque_40 ne 0))=1.
434
435 if total(power_map*masque_30_test) gt total(power_map*masque_40_test) then
begin
436   print, 30
437   masque_me=masque_30
438   distance=30.
439 endif else begin
440   print, 40
441   masque_me=masque_40
442   distance=40.
443 endelse
444
445 endif
446
447 save, filename='/home/LPAP/groulard/juno/'+pj+'/masque_v_'+pj+'_'+hemi+'.idl',
   masque_me, distance
448
449 ;endif
450 ;endfor
451
452 end
```


create_me_mask_groulard_V2.pro

```

1 pro create_me_mask_groulard_V2, pj, hemi, thickness_me, threshold, delta, sym,
  n_harmonic, polar
2 ; pj = perijove number. 'PJ#' in entry.
3 ; hemi = hemisphere. 'N' or 'S' in entry.
4 ; thickness_me = thickness of the mask.
5 ; threshold = threshohld of brightness in an area to look for the peak. 0.X in
  entry.
6 ; delta = maximum difference to the b mask.
7 ; sym = symmetry on delta : 1 -> symmetrical. ; 2 -> delta only applied inside
  of the b mask. ; 3 -> delta only applied outside of the b mask.
8 ; n_harmonic = number of harmonics for the Fourier fit.
9 ; polar = minimum distance to the barycentre to avoid taking into account too
  powerful polar emissions.
10
11 if sym ne 1 and sym ne 2 and sym ne 3 then sym = 1
12 if n_elements(polar) eq 0 then polar = 0.
13
14 if sym eq 1 then begin
15     delta_minus = delta
16     delta_plus = delta
17 endif
18 if sym eq 2 then begin
19     delta_minus = delta
20     delta_plus = 0.
21 endif
22 if sym eq 3 then begin
23     delta_minus = 0
24     delta_plus = delta
25 endif
26
27
28 ;           SOUTH                               NORTH
29
30 ; 1 : 'PJ1' , 'S', 15, 0.2 , 15, 1, 7, 70           1 : 'PJ1' , 'N', 15, 0.25, 40, 2, 7, 80
31 ; 3 : 'PJ3' , 'S', 15, 0.2 , 15, 1, 7, 0           3 : 'PJ3' , 'N', 15, 0.13, 25, 3, 5, 80
32 ; 4 : 'PJ4' , 'S', 15, 0.25, 15, 2, 3, 100          4 : 'PJ4' , 'N', 15, 0.15, 15, 2, 5, 80
33 ; 5 : 'PJ5' , 'S', 15, 0.2 , 5, 3, 4, 0            5 : 'PJ5' , 'N', 15, 0.2 , 25, 1, 5, 0
34 ; 6 : 'PJ6' , 'S', 15, 0.3 , 18, 3, 4, 90          6 : 'PJ6' , 'N', 15, 0.2 , 14, 2, 5, 0
35 ; 7 : 'PJ7' , 'S', 15, 0.15, 25, 2, 4, 110          7 : 'PJ7' , 'N', 15, 0.2 , 5, 1, 5, 0
36 ; 8 : 'PJ8' , 'S', 15, 0.15, 5, 1, 6, 0            8 : 'PJ8' , 'N', 15, 1.1 , 30, 3, 5, 0
37 ; 9 : 'PJ9' , 'S', 15, 0.1 , 10, 1, 4, 100          9 : 'PJ9' , 'N', 15, 0.2 , 5, 2, 5, 0
38 ; 10 : 'PJ10' , 'S', 15, 0.2 , 15, 1, 5, 0          10 : 'PJ10' , 'N', 15, 0.2 , 20, 1, 5, 0
39 ; 11 : 'PJ11' , 'S', 15, 0.2 , 15, 1, 4, 0          11 : 'PJ11' , 'N', 15, 0.2 , 20, 1, 5, 70
40 ; 12 : 'PJ12' , 'S', 15, 0.15, 5, 1, 6, 0           12 : 'PJ12' , 'N', 15, 0.15, 15, 1, 4, 70
41 ; 13 : 'PJ13' , 'S', 15, 0.2 , 15, 1, 7, 0          13 : 'PJ13' , 'N', 15, 0.2 , 5, 1, 5, 70
42 ; 14 : 'PJ14' , 'S', 15, 0.2 , 10, 1, 5, 115         14 : 'PJ14' , 'N', 15, 0.1 , 15, 1, 5, 0
43 ; 15 : 'PJ15' , 'S', 15, 0.15, 20, 1, 5, 0          15 : 'PJ15' , 'N', 15, 0.25, 20, 1, 5, 0
44 ; 16 : 'PJ16' , 'S', 15, 0.2 , 15, 1, 4, 0          16 : 'PJ16' , 'N', 15, 0.25, 10, 1, 5, 80
45 ; 17 : 'PJ17' , 'S', 15, 0.25, 5, 3, 4, 90          17 : 'PJ17' , 'N', 15, 0.25, 15, 1, 5, 80
46 ; 18 : 'PJ18' , 'S', 15, 0.2 , 15, 1, 6, 0          18 : 'PJ18' , 'N', 15, 0.25, 10, 1, 5, 0
47 ; 19 : 'PJ19' , 'S', 15, 0.35, 12, 3, 5, 0          19 : 'PJ19' , 'N', 15, 0.25, 10, 2, 5, 80
48 ; 20 : 'PJ20' , 'S', 15, 0.2 , 15, 2, 4, 105         20 : 'PJ20' , 'N', 15, 1.1 , 15, 1, 5, 80
49 ; 21 : 'PJ21' , 'S', 15, 0.15, 20, 1, 3, 0          21 : 'PJ21' , 'N', 15, 0.2 , 20, 3, 5, 0
50 ; 22 : 'PJ22' , 'S', 15, 0.25, 9, 3, 5, 120          22 : 'PJ22' , 'N', 15, 0.2 , 26, 3, 5, 0
51 ; 23 : 'PJ23' , 'S', 15, 0.1 , 25, 3, 5, 0          23 : 'PJ23' , 'N', 15, 0.2 , 0, 1, 5, 0
52 ; 24 : 'PJ24' , 'S', 15, 0.2 , 15, 1, 3, 0          24 : 'PJ24' , 'N', 15, 0.15, 15, 3, 5, 0
53 ; 25 : 'PJ25' , 'S', 15, 0.15, 15, 1, 4, 105         25 : 'PJ25' , 'N', 15, 0.15, 15, 3, 5, 0
54 ; 26 : 'PJ26' , 'S', 15, 0.1 , 20, 2, 5, 100         26 : 'PJ26' , 'N', 15, 0.20, 15, 2, 5, 0

```

APPENDIX I. IDL ROUTINES

```

55 ; 27 : 'PJ27','S',15,0.2 ,15,1,5, 0          27 : 'PJ27','N',15,0.15,15,1,5, 80
56 ; 28 : 'PJ28','S',15,0.2 , 5,3,5,115       28 : 'PJ28','N',15,0.15,20,1,5, 80
57 ; 29 : 'PJ29','S',15,0.2 ,15,1,4, 0
58 ; 30 : 'PJ30','S',15,0.2 ,15,1,5, 0          30 : 'PJ30','N',15,0.15,30,1,5, 80
59 ; 31 : 'PJ31','S',15,0.15,20,1,4, 0
60 ; 32 : 'PJ32','S',15,0.15,20,1,5, 0          32 : 'PJ32','N',15,0.15,15,1,5, 80
61 ; 33 : 'PJ33','S',15,0.1 , 5,2,5,110        33 : 'PJ33','N',15,0.15,10,1,5, 80
62 ; 34 : 'PJ34','S',15,0.15, 5,1,5, 0          34 : 'PJ34','N',15,0.15,20,1,5, 80
63 ; 35 : 'PJ35','S',15,0.2 ,15,1,7, 0          35 : 'PJ35','N',15,0.15,15,1,5, 80
64 ; 36 : 'PJ36','S',15,0.25,12,3,6,113        36 : 'PJ36','N',15,0.15, 5,1,5, 80
65 ; 37 : 'PJ37','S',15,0.1 , 7,1,4,100        37 : 'PJ37','N',15,0.15,15,1,5, 90
66 ; 38 : 'PJ38','S',15,0.2 ,15,1,7, 0          38 : 'PJ38','N',15,0.1 ,10,1,5, 80
67 ; 39 : 'PJ39','S',15,0.15, 5,1,5, 0          39 : 'PJ39','N',15,0.1 , 5,1,5, 80
68
69
70 restore, '/home/LPAP/groulard/juno/'+pj+'/auroral_power_'+pj+'_'+hemi+'.idl'
71 loadct,1, file='/home/LPAP/groulard/Memoire/colors_blwh01.tbl'
72 restore, '/LPAP/HST/redu/juno/'+pj+'/ephem/'+pj+'_ephem03.idl'
73 restore, '/home/LPAP/groulard/juno/'+pj+'/masque_b_'+pj+'_'+hemi+'.idl'
74
75
76 ; -----
77 ; |                               South                               |
78 ; -----
79
80
81 if hemi eq 'S' then begin
82
83     lon_lat_bary=[31.9209,-81.9309]
84     pos_bary_s=[474.,451.]
85     x_photo=438
86     y_photo=460
87
88     ;-----
89     ; Sometimes another b mask is needed to more easily create the g1 mask
90     ;-----
91
92     ;      PJ              5              7              15
93     ;      17              19              24              25              26              28
94     ;      30              31              32              33              36              39
95     mask=[' ',' ',' ',' ',' ',' ','February',' ',' ','June',' ',' ',' ',' ',' ',' ',' ',' ','February',' ','
96     ','February',' ',' ','April',' ',' ',' ',' ',' ','April','February','June',' ',' ','June',' ',' ','
97     June','February','June','June',' ',' ',' ','February',' ',' ',' ','April']
98
99     for i=1,39 do begin
100         pj_str='PJ'+strcompress(i,/re)
101         if pj_str eq pj then begin
102             if mask(i) ne '' then begin
103                 restore, '/LPAP/HST/work/bonfond/local_time_zones/oval_bands_'+mask(i)
104                 +'_S_15_a01.idl'
105                 masque_me=implan_me_area(0:3599,*)
106                 masque_me(3600-lon_lat_bary(0)*10.-150.:3600-lon_lat_bary(0)*10.+150.,
107                 lon_lat_bary(1)*10.+875.:lon_lat_bary(1)*10.+925.)=0.
108                 masque_me=shift(masque_me,1800,0)
109                 endif
110             endif
111         endfor
112
113     implan_south_area=fltarr(3600,1800)
114     oval_south_area_lon=fltarr(3600)
115     oval_south_area_lat=fltarr(3600)

```

APPENDIX I. IDL ROUTINES

```

110
111 ;-----
112 ; Smooth the map to work on it later
113 ;-----
114
115 if 1 eq 0 then begin
116 ind=where(implan_clean lt 25)
117 implan_clean2=smooth(implan_clean,21)
118 implan_clean2(ind)=0.
119 bpglobe,90-180.*(ephem_orb(st).lat_ssc lt 0.),0.,180.*(ephem_orb(st).lat_ssc
    lt 0.),rotate(implan_clean2,5.*(ephem_orb(st).lat_ssc lt 0.)),res,/grid,/
    horizon,/linscl, min=0., max=1000., londel=10, latdel=10, glinestyle=2
120
121 photo=tvrd(x_photo,y_photo,780,780,true=1)
122 tvlct, r,g,b,/get
123 fnameout='/home/LPAP/groulard/juno/' + pj + '/' + pj + '_smooth_' + hemi + '.png'
124 write_png, fnameout, photo, r, g, b
125
126 ind=where(implan_clean2 lt threshold*max(implan_clean2))
127 implan_clean3=implan_clean2
128 implan_clean3(ind)=0.
129 implan_clean3(where(implan_clean3 ne 0)) = 1.
130 bpglobe,90-180.*(ephem_orb(st).lat_ssc lt 0.),0.,180.*(ephem_orb(st).lat_ssc
    lt 0.),rotate(implan_clean3,5.*(ephem_orb(st).lat_ssc lt 0.)),res,/horizon
    ,/linscl, min=0., max=1., londel=10, latdel=10, glinestyle=2
131
132 photo=tvrd(x_photo,y_photo,780,780,true=1)
133 tvlct, r,g,b,/get
134 fnameout='/home/LPAP/groulard/juno/' + pj + '/' + pj + '_threshold_' + hemi + '.png'
135 write_png, fnameout, photo, r, g, b
136
137 pos_centre=fltarr(3600,1800)
138
139 print, max(implan_clean2)
140 oval_manual=PROJPOL(implan_clean2,512,512,0,-90,0)
141 val_max=max(oval_manual)
142 oval_bonfond=PROJPOL(masque_me,512,512,0,-90,0)
143
144 angl=fltarr(1024,1024)
145 endif
146
147
148 implan_clean2=implan_clean
149 for i=0, 180-1 do begin
150     profil=fltarr(1800)
151     for j=0, 19 do begin
152         profil=profil+implan_clean(20*i+j,*)
153     endfor
154     for j=0, 19 do begin
155         implan_clean2(20*i+j,*)=profil
156     endfor
157 endfor
158
159 bpglobe,90-180.*(ephem_orb(st).lat_ssc lt 0.),0.,180.*(ephem_orb(st).lat_ssc
    lt 0.),rotate(implan_clean2,5.*(ephem_orb(st).lat_ssc lt 0.)),res,/horizon
    ,/linscl, min=0., max=max(implan_clean2), londel=10, latdel=10, glinestyle=2
160 photo=tvrd(x_photo,y_photo,780,780,true=1)
161 tvlct, r,g,b,/get
162 fnameout='/home/LPAP/groulard/juno/' + pj + '/' + pj + '_implan_clean2_' + hemi + '.png'
163 write_png, fnameout, photo, r, g, b
164

```

APPENDIX I. IDL ROUTINES

```

165  ind=where(implan_clean2 lt threshold*max(implan_clean2))
166  implan_clean3=implan_clean2
167  implan_clean3(ind)=0.
168  implan_clean3(where(implan_clean3 ne 0)) = 1.
169  bpglobe,90-180.*(ephem_orb(st).lat_ssc lt 0.),0.,180.*(ephem_orb(st).lat_ssc
    lt 0.),rotate(implan_clean3,5.*(ephem_orb(st).lat_ssc lt 0.)),res,/horizon
    ,/linscl, min=0., max=1., londe1=10, latde1=10, glinestyle=2

170
171  photo=tvrd(x_photo,y_photo,780,780,true=1)
172  tvlct, r,g,b,/get
173  fnameout='/home/LPAP/groulard/juno/' + pj + '/' + pj + '_threshold2_' + hemi + '.png'
174  write_png, fnameout, photo, r, g, b
175
176  pos_centre=fltarr(3600,1800)
177
178  print, max(implan_clean2)
179  oval_manual=PROJPOL(implan_clean2,512,512,0,-90,0)
180  val_max=max(oval_manual)
181  oval_bonfond=PROJPOL(masque_me,512,512,0,-90,0)
182  oval_bonfond(where(oval_bonfond lt 0.1))=0.
183
184
185  ;-----
186  ; Create the 1 thickness mask (ribbon)
187  ;-----
188
189  for i=0, 3600-1 do begin
190
191      if i mod 500 eq 0 then print, i
192
193      ;-----
194      ; Find the centre of the b mask for each slice
195      ;-----
196
197      imrotbo=rot(oval_bonfond,i*0.1,1,pos_bary_s(0),pos_bary_s(1),/pivot)
198      ind1=min(where(imrotbo(pos_bary_s(0):*,pos_bary_s(1)) ne 0))
199      ind2=max(where(imrotbo(pos_bary_s(0):*,pos_bary_s(1)) ne 0))
200      dista=round((ind1+ind2)/2)
201      ;print, dista
202
203      imrotov=rot(oval_manual,i*0.1,1,pos_bary_s(0),pos_bary_s(1),/pivot)
204
205
206      ;-----
207      ; Create the mask based on the centre just found
208      ;-----
209
210      indx=0
211      val=0
212
213      for k=0,2 do begin ; If no data is found, look for greater distances to
the b mask.
214          if val eq 0. then begin
215              if dista-(2^k)*delta_minus lt polar then j_min = polar else j_min=
dista-(2^k)*delta_minus
216              for j=j_min, dista+delta_plus do begin
217                  if imrotov(pos_bary_s(0)+j,pos_bary_s(1)) gt threshold*val_max and
imrotov(pos_bary_s(0)+j,pos_bary_s(1)) gt val then begin ; If the brightness
is high, this is the main emission for sure...
218                      indx = j
219                      val = imrotov(pos_bary_s(0)+j,pos_bary_s(1))

```

APPENDIX I. IDL ROUTINES

```

220         endif else begin ; ... if not, look for the greatest gradient.
221             val1=imrotov(pos_bary_s(0)+j-1,pos_bary_s(1))
222             val2=imrotov(pos_bary_s(0)+j,pos_bary_s(1))
223             if val1 ne 0 and val2 ne 0 then begin
224                 if abs(val2-val1) gt val then begin
225                     indx = j
226                     val = abs(val2-val1)
227                 endif
228             endif
229         endelse
230     endfor
231 endif
232 endfor
233
234
235 ;-----
236 ; Forcing
237 ;-----
238
239 if pj eq 'PJ1' then begin
240     if i gt 1200 and i lt 1400 then indx=125
241     if indx ne 0 then begin
242         if i gt 450 and i lt 650 then indx=indx+20
243         if i gt 850 and i lt 900 then indx=indx+5
244     endif
245 endif
246
247 if pj eq 'PJ7' then begin
248     if indx ne 0 then begin
249         if i gt 200 and i lt 900 then indx=indx+5
250         if i gt 1850 and i lt 2350 then indx=indx-5
251     endif
252 endif
253
254 if pj eq 'PJ9' then begin
255     if indx ne 0 then begin
256         if i gt 580 and i lt 660 then indx=indx+20
257     endif
258 endif
259
260 if pj eq 'PJ14' then begin
261     if indx ne 0 then begin
262         if i gt 1800 and i lt 2100 then indx=indx-5
263     endif
264 endif
265
266 if pj eq 'PJ25' then begin
267     if indx ne 0 then begin
268         if i gt 0 and i lt 550 then indx=indx+15
269         if i gt 550 and i lt 650 then indx=indx+10
270     endif
271 endif
272
273 if pj eq 'PJ30' then begin
274     if indx ne 0 then begin
275         if i gt 2150 and i lt 2550 then indx=indx-10
276     endif
277 endif
278
279 ;-----
280 ; Polar coordinates to cylindrical

```

APPENDIX I. IDL ROUTINES

```

281     ; -----
282
283     if indx ne 0 then begin
284         xp=pos_bary_s(0)+indx*cos(i*0.1/180.*!pi)
285         yp=pos_bary_s(1)+indx*sin(i*0.1/180.*!pi)
286
287         fi=atan((xp-512.)/((yp-512.)*1.))
288         teta=acos(((yp-512.)/512.)*(1./cos(fi)))
289         ind=where(teta gt !pi/2.)
290         if ind(0) ne -1 then teta(ind)=!pi-teta(ind)
291         if ind(0) ne -1 then fi(ind)=!pi+fi(ind)
292
293         oval_south_area_lon(i)=-(-180.+fi*180./!pi)
294         oval_south_area_lat(i)=-teta*180./!pi
295         if round(oval_south_area_lon(i)*10.) lt 0 then oval_south_area_lon(i) =
oval_south_area_lon(i)+360.
296         if round(oval_south_area_lon(i)*10.) gt 3599 then oval_south_area_lon(i)
= oval_south_area_lon(i)-360.
297         pos_centre(round(oval_south_area_lon(i)*10.),round(oval_south_area_lat(i)
)*10.+900.))=1000.
298     endif
299 endfor
300
301 pos_centre=shift(pos_centre,1800,0)
302
303
304 ; -----
305 ; Smooth the ribbon
306 ; -----
307
308
309 ; -----
310 ; First try : polynomial fit
311 ; -----
312
313 if 1 eq 0 then begin
314     coef=poly_fit(oval_south_area_lon,oval_south_area_lat,3)
315     print, coef
316
317     pos_fit=fltarr(3600,1800)
318     for i=0, 3599 do begin
319         lon=i
320         lat=round(coef[0]+coef[1]*i+coef[2]*i^2+coef[3]*i^3)
321         pos_fit(lon,lat)=1000.
322     endfor
323 endif
324
325
326 ; -----
327 ; Second try : smooth the mask
328 ; -----
329
330 if 1 eq 0 then begin
331     for j=0,9 do begin
332         print, j
333         pos_centre2=smooth(pos_centre,25)
334         pos_centre3=fltarr(3600,1800)
335         for i=0, 3599 do begin
336             ind= where(pos_centre2(i,*) ne 0)
337             if max(pos_centre2(i,*)) ne 0 then pos_centre3(i, (min(ind)+max(ind))/2)
=1000.

```

APPENDIX I. IDL ROUTINES

```

338     endfor
339 pos_centre=pos_centre3
340 endfor
341 endif
342
343
344 ;-----
345 ; Third try : Fourier series fit
346 ;-----
347
348 absc=oval_south_area_lon(where(oval_south_area_lon ne 0))
349 ordo=oval_south_area_lat(where(oval_south_area_lon ne 0))
350
351 theta=absc*!pi/180.
352 fitvect=ordo
353
354 fit_fourier_1d_mat,theta,fitvect,n_harmonic,par
355 x=findgen(3600.)/10.
356 fourier_s,x*!pi/180,par,y_f
357
358 me_track=fltarr(3600,1800)
359 me_track(10*x,y_f*10+900)=1.
360 me_track=shift(me_track,1800,0)
361
362
363 ;-----
364 ; Visualise the ribbon
365 ;-----
366
367 aurore_visu=fltarr(3600,1800)
368 aurore=fltarr(3600,1800)
369 aurore(10*x,y_f*10+900)=1000.
370 aurore(round(oval_south_area_lon*10.),round(oval_south_area_lat*10+900.))=
1000.
371 aurore=shift(aurore,1800,0)
372 aurore_visu(where(aurore ne 0))=aurore_visu(where(aurore ne 0))+1000.
373 aurore_visu=aurore_visu+implan_clean
374
375 pos_centre_visu=implan_clean
376 pos_centre_visu(where(pos_centre ne 0))=pos_centre_visu(where(pos_centre ne
0))+1000.
377
378 bpglobe,90-180.*(ephem_orb(st).lat_ssc lt 0.),0.,180.*(ephem_orb(st).lat_ssc
lt 0.),rotate(aurore_visu,5.*(ephem_orb(st).lat_ssc lt 0.)),res,/grid,/
horizon,/linscl, min=0., max=max(pos_centre), londel=10, latdel=10,
glinestyle=2
379 photo=tvrd(x_photo,y_photo,780,780,true=1)
380 tvlct, r,g,b,/get
381 fnameout='/home/LPAP/groulard/juno/' + pj + '/' + pj + '_test_centre_visu2_' + hemi + '.
png'
382 write_png, fnameout, photo, r, g, b
383
384 cent=pos_centre
385 cent=shift(cent, -900,0)
386 cent(lon_lat_bary(0)*10-20:lon_lat_bary(0)*10+20,lon_lat_bary(1)*10+900)=
1000.
387 cent(lon_lat_bary(0)*10,lon_lat_bary(1)*10+900-5:lon_lat_bary(1)*10+900+5)=
1000.
388 cent=shift(cent, 900,0)
389 bpglobe,90-180.*(ephem_orb(st).lat_ssc lt 0.),0.,180.*(ephem_orb(st).lat_ssc
lt 0.),rotate(cent,5.*(ephem_orb(st).lat_ssc lt 0.)),res,/horizon,/linscl,

```


APPENDIX I. IDL ROUTINES

```

min=0., max=max(pos_centre), londel=10, latdel=10, glinestyle=2
390 photo=tvrd(x_photo,y_photo,780,780,true=1)
391 tvlct, r,g,b,/get
392 fnameout='/home/LPAP/groulard/juno/'+pj+'/' +pj+'_test_centre2_'+hemi+'.png'
393 write_png,fnameout,photo,r,g,b
394
395
396 ;stop ; Stop here to only have the ribbon
397
398 ;-----
399 ; Create the final mask
400 ;-----
401
402 implan_south_area=fltarr(3600,1800)
403 oval_south_area_lon=fltarr(3600)
404 oval_south_area_lat=fltarr(3600)
405
406 proj_me_track=PROJPOL(smooth(me_track,3),512,512,0,-90,0)
407
408 for i=0,7200-1 do begin
409
410     if i mod 500 eq 0 then print, i
411
412     imrotov=rot(proj_me_track,i*0.05,1,pos_bary_s(0),pos_bary_s(1),/pivot) gt
0
413
414     indx=where(imrotov(pos_bary_s(0):pos_bary_s(0)+250,pos_bary_s(1)) ne 0)
415     indx=indx(floor(n_elements(indx)/2.))
416     indx2=indx+indgen(thickness_me)-floor(thickness_me/2)
417
418     pos_max=indx2
419
420     xp=pos_bary_s(0)+pos_max*cos(i*0.05/180.*!pi)
421     yp=pos_bary_s(1)+pos_max*sin(i*0.05/180.*!pi)
422
423     fi=atan((xp-512.)/((yp-512.)*1.))
424     teta=acos(((yp-512.)/512.)*(1./cos(fi)))
425     ind=where(teta gt !pi/2.)
426     if ind(0) ne -1 then teta(ind)=!pi-teta(ind)
427     if ind(0) ne -1 then fi(ind)=!pi+fi(ind)
428
429     oval_south_area_lon=-(-180.+fi*180./!pi) ;*(flag ne 1)
430     oval_south_area_lat=-teta*180./!pi;*(flag ne 1)
431
432     steps=20
433
434     order=sort(oval_south_area_lon)
435     oval_south_area_lon2=interpol(oval_south_area_lon(order),findgen(
n_elements(oval_south_area_lon)),findgen((n_elements(oval_south_area_lon)-1)
*steps)/steps)
436     oval_south_area_lat2=interpol(oval_south_area_lat(order),findgen(
n_elements(oval_south_area_lat)),findgen((n_elements(oval_south_area_lat)-1)
*steps)/steps)
437
438     indi=where(oval_south_area_lon2 lt 0)
439     if indi(0) ne -1 then oval_south_area_lon2(indi)=oval_south_area_lon2(
indi)+360.
440     indi=where(oval_south_area_lon2 gt 360)
441     if indi(0) ne -1 then oval_south_area_lon2(indi)=oval_south_area_lon2(
indi)-360.
442     indi=where(oval_south_area_lon lt 0)

```

APPENDIX I. IDL ROUTINES

```

443     if indi(0) ne -1 then oval_south_area_lon(indi)=oval_south_area_lon(indi)
+360.
444     indi=where(oval_south_area_lon gt 360)
445     if indi(0) ne -1 then oval_south_area_lon(indi)=oval_south_area_lon(indi)
-360.
446
447     indi=where(oval_south_area_lon2 gt min(oval_south_area_lon) and
oval_south_area_lon2 lt max(oval_south_area_lon))
448     oval_south_area_lon2=oval_south_area_lon2(indi)
449     oval_south_area_lat2=oval_south_area_lat2(indi)
450
451     implan_south_area(round(oval_south_area_lon*10.),round(oval_south_area_lat
*10+900.))=1.+i
452     endfor
453
454     implan_south_area=shift(implan_south_area,1800,0)
455
456
457     ;-----
458     ; Do 15 smoothing of the mask to cover the holes in the mask
459     ;-----
460
461     masque=fltarr(3600,1800) ; Array that will be used to be sure that the mask
does not extend during the smoothing.
462     masque_me=implan_south_area
463     masque_me=shift(masque_me,1800,0)
464     masque_me(3600-lon_lat_bary(0)*10.-150.:3600-lon_lat_bary(0)*10.+150.,
lon_lat_bary(1)*10.+875.:lon_lat_bary(1)*10.+925.)=0.
465     masque_me=shift(masque_me,1800,0)
466
467     ;if 1 eq 0 then begin
468     for i=0, 3599 do begin
469         ind_max=max(where(masque_me(i,*) ne 0))
470         ind_min=min(where(masque_me(i,*) ne 0))
471         masque(i,ind_min:ind_max)=1
472     endfor
473
474     masque_me_smooth=masque_me
475     ind=where(masque_me ne 0)
476     for i=0, 14 do begin
477         masque_me_smooth=smooth(masque_me_smooth,2)
478         masque_me_smooth(ind)=masque_me(ind)
479     endfor
480
481     masque_me=masque_me_smooth
482     masque_me=masque_me*masque
483     ;endif
484
485     ;-----
486     ; Images
487     ;-----
488
489     bpglobe,90-180.*(lat_sun lt 0.),0.,180.*(lat_sun lt 0.),rotate(masque_me
,5.*(lat_sun lt 0.)),res,/grid,/horizon,/linscl, min=0., max=7200, londel=10
, latdel=10, glinestyle=2
490     photo=tvrd(x_photo,y_photo,780,780,true=1)
491     tvlct, r,g,b,/get
492     fnameout='/home/LPAP/groulard/juno/'+pj+'/' +pj+'_mask_g2_'+hemi+'.png'
493     write_png,fnameout,photo,r,g,b
494
495     mask_on=implan_clean_visu

```


APPENDIX I. IDL ROUTINES

```

lon_lat_bary(1)*10.+875.:lon_lat_bary(1)*10.+925.)=0.
547     masque_me=shift(masque_me,1800,0)
548     endif
549     endif
550     endfor
551
552     implan_north_area=fltarr(3600,1800)
553     oval_north_area_lon=fltarr(3600)
554     oval_north_area_lat=fltarr(3600)
555     angl=fltarr(3600)
556     distance=fltarr(3600)
557
558
559     ;-----
560     ; Smooth the map to work on it later
561     ;-----
562
563     ind=where(implan_clean lt 25)
564     implan_clean2=smooth(implan_clean,21)
565     implan_clean2(ind)=0.
566     bpglobe,90-180.*(ephem_orb(st).lat_ssc lt 0.),0.,180.*(ephem_orb(st).lat_ssc
567     lt 0.),rotate(implan_clean2,5.*(ephem_orb(st).lat_ssc lt 0.)),res,/grid,/
568     horizon,/linscl, min=0., max=1000., londel=10, latdel=10, glinestyle=2
569
570     photo=tvrd(x_photo,y_photo,780,780,true=1)
571     tvlct, r,g,b,/get
572     fnameout='/home/LPAP/groulard/juno/' + pj + '/' + pj + '_smooth_' + hemi + '.png'
573     write_png, fnameout, photo, r, g, b
574
575     ind=where(implan_clean2 lt threshold*max(implan_clean2))
576     implan_clean3=implan_clean2
577     implan_clean3(ind)=0.
578     implan_clean3(where(implan_clean3 ne 0)) = 1.
579     bpglobe,90-180.*(ephem_orb(st).lat_ssc lt 0.),0.,180.*(ephem_orb(st).lat_ssc
580     lt 0.),rotate(implan_clean3,5.*(ephem_orb(st).lat_ssc lt 0.)),res,/horizon
581     ,/linscl, min=0., max=1., londel=10, latdel=10, glinestyle=2
582
583     photo=tvrd(x_photo,y_photo,780,780,true=1)
584     tvlct, r,g,b,/get
585     fnameout='/home/LPAP/groulard/juno/' + pj + '/' + pj + '_threshold_' + hemi + '.png'
586     write_png, fnameout, photo, r, g, b
587
588     pos_centre=fltarr(3600,1800)
589
590     print, max(implan_clean2)
591     oval_manual=PROJPOL(implan_clean2,512,512,!pi,-90,90)
592     val_max=max(oval_manual)
593     oval_bonfond=PROJPOL(masque_me,512,512,!pi,-90,90)
594
595     weight=[1,1,1,1.05,1.1,1.15,1.2,1.25,1.35,1.5,1.6,1.65,1.65,1.55,1.45,1.45,1
596     .35,1.35,1.35,1.35,1.35,1.35,1.35,1.35,1.35,1.35,1.45,1.55,1.65,1.9,2,2.1,1.8,1
597     .5,1.1,1,1]
598
599     ;-----
600     ; Create the 1 thickness mask (ribbon)
601     ;-----
602
603     for i=0, 3599 do begin
604
605         if i mod 500 eq 0 then print, i
606

```

APPENDIX I. IDL ROUTINES

```

601 ; -----
602 ; Find the centre of the b mask for each slice
603 ; -----
604
605 imrotbo=rot(oval_bonfond,i*0.1,1,pos_bary_n(0),pos_bary_n(1),/pivot)
606 ind1=min(where(imrotbo(pos_bary_n(0):*,pos_bary_n(1)) ne 0))
607 ind2=max(where(imrotbo(pos_bary_n(0):*,pos_bary_n(1)) ne 0))
608 dista=round((ind1+ind2)/2)
609 ;print, dista
610
611 imrotov=rot(oval_manual,i*0.1,1,pos_bary_n(0),pos_bary_n(1),/pivot)
612
613
614 ; -----
615 ; Create the mask based on the centre just found
616 ; -----
617
618 indx=0
619 val=0
620
621 for k=0,2 do begin ; If no data is found, look for greater distances to
the b mask.
622     if val eq 0. then begin
623         if dista-(2^k)*delta_minus lt weight(round(i/100))*polar then j_min =
weight(round(i/100))*polar else j_min=dista-(2^k)*delta_minus
624         for j=j_min, dista+delta_plus do begin
625             if imrotov(pos_bary_n(0)+j,pos_bary_n(1)) gt threshold*val_max and
imrotov(pos_bary_n(0)+j,pos_bary_n(1)) gt val then begin ; If the brightness
is high, this is the main emission for sure...
626                 indx = j
627                 val = imrotov(pos_bary_n(0)+j,pos_bary_n(1))
628             endif else begin ; ... if not, look for the greatest gradient.
629                 val1=imrotov(pos_bary_n(0)+j-1,pos_bary_n(1))
630                 val2=imrotov(pos_bary_n(0)+j,pos_bary_n(1))
631                 if val1 ne 0 and val2 ne 0 then begin
632                     if abs(val2-val1) gt val then begin
633                         indx = j
634                         val = abs(val2-val1)
635                     endif
636                 endif
637             endelse
638         endfor
639     endif
640 endfor
641 ;endif
642
643
644 ; -----
645 ; Forcing
646 ; -----
647
648 if pj eq 'PJ4' then begin
649     if i lt 2400 and i gt 2000 then indx = indx-10
650 endif
651
652 if pj eq 'PJ7' then begin
653     if indx ne 0 then begin
654         if i gt 3100 and i lt 3200 then indx=indx+10
655         if i gt 3200 and i lt 3250 then indx=indx+20
656         if i gt 3250 and i lt 3300 then indx=indx+30
657         if i gt 3300 and i lt 3400 then indx=indx+25

```

APPENDIX I. IDL ROUTINES

```
658         if i gt 3400 and i lt 3500 then indx=indx+20
659     endif
660 endif
661
662 if pj eq 'PJ8' then begin
663     if indx ne 0 then begin
664         if i gt 1500 and i lt 1650 and indx gt 80 then indx=indx-10
665         if i gt 1750 and i lt 2150 and indx gt 80 then indx=indx-15
666         if i gt 2150 and i lt 2400 and indx gt 80 then indx=indx-25
667         if i gt 2400 and i lt 2650 and indx gt 80 then indx=indx-20
668         if i gt 2650 and i lt 2800 and indx gt 80 then indx=indx-15
669         if i gt 2800 and i lt 3000 and indx gt 80 then indx=indx-10
670     endif
671 endif
672
673 if pj eq 'PJ9' then begin
674     if indx ne 0 then begin
675         if i gt 1350 and i lt 1800 and indx gt 80 then indx=indx-15
676         if i gt 1800 and i lt 2250 and indx gt 80 then indx=indx-20
677         if i gt 2250 and i lt 2700 and indx gt 80 then indx=indx-15
678         if i gt 2800 and i lt 3000 and indx gt 80 then indx=indx-15
679         if i gt 3000 and i lt 3100 and indx gt 80 then indx=indx-10
680     endif
681 endif
682
683 if pj eq 'PJ11' then begin
684     if indx ne 0 then begin
685         if i gt 1800 and i lt 1900 and indx gt 80 then indx=indx-9
686         if i gt 2900 and i lt 3250 and indx gt 80 then indx=indx-7
687     endif
688 endif
689
690 if pj eq 'PJ13' then begin
691     if i gt 3150 and i lt 3400 then indx=180
692     if indx ne 0 then begin
693         if i gt 1700 and i lt 2700 and indx gt 80 then indx=indx-5
694     endif
695 endif
696
697 if pj eq 'PJ14' then begin
698     if indx ne 0 then begin
699         if i gt 1200 and i lt 2700 and indx gt 80 then indx=indx-5
700     endif
701 endif
702
703 if pj eq 'PJ15' then begin
704     if indx ne 0 then begin
705         if i gt 450 and i lt 650 and indx gt 80 then indx=indx-10
706         if i gt 1600 and i lt 1700 and indx gt 80 then indx=indx+10
707         if i gt 2700 and i lt 3150 and indx gt 80 then indx=indx-10
708         if i gt 3300 and i lt 3450 and indx gt 80 then indx=indx+10
709     endif
710 endif
711
712 if pj eq 'PJ16' then begin
713     if i gt 3150 and i lt 3470 then indx=175
714     if indx ne 0 then begin
715         if i gt 900 and i lt 1800 and indx gt 70 then indx=indx-5
716         if i gt 1800 and i lt 2000 and indx gt 70 then indx=indx-10
717         if i gt 2000 and i lt 3050 and indx gt 70 then indx=indx-5
718         if i gt 3050 and i lt 3150 and indx gt 70 then indx=indx-10
```

APPENDIX I. IDL ROUTINES

```

719     endif
720 endif
721
722 if pj eq 'PJ17' then begin
723     if i gt 3150 and i lt 3400 then indx=175
724     if indx ne 0 then begin
725         if i gt 1350 and i lt 1800 and indx gt 70 then indx=indx-5
726         if i gt 1800 and i lt 2000 and indx gt 70 then indx=indx-10
727         if i gt 2000 and i lt 2700 and indx gt 70 then indx=indx-5
728     endif
729 endif
730
731 if pj eq 'PJ19' then begin
732     if i gt 3050 and i lt 3450 then indx=170
733     if indx ne 0 then begin
734         if i gt 450 and i lt 900 and indx gt 70 then indx=indx-5
735         if i gt 900 and i lt 1300 and indx gt 70 then indx=indx+5
736     endif
737 endif
738
739 if pj eq 'PJ20' then begin
740     if indx ne 0 then begin
741         if i gt 1700 and i lt 1900 and indx gt 70 then indx=indx-10
742         if i gt 1900 and i lt 2400 and indx gt 70 then indx=indx-15
743         if i gt 2400 and i lt 3150 and indx gt 70 then indx=indx-10
744     endif
745 endif
746
747 if pj eq 'PJ21' then begin
748     if indx ne 0 then begin
749         if i gt 1800 and i lt 2400 and indx gt 70 then indx=indx-15
750         if i gt 2400 and i lt 2700 and indx gt 70 then indx=indx-5
751         if i gt 3050 and i lt 3200 and indx gt 70 then indx=indx-5
752     endif
753 endif
754
755 if pj eq 'PJ22' then begin
756     if indx ne 0 then begin
757         if i gt 1700 and i lt 2200 and indx gt 70 then indx=indx-15
758         if i gt 2200 and i lt 2700 and indx gt 70 then indx=indx-10
759         if i gt 2700 and i lt 2900 and indx gt 70 then indx=indx-5
760         if i gt 2900 and i lt 3000 and indx gt 70 then indx=indx-15
761     endif
762 endif
763
764 if pj eq 'PJ23' then begin
765     if indx ne 0 then begin
766         if i gt 1300 and i lt 2700 and indx gt 70 then indx=indx-15
767     endif
768 endif
769
770 if pj eq 'PJ24' then begin
771     if i gt 3150 and i lt 3400 then indx=175
772     if indx ne 0 then begin
773         if i gt 1700 and i lt 2300 and indx gt 70 then indx=indx-5
774     endif
775 endif
776
777 if pj eq 'PJ26' then begin
778     if indx ne 0 then begin
779         if i gt 450 and i lt 1000 and indx gt 70 then indx=indx-10

```


APPENDIX I. IDL ROUTINES

```
780         if i gt 1800 and i lt 2600 and indx gt 70 then indx=indx-10
781         if i gt 2600 and i lt 3100 and indx gt 70 then indx=indx-5
782         if i gt 3200 and i lt 3400 and indx gt 70 then indx=indx+5
783     endif
784 endif
785
786 if pj eq 'PJ32' then begin
787     if indx ne 0 then begin
788         if i gt 1350 and i lt 1700 and indx gt 70 then indx=indx-15
789         if i gt 1700 and i lt 1850 and indx gt 70 then indx=indx-10
790         if i gt 1850 and i lt 2250 and indx gt 70 then indx=indx-15
791         if i gt 2700 and i lt 3150 and indx gt 70 then indx=indx-5
792     endif
793 endif
794
795 if pj eq 'PJ33' then begin
796     if indx ne 0 then begin
797         if i gt 700 and i lt 900 and indx gt 70 then indx=indx-15
798         if i gt 1850 and i lt 2300 and indx gt 70 then indx=indx-10
799     endif
800 endif
801
802 if pj eq 'PJ34' then begin
803     if indx ne 0 then begin
804         if i gt 1800 and i lt 2400 and indx gt 70 then indx=indx-10
805         if i gt 2600 and i lt 3200 and indx gt 70 then indx=indx-5
806     endif
807 endif
808
809 if pj eq 'PJ35' then begin
810     if indx ne 0 then begin
811         if i gt 1800 and i lt 2700 and indx gt 70 then indx=indx-10
812     endif
813 endif
814
815 if pj eq 'PJ36' then begin
816     if i gt 3150 and i lt 3500 then indx=175
817     if indx ne 0 then begin
818         if i gt 0 and i lt 200 and indx gt 70 then indx=indx+15
819         if i gt 200 and i lt 300 and indx gt 70 then indx=indx+10
820         if i gt 1100 and i lt 2000 and indx gt 70 then indx=indx-5
821         if i gt 2600 and i lt 2900 and indx gt 70 then indx=indx-5
822     endif
823 endif
824
825 if pj eq 'PJ37' then begin
826     if i gt 3000 and i lt 3400 then indx=175
827     if indx ne 0 then begin
828         if i gt 1100 and i lt 1700 and indx gt 70 then indx=indx-10
829         if i gt 1800 and i lt 2250 and indx gt 70 then indx=indx-20
830         if i gt 2250 and i lt 3000 and indx gt 70 then indx=indx-15
831     endif
832 endif
833
834 if pj eq 'PJ38' then begin
835     if indx ne 0 then begin
836         if i gt 700 and i lt 900 and indx gt 70 then indx=indx-5
837         if i gt 1800 and i lt 2350 and indx gt 70 then indx=indx-10
838         if i gt 2350 and i lt 2600 and indx gt 70 then indx=indx-5
839         if i gt 2700 and i lt 3300 and indx gt 70 then indx=indx-5
840     endif
```

APPENDIX I. IDL ROUTINES

```

841     endif
842
843     if pj eq 'PJ39' then begin
844         if i gt 3000 and i lt 3400 then indx=175
845         if indx ne 0 then begin
846             if i gt 1350 and i lt 2250 and indx gt 70 then indx=indx-10
847             if i gt 2250 and i lt 2700 and indx gt 70 then indx=indx-5
848         endif
849     endif
850
851     if indx ne 0 then begin
852         angl(i)=i*0.1
853         distance(i)=indx
854     endif
855
856     endfor
857
858
859     ;-----
860     ; Smooth the ribbon
861     ;-----
862
863
864     ;-----
865     ; Fourier series fit
866     ;-----
867
868     absc=angl(where(distance ne 0))
869     ordo=distance(where(distance ne 0))
870
871     theta=absc*!dior
872     fitvect=ordo
873
874     fit_fourier_1d_mat,theta,fitvect,n_harmonic,par
875     x=findgen(7200.)/20.
876     fourier_s,x*!pi/180,par,y_f
877
878
879     ;-----
880     ; Visualise the ribbon
881     ;-----
882
883     aurore_visu=projpol(implan_clean_visu,512,512,!pi,-90,90)
884     for i=0, 3600-1 do begin
885         aurore_visu(pos_bary_n(0)+distance(i)*cos(i*!dior/10), pos_bary_n(1)+
886         distance(i)*sin(i*!dior/10))=1000
887     endfor
888
889     dgtv, congrid(aurore_visu,1024,1024)
890     photo=tvrd(256,160,512,512,true=1)
891     tvlct, r,g,b,/get
892     fnameout='/home/LPAP/groulard/juno/'+pj+'/' +pj+'_test_centre_visu2_'+hemi+'.
893     png'
894     write_png,fnameout,photo,r,g,b
895
896     cent=fltarr(1024,1024)
897     for i=0, 3600-1 do begin
898         cent(pos_bary_n(0)+distance(i)*cos(i*!dior/10), pos_bary_n(1)+distance(i)*
899         sin(i*!dior/10))=1000
900     endfor
901
902
903
904
905
906
907
908

```

APPENDIX I. IDL ROUTINES

```

899   dgtv, congrid(cent,1024,1024)
900   photo=tvrd(256,160,512,512,true=1)
901   tvlct, r,g,b,/get
902   fnameout='/home/LPAP/groulard/juno/'+pj+'/' +pj+'_test_centre2_'+hemi+'.png'
903   write_png, fnameout, photo, r, g, b
904
905 ;stop ; Stop here to only have the ribbon
906
907 ;-----
908 ; Create the final mask
909 ;-----
910
911   oval_north_area_lon=fltarr(3600)
912   oval_north_area_lat=fltarr(3600)
913
914   proj_me_track=PROJPOL(smooth(implan_north_area,3),512,512,0,-90,0)
915
916   for i=0,7200-1 do begin
917
918       if i mod 1000 eq 0 then print, i
919
920       indx=y_f(i)
921       indx2=indx+indgen(thickness_me*50.)/50.-floor(thickness_me/2)
922
923       pos_max=indx2
924       ;pos_max=indx
925
926       xp=pos_bary_n(0)+pos_max*cos(i*0.05/180.*!pi)
927       yp=pos_bary_n(1)+pos_max*sin(i*0.05/180.*!pi)
928
929       fi=atan((xp-512.)/((yp-512.)*1.))
930       teta=acos(((yp-512.)/512.)*(1./cos(fi)))
931       ind=where(teta gt !pi/2.)
932       if ind(0) ne -1 then teta(ind)=!pi-teta(ind)
933       if ind(0) ne -1 then fi(ind)=!pi+fi(ind)
934
935       oval_north_area_lon=-(-180.+fi*180./!pi)
936       oval_north_area_lat=teta*180./!pi
937
938       steps=20
939
940       order=sort(oval_north_area_lon)
941       oval_north_area_lon2=interpol(oval_north_area_lon(order),findgen(
n_elements(oval_north_area_lon)),findgen((n_elements(oval_north_area_lon)-1)
*steps)/steps)
942       oval_north_area_lat2=interpol(oval_north_area_lat(order),findgen(
n_elements(oval_north_area_lat)),findgen((n_elements(oval_north_area_lat)-1)
*steps)/steps)
943
944       indi=where(oval_north_area_lon2 lt 0)
945       if indi(0) ne -1 then oval_north_area_lon2(indi)=oval_north_area_lon2(
indi)+360.
946       indi=where(oval_north_area_lon2 gt 360)
947       if indi(0) ne -1 then oval_north_area_lon2(indi)=oval_north_area_lon2(
indi)-360.
948       indi=where(oval_north_area_lon lt 0)
949       if indi(0) ne -1 then oval_north_area_lon(indi)=oval_north_area_lon(indi)
+360.
950       indi=where(oval_north_area_lon gt 360)
951       if indi(0) ne -1 then oval_north_area_lon(indi)=oval_north_area_lon(indi)
-360.

```

APPENDIX I. IDL ROUTINES

```

952
953     indi=where(oval_north_area_lon2 gt min(oval_north_area_lon) and
oval_north_area_lon2 lt max(oval_north_area_lon))
954     oval_north_area_lon2=oval_north_area_lon2(indi)
955     oval_north_area_lat2=oval_north_area_lat2(indi)
956
957     implan_north_area(round(oval_north_area_lon*10.),round(oval_north_area_lat
*10+900.))=1.+i
958     endfor
959
960     ;implan_south_area=shift(implan_south_area,1800,0)
961
962     masque_me=implan_north_area
963
964     ;-----
965     ; Images
966     ;-----
967
968     bpglobe,90-180.*(lat_sun lt 0.),0.,180.*(lat_sun lt 0.),rotate(masque_me
,5.*(lat_sun lt 0.)),res,/horizon,/linscl, min=0., max=7200, londel=10,
latdel=10, glinestyle=2
969     photo=tvrd(x_photo,y_photo,780,780,true=1)
970     tvlct, r,g,b,/get
971     fnameout='/home/LPAP/groulard/juno/'+pj+'/' +pj+'_mask_g2_'+hemi+'.png'
972     write_png,fnameout,photo,r,g,b
973
974     mask_on=implan_clean_visu
975     ind=where(masque_me ne 0)
976     mask_on(ind)=1000
977     bpglobe,90-180.*(lat_sun lt 0.),0.,180.*(lat_sun lt 0.),rotate(mask_on,5.*(
lat_sun lt 0.)),res,/grid,/horizon,/linscl, min=0., max=1000, londel=10,
latdel=10, glinestyle=2
978
979     photo=tvrd(x_photo,y_photo,780,780,true=1)
980     tvlct, r,g,b,/get
981     fnameout='/home/LPAP/groulard/juno/'+pj+'/' +pj+'_mask_on_g2_'+hemi+'.png'
982     write_png,fnameout,photo,r,g,b
983
984     mask_add_on=implan_clean_visu
985     ind=where(masque_me ne 0)
986     mask_add_on(ind)=mask_add_on(ind)+400.
987     bpglobe,90-180.*(lat_sun lt 0.),0.,180.*(lat_sun lt 0.),rotate(mask_add_on
,5.*(lat_sun lt 0.)),res,/grid,/horizon,/linscl, min=0., max=max(mask_add_on
), londel=10, latdel=10, glinestyle=2
988
989     photo=tvrd(x_photo,y_photo,780,780,true=1)
990     tvlct, r,g,b,/get
991     fnameout='/home/LPAP/groulard/juno/'+pj+'/' +pj+'_mask_add_on_g2_'+hemi+'.png'
,
992     write_png,fnameout,photo,r,g,b
993
994     endif
995
996     save, filename='/home/LPAP/groulard/juno/'+pj+'/' +pj+'_masque_g_'+pj+'_'+hemi+'.idl',
masque_me
997
998 end

```

create_me_mask_groulard_vari.pro

```

1 pro create_me_mask_groulard_vari, pj, hemi, delta, threshold1, threshold2,
  n_harmonic_int, n_harmonic_ext, sym
2 ; pj = perijove number. 'PJ#' in entry.
3 ; hemi = hemisphere. 'N' or 'S' in entry.
4 ; delta = maximum difference to the b mask.
5 ; threshold1 = threshohld of brightness in an area to look for the peak (
  regarding the maximum brightness of the slice). 0.X in entry.
6 ; threshold2 = threshold of brightness to modifie the width of the mask (
  regarding the maximum brightness of the mask). 0.X in entry.
7 ; n_harmonic_int = number of harmonics for the Fourier fit (internal ribbon).
8 ; n_harmonic_ext = number of harmonics for the Fourier fit (external ribbon).
9 ; sym = symmetry on delta : 1 -> symmetrical. ; 2 -> delta only applied inside
  of the g mask. ; 3 -> delta only applied outside of the g mask.
10
11
12 if sym ne 1 and sym ne 2 and sym ne 3 then sym = 1
13 if sym eq 1 then begin
14   delta_minus = delta
15   delta_plus = delta
16 endif
17 if sym eq 2 then begin
18   delta_minus = delta
19   delta_plus = 0.
20 endif
21 if sym eq 3 then begin
22   delta_minus = 0
23   delta_plus = delta
24 endif
25
26 ;           SOUTH                               NORTH
27
28 ; 1 : 'PJ1'  , 'S', 20,0.6 ,0.15, 9,3,1
29 ; 3 : 'PJ3'  , 'S', 10,0.7 ,0.1 ,10,4,1
30 ; 5 : 'PJ5'  , 'S', 20,0.7 ,0.1 ,10,4,1
31 ;
32 ;
33 ; 10 : 'PJ10', 'S', 40,0.3 ,0.05, 4,4,2
34 ; 12 : 'PJ12', 'S', 15,0.5 ,0.1 , 5,4,1
35 ;
36 ; 15 : 'PJ15', 'S', 40,0.2 ,0.25, 3,4,2
37 ; 18 : 'PJ18', 'S', 10,0.2 ,0.25, 4,4,1
38 ; 19 : 'PJ19', 'S', 35,0.7 ,0.1 , 6,4,2
39 ;
40 ; 21 : 'PJ21', 'S', 3,0.7 ,0.1 , 4,4,1
41 ; 23 : 'PJ23', 'S', 15,0.5 ,0.1 , 4,4,1
42 ; 25 : 'PJ25', 'S', 40,0.6 ,0.05, 6,4,2
43 ; 27 : 'PJ27', 'S', 25,0.7 ,0.1 , 6,4,2
44 ; 28 : 'PJ28', 'S', 20,0.8 ,0.2 ,25,4,2
45 ; 29 : 'PJ29', 'S', 20,0.4 ,0.1 , 6,4,2
46 ; 31 : 'PJ31', 'S', 45,0.99,0.2 , 6,4,2
47 ; 32 : 'PJ32', 'S', 35,0.7 ,0.1 , 6,4,1
48 ; 33 : 'PJ33', 'S', 20,0.6 ,0.1 ,10,4,2
49 ; 35 : 'PJ35', 'S', 20,0.4 ,0.3 , 10,6,1
50 ; 38 : 'PJ38', 'S', 30,0.4 ,0.2 ,15,4,2
51
52
53 restore, '/home/LPAP/groulard/juno/'+pj+'/auroral_power_'+pj+'_'+hemi+'.idl'
54 loadct,1, file='/home/LPAP/groulard/Memoire/colors_blwh01.tbl'

```

APPENDIX I. IDL ROUTINES

```

55  restore, '/LPAP/HST/redu/juno/'+pj+'/ephem/'+pj+'_ephem03.idl'
56  restore, '/home/LPAP/groulard/juno/'+pj+'/masque_g_'+pj+'_'+hemi+'.idl'
57
58
59 ; -----
60 ; |                               South                               |
61 ; -----
62
63
64  if hemi eq 'S' then begin
65
66      lon_lat_bary=[31.9209,-81.9309]
67      pos_bary_s=[474.,451.]
68      x_photo=438
69      y_photo=460
70
71      angl=fltarr(3600)
72      deb_arr=fltarr(3600)
73      fin_arr=fltarr(3600)
74
75      ; -----
76      ; Bin the brightness map
77      ; -----
78
79      implan_clean2=implan_clean
80      for i=0, 180-1 do begin
81          profil=fltarr(1800)
82          for j=0, 19 do begin
83              profil=profil+implan_clean(20*i+j,*)
84          endfor
85          for j=0, 19 do begin
86              implan_clean2(20*i+j,*)=profil
87          endfor
88      endfor
89
90      bpglobe,90-180.*(ephem_orb(st).lat_ssc lt 0.),0.,180.*(ephem_orb(st).lat_ssc
91      lt 0.),rotate(implan_clean2,5.*(ephem_orb(st).lat_ssc lt 0.)),res,/grid,/
92      horizon,/linscl, min=0., max=max(implan_clean2), londel=10, latdel=10,
93      glinestyle=2
94
95      photo=tvrd(x_photo,y_photo,780,780,true=1)
96      tvlct, r,g,b,/get
97      fnameout='/home/LPAP/groulard/juno/'+pj+'/'+pj+'_implan_clean2_'+hemi+'.png'
98      write_png,fnameout,photo,r,g,b
99
100
101      oval_manual=PROJPOL(implan_clean2,512,512,0,-90,0)
102      masque_manual=PROJPOL(masque_me,512,512,0,-90,0)
103      masque_manual(where(masque_manual lt 0.1))=0.
104
105      implan_south_area=fltarr(3600,1800)
106      oval_south_area_lon=fltarr(3600)
107      oval_south_area_lat=fltarr(3600)
108
109      ind=where(masque_me ne 0)
110      implan=implan_clean2(ind)
111      max_mask=max(implan)
112
113      implan_clean3=implan_clean2
114      ind=where(implan_clean2 lt threshold2*max_mask)
115      implan_clean3(ind)=0
116      bpglobe,90-180.*(ephem_orb(st).lat_ssc lt 0.),0.,180.*(ephem_orb(st).lat_ssc

```

APPENDIX I. IDL ROUTINES

```

    lt 0.),rotate(implan_clean3,5.*(ephem_orb(st).lat_ssc lt 0.)),res,/grid,/
horizon,/linscl, min=0., max=max(implan_clean3), londel=10, latdel=10,
glinestyle=2
113
114 photo=tvrd(x_photo,y_photo,780,780,true=1)
115 tvlct, r,g,b,/get
116 fnameout='/home/LPAP/groulard/juno/'+pj+'/' +pj+'_implan_clean2_threshold_'+
hemi+'.png'
117 write_png,fnameout,photo,r,g,b
118
119
120 ;-----
121 ; Search the inner and outer limits of the mask
122 ;-----
123
124 for i=0, 3599 do begin
125
126     if i mod 500 eq 0 then print, i
127
128     imrotov=rot(oval_manual,i*0.1,1,pos_bary_s(0),pos_bary_s(1),/pivot)
129     imrotma=rot(masque_manual,i*0.1,1,pos_bary_s(0),pos_bary_s(1),/pivot)
130
131     ind0=where(imrotma(pos_bary_s(0):*,pos_bary_s(1)) gt 0.8*max(imrotma(
pos_bary_s(0):*,pos_bary_s(1))))
132     ind1=min(ind0)
133     ind2=max(ind0)
134
135     coupe=imrotov(pos_bary_s(0)+ind1:pos_bary_s(0)+ind2,pos_bary_s(1))
136     ind3=where(coupe eq max(coupe))
137     maxi=max(coupe)
138
139     if maxi ge threshold2*max_mask then begin ; If we are in a high
brightness region, the G1 mask is modified. If not, it is kept.
140         if ind1-delta_minus lt 0 then ind_min=0 else ind_min=ind1-delta_minus
141         if ind2+delta_plus gt 512 then ind_max=512 else ind_max=ind2+delta_plus
142
143         coupe2=imrotov(pos_bary_s(0):*,pos_bary_s(1))
144         ind4=where(coupe2 gt threshold1*maxi) ; Found the region where the mask
is bright enough to be modified ...
145         ind5=ind4(where(ind4 ge ind_min and ind4 le ind_max)) ; ... and limit
this region to the area of interest around the G1 mask ...
146         debut=min(ind5)-5 ; ... with a small margin to encompass the edges of
the region.
147         fin=max(ind5)+5
148         if debut gt ind1 then debut=ind1 ; The new mask has to be at least the
width of the G1 mask.
149         if fin lt ind2 then fin=ind2
150     endif else begin
151         debut=ind1
152         fin=ind2
153     endelse
154
155     angl(i)=i*0.1
156     deb_arr(i)=debut
157     fin_arr(i)=fin
158 endfor
159
160 inter=fltarr(1024,1024)
161 for i=0, 3600-1 do begin
162     inter(pos_bary_s(0)+deb_arr(i)*cos(i*!dior/10), pos_bary_s(1)+deb_arr(i)*
sin(i*!dior/10))=1000

```

APPENDIX I. IDL ROUTINES

```

163     inter(pos_bary_s(0)+fin_arr(i)*cos(i*!dtor/10), pos_bary_s(1)+fin_arr(i)*
sin(i*!dtor/10))=1000
164     endfor
165
166     dgtv, congrid(inter,1024,1024)
167     photo=tvrd(256,160,512,512,true=1)
168     tvlct, r,g,b,/get
169     fnameout='/home/LPAP/groulard/juno/'+pj+'/' +pj+'_inter_g2_'+hemi+'.png'
170     write_png,fnameout,photo,r,g,b
171
172
173     ;-----
174     ; Smooth the inner edge of the mask (inner ribbon)
175     ;-----
176
177     absc=angl(where(deb_arr ne 0))
178     ordo=deb_arr(where(deb_arr ne 0))
179
180     theta=absc*!dtor
181     fitvect=ordo
182
183     fit_fourier_1d_mat,theta,fitvect,n_harmonic_int,par
184     x=findgen(7200.)/20.
185     fourier_s,x*!pi/180,par,y_f
186
187
188     ;-----
189     ; Smooth the outer edge of the mask (outer ribbon)
190     ;-----
191
192     absc=angl(where(fin_arr ne 0))
193     ordo=fin_arr(where(fin_arr ne 0))
194
195     theta=absc*!dtor
196     fitvect=ordo
197
198     fit_fourier_1d_mat,theta,fitvect,n_harmonic_ext,par
199     x=findgen(7200.)/20.
200     fourier_s,x*!pi/180,par,y_f2
201
202
203     ;-----
204     ; Create the mask based on the two ribbons
205     ;-----
206
207     for i=0, 7199 do begin
208
209         if i mod 1000 eq 0 then print, i
210         thickness_me=y_f2(i)-y_f(i)
211         if thickness_me eq 0 then thickness_me=1.
212
213
214         indx=y_f(i)+indgen(thickness_me*20.)/20.
215
216         pos_max=indx
217
218         xp=pos_bary_s(0)+pos_max*cos(i*0.05/180.*!pi)
219         yp=pos_bary_s(1)+pos_max*sin(i*0.05/180.*!pi)
220
221         fi=atan((xp-512.)/((yp-512.)*1.))
222         teta=acos(((yp-512.)/512.)*(1./cos(fi)))

```


APPENDIX I. IDL ROUTINES

```

223     ind=where(teta gt !pi/2.)
224     if ind(0) ne -1 then teta(ind)=!pi-teta(ind)
225     if ind(0) ne -1 then fi(ind)=!pi+fi(ind)
226
227     oval_south_area_lon=-(-180.+fi*180./!pi)
228     oval_south_area_lat=-teta*180./!pi
229
230     steps=20
231
232     order=sort(oval_south_area_lon)
233     oval_south_area_lon2=interpol(oval_south_area_lon(order),findgen(
n_elements(oval_south_area_lon)),findgen((n_elements(oval_south_area_lon)-1
*steps)/steps)
234     oval_south_area_lat2=interpol(oval_south_area_lat(order),findgen(
n_elements(oval_south_area_lat)),findgen((n_elements(oval_south_area_lat)-1
*steps)/steps)
235
236     indi=where(oval_south_area_lon2 lt 0)
237     if indi(0) ne -1 then oval_south_area_lon2(indi)=oval_south_area_lon2(
indi)+360.
238     indi=where(oval_south_area_lon2 gt 360)
239     if indi(0) ne -1 then oval_south_area_lon2(indi)=oval_south_area_lon2(
indi)-360.
240     indi=where(oval_south_area_lon lt 0)
241     if indi(0) ne -1 then oval_south_area_lon(indi)=oval_south_area_lon(indi)
+360.
242     indi=where(oval_south_area_lon gt 360)
243     if indi(0) ne -1 then oval_south_area_lon(indi)=oval_south_area_lon(indi)
-360.
244
245     indi=where(oval_south_area_lon2 gt min(oval_south_area_lon) and
oval_south_area_lon2 lt max(oval_south_area_lon))
246     oval_south_area_lon2=oval_south_area_lon2(indi)
247     oval_south_area_lat2=oval_south_area_lat2(indi)
248
249     implan_south_area(round(oval_south_area_lon*10.),round(oval_south_area_lat
*10+900.))=1.+i
250     endfor
251
252     implan_south_area=shift(implan_south_area,1800,0)
253     masque_me=implan_south_area
254
255     ;-----
256     ; Images
257     ;-----
258
259     bpglobe,90-180.*(lat_sun lt 0.),0.,180.*(lat_sun lt 0.),rotate(masque_me
,5.*(lat_sun lt 0.)),res,/grid,/horizon,/linscl, min=0., max=7200, londel=10
, latdel=10, glinestyle=2
260     photo=tvrd(x_photo,y_photo,780,780,true=1)
261     tvlct, r,g,b,/get
262     fnameout='/home/LPAP/groulard/juno/'+pj+'/' +pj+'_mask_g_vari_'+hemi+'.png'
263     write_png,fnameout,photo,r,g,b
264
265     mask_add_on=implan_clean_visu
266     ind=where(masque_me ne 0)
267     mask_add_on(ind)=mask_add_on(ind)+400.
268     bpglobe,90-180.*(lat_sun lt 0.),0.,180.*(lat_sun lt 0.),rotate(mask_add_on
,5.*(lat_sun lt 0.)),res,/grid,/horizon,/linscl, min=0., max=max(mask_add_on
), londel=10, latdel=10, glinestyle=2
269

```

APPENDIX I. IDL ROUTINES

```

270   photo=tvrd(x_photo,y_photo,780,780,true=1)
271   tvlct, r,g,b,/get
272   fnameout='/home/LPAP/groulard/juno/'+pj+'/' +pj+'_mask_add_on_g_vari_'+hemi+'
      .png'
273   write_png,fnameout,photo,r,g,b
274
275   save, filename='/home/LPAP/groulard/juno/'+pj+'masque_g2_'+pj+'_'+hemi+'.
      idl', masque_me
276 endif
277
278
279 ; -----
280 ; |                               North                               |
281 ; -----
282
283
284 if hemi eq 'N' then begin
285
286   lon_lat_bary=[185.670,73.9340]
287   pos_bary_n=[498.,371.]
288   x_photo=363
289   y_photo=170
290
291   angl=fltarr(3600)
292   deb_arr=fltarr(3600)
293   fin_arr=fltarr(3600)
294
295   ; -----
296   ; Bin the brightness map
297   ; -----
298
299   implan_clean2=implan_clean
300   for i=0, 180-1 do begin
301     profil=fltarr(1800)
302     for j=0, 19 do begin
303       profil=profil+implan_clean(20*i+j,*)
304     endfor
305     for j=0, 19 do begin
306       implan_clean2(20*i+j,*)=profil
307     endfor
308   endfor
309
310   bpglobe,90-180.*(ephem_orb(st).lat_ssc lt 0.),0.,180.*(ephem_orb(st).lat_ssc
      lt 0.),rotate(implan_clean2,5.*(ephem_orb(st).lat_ssc lt 0.)),res,/grid,/
      horizon,/linscl, min=0., max=max(implan_clean2), londel=10, latdel=10,
      glinestyle=2
311
312   photo=tvrd(x_photo,y_photo,780,780,true=1)
313   tvlct, r,g,b,/get
314   fnameout='/home/LPAP/groulard/juno/'+pj+'/' +pj+'_implan_clean2_'+hemi+'.png'
315   write_png,fnameout,photo,r,g,b
316
317   oval_manual=PROJPOL(implan_clean2,512,512,!pi,-90,90)
318   masque_manual=PROJPOL(masque_me,512,512,!pi,-90,90)
319
320   implan_north_area=fltarr(3600,1800)
321   oval_north_area_lon=fltarr(3600)
322   oval_north_area_lat=fltarr(3600)
323
324   ind=where(masque_me ne 0)
325   implan=implan_clean2(ind)

```

APPENDIX I. IDL ROUTINES

```

326     max_mask=max(implan)
327
328     implan_clean3=implan_clean2
329     ind=where(implan_clean2 lt threshold2*max_mask)
330     implan_clean3(ind)=0
331     bpglobe,90-180.*(ephem_orb(st).lat_ssc lt 0.),0.,180.*(ephem_orb(st).lat_ssc
    lt 0.),rotate(implan_clean3,5.*(ephem_orb(st).lat_ssc lt 0.)),res,/grid,/
    horizon,/linscl, min=0., max=max(implan_clean3), londel=10, latdel=10,
    glinestyle=2
332
333     photo=tvrd(x_photo,y_photo,780,780,true=1)
334     tvlct, r,g,b,/get
335     fnameout='/home/LPAP/groulard/juno/'+pj+'/' +pj+'_implan_clean2_threshold_'+
    hemi+'.png'
336     write_png,fnameout,photo,r,g,b
337
338
339     ;-----
340     ; Search the inner and outer limits of the mask
341     ;-----
342
343     for i=0, 3599 do begin
344
345         if i mod 500 eq 0 then print, i
346
347         imrotov=rot(oval_manual,i*0.1,1,pos_bary_n(0),pos_bary_n(1),/pivot)
348         imrotma=rot(masque_manual,i*0.1,1,pos_bary_n(0),pos_bary_n(1),/pivot)
349
350         ind0=where(imrotma(pos_bary_n(0):*,pos_bary_n(1)) ne 0)
351         ind1=min(ind0)
352         ind2=max(ind0)
353         ;ind_mid=ind1+floor((ind2-ind1)/2.)
354
355         coupe=imrotov(pos_bary_n(0)+ind1:pos_bary_n(0)+ind2,pos_bary_n(1))
356         ind3=where(coupe eq max(coupe))
357         maxi=max(coupe)
358         ;print, maxi
359
360         if maxi ge threshold2*max_mask then begin ; If we are in a high brightness
    region, the G1 mask is modified. If not, it is kept.
361             if ind1-delta_minus lt 0 then ind_min=0 else ind_min=ind1-delta_minus
362             if ind2+delta_plus gt 512 then ind_max=512 else ind_max=ind2+delta_plus
363
364             coupe2=imrotov(pos_bary_n(0):*,pos_bary_n(1))
365             ind4=where(coupe2 gt threshold1*maxi) ; Found the region where the mask
    is bright enough to be modified ...
366             ind5=ind4(where(ind4 ge ind_min and ind4 le ind_max)) ; ... and limit
    this region to the area of interest around the G1 mask ...
367             debut=min(ind5)-4 ; with a small margin to encompass the edges of the
    region.
368             fin=max(ind5)+4
369             if debut gt ind1 then debut=ind1 ; The new mask has to be at least the
    width of the G1 mask.
370             if fin lt ind2 then fin=ind2
371         endif else begin
372             debut=ind1
373             fin=ind2
374         endelse
375
376
377     ;-----

```

APPENDIX I. IDL ROUTINES

```

378     ; Forcing
379     ;-----
380
381     if pj eq 'PJ13' then begin
382         if i gt 0 and i lt 200 then fin=fin+35
383         if i ge 200 and i lt 400 then fin=fin+15
384         if i ge 400 and i lt 500 then fin=fin+10
385         if i gt 3500 and i lt 3600 then fin=fin+37
386     endif
387
388     if pj eq 'PJ19' then begin
389         if i ge 0 and i lt 200 then fin=fin+20
390         if i gt 3200 and i lt 3600 then fin=fin+25
391         if i ge 0 and i lt 100 then debut=debut-15
392         if i gt 3300 and i lt 3600 then debut=debut-25
393         if i ge 100 and i lt 200 then debut=debut-10
394         if i ge 200 and i lt 900 then debut=debut-15
395         if i ge 900 and i lt 1100 then debut=debut-30
396         if i ge 1100 and i lt 1200 then debut=debut-20
397         if i ge 1200 and i lt 1300 then debut=debut-10
398     endif
399
400
401     angl(i)=i*0.1
402     deb_arr(i)=debut
403     fin_arr(i)=fin
404 endfor
405
406     inter=fltarr(1024,1024)
407     for i=0, 3600-1 do begin
408         inter(pos_bary_n(0)+deb_arr(i)*cos(i*!dtor/10), pos_bary_n(1)+deb_arr(i)*
409         sin(i*!dtor/10))=1000
410         inter(pos_bary_n(0)+fin_arr(i)*cos(i*!dtor/10), pos_bary_n(1)+fin_arr(i)*
411         sin(i*!dtor/10))=1000
412     endfor
413
414     dgtv, congrid(inter,1024,1024)
415     photo=tvrd(256,160,512,512,true=1)
416     tvlct, r,g,b,/get
417     fnameout='/home/LPAP/groulard/juno/'+pj+'/' +pj+'_inter_g2_'+hemi+'.png'
418     write_png, fnameout, photo, r, g, b
419
420     ;-----
421     ; Smooth the inner edge of the mask (inner ribbon)
422     ;-----
423
424     absc=angl(where(deb_arr ne 0))
425     ordo=deb_arr(where(deb_arr ne 0))
426
427     theta=absc*!dtor
428     fitvect=ordo
429
430     fit_fourier_1d_mat, theta, fitvect, n_harmonic_int, par
431     x=findgen(7200.)/20.
432     fourier_s, x*!pi/180, par, y_f
433
434     ;-----
435     ; Smooth the outer edge of the mask (outer ribbon)
436     ;-----
437
438     absc=angl(where(fin_arr ne 0))

```

APPENDIX I. IDL ROUTINES

```

437   ordo=fin_arr(where(fin_arr ne 0))
438
439   theta=absc*!dior
440   fitvect=ordo
441
442   fit_fourier_1d_mat,theta,fitvect,n_harmonic_ext,par
443   x=findgen(7200.)/20.
444   fourier_s,x*!pi/180,par,y_f2
445
446
447   ;-----
448   ; Create the mask based on the two ribbons
449   ;-----
450
451   for i=0, 7199 do begin
452
453       if i mod 1000 eq 0 then print, i
454       thickness_me=y_f2(i)-y_f(i)
455       if thickness_me eq 0 then thickness_me=1.
456
457       indx=y_f(i)+indgen(thickness_me*20.)/20.
458
459       pos_max=indx
460
461       xp=pos_bary_n(0)+pos_max*cos(i*0.05/180.*!pi)
462       yp=pos_bary_n(1)+pos_max*sin(i*0.05/180.*!pi)
463
464       fi=atan((xp-512.)/((yp-512.)*1.))
465       teta=acos(((yp-512.)/512.)*(1./cos(fi)))
466       ind=where(teta gt !pi/2.)
467       if ind(0) ne -1 then teta(ind)=!pi-teta(ind)
468       if ind(0) ne -1 then fi(ind)=!pi+fi(ind)
469
470       oval_north_area_lon=-(-180.+fi*180./!pi)
471       oval_north_area_lat=teta*180./!pi
472
473       steps=20
474
475       order=sort(oval_north_area_lon)
476       oval_north_area_lon2=interpol(oval_north_area_lon(order),findgen(
n_elements(oval_north_area_lon)),findgen((n_elements(oval_north_area_lon)-1)
*steps)/steps)
477       oval_north_area_lat2=interpol(oval_north_area_lat(order),findgen(
n_elements(oval_north_area_lat)),findgen((n_elements(oval_north_area_lat)-1)
*steps)/steps)
478
479       indi=where(oval_north_area_lon2 lt 0)
480       if indi(0) ne -1 then oval_north_area_lon2(indi)=oval_north_area_lon2(
indi)+360.
481       indi=where(oval_north_area_lon2 gt 360)
482       if indi(0) ne -1 then oval_north_area_lon2(indi)=oval_north_area_lon2(
indi)-360.
483       indi=where(oval_north_area_lon lt 0)
484       if indi(0) ne -1 then oval_north_area_lon(indi)=oval_north_area_lon(indi)
+360.
485       indi=where(oval_north_area_lon gt 360)
486       if indi(0) ne -1 then oval_north_area_lon(indi)=oval_north_area_lon(indi)
-360.
487
488       indi=where(oval_north_area_lon2 gt min(oval_north_area_lon) and
oval_north_area_lon2 lt max(oval_north_area_lon))

```

APPENDIX I. IDL ROUTINES

```

489     oval_north_area_lon2=oval_north_area_lon2(indi)
490     oval_north_area_lat2=oval_north_area_lat2(indi)
491
492
493     implan_north_area(round(oval_north_area_lon*10.),round(oval_north_area_lat
*10+900.))=1.+i
494     endfor
495
496     masque_me=implan_north_area
497
498     ;-----
499     ; Images
500     ;-----
501
502     bpglobe,90-180.*(lat_sun lt 0.),0.,180.*(lat_sun lt 0.),rotate(masque_me
,5.*(lat_sun lt 0.)),res,/grid,/horizon,/linscl, min=0., max=7200, londel=10
, latdel=10, glinestyle=2
503     photo=tvrd(x_photo,y_photo,780,780,true=1)
504     tvlct, r,g,b,/get
505     fnameout='/home/LPAP/groulard/juno/'+pj+'/' +pj+'_mask_g_vari_'+hemi+'.png'
506     write_png,fnameout,photo,r,g,b
507
508     mask_add_on=implan_clean_visu
509     ind=where(masque_me ne 0)
510     mask_add_on(ind)=mask_add_on(ind)+400.
511     bpglobe,90-180.*(lat_sun lt 0.),0.,180.*(lat_sun lt 0.),rotate(mask_add_on
,5.*(lat_sun lt 0.)),res,/grid,/horizon,/linscl, min=0., max=max(mask_add_on
), londel=10, latdel=10, glinestyle=2
512
513     photo=tvrd(x_photo,y_photo,780,780,true=1)
514     tvlct, r,g,b,/get
515     fnameout='/home/LPAP/groulard/juno/'+pj+'/' +pj+'_mask_add_on_g_vari_'+hemi+'
.png'
516     write_png,fnameout,photo,r,g,b
517
518     save, filename='/home/LPAP/groulard/juno/'+pj+'/' +pj+'_masque_g2_'+pj+'_' +hemi+'
idl', masque_me
519     endif
520
521
522 end

```

measure_power_arc.pro

```

1 pro measure_power_arc, hemi, pj, modele, lt_11, lt_12, lt_21, lt_22
2 ; hemi = hemisphere. 'N' or 'S' in entry.
3 ; pj = perijove number. 'PJ#' in entry.
4 ; modele = mask to be used : 'v' for Vogt, 'b' for Bonfond, 'g' for Groulard,
5 ; 'g2' for Groulard with variable width.
6 ; lt_11 = local time of the begining of the dawn region
7 ; lt_12 = local time of the end of the dawn region
8 ; lt_21 = local time of the begining of the dusk region
9 ; lt_22 = local time of the end of the dusk region
10
11 for k=1, 39 do begin
12   pj='PJ'+strcompress(k,/re)
13   print, pj
14 if file_test('/home/LPAP/groulard/juno/'+pj+'/masque_'+modele+'_'+pj+'_'+hemi+'.
15   idl') then begin
16   ;-----
17   ; default local time dawn : 6h to 8h ; default local time dusk : 16h to 18h
18   ;-----
19
20   if n_elements(lt_11) eq 0 then lt_11=6.
21   if n_elements(lt_12) eq 0 then lt_12=8.
22   if n_elements(lt_21) eq 0 then lt_21=16.
23   if n_elements(lt_22) eq 0 then lt_22=18.
24
25   ;print, 'dusk: ', lt_21, lt_22, '      dawn: ', lt_11,  lt_12
26   distance=30. ; Rj
27
28   restore, '/home/LPAP/groulard/juno/'+pj+'/auroral_power_'+pj+'_'+hemi+'.idl'
29   loadct,1, file='/home/LPAP/groulard/Memoire/colors_blwh01.tbl'
30   restore, '/LPAP/HST/redu/juno/'+pj+'/ephem/'+pj+'_ephem03.idl'
31   restore, '/home/LPAP/groulard/juno/'+pj+'/masque_'+modele+'_'+pj+'_'+hemi+'.
32   idl'
33
34   if hemi eq 'N' then begin
35     x_photo=363
36     y_photo=170
37   endif
38   if hemi eq 'S' then begin
39     x_photo=438
40     y_photo=460
41   endif
42
43   ;-----
44   ; Use the Vogt et al. magnetosphere model
45   ;-----
46
47   if hemi eq 'N' then hemi_str='north' else if $
48     hemi eq 'S' then hemi_str='south' else stop
49
50   pos11 = mapping_function2019('mag_to_ion_'+hemi_str, lon_sun, distance, lt_11,
51     'jrm09')
52   a_11=latlon2angle_AG(pos11(0),pos11(1))
53   angle_11=a_11(0)
54   dist_11=a_11(1)

```

APPENDIX I. IDL ROUTINES

```

55  pos12 = mapping_function2019('mag_to_ion_'+hemi_str, lon_sun, distance, lt_12,
    'jrm09')
56  a_12=latlon2angle_AG(pos12(0),pos12(1))
57  angle_12=a_12(0)
58  dist_12=a_12(1)
59
60  pos21 = mapping_function2019('mag_to_ion_'+hemi_str, lon_sun, distance, lt_21,
    'jrm09')
61  a_21=latlon2angle_AG(pos21(0),pos21(1))
62  angle_21=a_21(0)
63  dist_21=a_21(1)
64
65  pos22 = mapping_function2019('mag_to_ion_'+hemi_str, lon_sun, distance, lt_22,
    'jrm09')
66  a_22=latlon2angle_AG(pos22(0),pos22(1))
67  angle_22=a_22(0)
68  dist_22=a_22(1)
69
70
71  ;-----
72  ; Chose the mask
73  ;-----
74
75  restore, '/home/LPAP/groulard/juno/'+pj+'/masque_'+modele+'_'+pj+'_'+hemi+'.
    idl'
76  if modele eq 'v' then masque_me=shift(masque_me,180,0) ; The V mask is
    accidentally shifted when loaded
77
78  if 1 eq 0 then begin
79  bpglobe,90-180.*(lat_sun lt 0.),0.,180.*(lat_sun lt 0.),rotate(masque_me,5.*(
    lat_sun lt 0.)),res,/grid,/horizon,/linscl, min=0., max=9000, lon del=10,
    lat del=10, gline style=2
80
81  photo=tvrd(x_photo,y_photo,780,780,true=1)
82  tvlct, r,g,b,/get
83  fnameout='/home/LPAP/groulard/juno/'+pj+'/'+'pj'+'_masque_me_'+modele+'_'+hemi+'
    .png'
84  write_png,fnameout,photo,r,g,b
85  endif
86
87  ;-----
88  ; Visualize the angles on the brightness map
89  ;-----
90
91  if 1 eq 0 then begin
92      if hemi eq 'N' then begin
93          lat_bary=73.9340
94          lon_bary=185.670
95
96          ; Modifies the reference axis to match the bpglobe function.
97          angle_11_visu=angle_11-90.
98          angle_11_visu=360-angle_11_visu
99          if angle_11_visu gt 360 then angle_11_visu=angle_11_visu-360
100         angle_12_visu=angle_12-90.
101         angle_12_visu=360-angle_12_visu
102         if angle_12_visu gt 360 then angle_12_visu=angle_12_visu-360
103         angle_21_visu=angle_21-90.
104         angle_21_visu=360-angle_21_visu
105         if angle_21_visu gt 360 then angle_21_visu=angle_21_visu-360
106         angle_22_visu=angle_22-90.
107         angle_22_visu=360-angle_22_visu

```


APPENDIX I. IDL ROUTINES

```

108     if angle_22_visu gt 360 then angle_22_visu=angle_22_visu-360
109 endif
110
111 if hemi eq 'S' then begin
112     lat_bary=-81.9309
113     lon_bary=31.9209
114
115     angle_11_visu=angle_11+90.
116     angle_11_visu=360-angle_11_visu
117     if angle_11_visu gt 360 then angle_11_visu=angle_11_visu-360
118     angle_12_visu=angle_12+90.
119     angle_12_visu=360-angle_12_visu
120     if angle_12_visu gt 360 then angle_12_visu=angle_12_visu-360
121     angle_21_visu=angle_21+90.
122     angle_21_visu=360-angle_21_visu
123     if angle_21_visu gt 360 then angle_21_visu=angle_21_visu-360
124     angle_22_visu=angle_22+90.
125     angle_22_visu=360-angle_22_visu
126     if angle_22_visu gt 360 then angle_22_visu=angle_22_visu-360
127 endif
128
129 ; Display the brightness map
130 bpglobe,90-180.*(lat_sun lt 0.),0.,180.*(lat_sun lt 0.),rotate(
implan_clean_visu,5.*(lat_sun lt 0.)),res,/grid,/horizon,/linscl, min=0.,
max=1000, londel=10, latdel=10, glinestyle=2
131
132 if 1 eq 0 then begin
133     print, 'sun ', lon_sun
134     print, pos11, angle_11_visu
135     print, ''
136     print, pos12, angle_12_visu
137     print, ''
138     print, pos21, angle_21_visu
139     print, ''
140     print, pos22, angle_22_visu
141     print, ''
142 endif
143
144 if angle_11_visu lt angle_12_visu then angle_11_visu=angle_11_visu+360
145 if angle_21_visu lt angle_22_visu then angle_21_visu=angle_21_visu+360
146
147 y11=dist_11*cos(angle_11_visu*!dtor)
148 x11=dist_11*sin(angle_11_visu*!dtor)
149 y12=dist_12*cos(angle_12_visu*!dtor)
150 x12=dist_12*sin(angle_12_visu*!dtor)
151 y21=dist_21*cos(angle_21_visu*!dtor)
152 x21=dist_21*sin(angle_21_visu*!dtor)
153 y22=dist_22*cos(angle_22_visu*!dtor)
154 x22=dist_22*sin(angle_22_visu*!dtor)
155
156 xbary=750.*cos((lat_bary)*!dtor)*(sin((lon_bary)*!dtor))+750.
157 ybary=750.*cos((lat_bary)*!dtor)*(cos((lon_bary)*!dtor))+750.
158
159 ; Display the dawn angles:
160 plots, [xbary,xbary+x11], [ybary,ybary+y11], thick=3, /device
161 plots, [xbary,xbary+x12], [ybary,ybary+y12], thick=3, /device
162 for m=0, 99 do plots, [xbary, xbary+50*sin(angle_12_visu*!dtor+m*(
angle_11_visu*!dtor-angle_12_visu*!dtor)/100)], [ybary, ybary+50*cos(
angle_12_visu*!dtor+m*(angle_11_visu*!dtor-angle_12_visu*!dtor)/100)], thick
=3, /device
163 xyouts, xbary+x11,ybary+y11,'6',color=255,/device, ali=0.5, charsize=2

```

APPENDIX I. IDL ROUTINES

```

164     xyouts, xbary+x12,ybary+y12,'10',color=255,/device, ali=0.5, charsize=2
165
166     ; Display the dusk angles:
167     plots, [xbary,xbary+x21], [ybary,ybary+y21], thick=3, /device
168     plots, [xbary,xbary+x22], [ybary,ybary+y22], thick=3, /device
169     for m=0, 99 do plots, [xbary, xbary+100*sin(angle_22_visu*!dtor+m*(
angle_21_visu*!dtor-angle_22_visu*!dtor)/100)], [ybary, ybary+100*cos(
angle_22_visu*!dtor+m*(angle_21_visu*!dtor-angle_22_visu*!dtor)/100)], thick
=3, /device
170     xyouts, xbary+x21,ybary+y21,'14',color=255,/device, ali=0.5, charsize=2
171     xyouts, xbary+x22,ybary+y22,'18',color=255,/device, ali=0.5, charsize=2
172
173     ; Adds the location of the Sun
174     if hemi eq 'N' then oplot, 180-lon_sun*[1,1], [lat_sun(0)+3,lat_sun(0)-4],
thick=3 else $
175     oplot, 180+lon_sun*[1,1], [lat_sun(0)+3,lat_sun(0)+7], thick=3
176
177     photo=tvrd(x_photo,y_photo,780,780,true=1)
178     tvlct, r,g,b,/get
179     fnameout='/home/LPAP/groulard/juno/' + pj + '/' + pj + '_angles_' + hemi + '.png'
180     write_png, fnameout, photo, r, g, b
181 endif
182
183
184 ; -----
185 ; Image of the mask on the brightness map to be sure it is not shifted
186 ; -----
187
188 if 1 eq 0 then begin
189     mask_on=implan_clean_visu
190     inde=where(masque_me ne 0)
191     mask_on(inde)=1000
192     bpglobe,90-180.*(lat_sun lt 0.),0.,180.*(lat_sun lt 0.),rotate(mask_on,5.*(
lat_sun lt 0.)),res,/grid,/horizon,/linscl, min=0., max=1000, londel=10,
latdel=10, glinestyle=2
193
194     photo=tvrd(x_photo,y_photo,780,780,true=1)
195     tvlct, r,g,b,/get
196     fnameout='/home/LPAP/groulard/juno/' + pj + '/' + pj + '_mask_on_' + modele + '_' + hemi +
strcompress(lt_11) + '-' + strcompress(lt_12) + '-' + strcompress(lt_21) + '-' +
strcompress(lt_22) + '.png'
197     write_png, fnameout, photo, r, g, b
198     fnameout='/home/LPAP/groulard/juno/all/' + pj + '_mask_on_' + modele + '_' + hemi +
strcompress(lt_11) + '-' + strcompress(lt_12) + '-' + strcompress(lt_21) + '-' +
strcompress(lt_22) + '.png'
199     write_png, fnameout, photo, r, g, b
200 endif
201
202
203 ; -----
204 ; Create two new masks based on the isolated dawn and dusk regions of the
initial mask
205 ; -----
206
207 ; Dawn:
208 if angle_12 gt angle_11 then implan_dawn_area=masque_me gt (angle_11*20.+1.)
and masque_me le (angle_12*20.+1.) $
209 else implan_dawn_area=(masque_me lt (angle_12*20.+1.) or masque_me ge (
angle_11*20.+1.)) and masque_me gt 0
210
211 inde_dawn=where(implan_dawn_area ne 0)

```

APPENDIX I. IDL ROUTINES

```

212  implan_dawn_area(inde_dawn)=1
213
214  if 1 eq 0 then begin
215  bpglobe,90-180.*(lat_sun lt 0.),0.,180.*(lat_sun lt 0.),rotate(
      implan_dawn_area,5.*(lat_sun lt 0.)),res,/grid,/horizon,/linscl, min=0., max
      =1000, londel=10, latdel=10, glinestyle=2
216
217  photo=tvrd(x_photo,y_photo,780,780,true=1)
218  tvlct, r,g,b,/get
219  fnameout='/home/LPAP/groulard/juno/'+pj+'/' +pj+'_masque_dawn_'+modele+'_'+hemi
      +'.png'
220  write_png,fnameout,photo,r,g,b
221  endif
222
223  ; Dusk:
224  if angle_22 gt angle_21 then implan_dusk_area=masque_me gt (angle_21*20.+1.)
      and masque_me le (angle_22*20.+1.) $
225  else implan_dusk_area=(masque_me lt (angle_22*20.+1.) or masque_me ge (
      angle_21*20.+1.)) and masque_me gt 0
226
227  inde_dusk=where(implean_dusk_area ne 0)
228  implan_dusk_area(inde_dusk)=1
229
230  if 1 eq 0 then begin
231  bpglobe,90-180.*(lat_sun lt 0.),0.,180.*(lat_sun lt 0.),rotate(
      implan_dusk_area,5.*(lat_sun lt 0.)),res,/grid,/horizon,/linscl, min=0., max
      =1000, londel=10, latdel=10, glinestyle=2
232
233  photo=tvrd(x_photo,y_photo,780,780,true=1)
234  tvlct, r,g,b,/get
235  fnameout='/home/LPAP/groulard/juno/'+pj+'/' +pj+'_masque_dusk_'+modele+'_'+hemi
      +'.png'
236  write_png,fnameout,photo,r,g,b
237  endif
238
239
240  ;-----
241  ; Image of the new masks on the brightness map to be sure they are not shifted
242  ;-----
243
244  if 1 eq 0 then begin
245  mask_on_dd=implean_clean_visu
246  inde=where(implean_dusk_area ne 0 or implan_dawn_area ne 0)
247  mask_on_dd(inde)=1000
248  bpglobe,90-180.*(lat_sun lt 0.),0.,180.*(lat_sun lt 0.),rotate(mask_on_dd,5.*(
      lat_sun lt 0.)),res,/grid,/horizon,/linscl, min=0., max=1000, londel=10,
      latdel=10, glinestyle=2
249
250  photo=tvrd(x_photo,y_photo,780,780,true=1)
251  tvlct, r,g,b,/get
252  fnameout='/home/LPAP/groulard/juno/'+pj+'/' +pj+'_mask_on_dd_'+modele+'_'+hemi+
      '.png'
253  write_png,fnameout,photo,r,g,b
254  fnameout='/home/LPAP/groulard/juno/all/'+pj+'_mask_on_dd_'+modele+'_'+hemi+'.'
      'png'
255  write_png,fnameout,photo,r,g,b
256  endif
257
258
259  ;-----
260  ; Compute the power emitted in bith regions

```

APPENDIX I. IDL ROUTINES

```
261 ;-----
262
263 power_dawn = total(power_map*implan_dawn_area)
264 power_dusk = total(power_map*implan_dusk_area)
265 print, 'total ', measured_total_power
266 print, 'dawn ', power_dawn
267 print, 'dusk ', power_dusk
268
269 lt_11=strcompress(string(lt_11), /re)
270 save, filename='/home/LPAP/groulard/juno/'+pj+'/dawn_dusk_power_'+modele+'_'+
    pj+'_'+hemi+'_'+lt_11+'.idl', power_dawn, power_dusk, measured_total_power
271
272
273 endif
274 endfor
275
276
277 end
```

stats_dawn_dusk.pro

```

1 pro stats_dawn_dusk, sta, fin, modele, lt_11
2 ; sta = first perijove to take into account
3 ; fin = last perijove to take into account
4 ; modele = mask to be used : 'v' for Vogt, 'b' for Bonfond, 'g' for Groulard,
5 ; 'g2' for Groulard with variable width.
6 ; lt_11 = local time of the beginning of the dawn region.
7
8 dawn=fltarr(fin+1,2)
9 dusk=fltarr(fin+1,2)
10 total_pow=fltarr(fin+1,2)
11 ratio=fltarr(fin+1,2)
12 lon=fltarr(fin+1,2)
13
14 dawn(*,*)=0.
15 dusk(*,*)=0.
16 total_pow(*,*)=1.
17
18 ;-----
19 ; List of the usable masks for both the HST and symmetric sectors of each
20 ; perijove
21 ;-----
22 ; 0 = mask not usable, 1 = mask usable
23
24 ; PJ 1 2 3 4 5 6 7 8 9 10 11 12 13 14 15 16 17 18 19 20 21 22
25 ; 23 24 25 26 27 28 29 30 31 32 33 34 35 36 37 38 39
26 ;usable_N=[0, 1, 0, 1, 1, 1, 1, 1, 1, 1, 1, 0, 1, 1, 1, 1, 1, 1, 0, 0, 1, 1, 1, 1,
27 ; 0, 1, 0, 1, 0, 0, 0, 0, 0, 1, 0, 0, 0, 1, 0, 1, 1] ; 'g' 6-8 16-18 & 4-8
28 ; 16-20 et 'g'+ 'g2' 6-8 16-18
29 ;usable_S=[0, 1, 0, 1, 1, 1, 1, 1, 1, 1, 1, 1, 1, 1, 1, 1, 1, 1, 1, 1, 1, 1, 1, 1,
30 ; 1, 1, 1, 1, 1, 1, 1, 1, 1, 1, 1, 1, 1, 1, 1, 1, 1, 1, 1, 1, 1, 1, 1, 1]
31 ;usable_N=[0, 1, 0, 1, 1, 1, 1, 1, 1, 1, 1, 1, 1, 1, 1, 1, 0, 0, 1, 1, 1, 1, 1, 1,
32 ; 0, 1, 0, 1, 0, 0, 0, 0, 0, 1, 0, 0, 0, 1, 0, 1, 1] ; 'g'+ 'g2' 4-8 16-20
33 ;usable_S=[0, 1, 0, 1, 1, 1, 1, 1, 1, 1, 1, 1, 1, 1, 1, 1, 1, 1, 1, 1, 1, 1, 1, 1,
34 ; 1, 1, 1, 1, 1, 1, 1, 1, 1, 1, 1, 1, 1, 1, 1, 1, 1, 1, 1, 1, 1, 1, 1, 1]
35 ;usable_N=[0, 0, 0, 0, 0, 0, 1, 1, 0, 0, 1, 0, 0, 1, 1, 0, 1, 0, 0, 0, 0, 1, 1, 0, 0,
36 ; 0, 0, 0, 0, 0, 0, 0, 0, 0, 0, 0, 0, 0, 0, 0, 0, 0] ; 'g2' 4-8 16-20
37 ;usable_S=[0, 1, 0, 1, 0, 1, 0, 0, 0, 0, 0, 1, 0, 1, 0, 0, 1, 0, 0, 1, 1, 0, 1, 0, 0,
38 ; 1, 0, 1, 0, 1, 1, 1, 0, 1, 1, 1, 0, 1, 0, 0, 1, 0, 0, 1, 1, 0, 1, 0, 1, 0,
39 ; 1, 0, 1, 0, 1, 1, 1, 0, 1, 1, 0, 1, 1, 0, 1, 1, 0, 0, 1, 1, 0, 0, 1, 1, 1, 1,
40 ; 0, 1, 0, 0, 0, 0, 0, 0, 0, 1, 0, 0, 0, 1, 0, 1, 1] ; 'v' 4-8 16-20

```

APPENDIX I. IDL ROUTINES

```

40 ;usable_S=[0, 1, 0, 1, 1, 1, 1, 1, 1, 1, 1, 1, 1, 1, 1, 1, 0, 1, 1, 1, 1, 1, 1, 0,
      1, 0, 1, 0, 0, 0, 1, 0, 1, 1, 1, 0, 1, 1, 1, 1, 1]
41 ;usable_N=[0, 1, 0, 1, 1, 1, 1, 1, 1, 1, 1, 1, 1, 1, 1, 1, 1, 1, 1, 1, 1, 1, 1, 1,
      1, 1, 1, 1, 1, 1, 1, 1, 1, 1, 1, 1, 1, 1, 1] ; all ok
42 ;usable_S=[0, 1, 0, 1, 1, 1, 1, 1, 1, 1, 1, 1, 1, 1, 1, 1, 1, 1, 1, 1, 1, 1, 1, 1,
      1, 1, 1, 1, 1, 1, 1, 1, 1, 1, 1, 1, 1, 1, 1]
43
44
45 ;-----
46 ; Fill the arrays with the power computed in the dawn region, dusk region, and
      in the whole main emission obtained with measure_power_arc.pro
47 ; PJ i --> north: array(i,0) ; south: array(i,1)
48 ;-----
49
50 lt_11=strcompress(string(lt_11),/re)
51 for i=sta, fin do begin
52     str_i=strcompress(string(i), /re)
53
54     if modele ne 'g2' then begin
55         if file_test('/home/LPAP/groulard/juno/PJ'+str_i+'/dawn_dusk_power_'+
modele+'_PJ'+str_i+'_N_'+lt_11+'.idl') then begin
56             restore, '/home/LPAP/groulard/juno/PJ'+str_i+'/dawn_dusk_power_'+modele+
'_PJ'+str_i+'_N_'+lt_11+'.idl'
57             restore, '/home/LPAP/groulard/juno/PJ'+str_i+'/auroral_power_PJ'+str_i+
'_N.idl'
58             dawn(i,0)=power_dawn
59             dusk(i,0)=power_dusk
60             total_pow(i,0)=measured_total_power
61             lon(i,0)=lon_sun
62             print, 'PJ', str_i, ' N ok'
63         endif
64         if file_test('/home/LPAP/groulard/juno/PJ'+str_i+'/dawn_dusk_power_'+
modele+'_PJ'+str_i+'_S_'+lt_11+'.idl') then begin
65             restore, '/home/LPAP/groulard/juno/PJ'+str_i+'/dawn_dusk_power_'+modele+
'_PJ'+str_i+'_S_'+lt_11+'.idl'
66             restore, '/home/LPAP/groulard/juno/PJ'+str_i+'/auroral_power_PJ'+str_i+
'_S.idl'
67             dawn(i,1)=power_dawn
68             dusk(i,1)=power_dusk
69             total_pow(i,1)=measured_total_power
70             lon(i,1)=lon_sun
71             print, 'PJ', str_i, ' S ok'
72         endif
73     endif
74
75     if modele eq 'g2' then begin
76         if file_test('/home/LPAP/groulard/juno/PJ'+str_i+'/dawn_dusk_power_'+
modele+'_PJ'+str_i+'_N_'+lt_11+'.idl') then begin
77             restore, '/home/LPAP/groulard/juno/PJ'+str_i+'/dawn_dusk_power_'+modele+
'_PJ'+str_i+'_N_'+lt_11+'.idl'
78             restore, '/home/LPAP/groulard/juno/PJ'+str_i+'/auroral_power_PJ'+str_i+
'_N.idl'
79             dawn(i,0)=power_dawn
80             dusk(i,0)=power_dusk
81             total_pow(i,0)=measured_total_power
82             lon(i,0)=lon_sun
83             print, 'PJ', str_i, ' N ok'
84         endif else begin
85             if file_test('/home/LPAP/groulard/juno/PJ'+str_i+'/dawn_dusk_power_g_PJ'+
str_i+'_N_'+lt_11+'.idl') then begin
86                 restore, '/home/LPAP/groulard/juno/PJ'+str_i+'/dawn_dusk_power_g_PJ'+

```

APPENDIX I. IDL ROUTINES

```

str_i+'_N_'+lt_11+'.idl'
87     restore, '/home/LPAP/groulard/juno/PJ'+str_i+'/auroral_power_PJ'+str_i
+'_N.idl'
88     dawn(i,0)=power_dawn
89     dusk(i,0)=power_dusk
90     total_pow(i,0)=measured_total_power
91     lon(i,0)=lon_sun
92     print, 'PJ', str_i, ' N ok'
93     endif
94     endelse
95     if file_test('/home/LPAP/groulard/juno/PJ'+str_i+'/dawn_dusk_power_'+
modele+'_PJ'+str_i+'_S_'+lt_11+'.idl') then begin
96         restore, '/home/LPAP/groulard/juno/PJ'+str_i+'/dawn_dusk_power_'+modele+
'_PJ'+str_i+'_S_'+lt_11+'.idl'
97         restore, '/home/LPAP/groulard/juno/PJ'+str_i+'/auroral_power_PJ'+str_i+'
_S.idl'
98         dawn(i,1)=power_dawn
99         dusk(i,1)=power_dusk
100        total_pow(i,1)=measured_total_power
101        lon(i,1)=lon_sun
102        print, 'PJ', str_i, ' S ok'
103        endif else begin
104        if file_test('/home/LPAP/groulard/juno/PJ'+str_i+'/dawn_dusk_power_g_PJ'
+str_i+'_S_'+lt_11+'.idl') then begin
105            restore, '/home/LPAP/groulard/juno/PJ'+str_i+'/dawn_dusk_power_g_PJ'+
str_i+'_S_'+lt_11+'.idl'
106            restore, '/home/LPAP/groulard/juno/PJ'+str_i+'/auroral_power_PJ'+str_i
+'_S.idl'
107            dawn(i,1)=power_dawn
108            dusk(i,1)=power_dusk
109            total_pow(i,1)=measured_total_power
110            lon(i,1)=lon_sun
111            print, 'PJ', str_i, ' S ok'
112            endif
113            endelse
114            endif
115        endfor
116
117    if 1 eq 0 then begin
118        print, 'dawn'
119        print, dawn(1:*,*)
120        print, 'dusk'
121        print, dusk(1:*,*)
122        print, 'total'
123        print, total_pow(1:*,*)
124    endif
125
126
127    ;-----
128    ; Compute the dusk-over-dawn ratios
129    ;-----
130
131    ratio_tot=0.
132    ind_ok=0.
133    equal=0.
134    ind_equal=fltarr(fin+1)
135    dusk_big=0.
136    ind_dusk=fltarr(fin+1)
137    dawn_big=0.
138    ind_dawn=fltarr(fin+1)
139

```

APPENDIX I. IDL ROUTINES

```

140  for i=sta, fin do begin
141      if usable_S(i) eq 1. then begin
142          ind_ok=ind_ok+1.
143          ratio(i,1)=dusk(i,1)/dawn(i,1)
144          ratio_tot=ratio_tot+ratio(i,1)
145
146          if dusk(i,1) gt dawn(i,1) then begin
147              if dusk(i,1)-dusk(i,1)/100 gt dawn(i,1) then begin ; More power from the
dusk region
148                  dusk_big=dusk_big+1.
149                  ind_dusk(i)=1.
150              endif else begin ; Equal emitted power
151                  equal=equal+1.
152                  ind_equal(i)=1.
153              endelse
154              endif else if dusk(i,1) lt dawn(i,1) then begin
155                  if dawn(i,1)-dawn(i,1)/100 gt dusk(i,1) then begin ; More power from
the dawn region
156                      dawn_big=dawn_big+1.
157                      ind_dawn(i)=1.
158                  endif else begin ; Equal emitted power
159                      equal=equal+1.
160                      ind_equal(i)=1.
161                  endelse
162                  endif
163              endif
164          endfor
165          ratio_tot=ratio_tot/(ind_ok)
166          pourcent_dawn=dawn_big/(ind_ok)
167          pourcent_dusk=dusk_big/(ind_ok)
168          pourcent_equal=equal/(ind_ok)
169          moy_dusk=total(dusk(*,1)*usable_S)/(ind_ok)
170          moy_dawn=total(dawn(*,1)*usable_S)/(ind_ok)
171          ratio_moy=moy_dusk/moy_dawn
172
173
174  ;-----
175  ; Computation of the medians and standard deviations for the ratios, dusk
region, and dawn region
176  ;-----
177
178  ind=where(ratio(*,1) ne 0) ; Ratios.
179  arr_med=ratio(ind,1)
180  arr_med=arr_med(sort(arr_med))
181  if ind_ok mod 2 eq 0 then begin
182      inf=arr_med((ind_ok/2)-1)
183      sup=arr_med(ind_ok/2)
184      med= (inf+sup)/2
185  endif else begin
186      med=arr_med(floor(ind_ok/2))
187  endelse
188
189  sigma=sqrt(total((arr_med(*)-ratio_tot)^2)/ind_ok)
190
191  ind=where(dusk(*,1)*usable_S ne 0) ; Dusk.
192  arr_med2=dusk(ind,1)
193  arr_med2=arr_med2(sort(arr_med2))
194  if ind_ok mod 2 eq 0 then begin
195      inf=arr_med2((ind_ok/2)-1)
196      sup=arr_med2(ind_ok/2)
197      med2=((inf+sup)/2)/1e+09

```


APPENDIX I. IDL ROUTINES

```

198   endif else begin
199       med2=arr_med2(floor(ind_ok/2))/1e+09
200   endelse
201
202   sigma2=sqrt(total((arr_med2(*)-moy_dusk)^2)/ind_ok)
203
204   ind=where(dawn(*,1)*usable_S ne 0) ; Dawn.
205   arr_med3=dawn(ind,1)
206   arr_med3=arr_med3(sort(arr_med3))
207   if ind_ok mod 2 eq 0 then begin
208       inf=arr_med3((ind_ok/2)-1)
209       sup=arr_med3(ind_ok/2)
210       med3=((inf+sup)/2)/1e+09
211   endif else begin
212       med3=arr_med2(floor(ind_ok/2))/1e+09
213   endelse
214
215   sigma3=sqrt(total((arr_med3(*)-moy_dawn)^2)/ind_ok)
216
217
218   ;-----
219   ; Print every information computed
220   ;-----
221
222   print, '-----SOUTH-----'
223   print, ind_ok, ' PJ ok'
224   print, ratio_tot, ' mean dusk/dawn'
225   print, moy_dusk/1e+09, ' GW mean dusk'
226   print, moy_dawn/1e+09, ' GW mean dawn'
227   print, ratio_moy, ' mean dusk/mean dawn'
228   print, med, ' median'
229   print, med2, ' GW median dusk'
230   print, med3, ' GW median dawn'
231   print, med2/med3, ' ratio of medians'
232   print, sigma, ' sigma of the ratio'
233   print, sigma2/1e+09, ' GW sigma dusk'
234   print, sigma3/1e+09, ' GW sigma dawn'
235   print, dusk_big, ' dusk, (', strcompress(100*pourcent_dusk), '%)'
236   print, dawn_big, ' dawn, (', strcompress(100*pourcent_dawn), '%)'
237   print, equal, ' equal, (', strcompress(100*pourcent_equal), '%)'
238   print, ''
239   print, 'dawn'
240   for i=sta, fin do begin
241       if ind_dawn(i) eq 1 then print, 'PJ', i
242   endfor
243   print, ''
244   print, 'equal'
245   for i=sta, fin do begin
246       if ind_equal(i) eq 1 then print, 'PJ', i
247   endfor
248
249
250 ; -----
251 ; |                               |
252 ; |                               |
253 ; |                               |
254 ; |                               |
255 ; -----
256 ; Compute the dusk-over-dawn ratios
257 ; -----
258

```

APPENDIX I. IDL ROUTINES

```

259  ratio_tot=0.
260  ind_ok=0.
261  equal=0.
262  ind_equal=fltarr(fin+1)
263  dusk_big=0.
264  ind_dusk=fltarr(fin+1)
265  dawn_big=0.
266  ind_dawn=fltarr(fin+1)
267
268  for i=sta, fin do begin
269      if usable_N(i) eq 1. then begin
270          ind_ok=ind_ok+1.
271          ratio(i,0)=dusk(i,0)/dawn(i,0)
272          ratio_tot=ratio_tot+ratio(i,0)
273
274          if dusk(i,0) gt dawn(i,0) then begin
275              if dusk(i,0)-dusk(i,0)/100 gt dawn(i,0) then begin ; More power from the
dusk region
276                  dusk_big=dusk_big+1.
277                  ind_dusk(i)=1.
278              endif else begin ; Equal emitted power
279                  equal=equal+1.
280                  ind_equal(i)=1.
281              endelse
282          endif else if dusk(i,0) lt dawn(i,0) then begin
283              if dawn(i,0)-dawn(i,0)/100 gt dusk(i,0) then begin ; More power from the
dawn region
284                  dawn_big=dawn_big+1.
285                  ind_dawn(i)=1.
286              endif else begin ; Equal emitted power
287                  equal=equal+1.
288                  ind_equal(i)=1.
289              endelse
290          endif
291      endif
292  endfor
293  ratio_tot=ratio_tot/(ind_ok)
294  pourcent_dawn=dawn_big/(ind_ok)
295  pourcent_dusk=dusk_big/(ind_ok)
296  pourcent_equal=equal/(ind_ok)
297  moy_dusk=total(dusk(*,0)*usable_N)/(ind_ok)
298  moy_dawn=total(dawn(*,0)*usable_N)/(ind_ok)
299  ratio_moy=moy_dusk/moy_dawn
300
301
302  ;-----
303  ; Computation of the medians and standard deviations for the ratios, dusk
region, and dawn region
304  ;-----
305
306  ind=where(ratio(*,0) ne 0) ; Ratios.
307  arr_med=ratio(ind,0)
308  arr_med=arr_med(sort(arr_med))
309  if ind_ok mod 2 eq 0 then begin
310      inf=arr_med((ind_ok/2)-1)
311      sup=arr_med(ind_ok/2)
312      med= (inf+sup)/2
313  endif else begin
314      med=arr_med(floor(ind_ok/2))
315  endelse
316

```

APPENDIX I. IDL ROUTINES

```

317  sigma=sqrt(total((arr_med(*)-ratio_tot)^2)/ind_ok)
318
319  ind=where(dusk(*,0)*usable_N ne 0) ; Dusk.
320  arr_med2=dusk(ind,0)
321  arr_med2=arr_med2(sort(arr_med2))
322  if ind_ok mod 2 eq 0 then begin
323      inf=arr_med2((ind_ok/2)-1)
324      sup=arr_med2(ind_ok/2)
325      med2=((inf+sup)/2)/1e+09
326  endif else begin
327      med2=arr_med2(floor(ind_ok/2))/1e+09
328  endelse
329
330  sigma2=sqrt(total((arr_med2(*)-moy_dusk)^2)/ind_ok)
331
332  ind=where(dawn(*,0)*usable_N ne 0) ; Dawn.
333  arr_med3=dawn(ind,0)
334  arr_med3=arr_med3(sort(arr_med3))
335  if ind_ok mod 2 eq 0 then begin
336      inf=arr_med3((ind_ok/2)-1)
337      sup=arr_med3(ind_ok/2)
338      med3=((inf+sup)/2)/1e+09
339  endif else begin
340      med3=arr_med3(floor(ind_ok/2))/1e+09
341  endelse
342
343  sigma3=sqrt(total((arr_med3(*)-moy_dawn)^2)/ind_ok)
344
345
346  ;-----
347  ; Print every information computed
348  ;-----
349
350  print, '-----NORTH-----'
351  print, ind_ok, ' PJ ok'
352  print, ratio_tot, ' mean dusk/dawn'
353  print, moy_dusk/1e+09, ' GW mean dusk'
354  print, moy_dawn/1e+09, ' GW mean dawn'
355  print, ratio_moy, ' mean dusk/mean dawn'
356  print, med, ' median'
357  print, med2, ' GW median dusk'
358  print, med3, ' GW median dawn'
359  print, med2/med3, ' ratio of medians'
360  print, sigma, ' sigma of ratio'
361  print, sigma2/1e+09, ' GW sigma dusk'
362  print, sigma3/1e+09, ' GW sigma dawn'
363  print, dusk_big, ' dusk, (', strcompress(100*pourcent_dusk), ' %)'
364  print, dawn_big, ' dawn, (', strcompress(100*pourcent_dawn), ' %)'
365  print, equal, ' equal, (', strcompress(100*pourcent_equal), ' %)'
366  print, ''
367  print, 'dawn'
368  for i=sta, fin do begin
369      if ind_dawn(i) eq 1 then print, 'PJ', i
370  endfor
371  print, ''
372  print, 'equal'
373  for i=sta, fin do begin
374      if ind_equal(i) eq 1 then print, 'PJ', i
375  endfor
376 end

```

error_V2.pro

```

1 pro error_V2, modele, hemi, sector
2 ; modele = model used. 'b', 'v', 'g', or 'g2' in entry.
3 ; hemi = hemisphere of interest. 'N' or 'S' in entry.
4 ; sector = sector of interest. 'HST' or 'sym' in entry.
5
6 arr_ratio=fltarr(40)
7 arr_err_ratio=fltarr(40)
8
9 for k=1, 39 do begin
10   pj='PJ'+strcompress(k,/re)
11   print, pj
12
13   if file_test('/home/LPAP/groulard/juno/'+pj+'/auroral_power_'+pj+'_'+hemi+'.
14   idl') then begin
15     restore, '/home/LPAP/groulard/juno/'+pj+'/auroral_power_'+pj+'_'+hemi+'.
16     idl'
17
18     ;-----
19     ; Select the maps to work on based on the sector, the modele and the
20     hemisphere selected
21     ;-----
22
23     if sector eq 'HST' then begin
24       lt_11=6
25       lt_12=8
26       lt_21=16
27       lt_22=18
28
29       if modele eq 'b' then begin
30         usable_N=[0, 1, 0, 1, 1, 1, 1, 0, 1, 1, 0, 1, 1, 0, 1, 1, 1, 0, 0, 1,
31         1, 0, 1, 0, 1, 0, 1, 0, 0, 0, 0, 0, 1, 0, 0, 0, 1, 0, 1, 0]
32         usable_S=[0, 1, 0, 1, 1, 1, 1, 0, 1, 1, 1, 1, 1, 1, 1, 1, 1, 1, 1, 1,
33         1, 1, 1, 1, 0, 1, 1, 1, 1, 0, 1, 1, 1, 1, 1, 1, 1, 0, 1, 1]
34       endif
35       if modele eq 'v' then begin
36         usable_N=[0, 1, 0, 1, 1, 1, 1, 1, 1, 1, 0, 1, 1, 1, 1, 1, 1, 0, 0, 1,
37         1, 1, 1, 0, 1, 0, 0, 0, 0, 0, 1, 0, 0, 0, 1, 0, 1, 1]
38         usable_S=[0, 1, 0, 1, 1, 1, 1, 1, 1, 1, 1, 1, 1, 1, 1, 1, 1, 1, 0, 1,
39         1, 1, 0, 1, 0, 1, 0, 0, 0, 1, 1, 1, 1, 1, 1, 1, 1, 1, 1]
40       endif
41       if modele eq 'g' or modele eq 'g2' then begin
42         usable_N=[0, 1, 0, 1, 1, 1, 1, 1, 1, 1, 0, 1, 1, 1, 1, 1, 1, 0, 0, 1,
43         1, 1, 1, 0, 1, 0, 1, 0, 0, 0, 0, 0, 1, 0, 0, 0, 1, 0, 1, 1]
44         usable_S=[0, 1, 0, 1, 1, 1, 1, 1, 1, 1, 1, 1, 1, 1, 1, 1, 1, 1, 1, 1,
45         1, 1, 1, 1, 1, 1, 1, 1, 1, 1, 1, 1, 1, 1, 1, 1, 1, 1]
46       endif
47       endif else begin
48         lt_11=4
49         lt_12=8
50         lt_21=16
51         lt_22=20
52
53         if modele eq 'b' then begin
54           usable_N=[0, 1, 0, 1, 1, 1, 1, 0, 0, 1, 0, 1, 1, 0, 1, 1, 1, 0, 0, 1,
55           1, 0, 0, 0, 1, 0, 1, 0, 0, 0, 0, 0, 1, 0, 0, 0, 1, 0, 1, 0]
56           usable_S=[0, 1, 0, 1, 1, 1, 1, 0, 1, 1, 1, 1, 1, 0, 1, 1, 1, 1, 1, 1,
57           1, 1, 0, 1, 0, 1, 1, 1, 1, 0, 1, 1, 1, 1, 1, 1, 1, 0, 1, 1]
58         endif
59       endif
60     end
61   end
62 end

```

APPENDIX I. IDL ROUTINES

```

48     if modele eq 'v' then begin
49         usable_N=[0, 1, 0, 1, 1, 1, 1, 1, 1, 1, 0, 1, 1, 1, 1, 1, 1, 0, 0, 1,
1, 1, 1, 0, 1, 0, 0, 0, 0, 0, 0, 1, 0, 0, 0, 1, 0, 1, 1]
50         usable_S=[0, 1, 0, 1, 1, 1, 1, 1, 1, 1, 1, 1, 1, 1, 1, 1, 0, 1, 1, 1,
1, 1, 0, 1, 0, 1, 0, 0, 0, 1, 0, 1, 1, 1, 0, 1, 1, 1, 1]
51     endif
52     if modele eq 'g' then begin
53         usable_N=[0, 1, 0, 1, 1, 1, 1, 1, 1, 1, 0, 1, 1, 1, 1, 1, 1, 0, 0, 1,
1, 1, 1, 0, 1, 0, 1, 0, 0, 0, 0, 0, 1, 0, 0, 0, 1, 0, 1, 1]
54         usable_S=[0, 1, 0, 1, 1, 1, 1, 1, 1, 1, 1, 1, 1, 1, 1, 1, 1, 1, 1, 1,
1, 1, 1, 1, 1, 1, 1, 1, 1, 1, 1, 1, 1, 1, 1, 1]
55     endif
56     if modele eq 'g2' then begin
57         usable_N=[0, 1, 0, 1, 1, 1, 1, 1, 1, 1, 1, 1, 1, 1, 1, 1, 1, 0, 0, 1,
1, 1, 1, 0, 1, 0, 1, 0, 0, 0, 0, 0, 1, 0, 0, 0, 1, 0, 1, 1]
58         usable_S=[0, 1, 0, 1, 1, 1, 1, 1, 1, 1, 1, 1, 1, 1, 1, 1, 1, 1, 1, 1,
1, 1, 1, 1, 1, 1, 1, 1, 1, 1, 1, 1, 1, 1, 1, 1]
59     endif
60     endelse
61
62     if hemi eq 'N' then usable=usable_N else usable=usable_S
63
64     distance=30. ; Rj
65
66     str_lt=strcompress(lt_11,/re)
67     if modele ne 'g2' then begin ; restore the data needed based on the model
(for b, v or g).
68         restore, '/home/LPAP/groulard/juno/'+pj+'/dawn_dusk_power_'+modele+'_'+
pj+'_'+hemi+'_'+str_lt+'.idl'
69         restore, '/home/LPAP/groulard/juno/'+pj+'/auroral_power_'+pj+'_'+hemi+'
idl'
70         restore, '/LPAP/HST/redu/juno/'+pj+'/ephem/'+pj+'_ephem03.idl'
71         restore, '/home/LPAP/groulard/juno/'+pj+'/masque_'+modele+'_'+pj+'_'+
hemi+'.idl'
72         restore, '/LPAP/HST/work/bonfond/Fichiers_de_reference/surface_vect.idl'
73     endif else begin ; restore the data needed if the model is g2.
74         if file_test('/home/LPAP/groulard/juno/'+pj+'/dawn_dusk_power_g2_'+pj+'_'
'+hemi+'_'+str_lt+'.idl') then begin ; if a g2 mask exists, restore the g2
data...
75             restore, '/home/LPAP/groulard/juno/'+pj+'/dawn_dusk_power_g2_'+pj+'_'
+hemi+'_'+str_lt+'.idl'
76             restore, '/home/LPAP/groulard/juno/'+pj+'/auroral_power_'+pj+'_'
+hemi+'
'.idl'
77             restore, '/LPAP/HST/redu/juno/'+pj+'/ephem/'+pj+'_ephem03.idl'
78             restore, '/home/LPAP/groulard/juno/'+pj+'/masque_g2_'+pj+'_'
+hemi+'
idl'
79             restore, '/LPAP/HST/work/bonfond/Fichiers_de_reference/surface_vect.
idl'
80         endif else begin
81             if file_test('/home/LPAP/groulard/juno/'+pj+'/dawn_dusk_power_g_'+pj+'_'
'+hemi+'_'+str_lt+'.idl') then begin ; ... if not, restore the g data.
82                 restore, '/home/LPAP/groulard/juno/'+pj+'/dawn_dusk_power_g_'+pj+'_'
'+hemi+'_'
'+str_lt+'.idl'
83                 restore, '/home/LPAP/groulard/juno/'+pj+'/auroral_power_'+pj+'_'
+hemi+'
'.idl'
84                 restore, '/LPAP/HST/redu/juno/'+pj+'/ephem/'+pj+'_ephem03.idl'
85                 restore, '/home/LPAP/groulard/juno/'+pj+'/masque_g_'+pj+'_'
+hemi+'
idl'
86                 restore, '/LPAP/HST/work/bonfond/Fichiers_de_reference/surface_vect.
idl'
87             endif

```

```

88         endelse
89     endelse
90
91     surf_mat=rebin(transpose(surface_vect),3600,1800) ;in km^2
92
93     if hemi eq 'N' then begin
94         x_photo=363
95         y_photo=170
96     endif
97     if hemi eq 'S' then begin
98         x_photo=438
99         y_photo=460
100    endif
101
102
103    ;-----
104    ; Using Vogt et al. 2011 model
105    ;-----
106
107    if hemi eq 'N' then hemi_str='north' else if $
108        hemi eq 'S' then hemi_str='south' else stop
109
110    pos11 = mapping_function2019('mag_to_ion_'+hemi_str, lon_sun, distance,
111    lt_11, 'jrm09')
112    a_11=latlon2angle_AG(pos11(0),pos11(1))
113    angle_11=a_11(0)
114    dist_11=a_11(1)
115    pos12 = mapping_function2019('mag_to_ion_'+hemi_str, lon_sun, distance,
116    lt_12, 'jrm09')
117    a_12=latlon2angle_AG(pos12(0),pos12(1))
118    angle_12=a_12(0)
119    dist_12=a_12(1)
120    pos21 = mapping_function2019('mag_to_ion_'+hemi_str, lon_sun, distance,
121    lt_21, 'jrm09')
122    a_21=latlon2angle_AG(pos21(0),pos21(1))
123    angle_21=a_21(0)
124    dist_21=a_21(1)
125    pos22 = mapping_function2019('mag_to_ion_'+hemi_str, lon_sun, distance,
126    lt_22, 'jrm09')
127    a_22=latlon2angle_AG(pos22(0),pos22(1))
128    angle_22=a_22(0)
129    dist_22=a_22(1)
130
131    if modele eq 'v' then masque_me=shift(masque_me,1800,0) ; the v mask is
132    accidentally shifted in comparison to the other masks.
133
134    ;-----
135    ; Create the dusk and dawn masks
136    ;-----
137
138    ; Dawn:
139    if angle_12 gt angle_11 then implan_dawn_area=masque_me gt (angle_11*20.+1
140    .) and masque_me le (angle_12*20.+1.) $
141    else implan_dawn_area=(masque_me lt (angle_12*20.+1.) or masque_me ge (
142    angle_11*20.+1.)) and masque_me gt 0
143
144    inde_dawn=where(implan_dawn_area ne 0)
145    implan_dawn_area(inde_dawn)=1
146
147    ; Dusk:

```

APPENDIX I. IDL ROUTINES

```

142     if angle_22 gt angle_21 then implan_dusk_area=masque_me gt (angle_21*20.+1
143     .) and masque_me le (angle_22*20.+1.) $
144     else implan_dusk_area=(masque_me lt (angle_22*20.+1.) or masque_me ge (
145     angle_21*20.+1.)) and masque_me gt 0
146
147     inde_dusk=where(implan_dusk_area ne 0)
148     implan_dusk_area(inde_dusk)=1
149
150     ind1=where(implan_dusk_area ne 0)
151     ind2=where(implan_dawn_area ne 0)
152     implan_clean_dusk=implan_clean(ind1)
153     implan_clean_dawn=implan_clean(ind2)
154     surf_dusk=surf_mat(ind1)
155     surf_dawn=surf_mat(ind2)
156
157     ;-----
158     ; Compute the uncertainty on the count
159     ;-----
160
161     mean_energy=1.65590e-18
162     bri_dusk=total(implan_clean_dusk*surf_dusk)/total(surf_dusk)
163     bri_dawn=total(implan_clean_dawn*surf_dawn)/total(surf_dawn)
164
165     count_dusk=total(25*implan_clean_dusk/10) ; 25 counts for 10kR (cf. Gerard
166     et al. 2019)
167     count_dawn=total(25*implan_clean_dawn/10)
168
169     print, 'counts: ', count_dusk, ' - ', count_dawn
170     print, ''
171     err_bri_dusk=bri_dusk*sqrt(count_dusk)/count_dusk
172     err_bri_dawn=bri_dawn*sqrt(count_dawn)/count_dawn
173
174     print, 'err dusk: ', 100*err_bri_dusk/bri_dusk, '%'
175     print, 'err dawn: ', 100*err_bri_dawn/bri_dawn, '%'
176     print, ''
177
178     print, 'dusk: ', bri_dusk, '+-', err_bri_dusk
179     print, 'dawn: ', bri_dawn, '+-', err_bri_dawn
180     print, ''
181
182     dusk=mean_energy*bri_dusk*1.e13*1.e6*total(surf_dusk) ; Power dusk.
183     dawn=mean_energy*bri_dawn*1.e13*1.e6*total(surf_dawn) ; Power dawn.
184     err_dusk=mean_energy*err_bri_dusk*1.e13*1.e6*total(surf_dusk) ; Counting
185     error on the power dusk.
186     err_dawn=mean_energy*err_bri_dawn*1.e13*1.e6*total(surf_dawn) ; Counting
187     error on the power dawn.
188
189     if dawn ne 0 then ratio=dusk/dawn else ratio = 0
190     if dawn ne 0 and dusk ne 0 then err_ratio=ratio*sqrt((err_dusk/dusk)^2+(
191     err_dawn/dawn)^2) else err_ratio = 0 ; Propagation of error on the ratio.
192
193     print, dusk/1e09, '+-', err_dusk/1e09, ' GW'
194     print, dawn/1e09, '+-', err_dawn/1e09, ' GW'
195     print, ratio, err_ratio
196
197     arr_ratio(k)=ratio
198     arr_err_ratio(k)=err_ratio
199

```

```
197     endif
198   endfor
199
200   ind=where(arr_ratio ne 0 and usable ne 0)
201   moy=total(arr_ratio*usable)/n_elements(ind)
202
203   moy_err=sqrt(total((arr_err_ratio*usable)^2))/n_elements(ind) ; Propagation of
      error on the mean.
204
205   print, ''
206   print, ind
207   print, arr_ratio(where(arr_ratio ne 0))
208   print, moy, '+-', moy_err
209
210 end
```


Appendix II: Auroral maps

The following pages are a collection of auroral maps (i.e. polar projections of the auroral regions displayed in System III, with the 0° meridian upward and increasing longitude counting clockwise) created during this master thesis. Each page is composed of a maximum of 12 images and corresponds to the maps created for a given perijove. 6 images are related to the southern hemisphere, and the 6 others to the northern hemisphere. The 2 first images of each series are a map of the aurorae with a scale indicating the brightness of each location and the date of first and last spins constituting the image, and the same map with the different local times of interest and the direction to the Sun. Figure 7.1 shows how to recognise the different local times. After that, the map is shown on 4 images with the different masks added on it. In order, their are the B, V, G1 and G2 masks, each of them being labelled in the top right corner.

It is worth mentioning that the 4 last maps are not always present, because not always useful. The data collected during some perijove are not enough to be used, and no mask has been created for these perijoves (e.g. PJ25 – north). In addition, when the main emission is made of a simple structure, the G1 mask covers it all and there is no reason to create the G2 mask for this perijove (e.g. PJ1 – north).

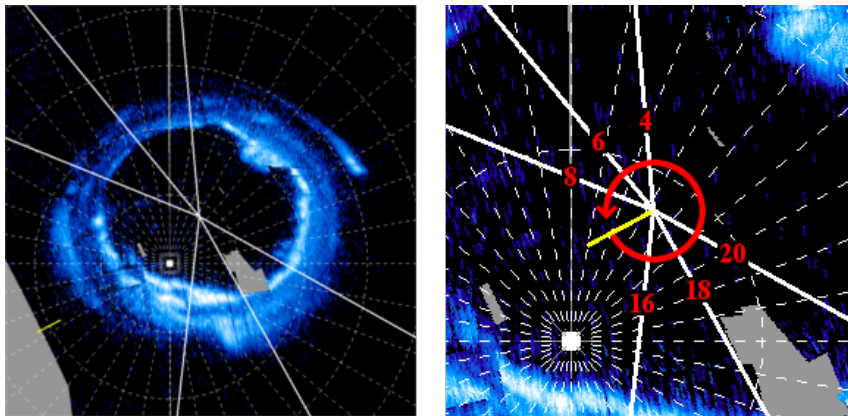
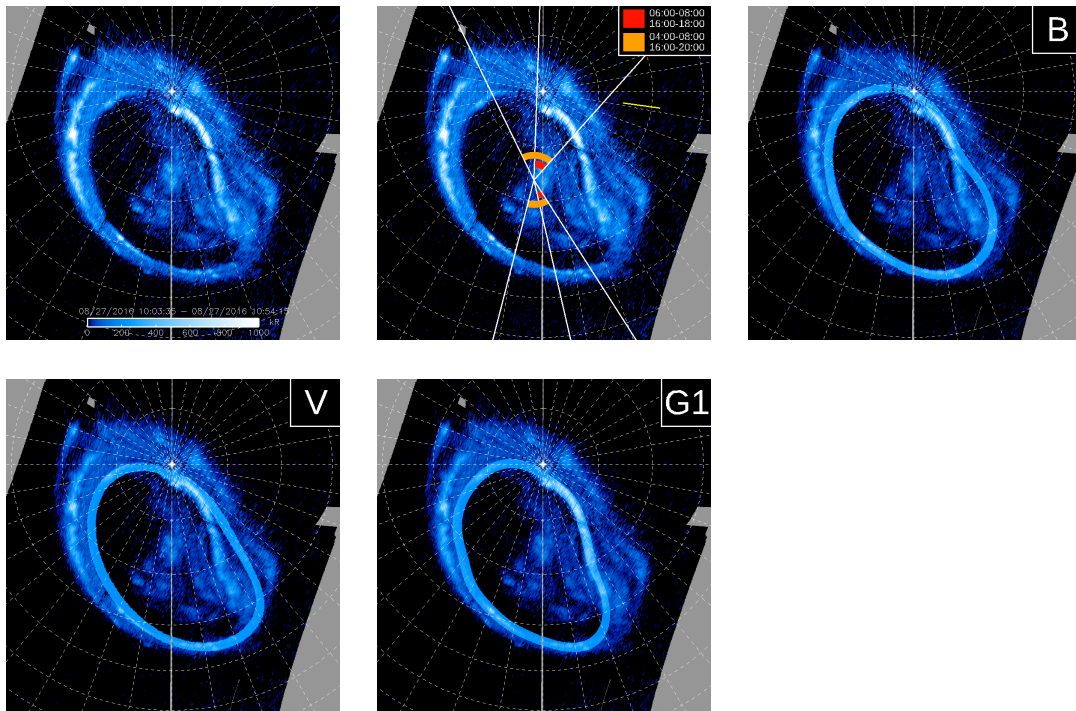
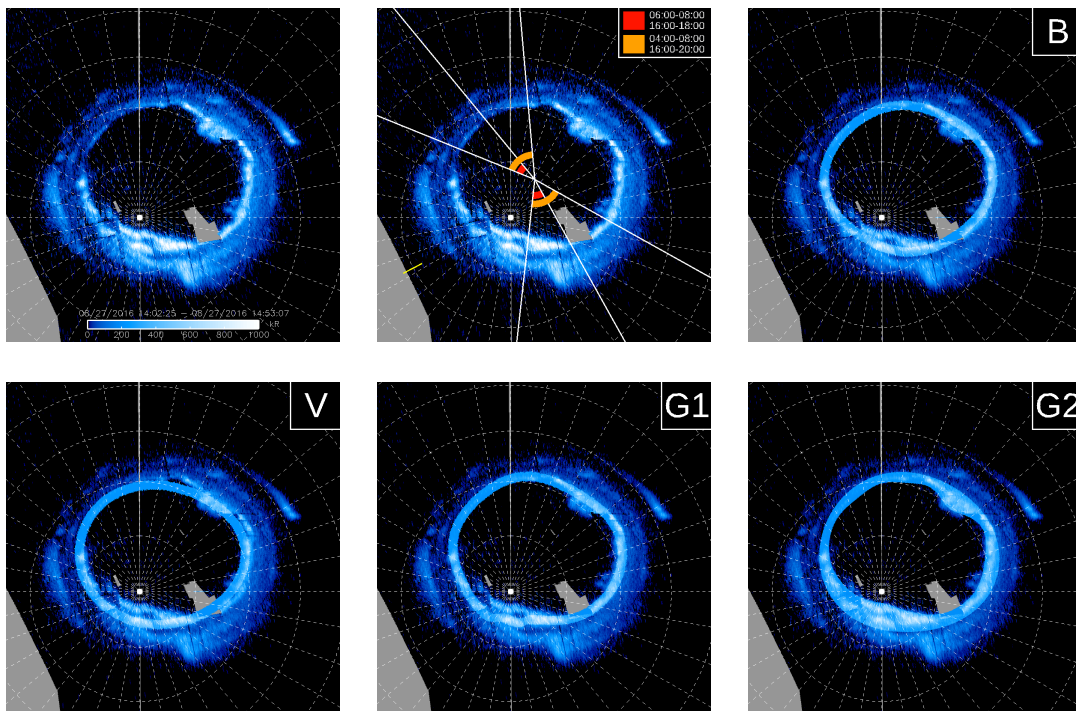


Figure 7.1: (left) A map of PJ1 – south, with the direction to the Sun in yellow and the six local times 4:00, 6:00, 8:00, 16:00, 18:00 and 20:00. (right) A zoom on the same map, with the different local times labelled. The auroral maps have been created so that Jupiter rotates in the trigonometric sense either in the northern hemisphere (i.e. the aurorae are seen from above the north pole) and in the southern hemisphere (i.e. the aurorae are seen from inside the planet). One can report the sunward direction by a rectilinear translation. This direction indicates noon. By rotating in the trigonometric sense, one thus find that the first local time reached is 16:00, then 18:00, and then 20:00. By continuing to the dawn part, one reaches 4:00, then 6:00, and finally 8:00.

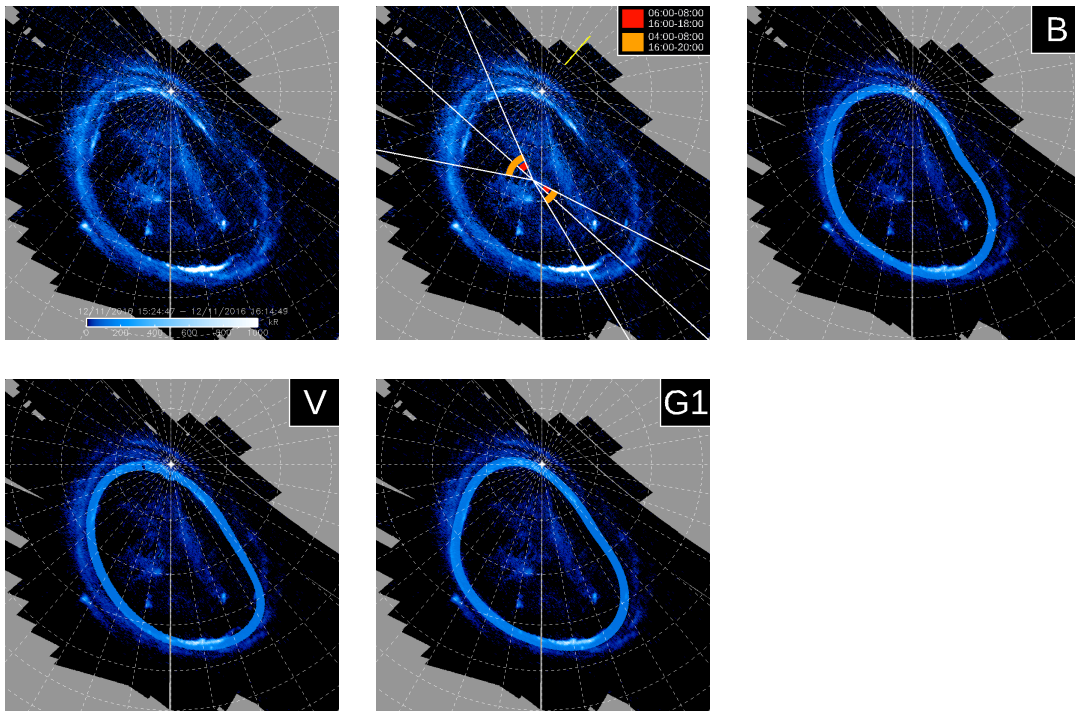
PJ1 – North



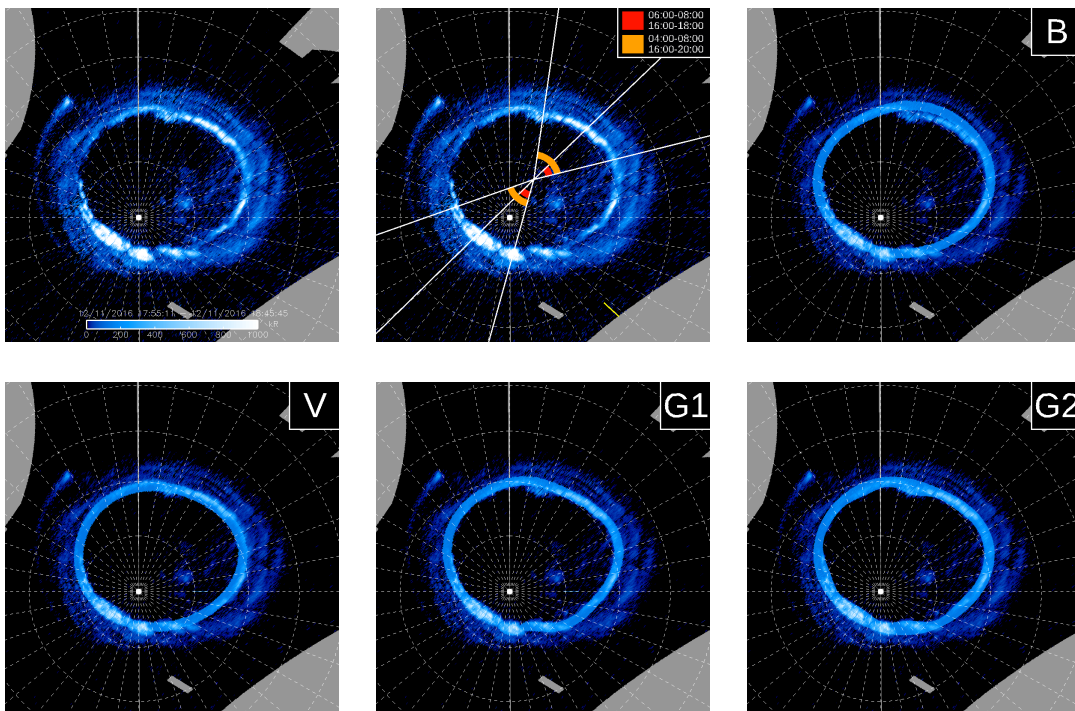
PJ1 – South



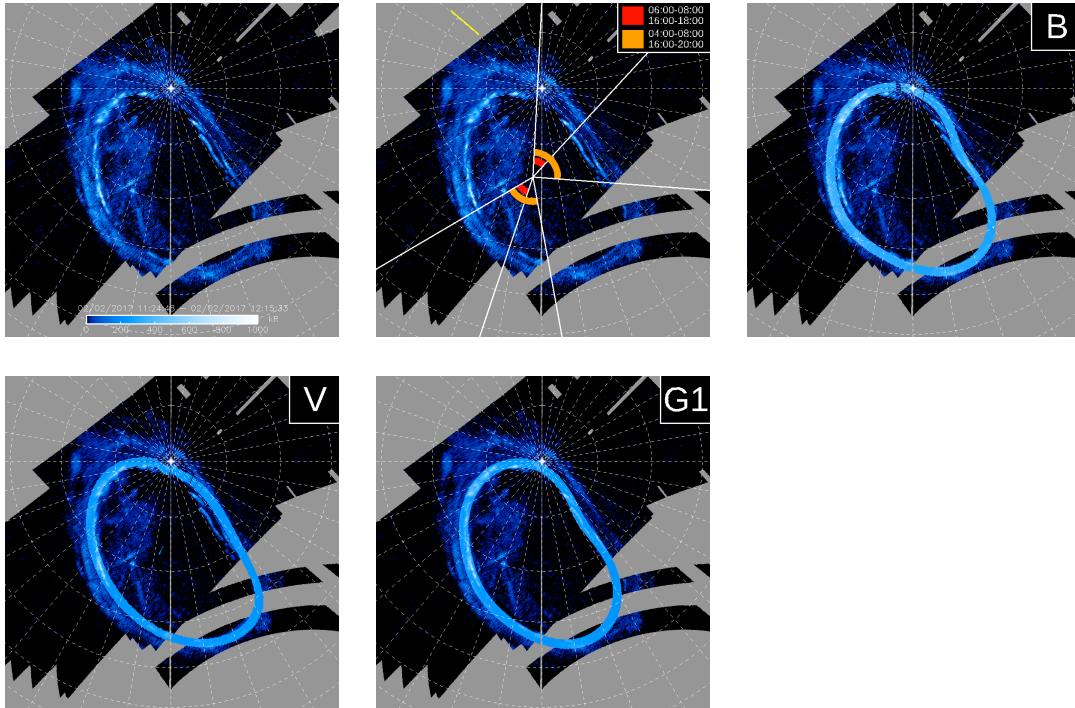
PJ3 – North



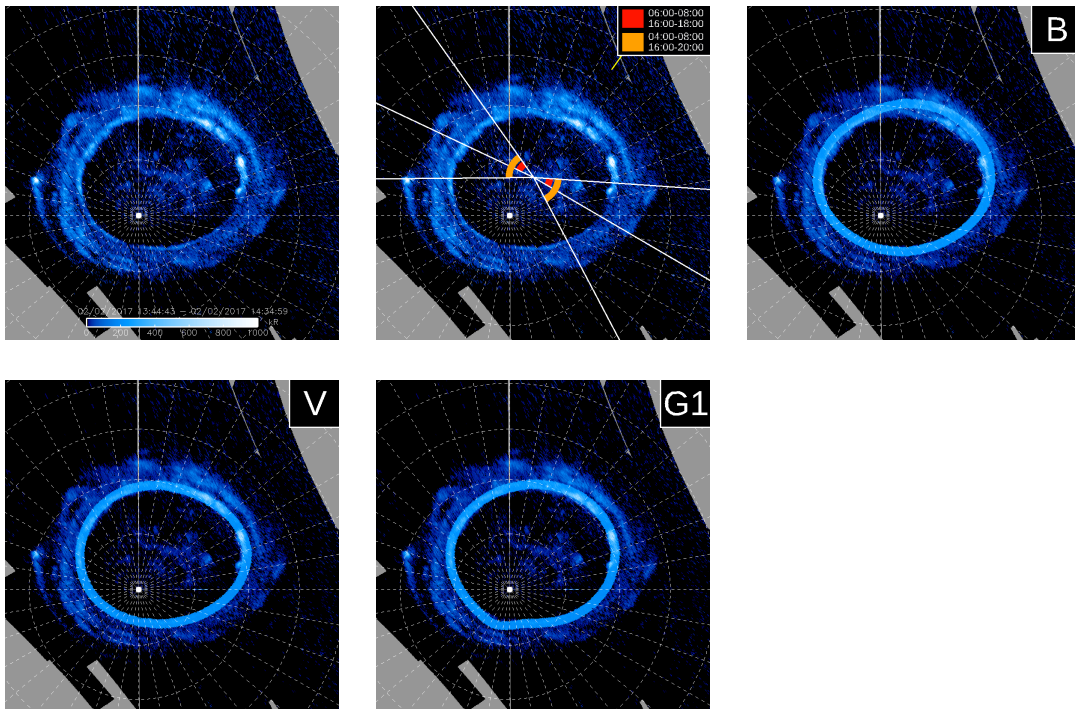
PJ3 – South



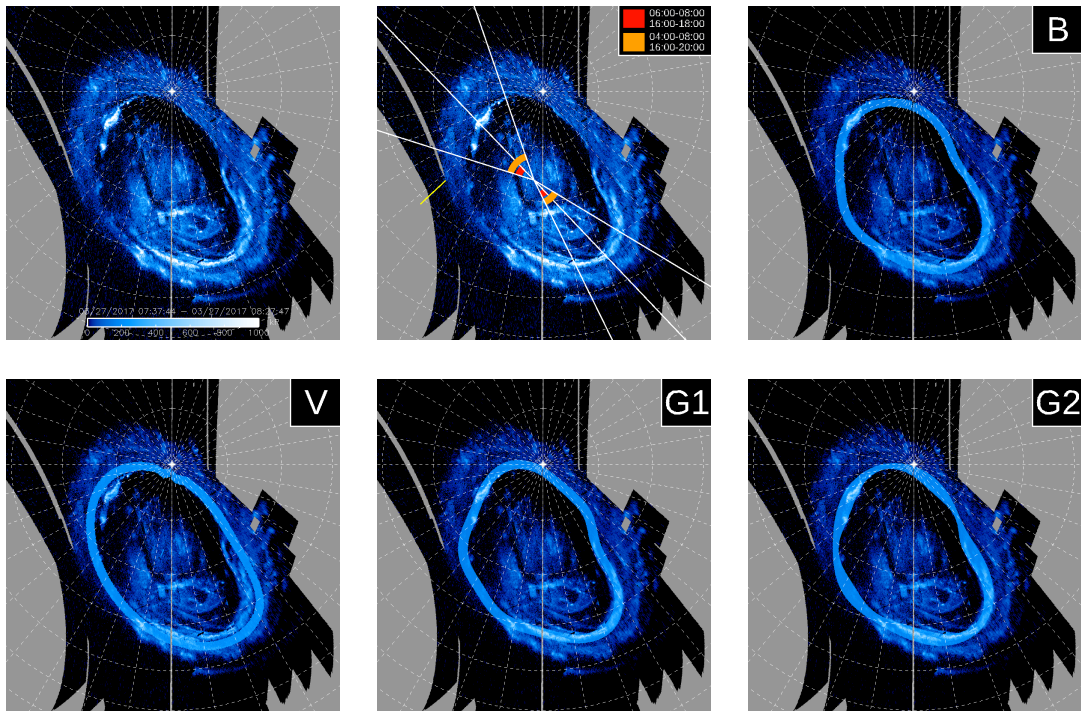
PJ4 – North



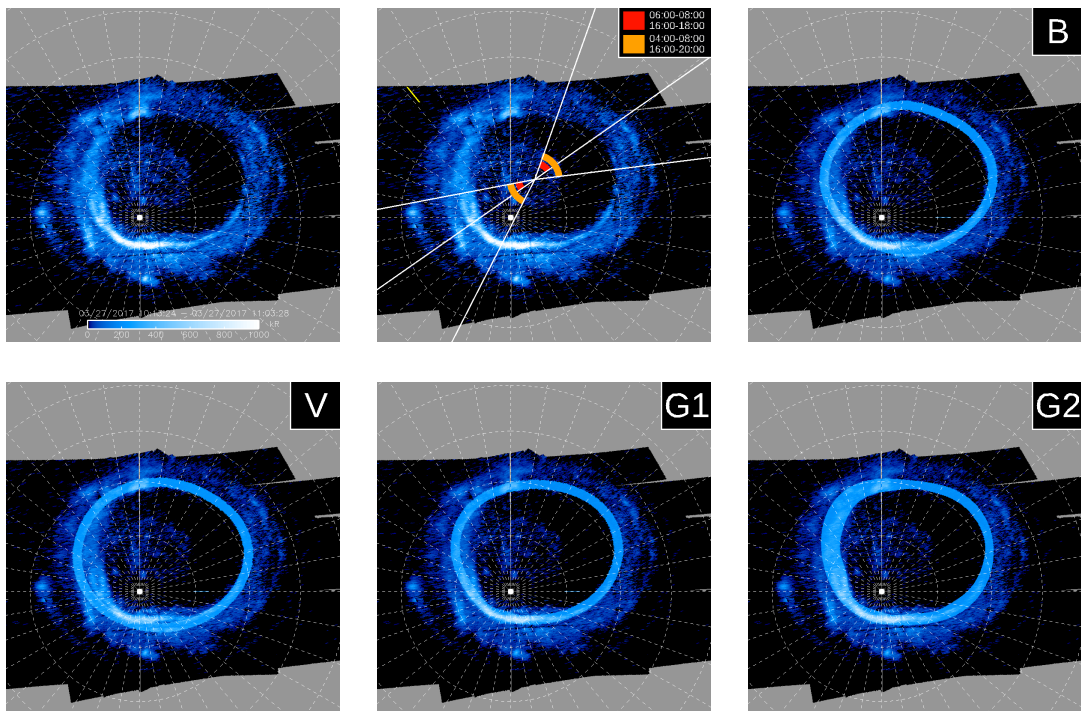
PJ4 – South



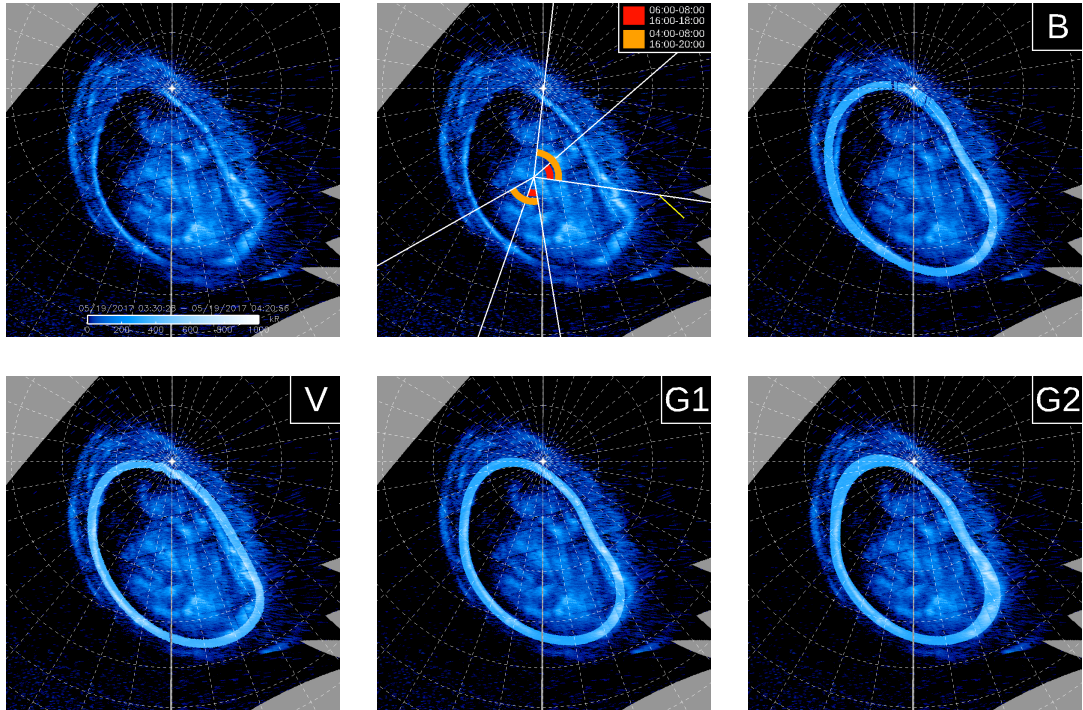
PJ5 – North



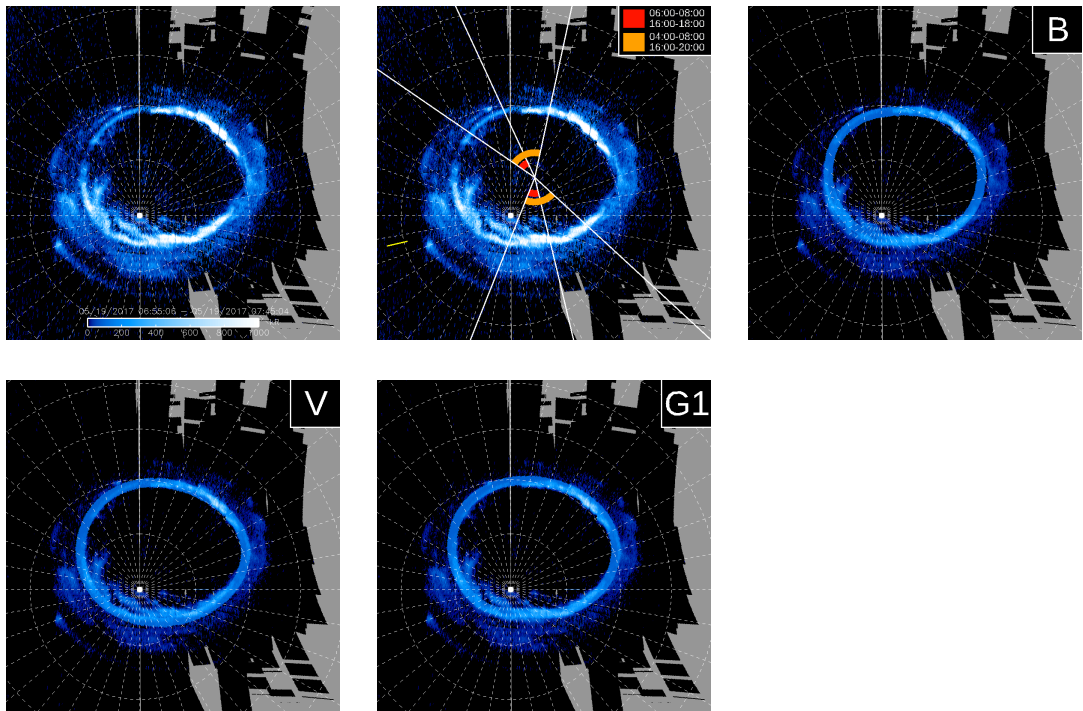
PJ5 – South



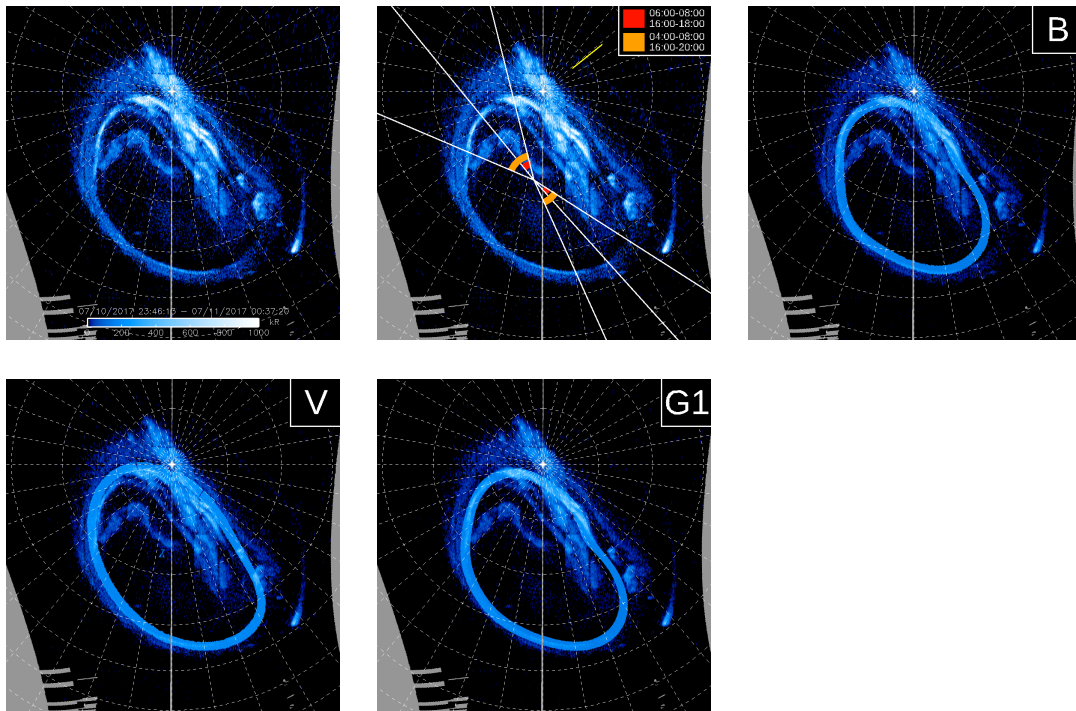
PJ6 – North



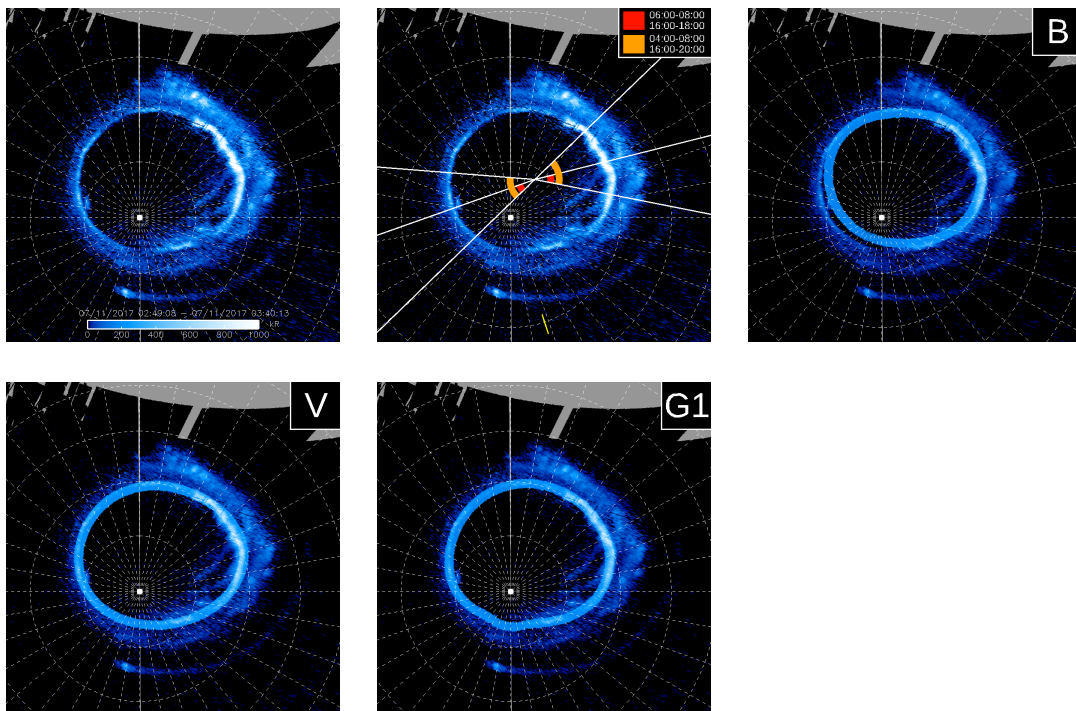
PJ6 – South



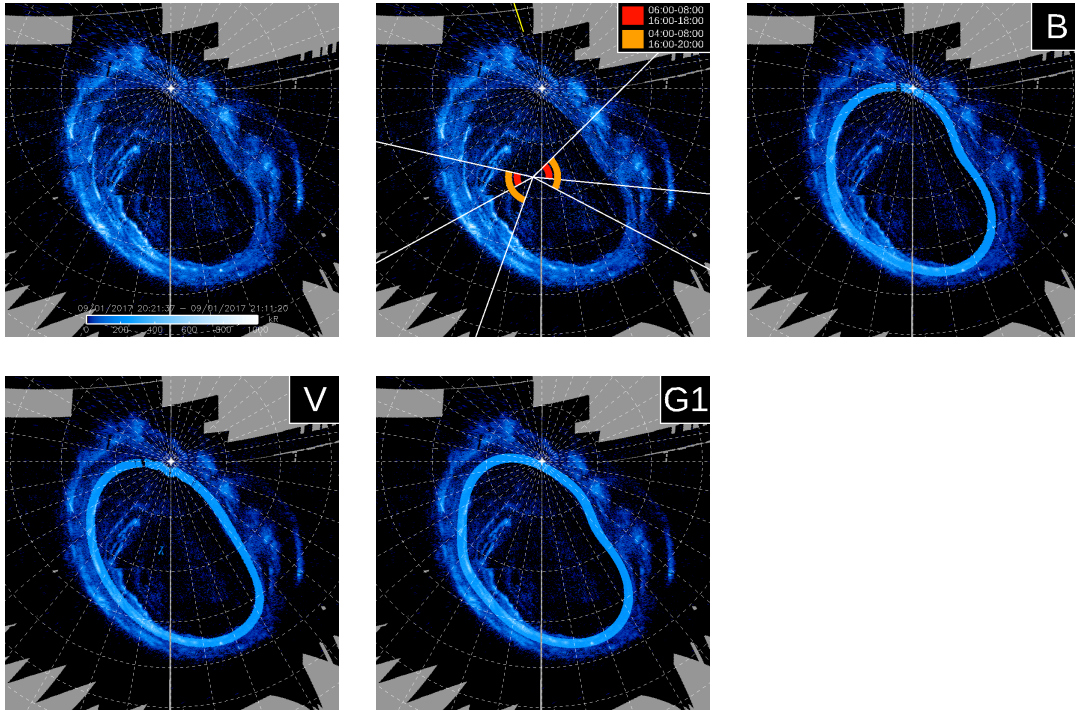
PJ7 – North



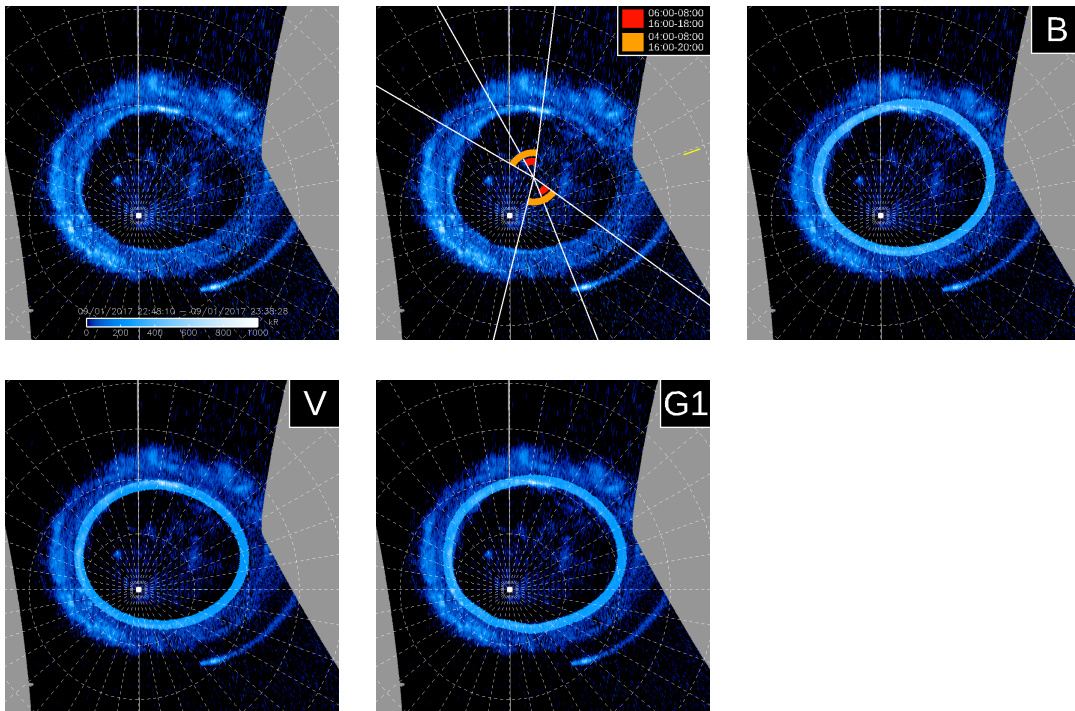
PJ7 – South



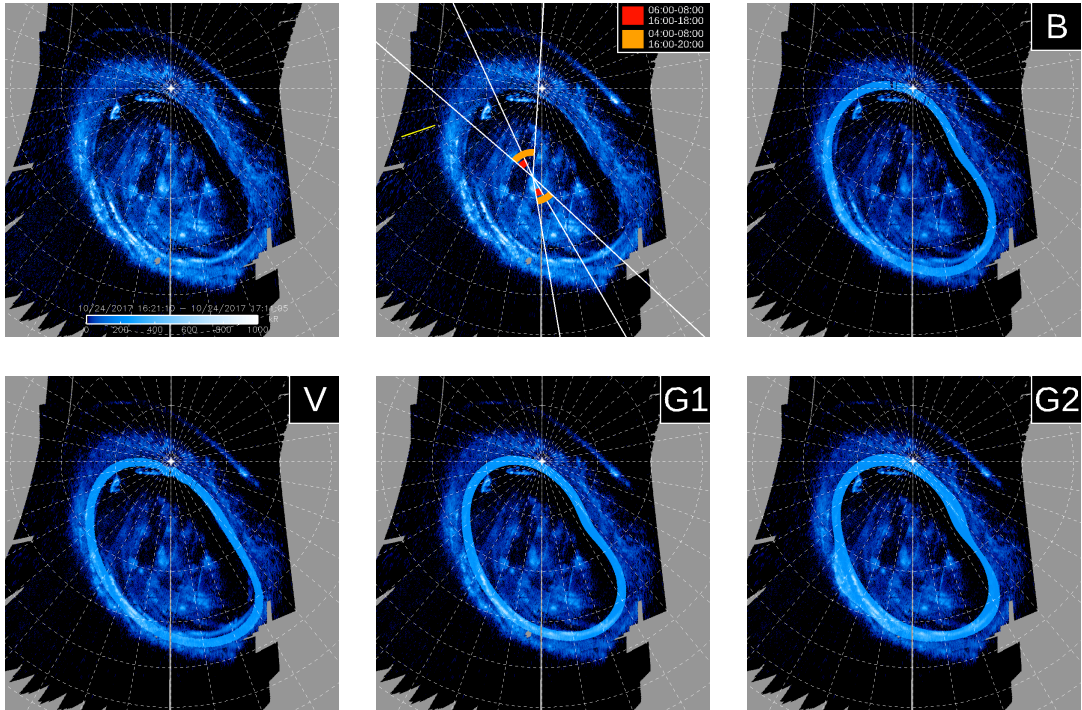
PJ8 – North



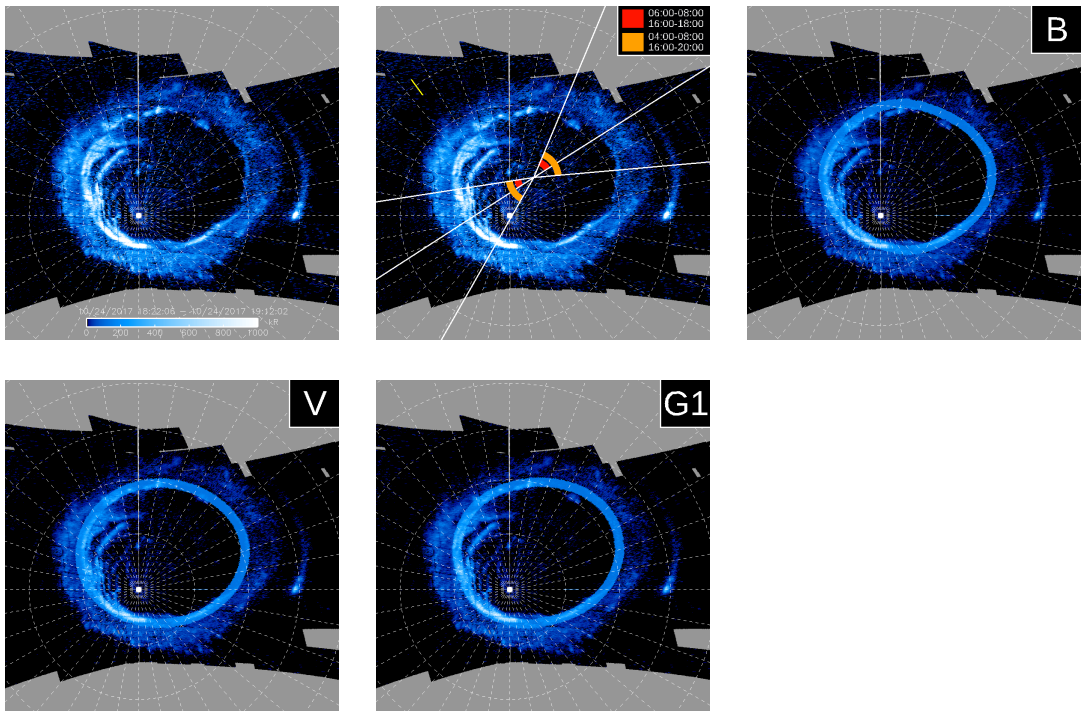
PJ8 – South



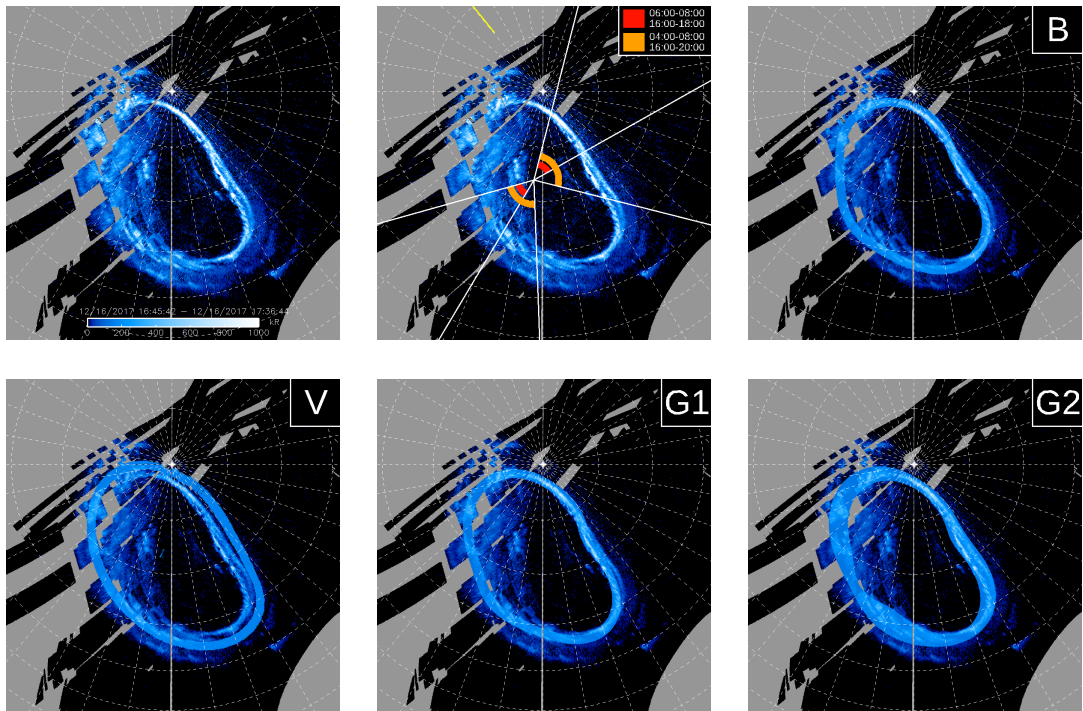
PJ9 – North



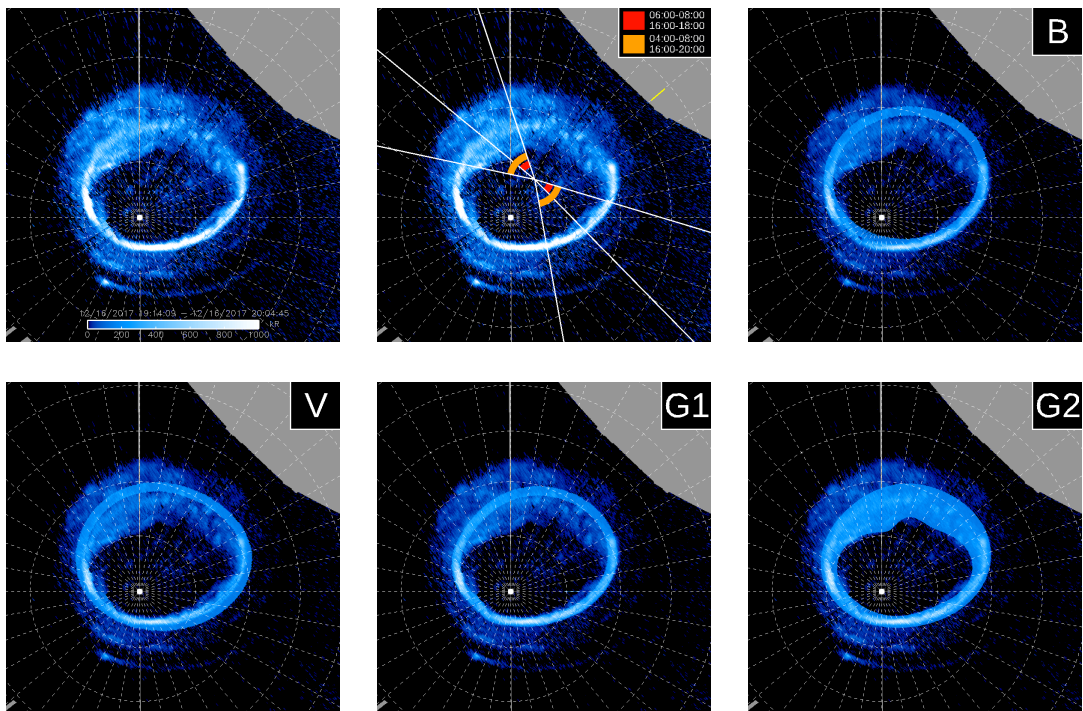
PJ9 – South



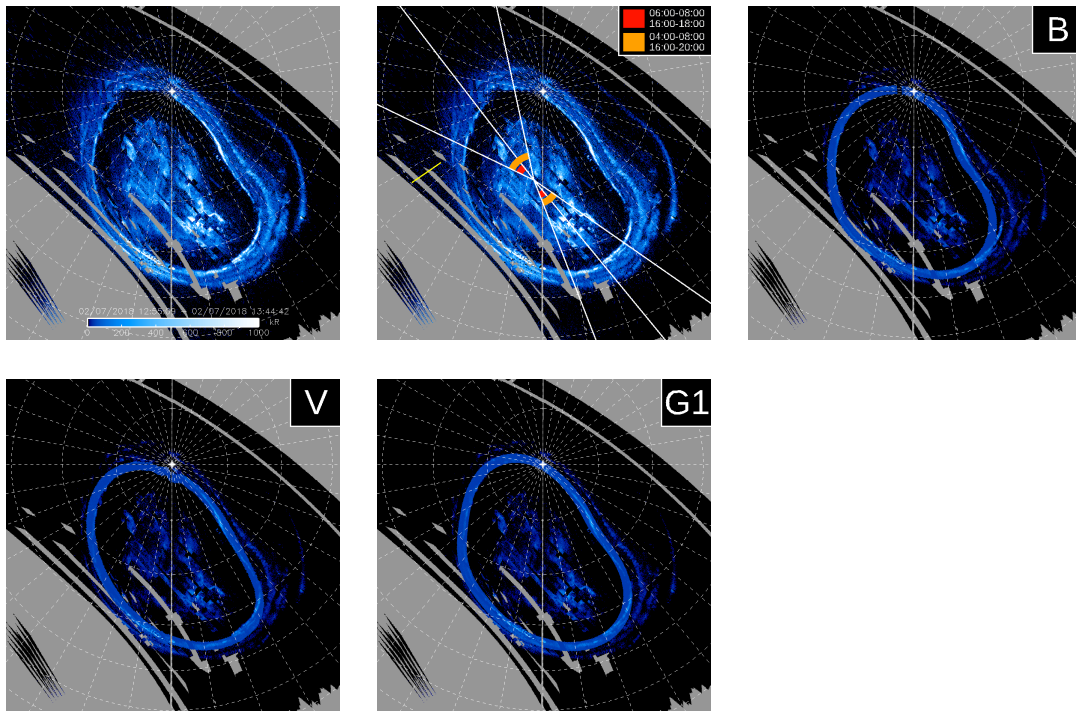
PJ10 – North



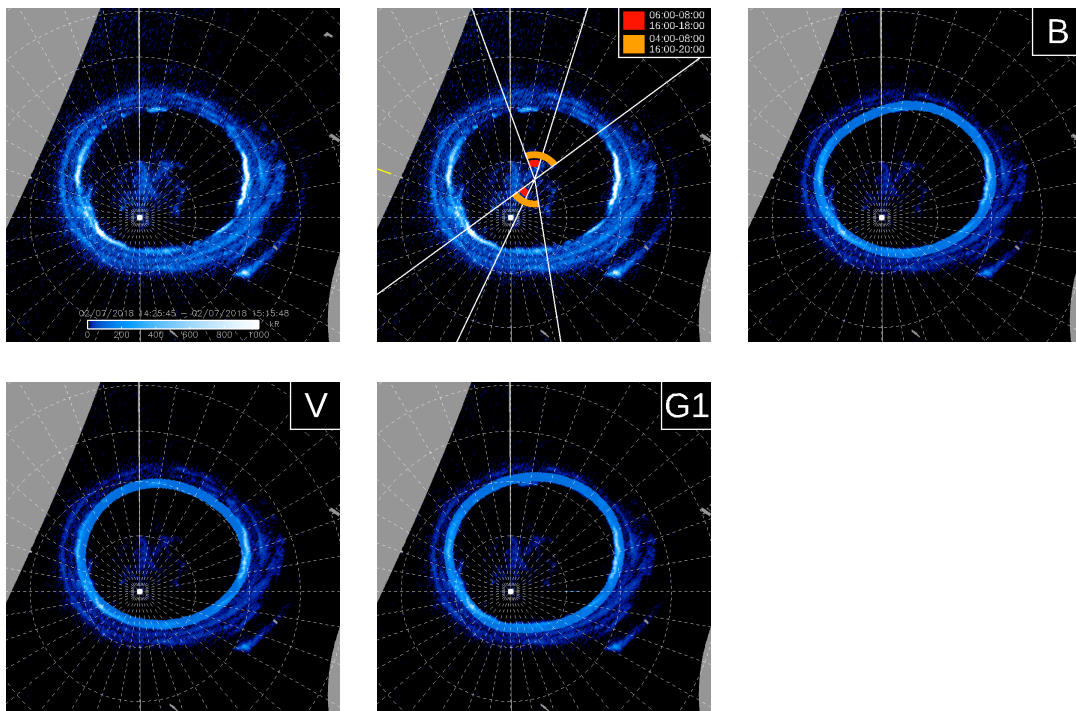
PJ10 – South



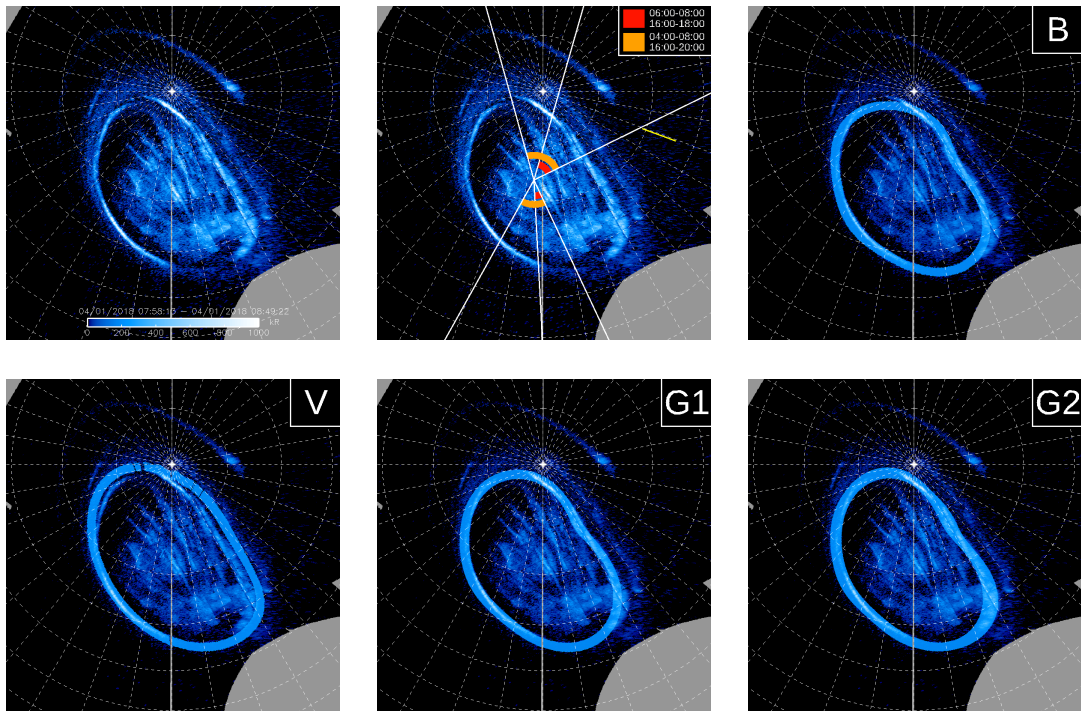
PJ11 – North



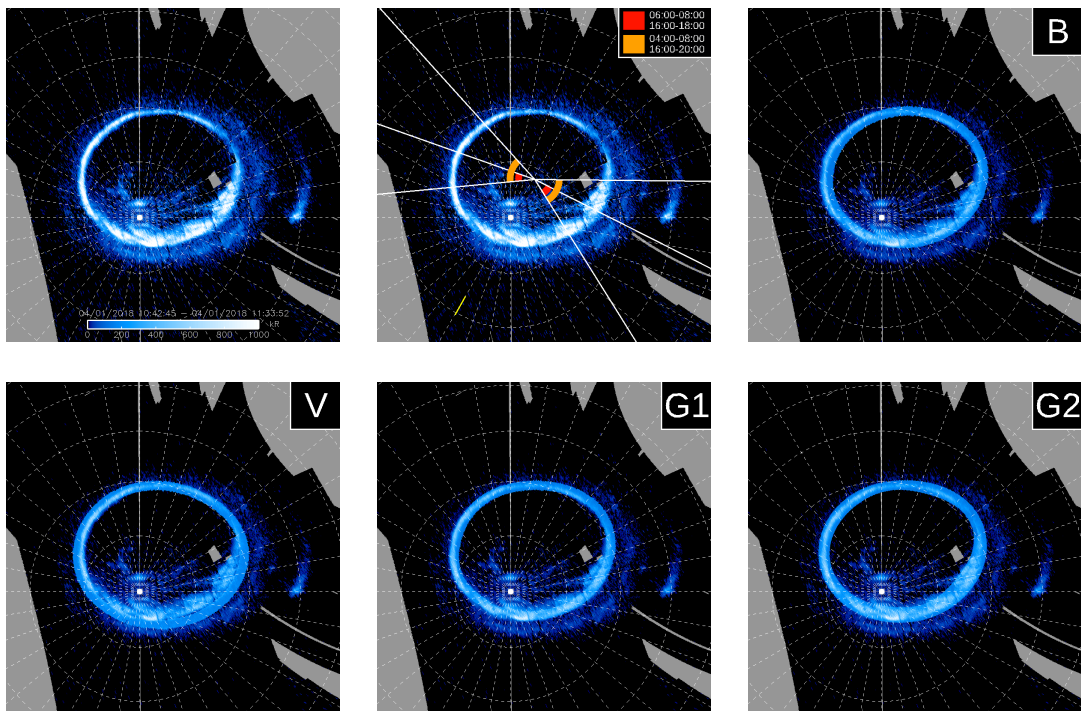
PJ11 – South



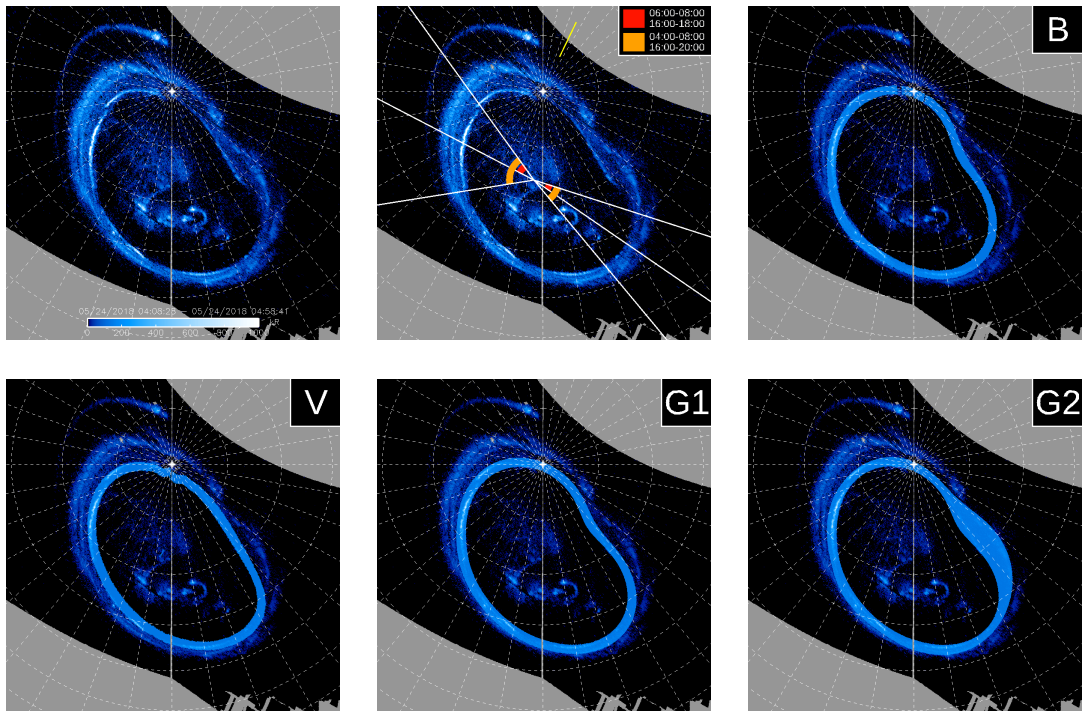
PJ12 – North



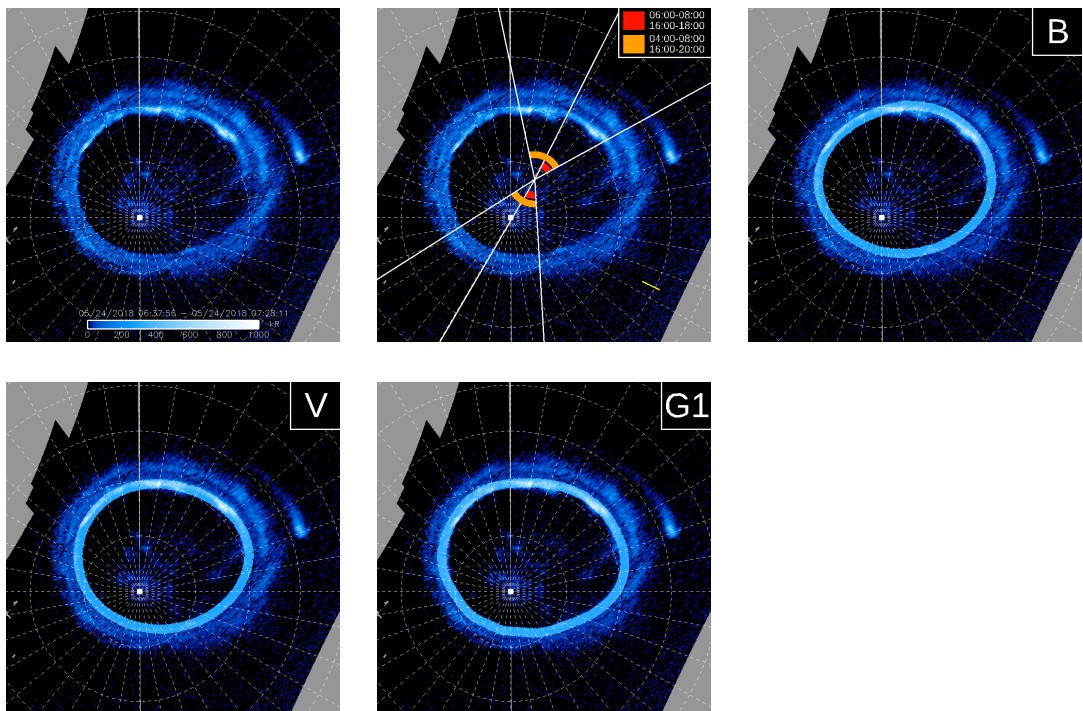
PJ12 – South



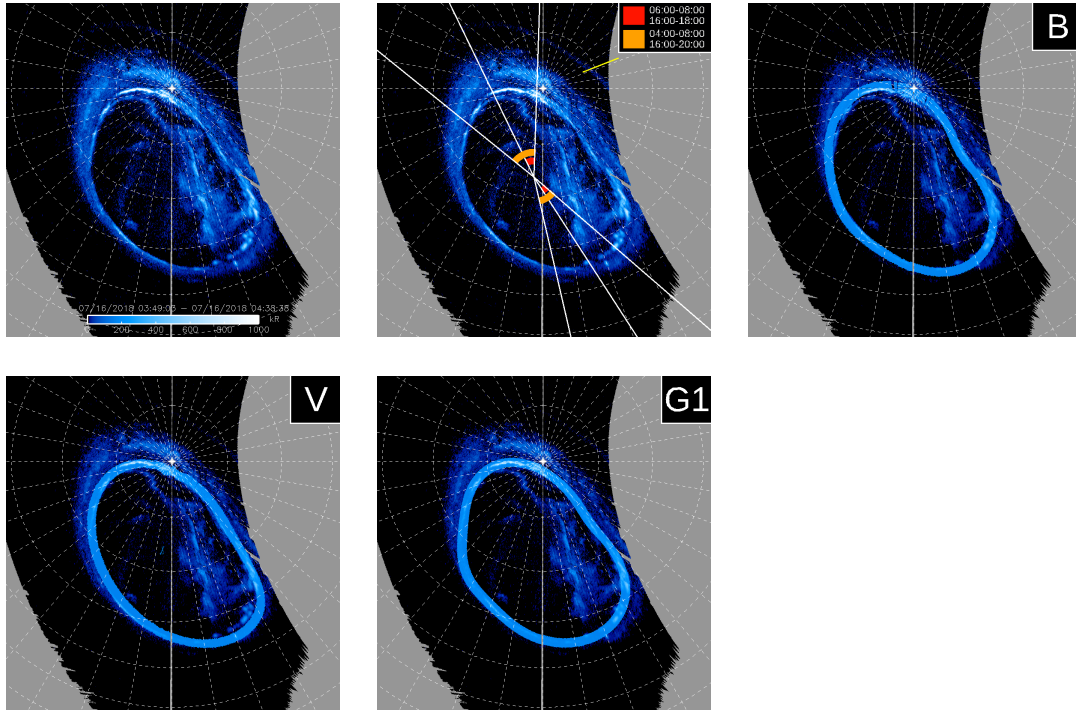
PJ13 – North



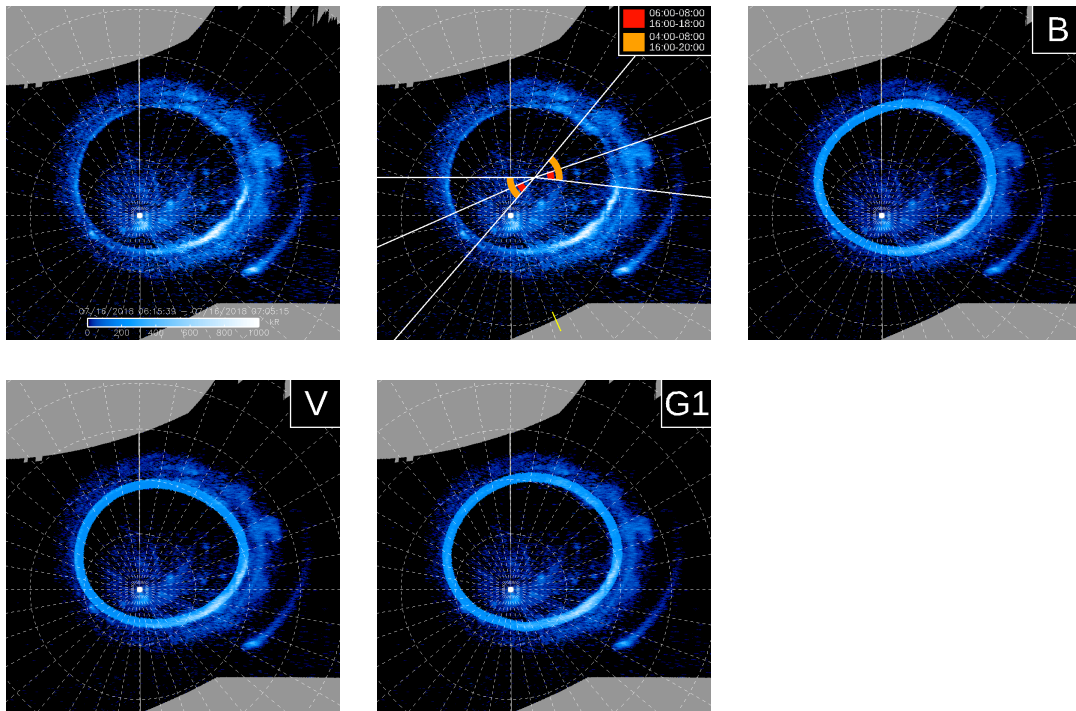
PJ13 – South



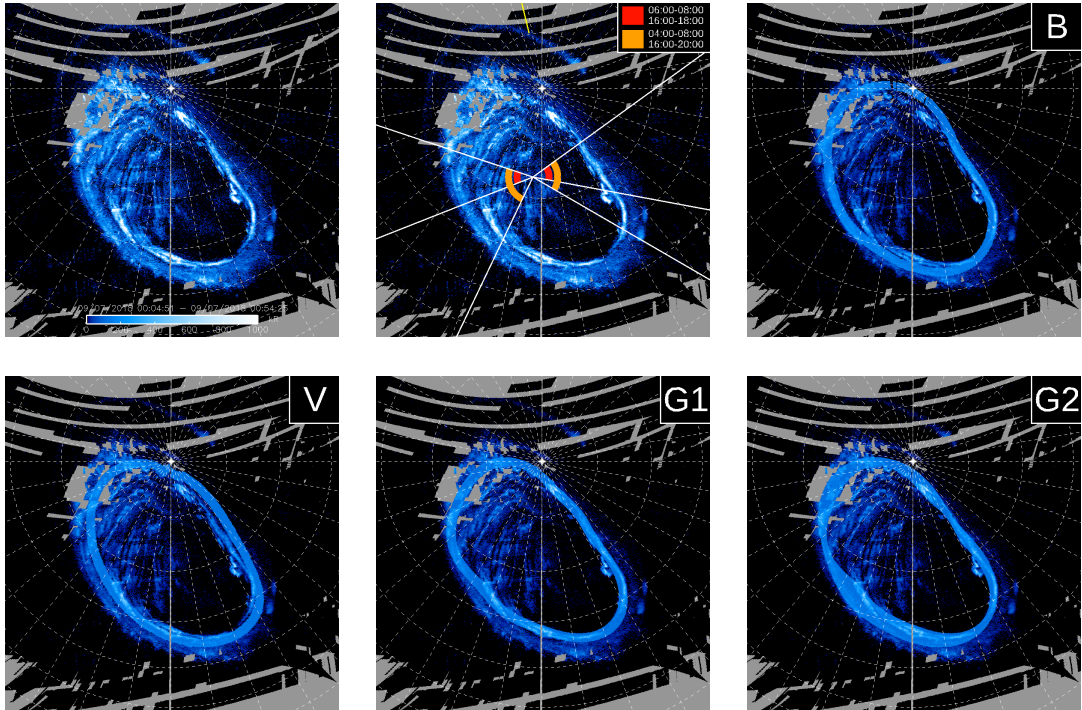
PJ14 – North



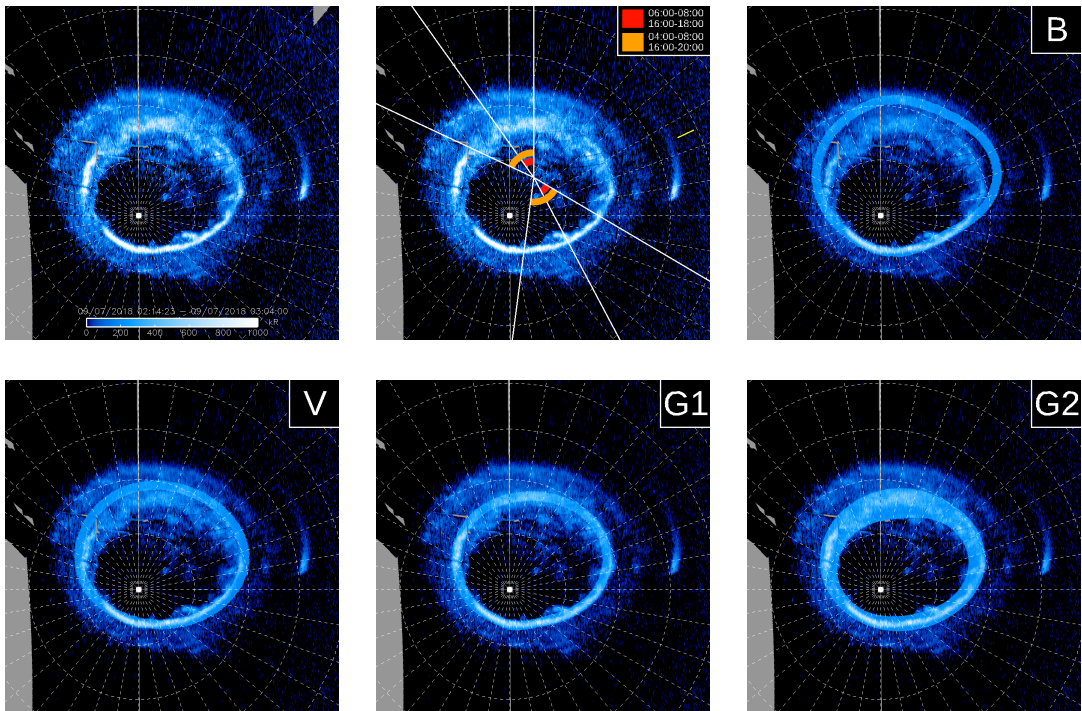
PJ14 – South



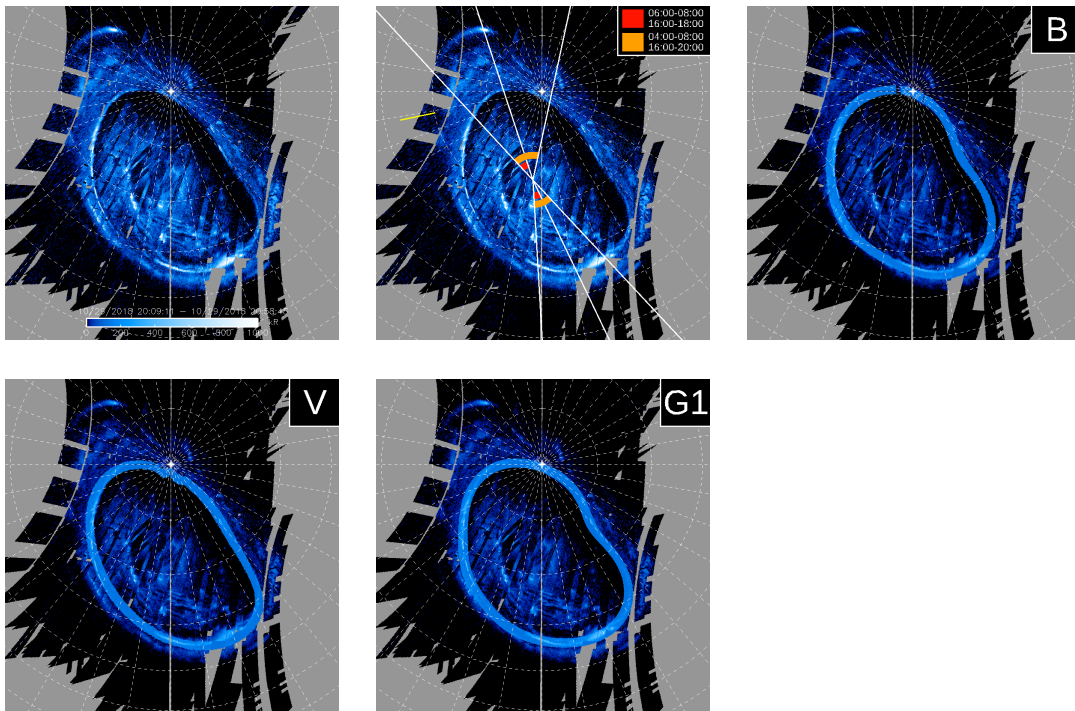
PJ15 – North



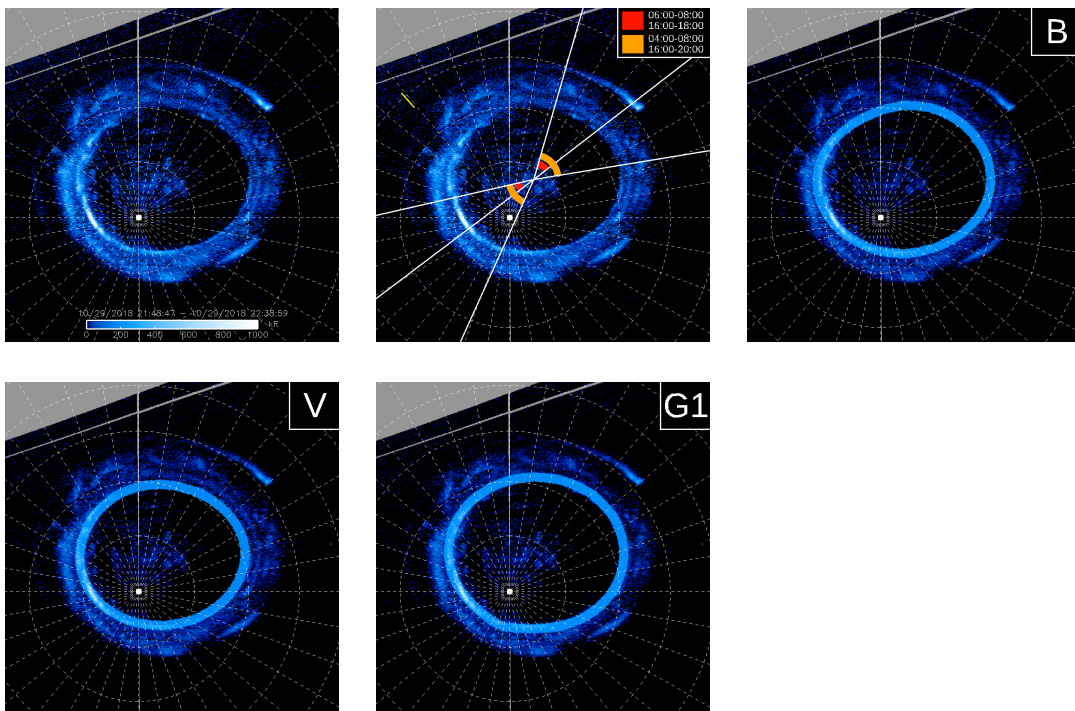
PJ15 – South



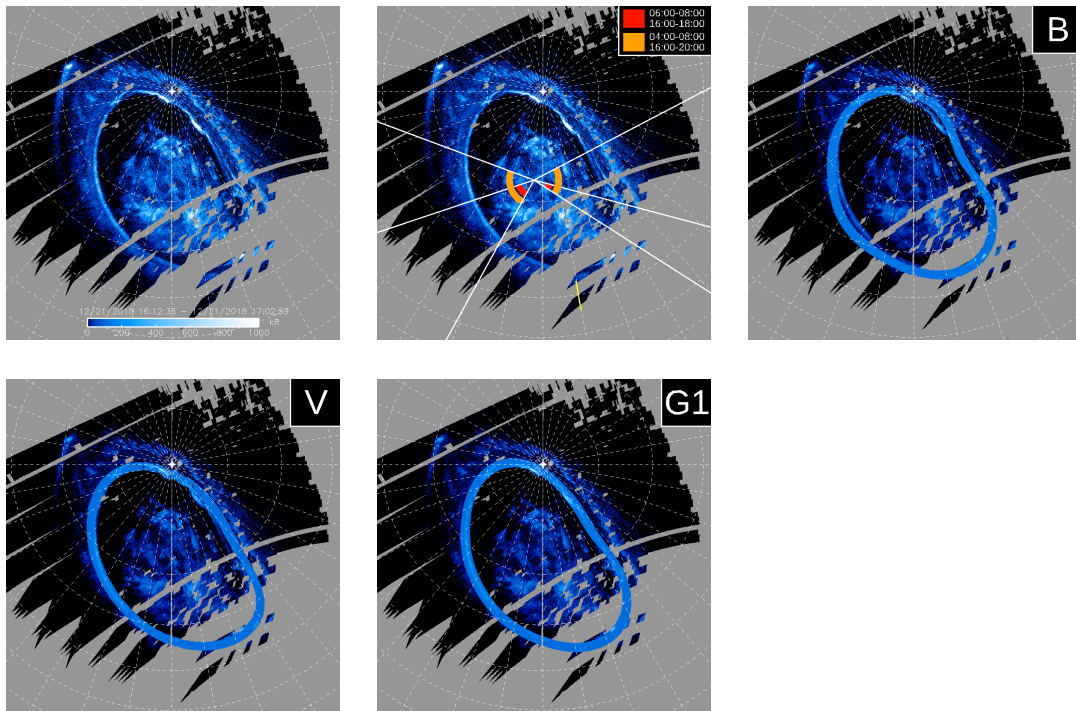
PJ16 – North



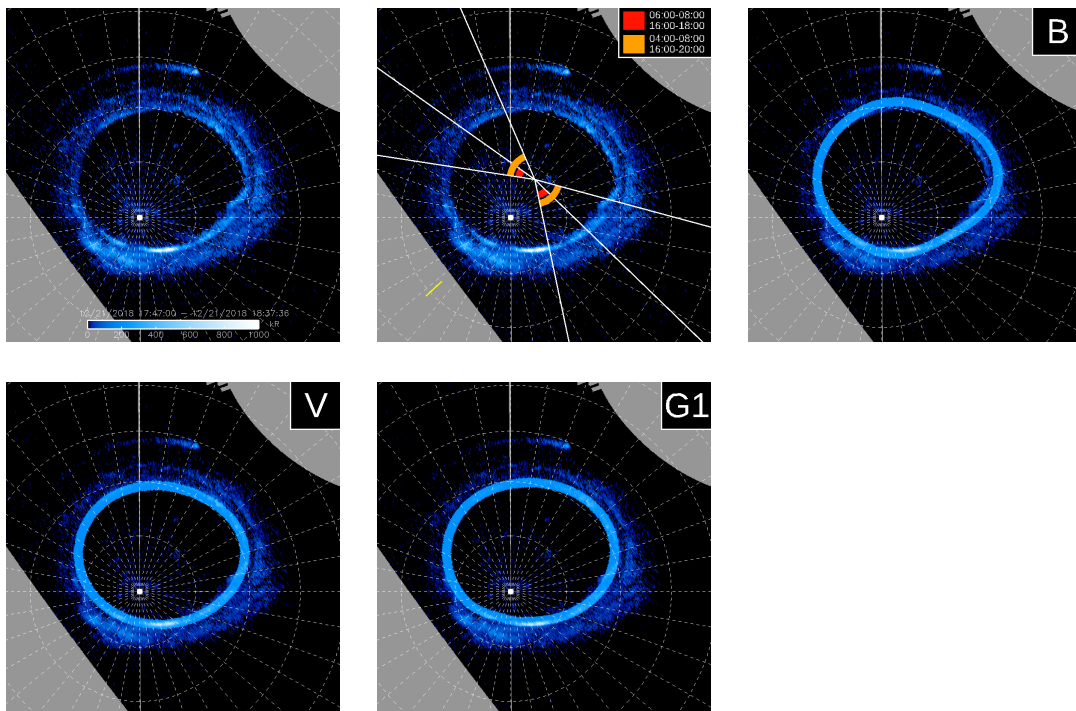
PJ16 – South



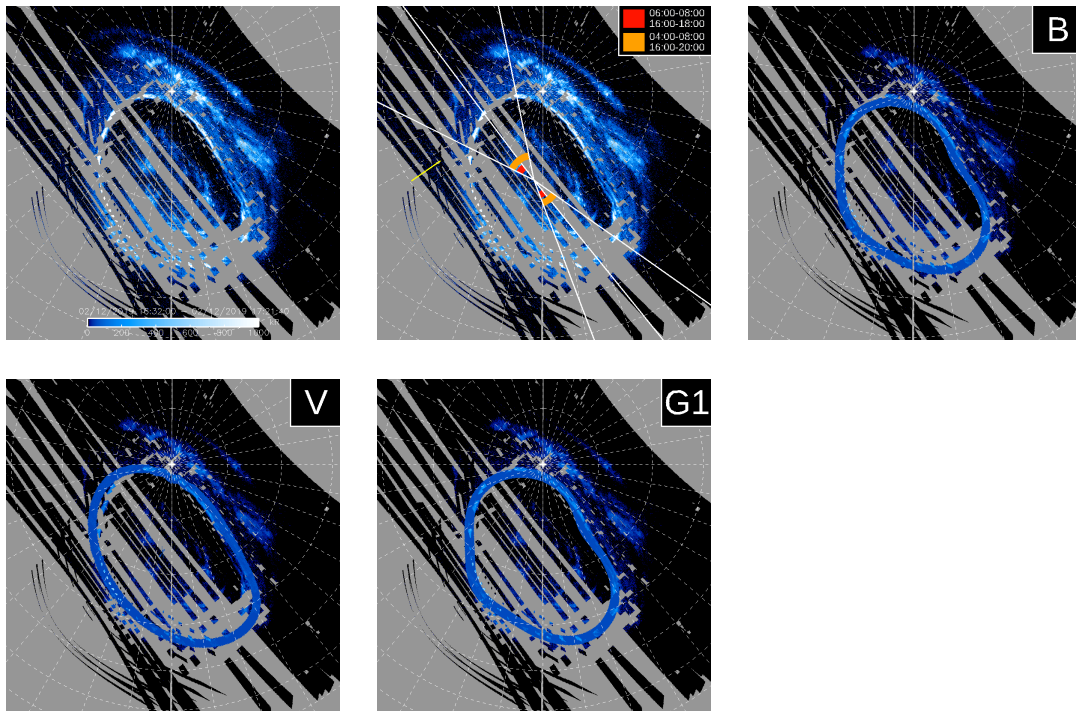
PJ17 – North



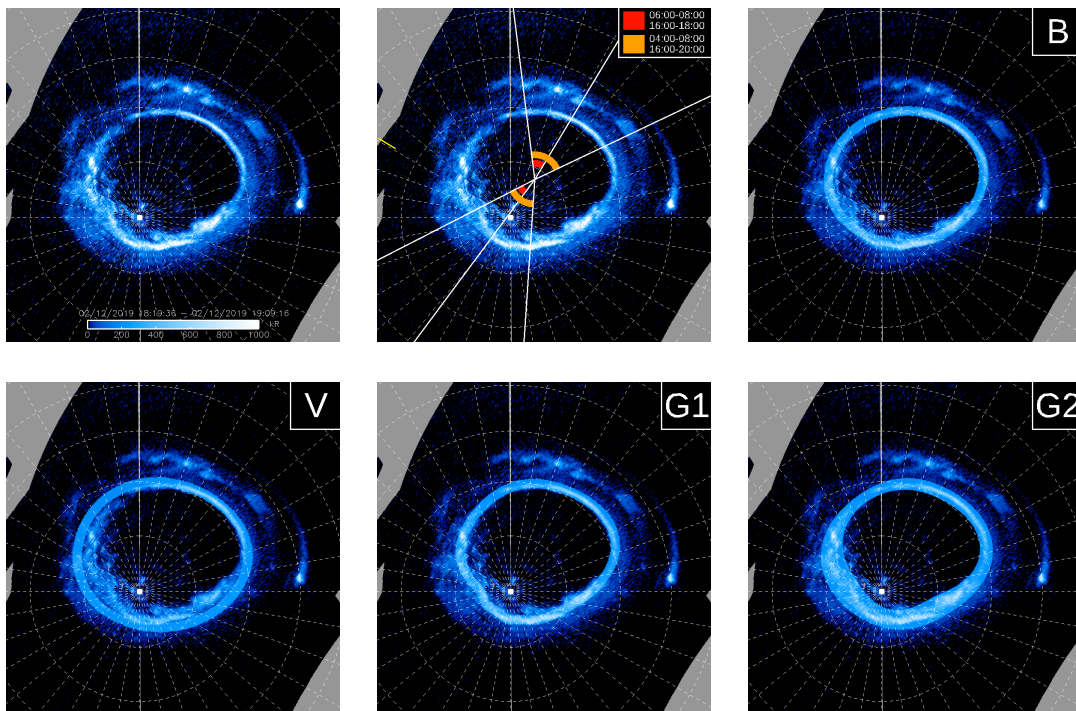
PJ17 – South



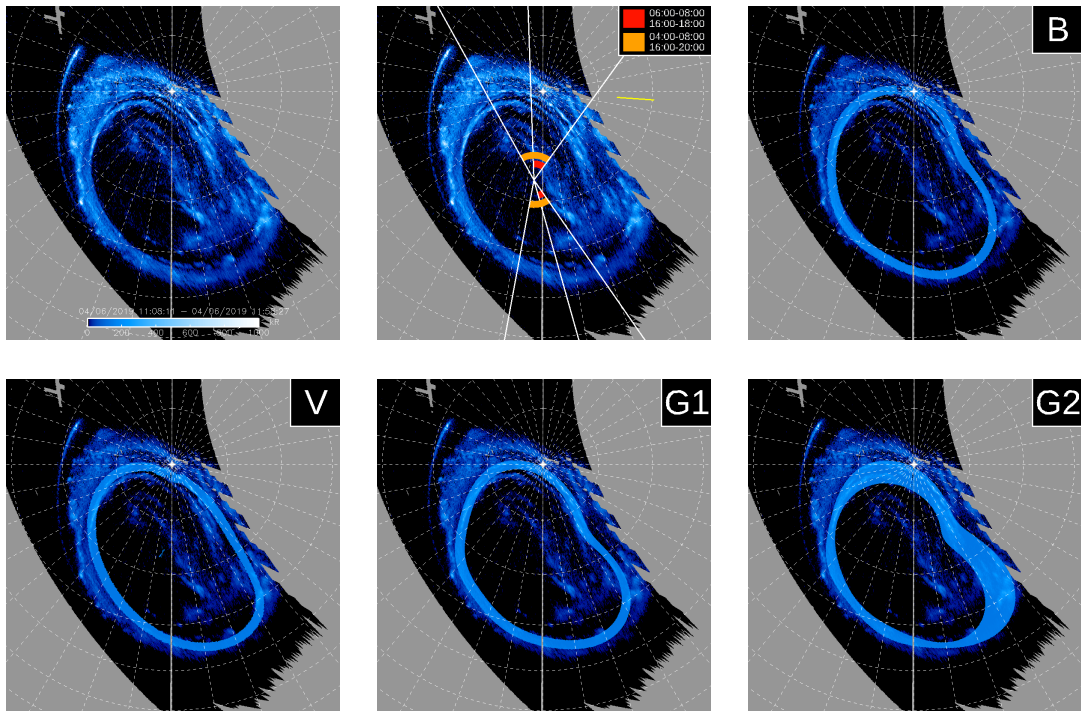
PJ18 – North



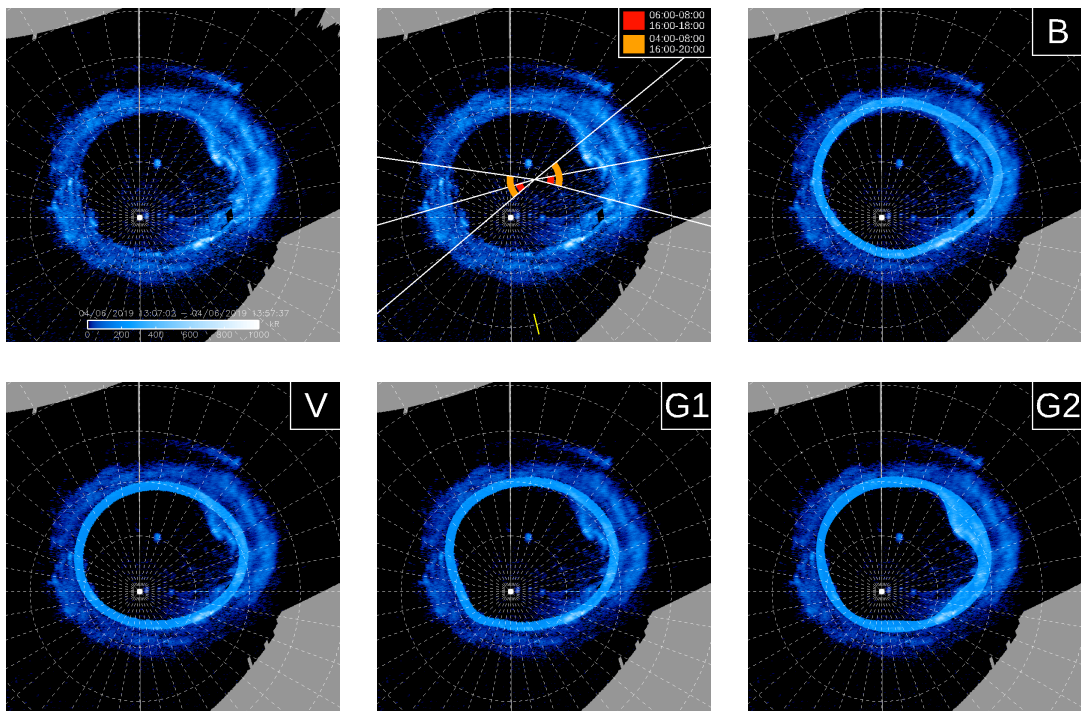
PJ18 – South



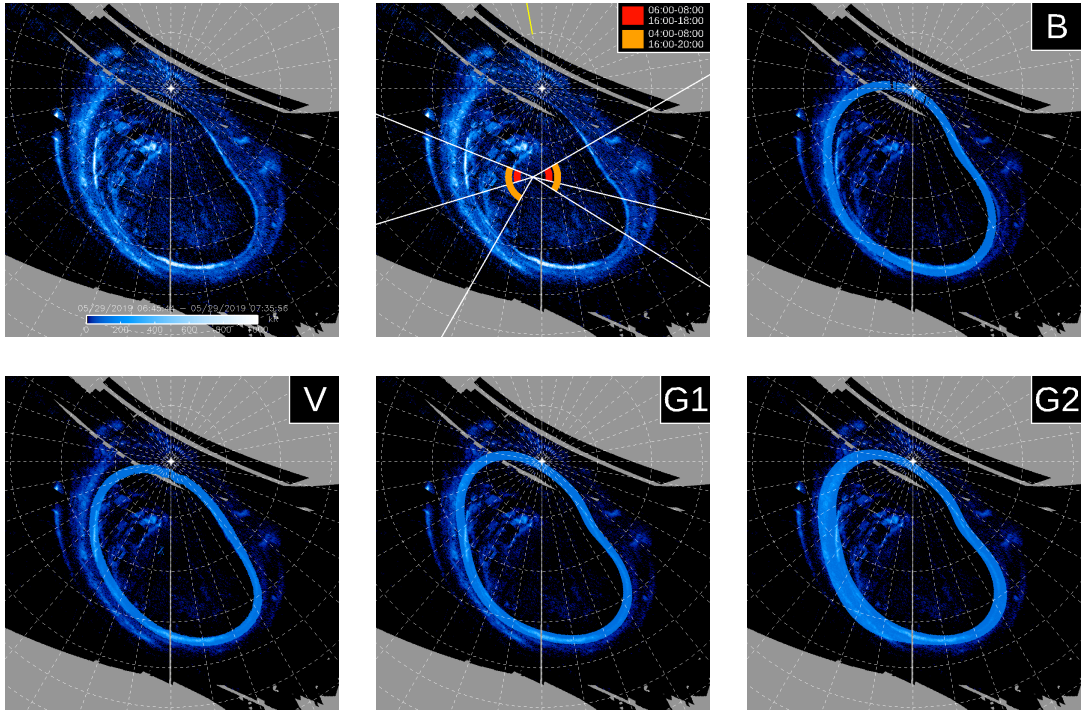
PJ19 – North



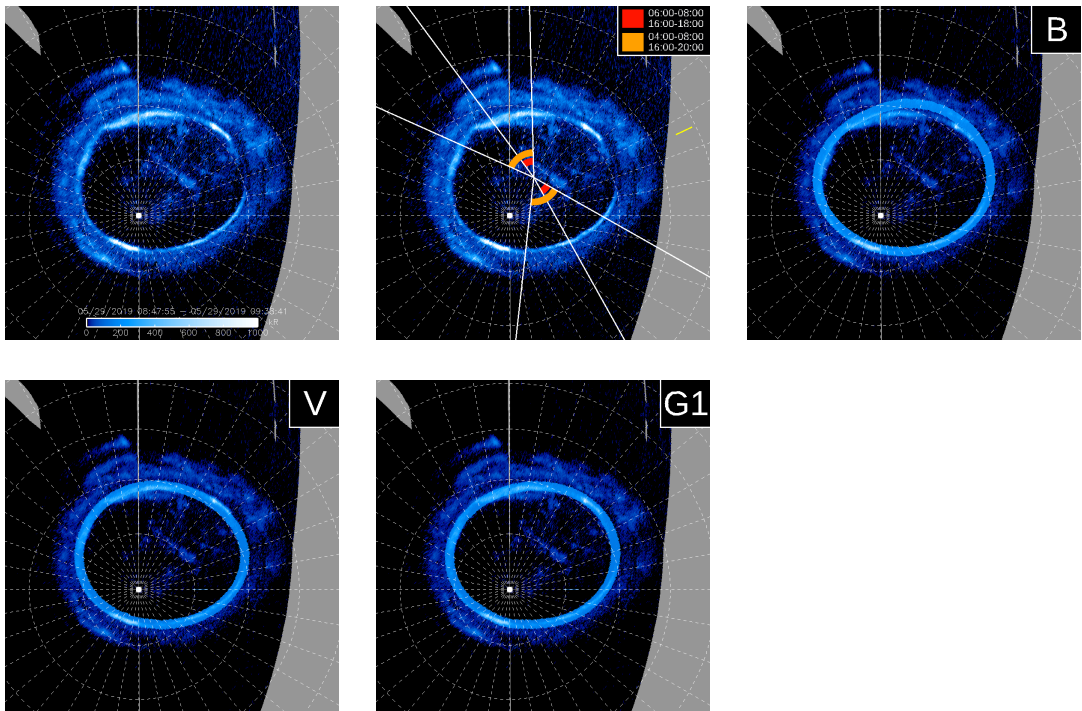
PJ19 – South



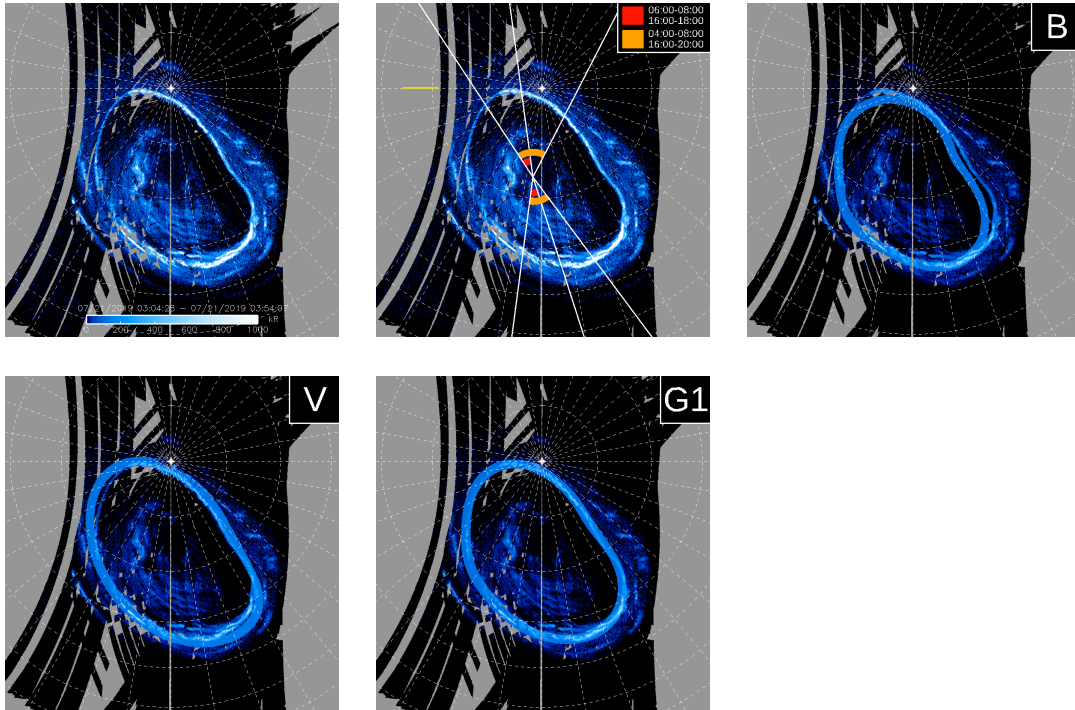
PJ20 – North



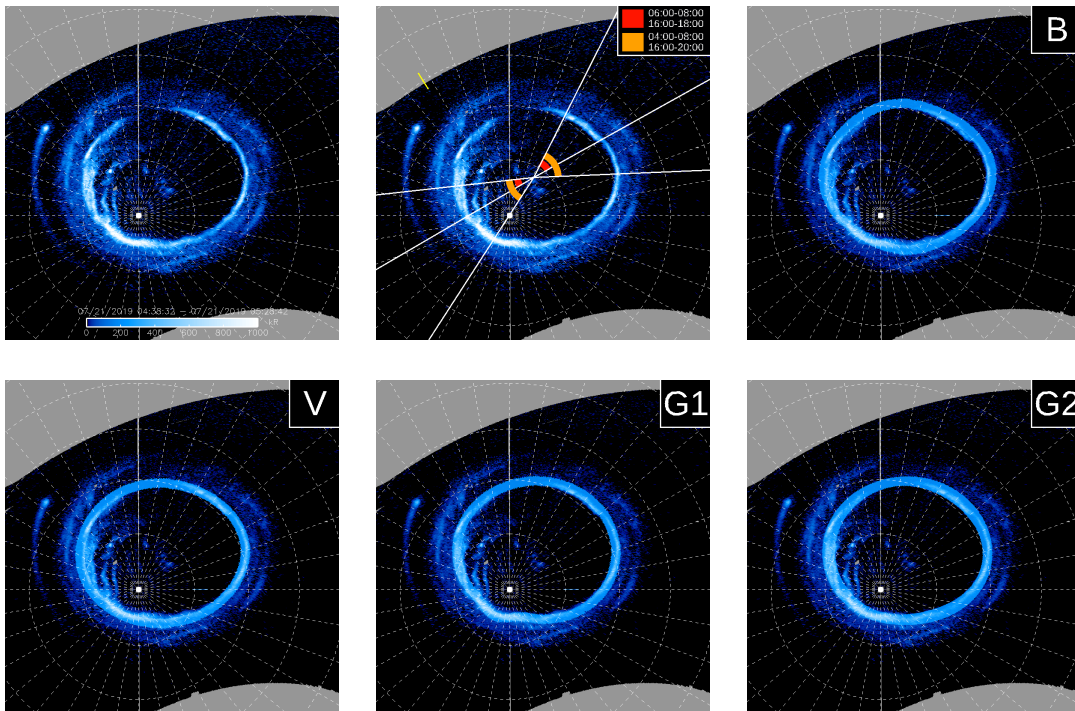
PJ20 – South



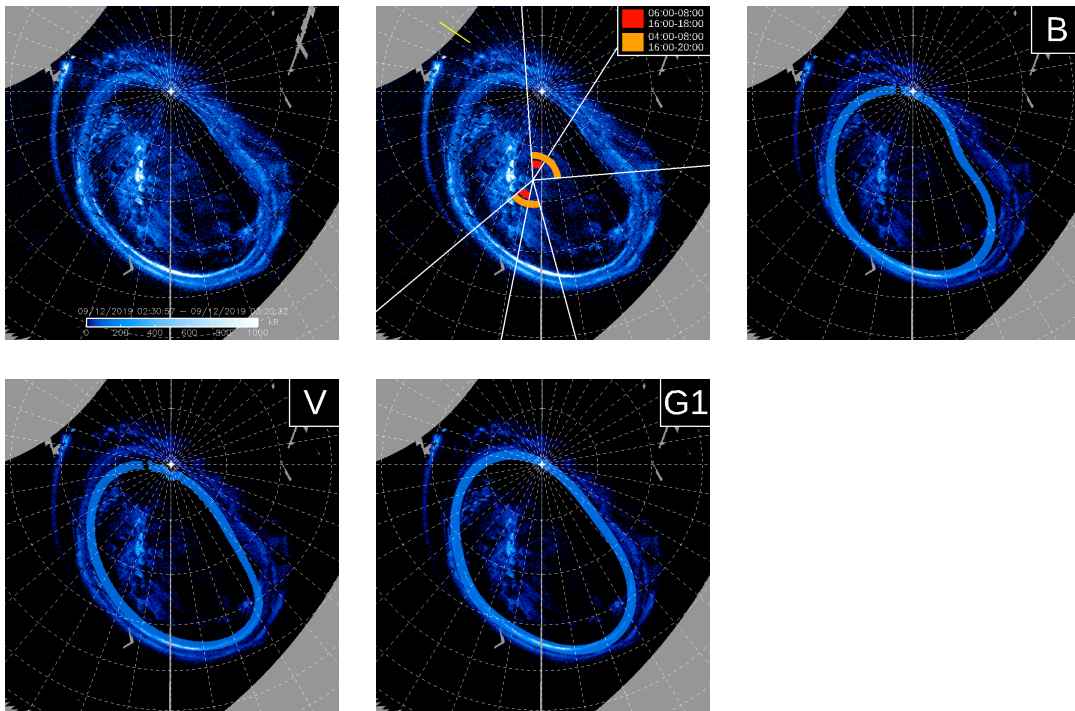
PJ21 – North



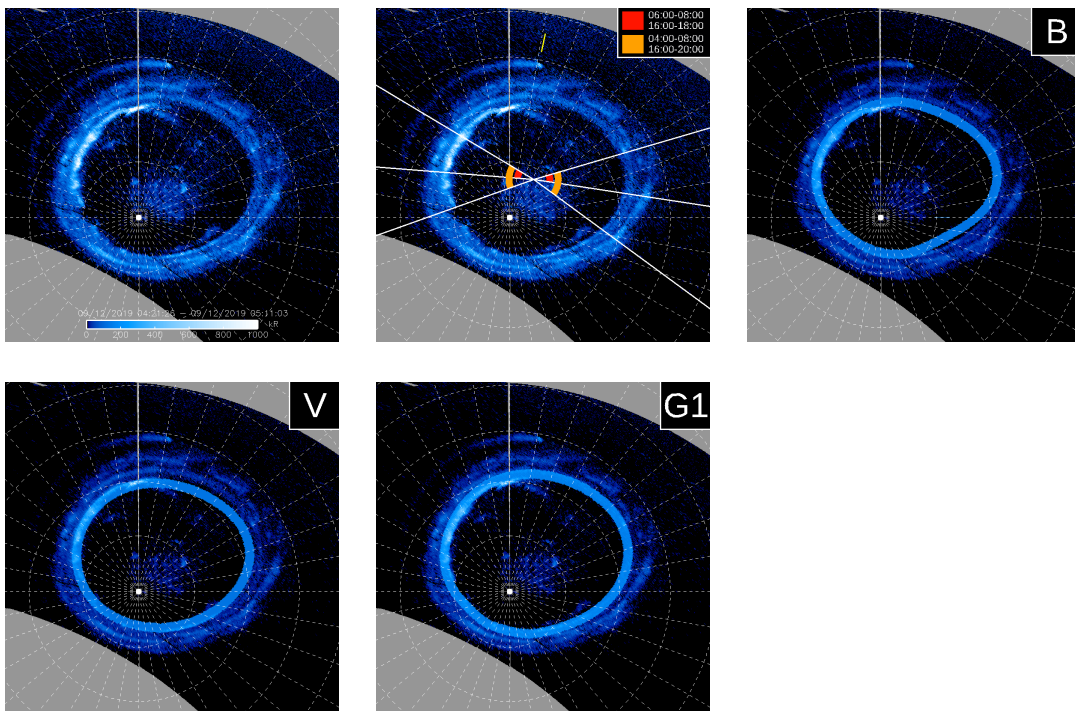
PJ21 – South



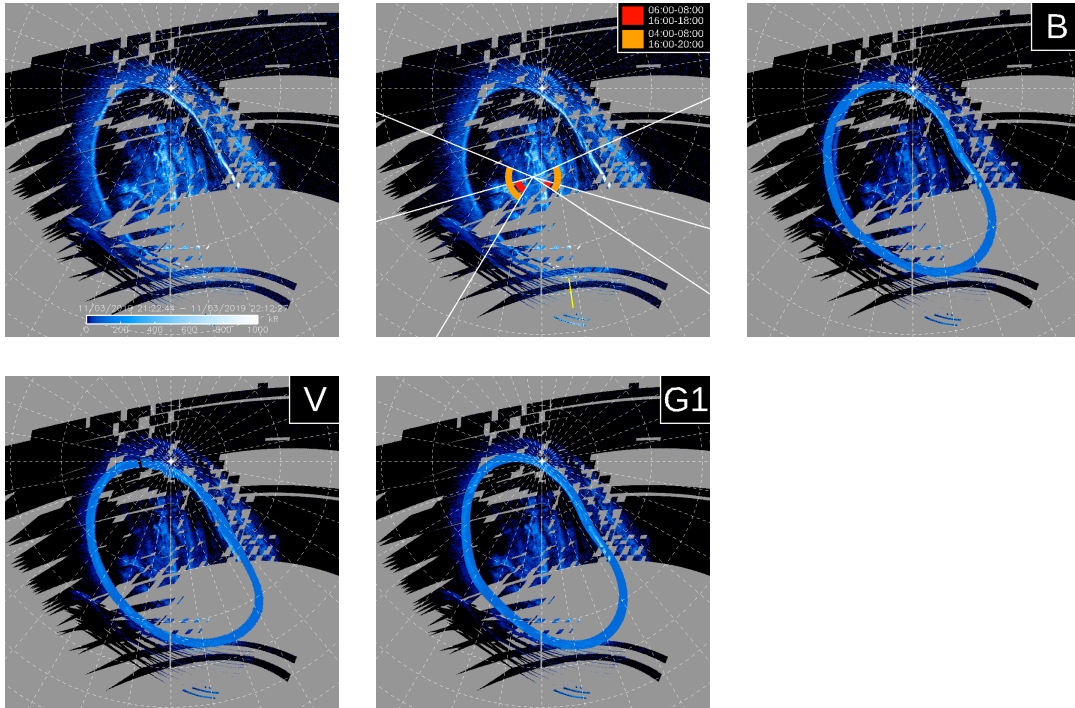
PJ22 – North



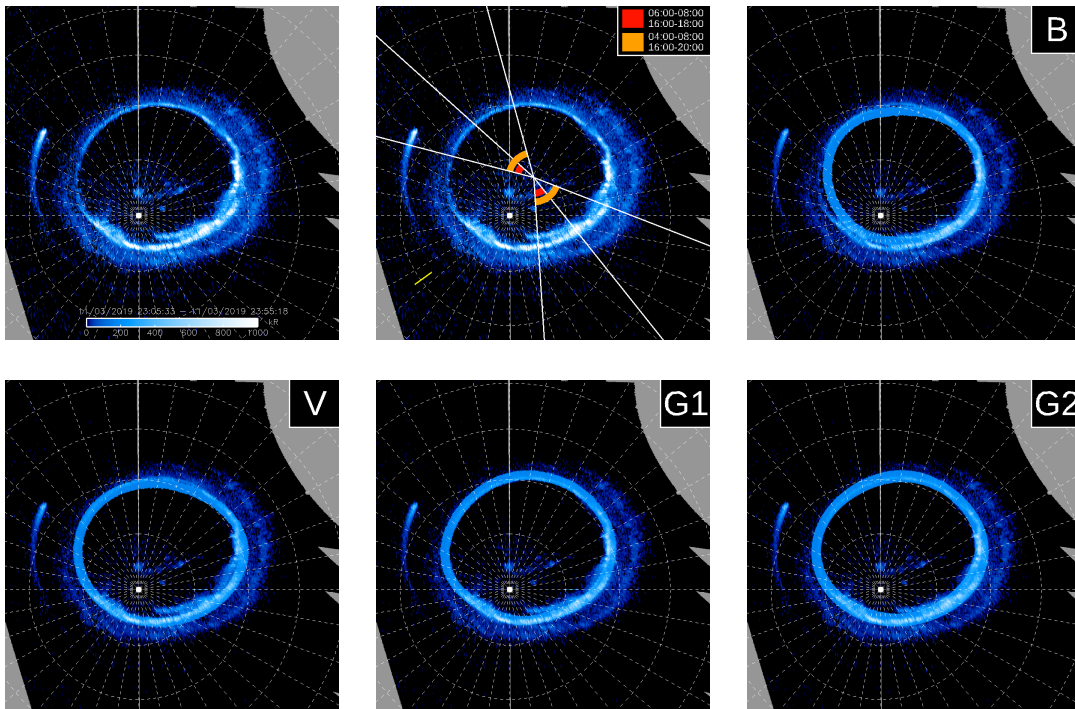
PJ22 – South



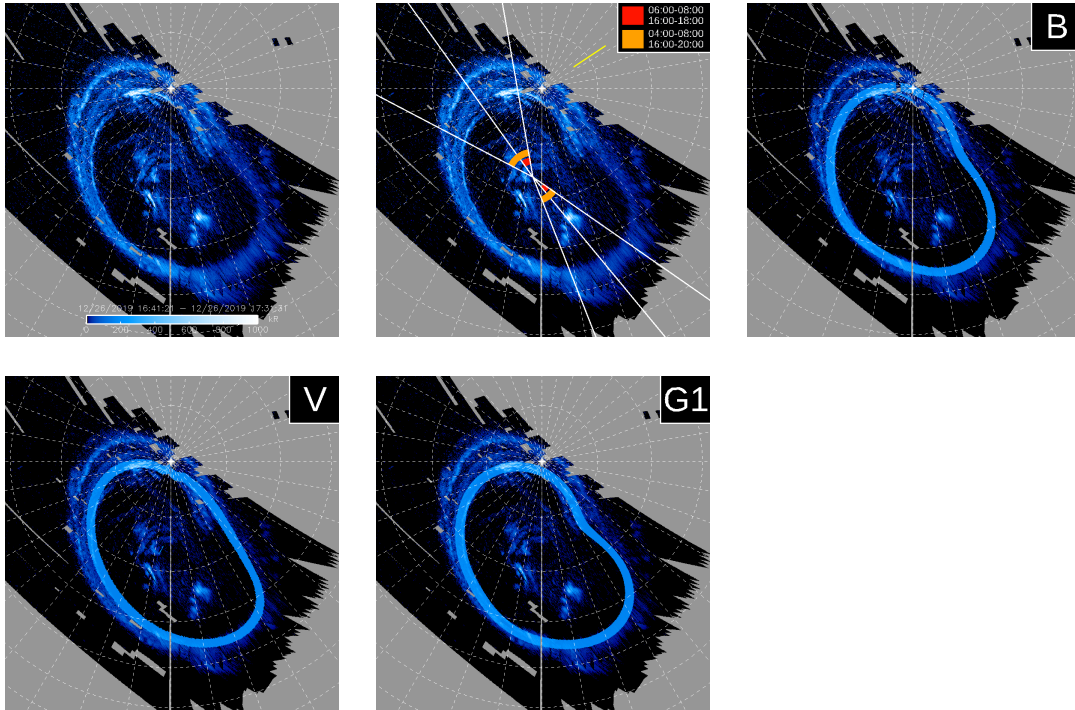
PJ23 – North



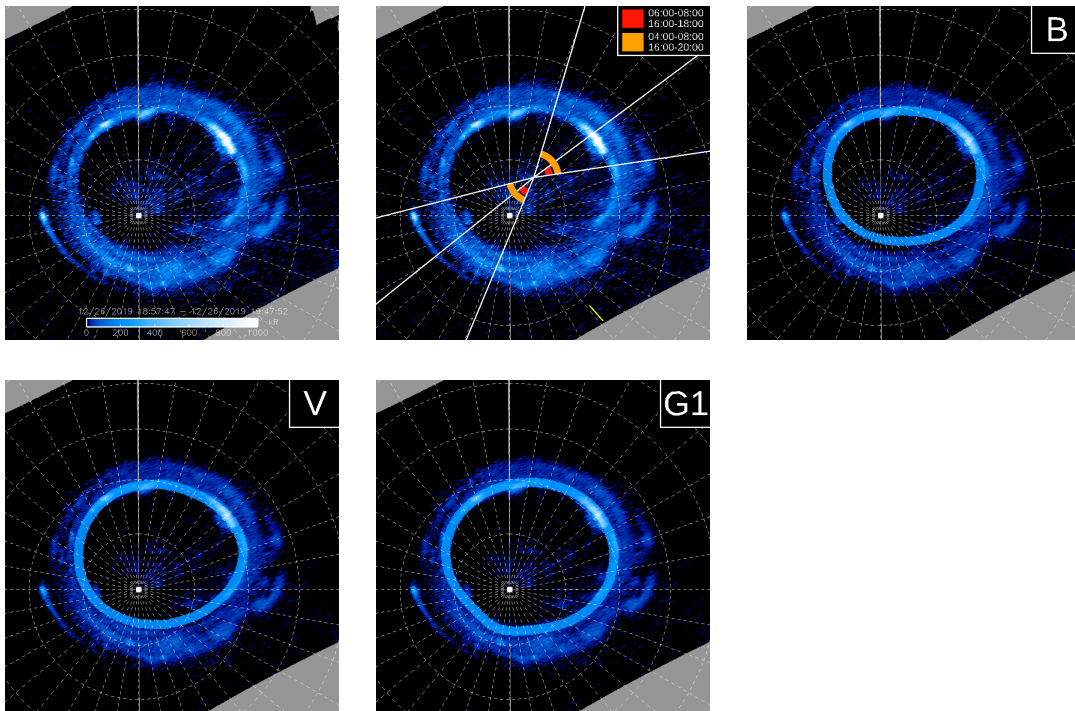
PJ23 – South



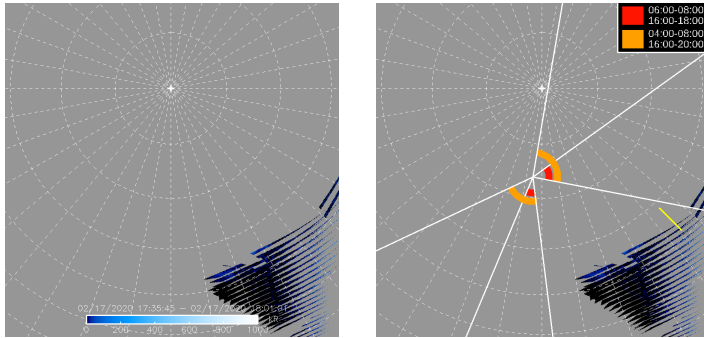
PJ24 – North



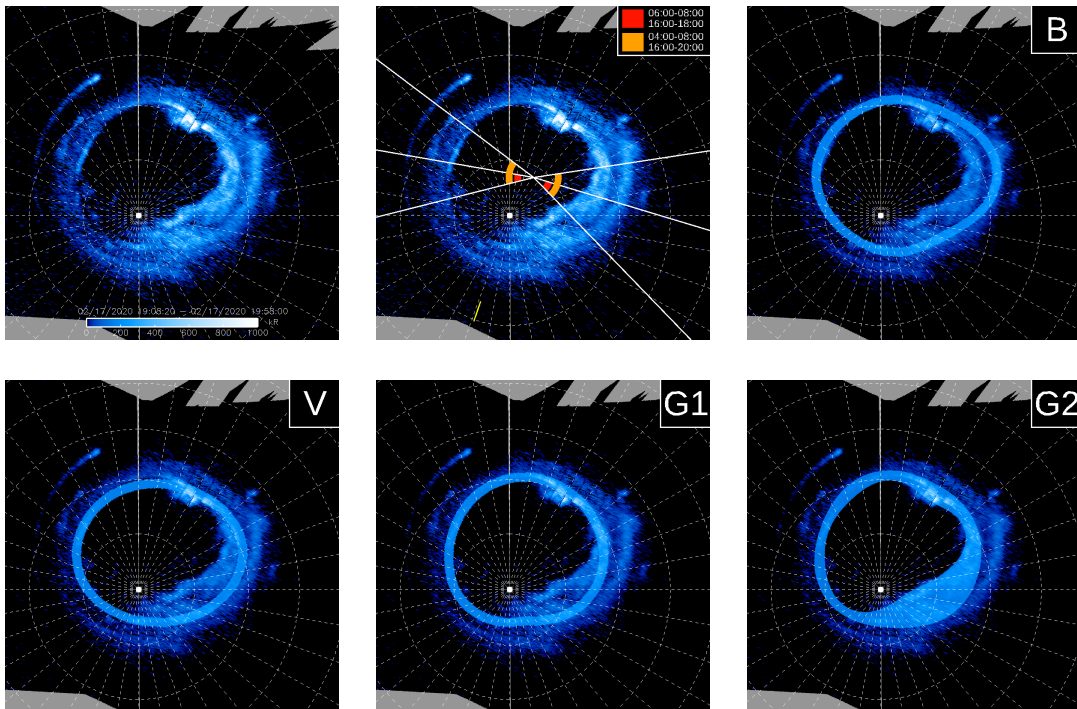
PJ24 – South



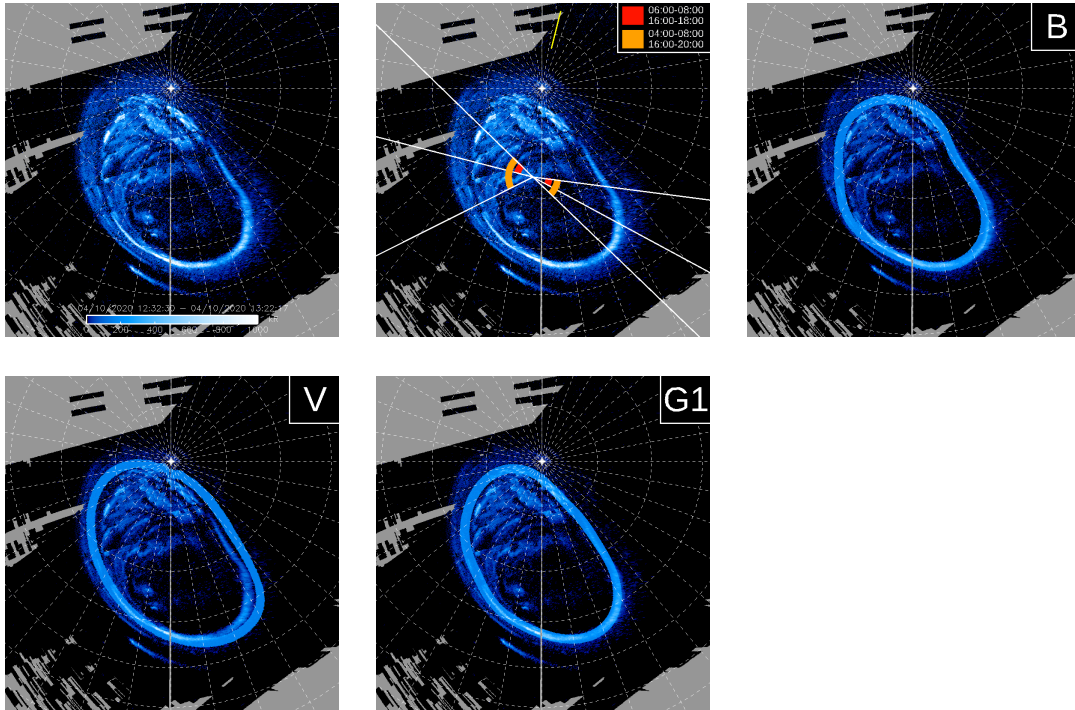
PJ25 – North



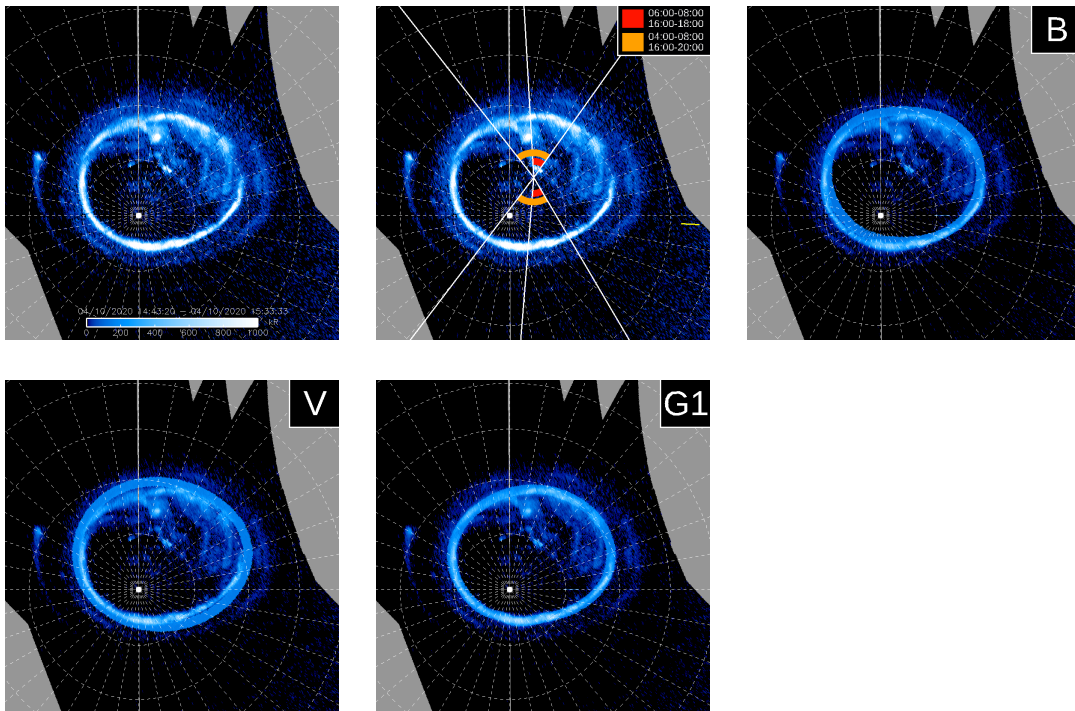
PJ25 – South



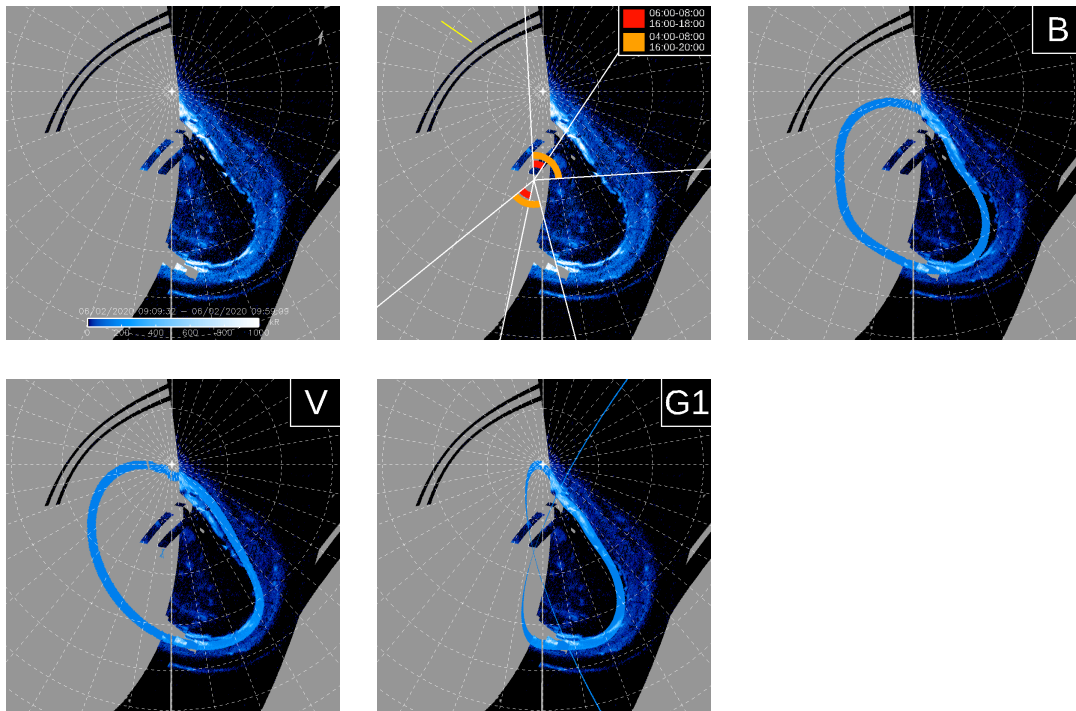
PJ26 – North



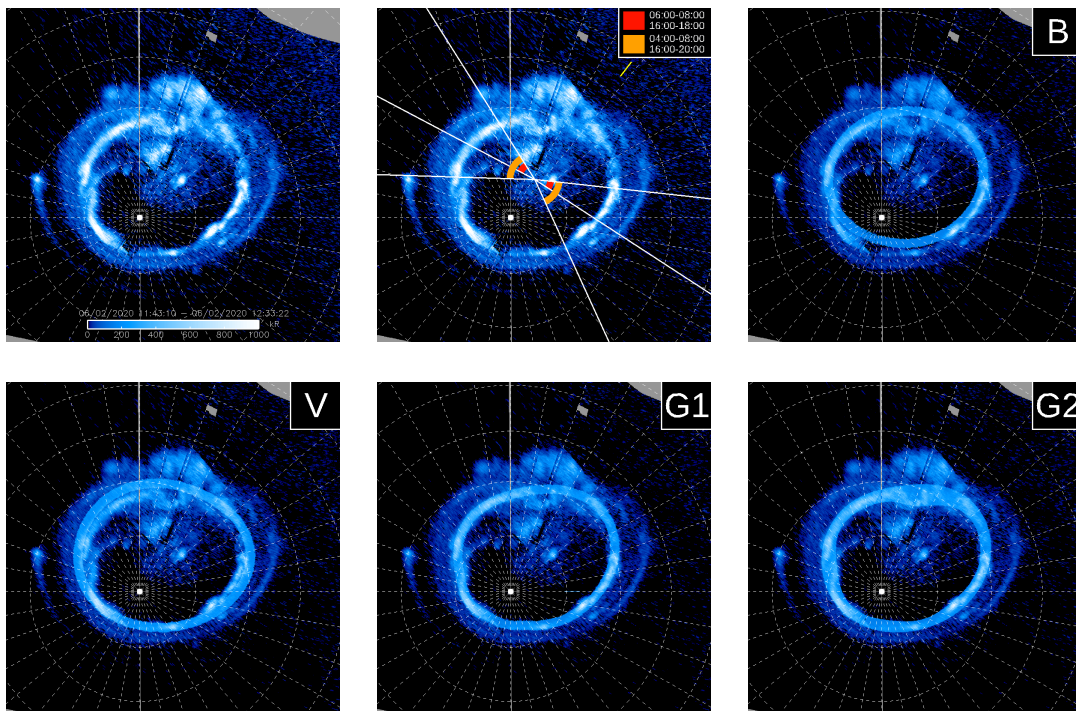
PJ26 – South



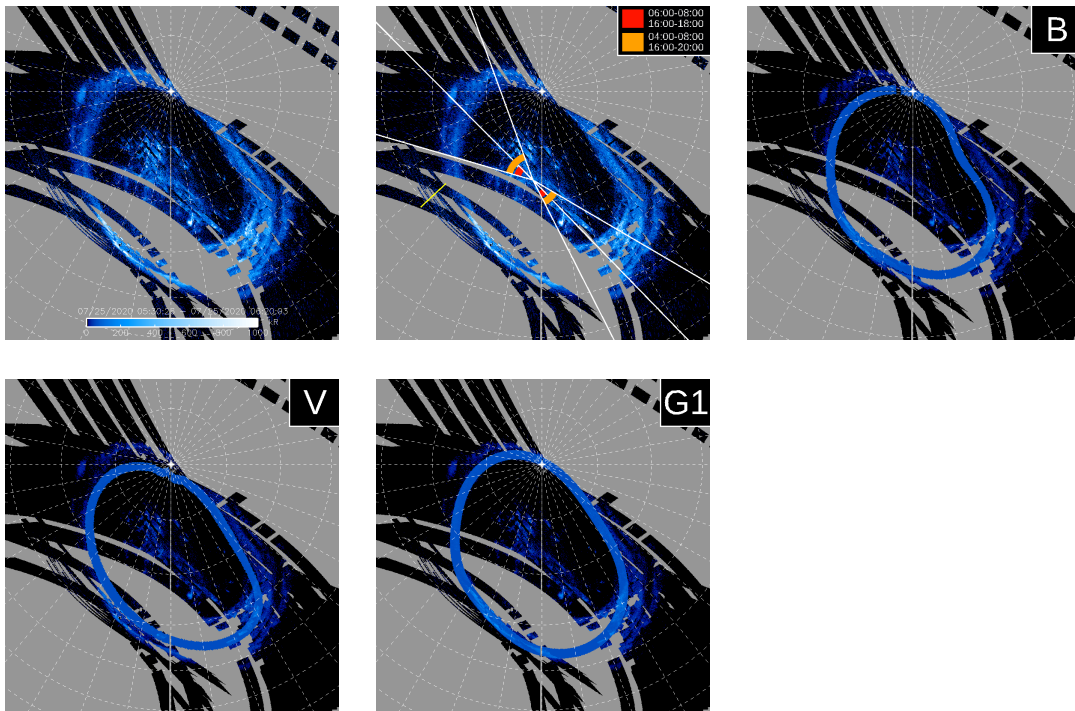
PJ27 – North



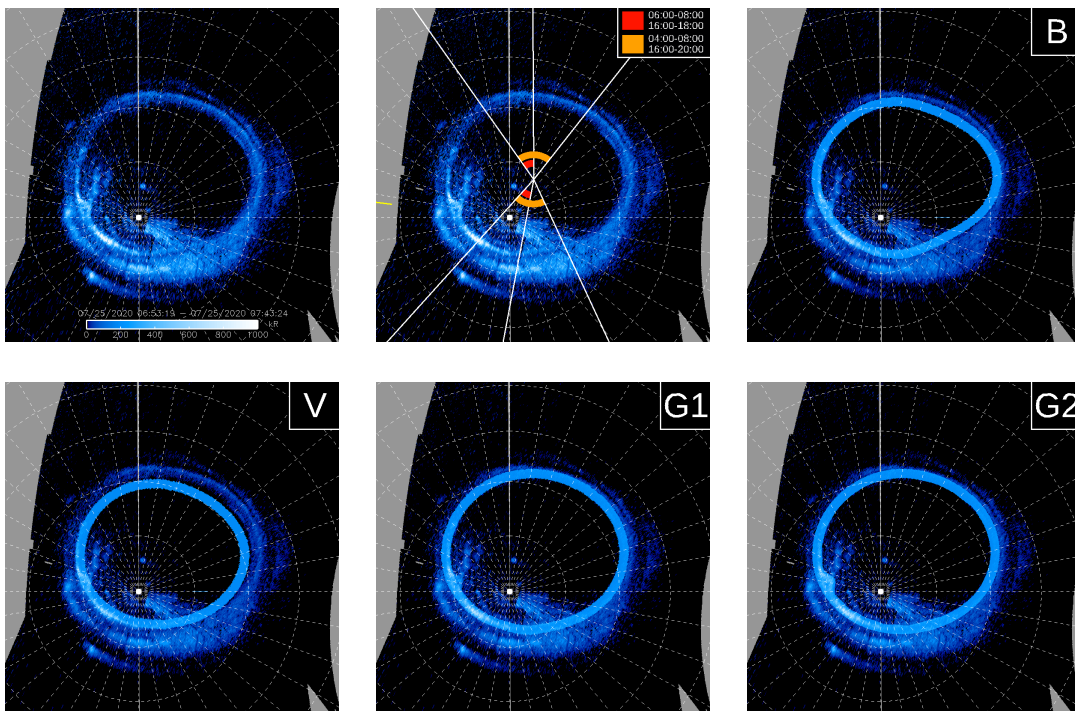
PJ27 – South



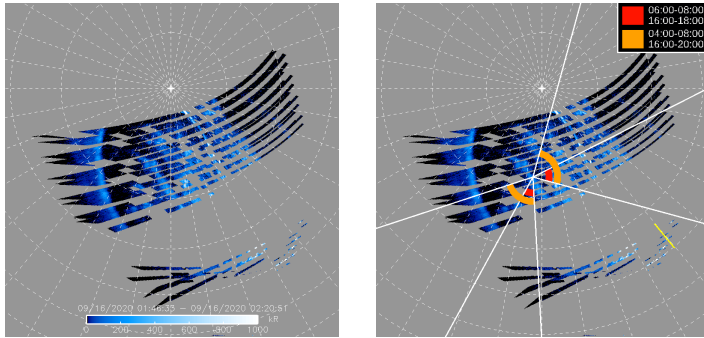
PJ28 – North



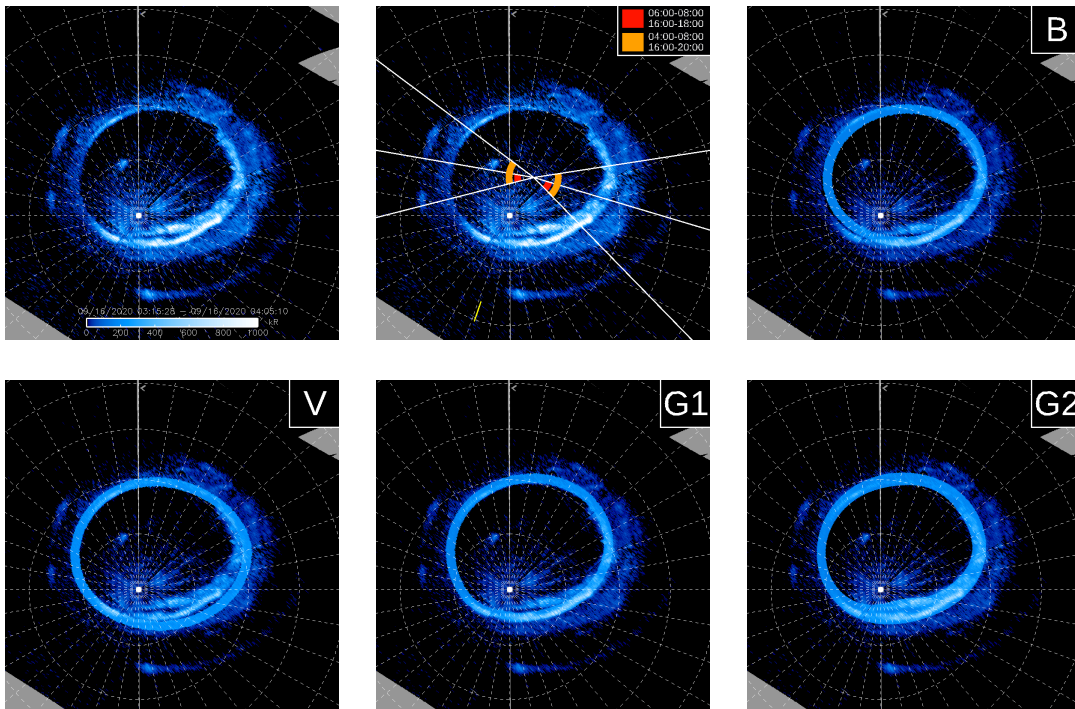
PJ28 – South



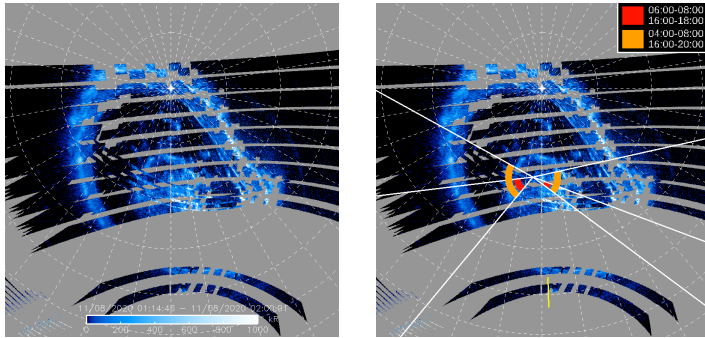
PJ29 – North



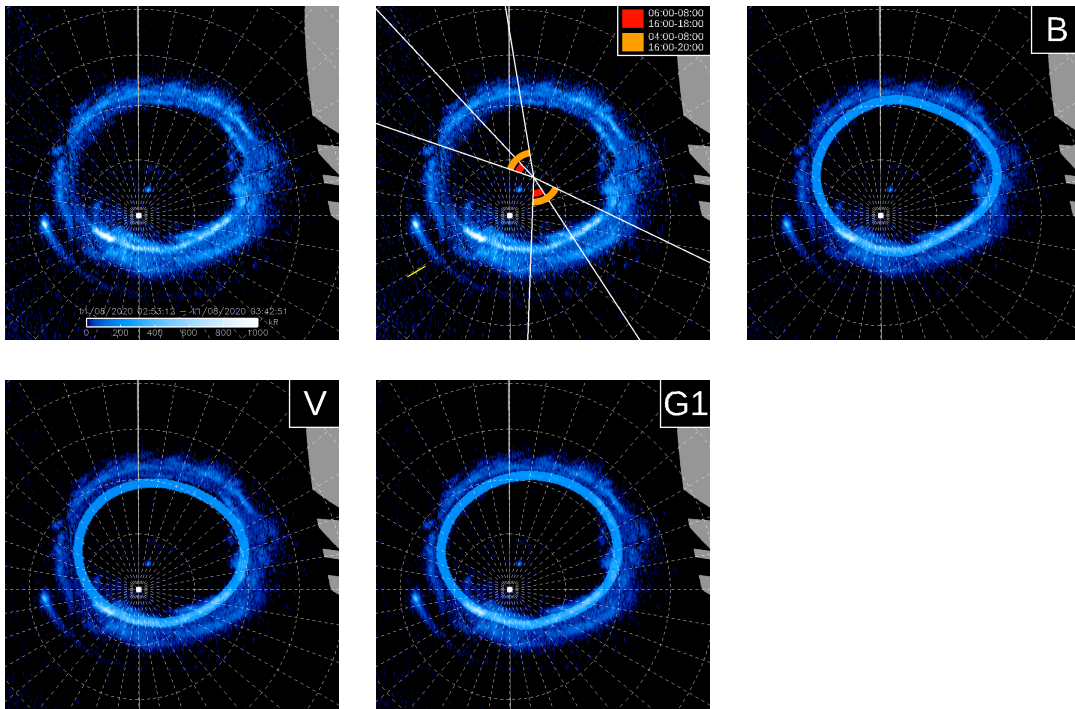
PJ29 – South



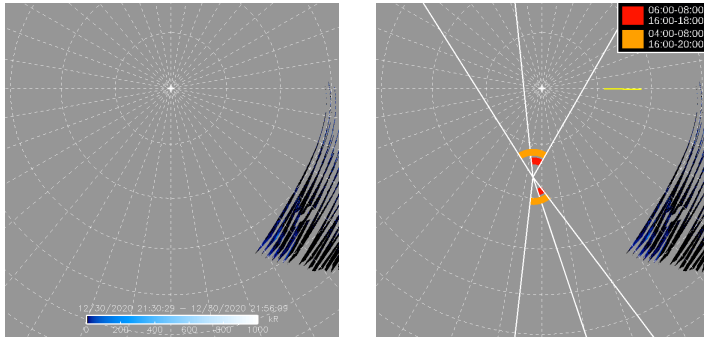
PJ30 – North



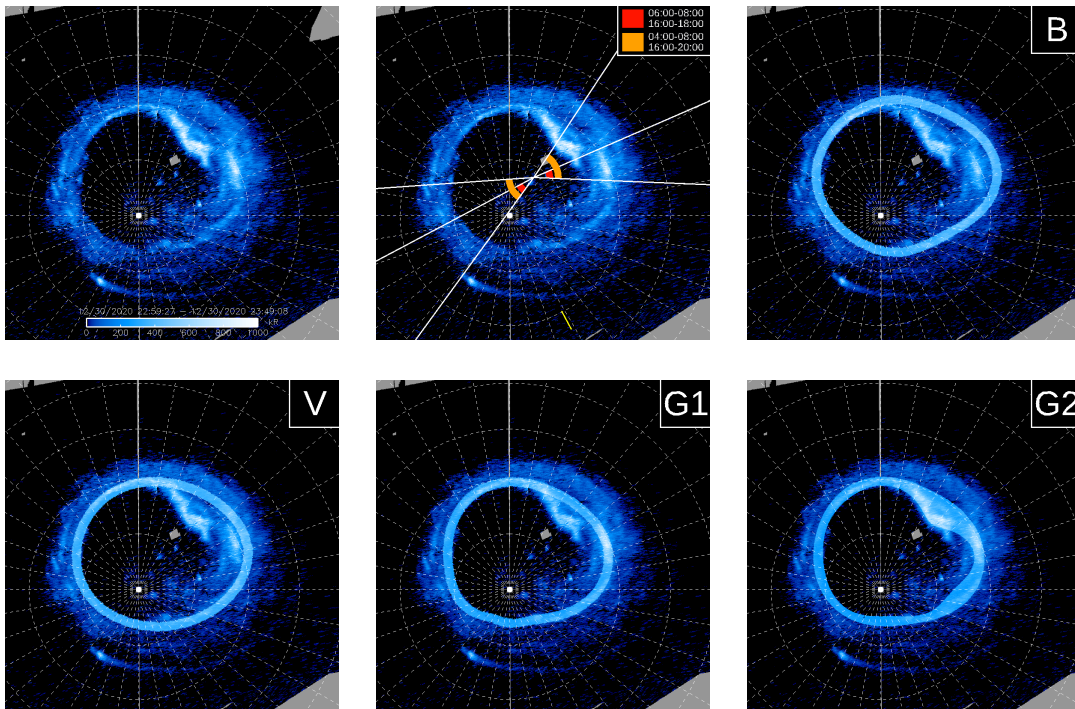
PJ30 – South



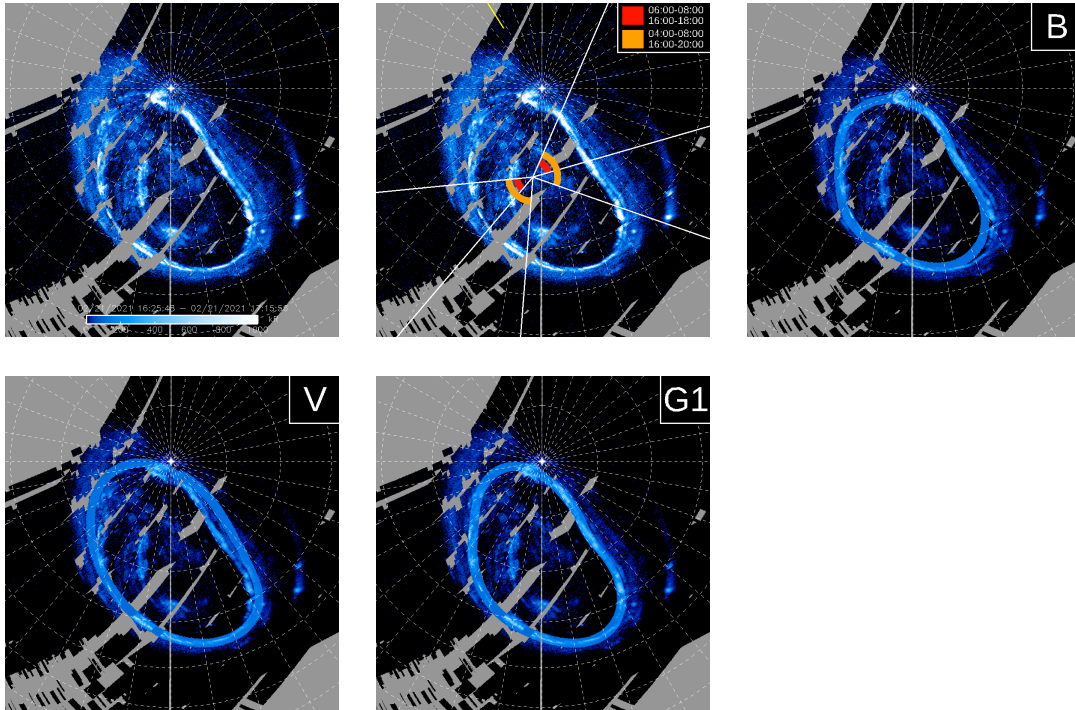
PJ31 – North



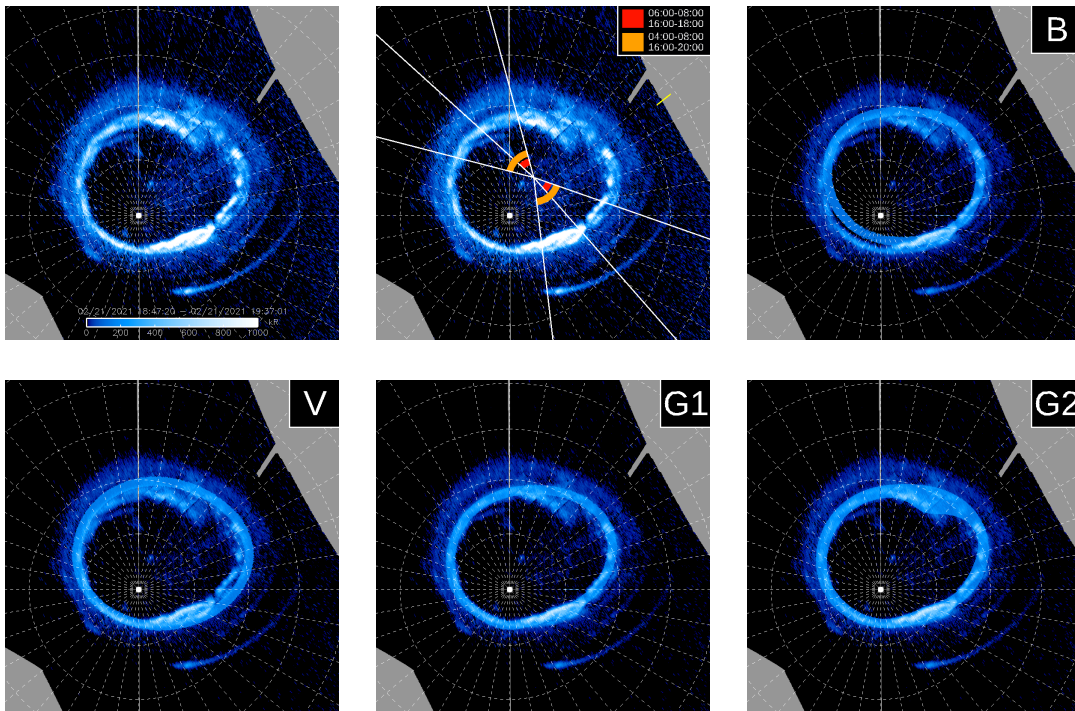
PJ31 – South



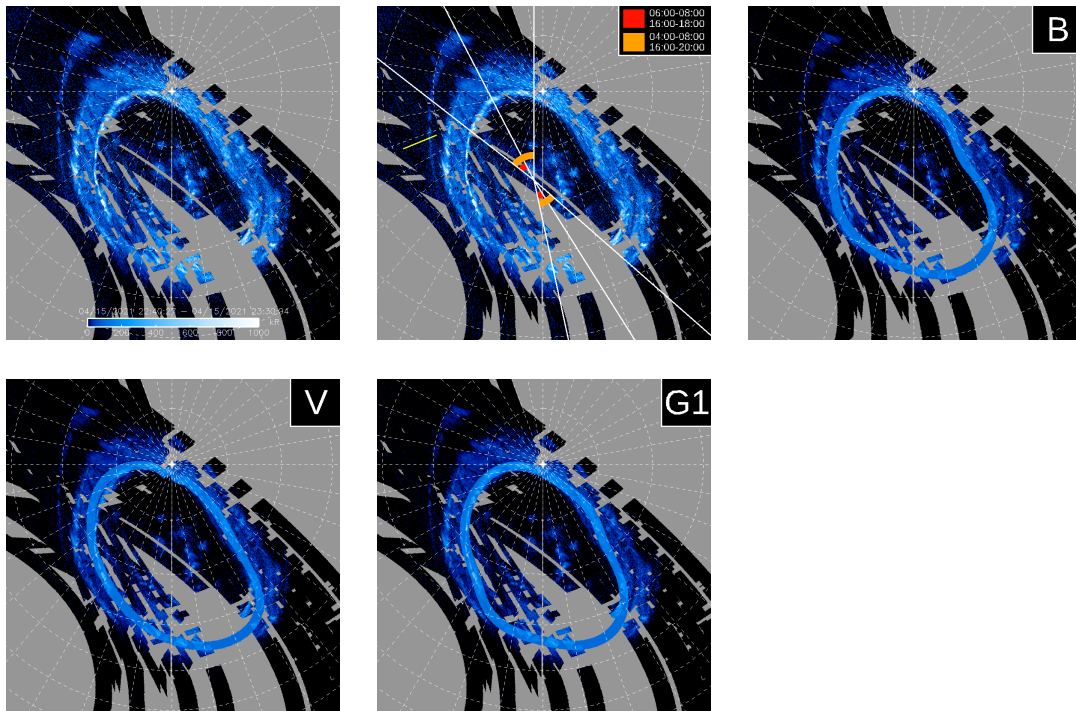
PJ32 – North



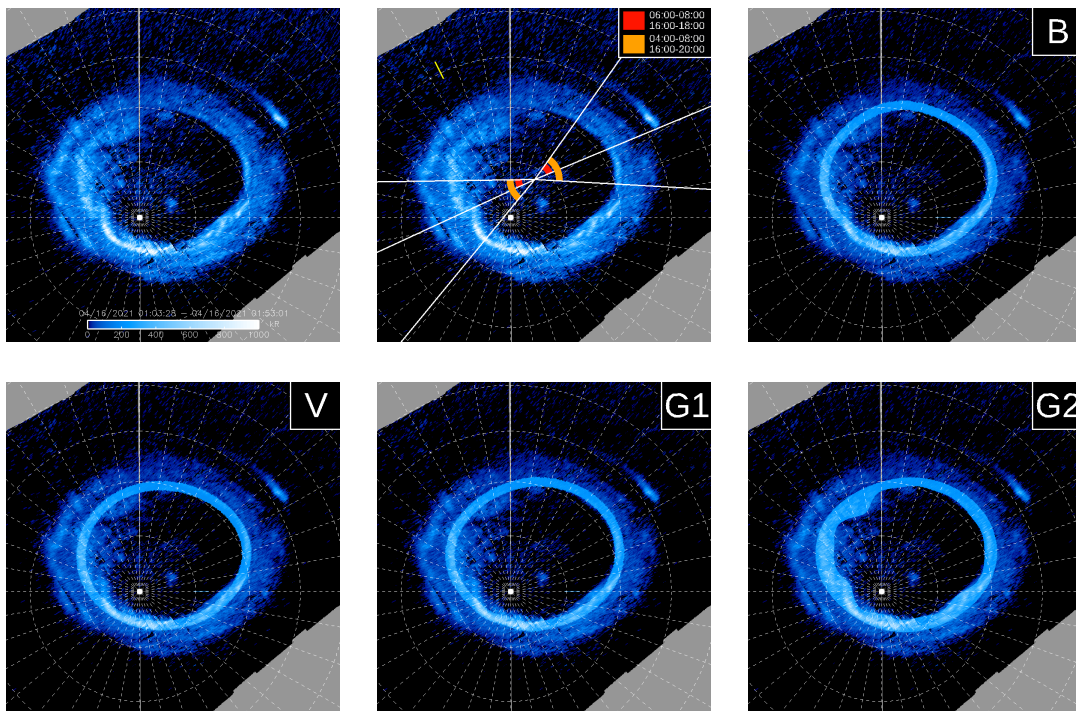
PJ32 – South



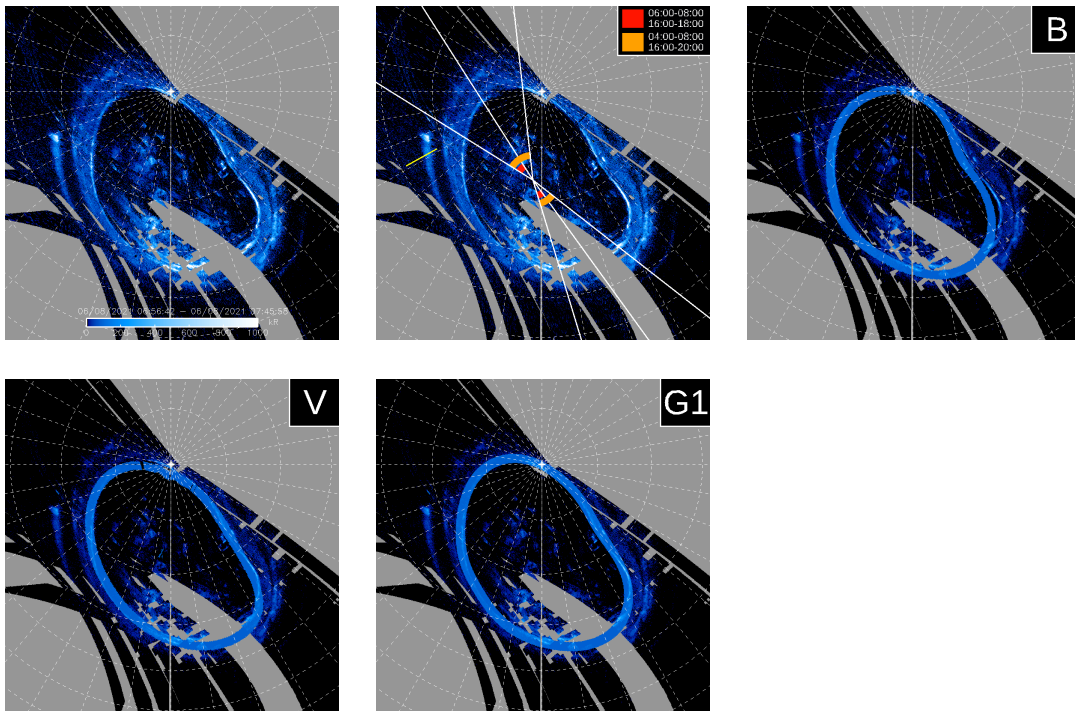
PJ33 – North



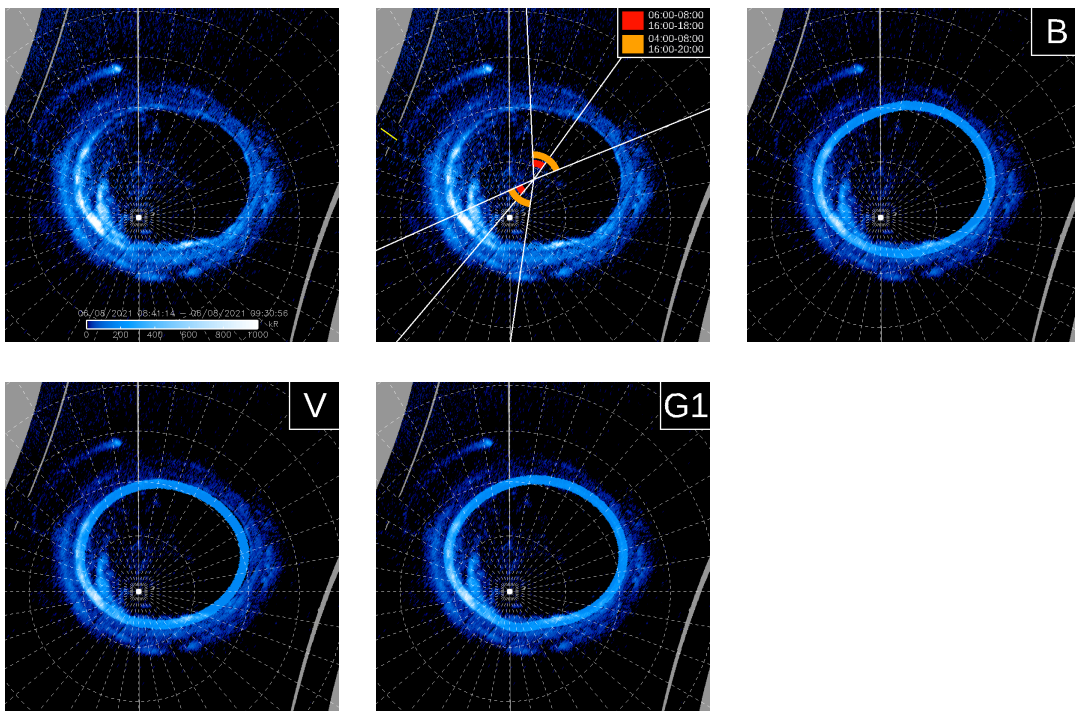
PJ33 – South



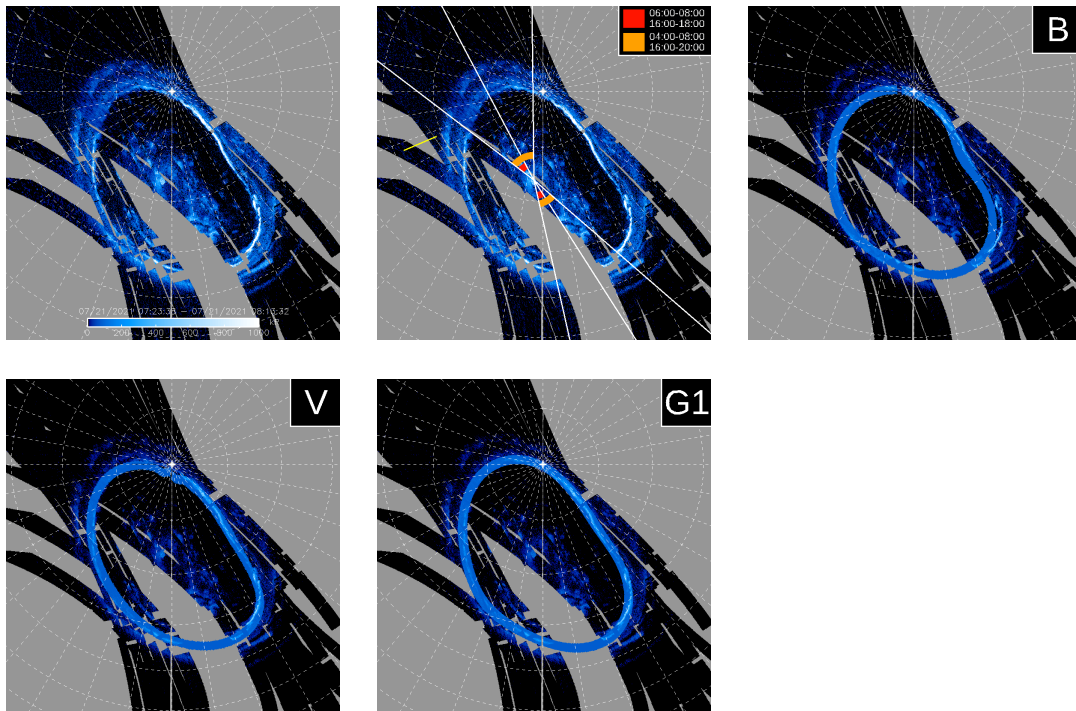
PJ34 – North



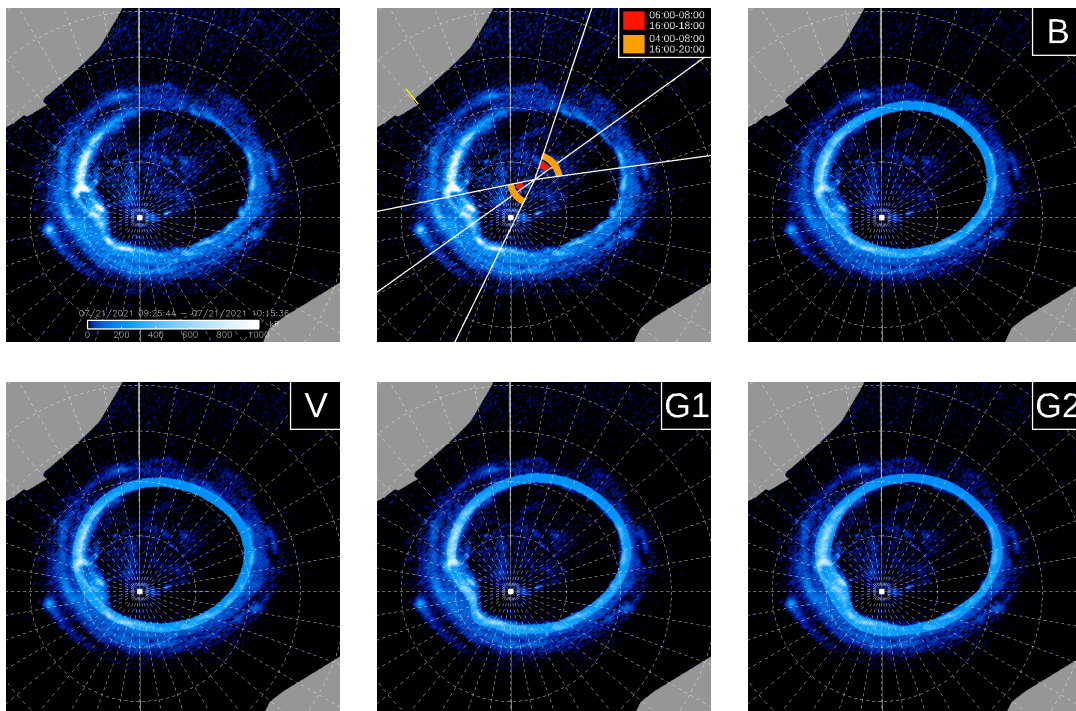
PJ34 – South



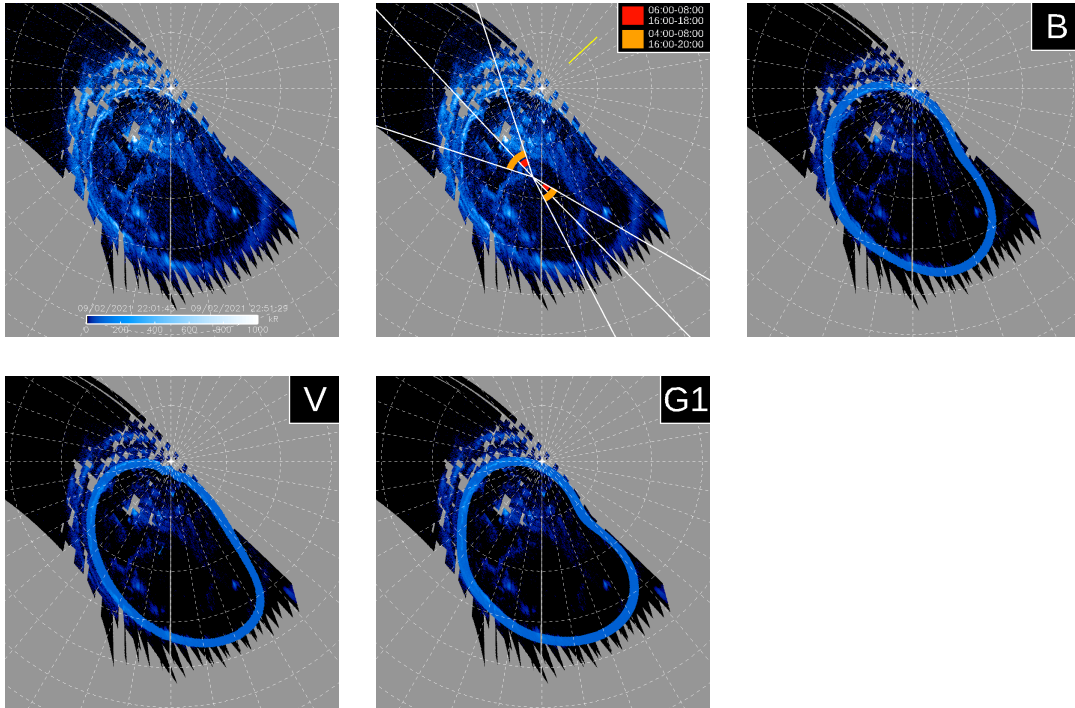
PJ35 – North



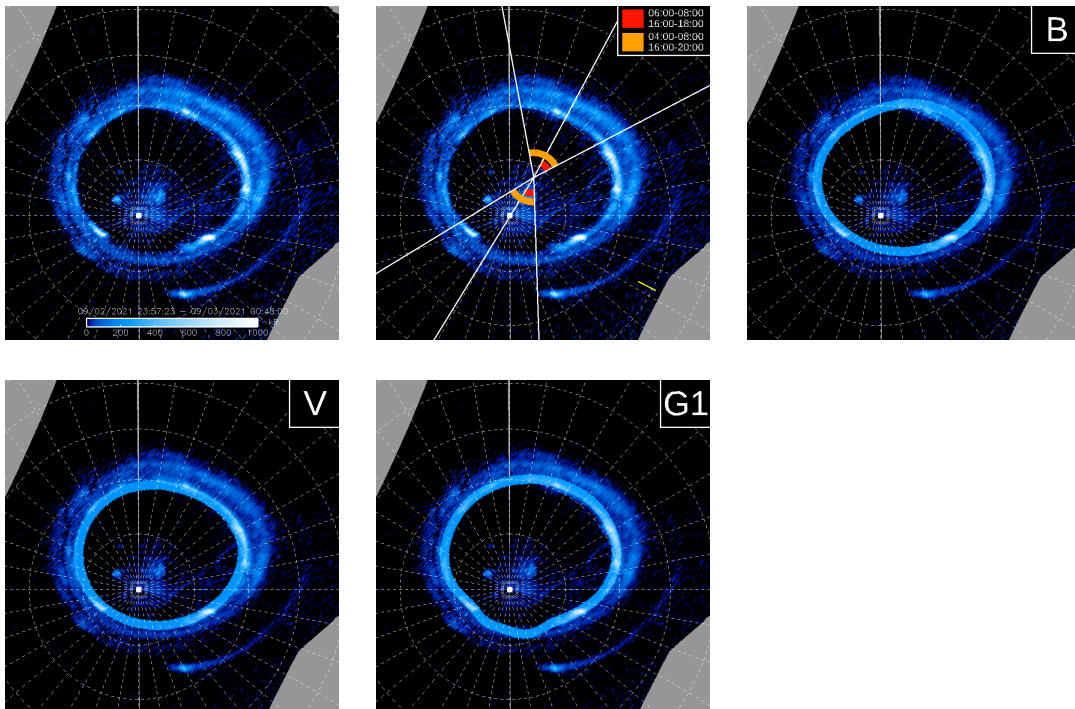
PJ35 – South



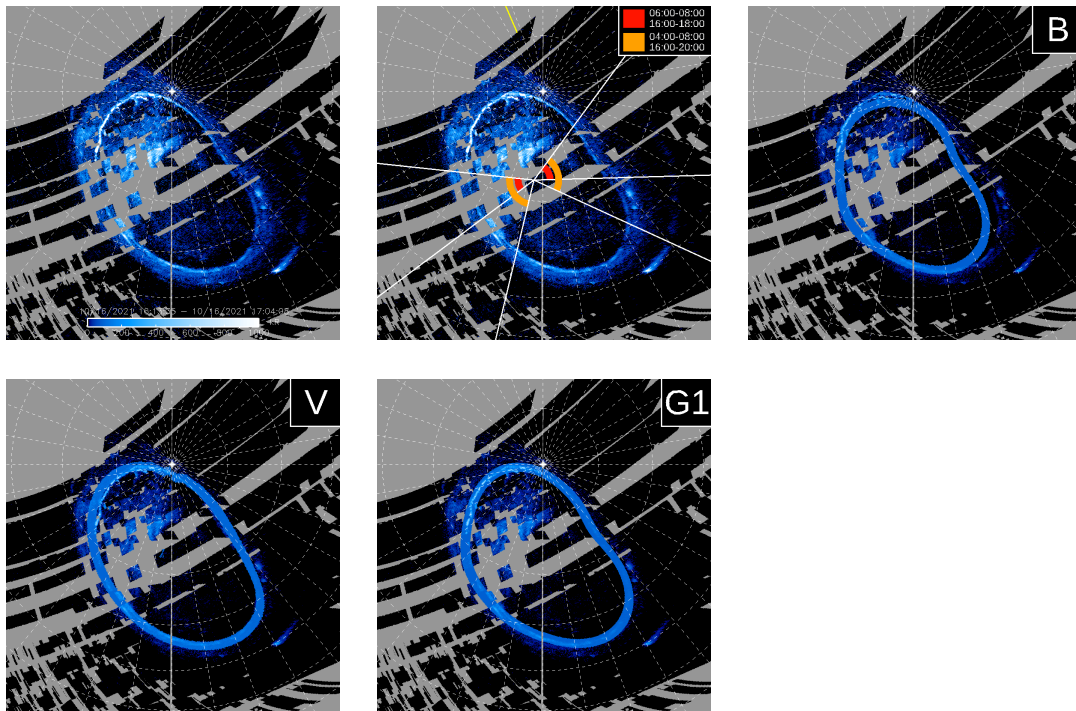
PJ36 – North



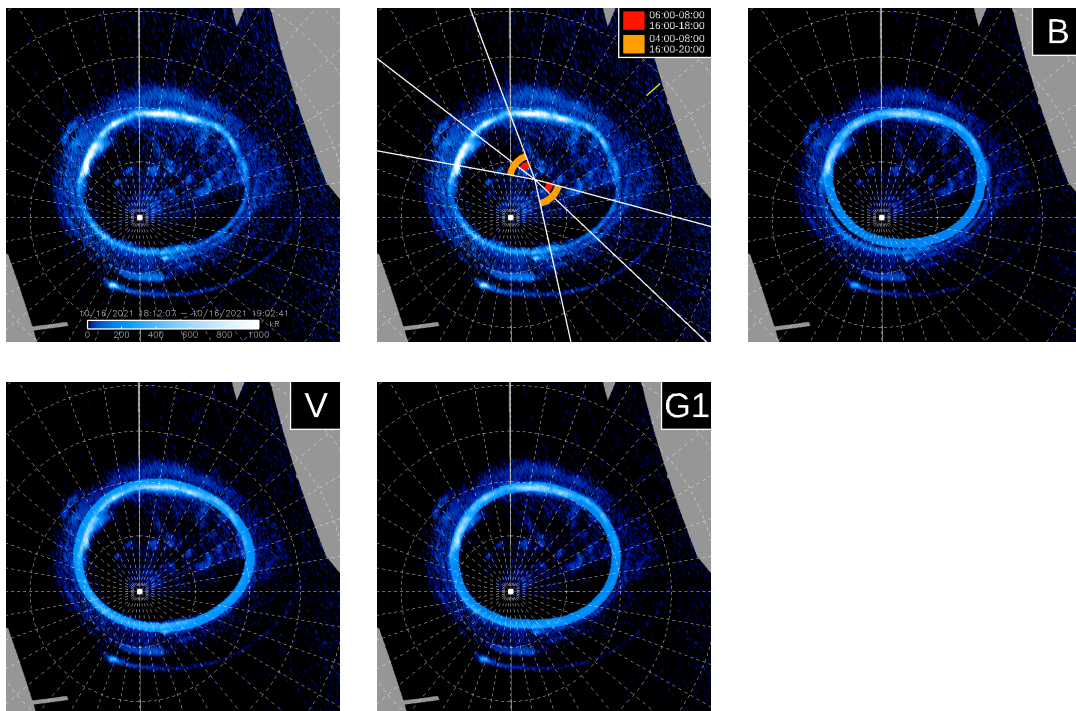
PJ36 – South



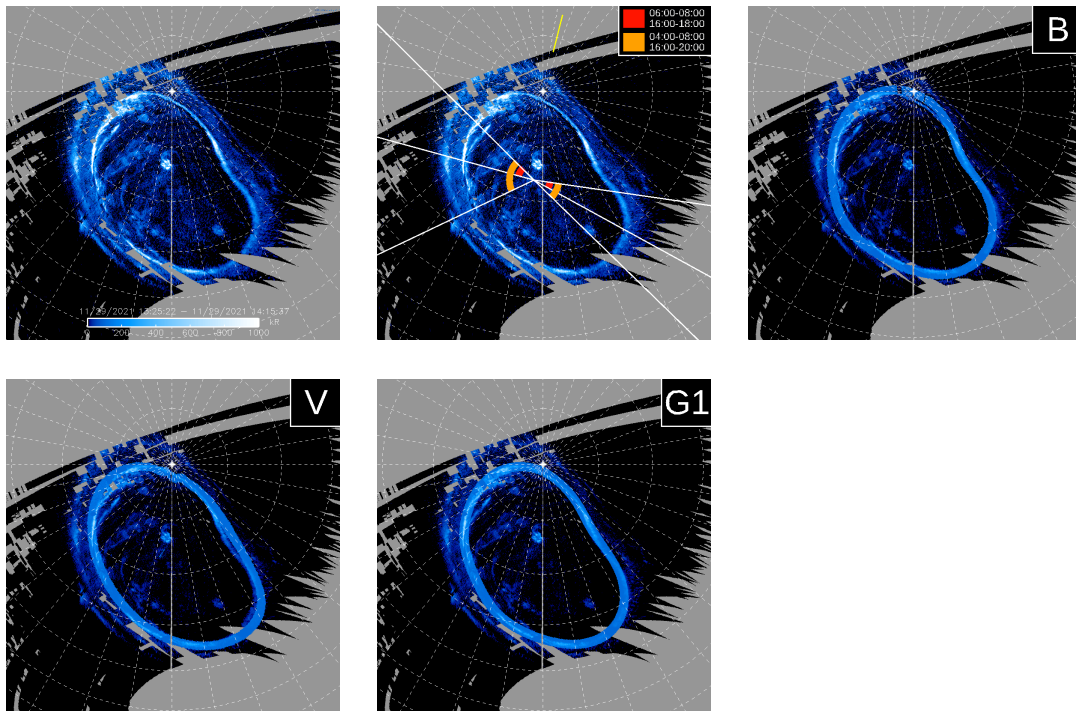
PJ37 – North



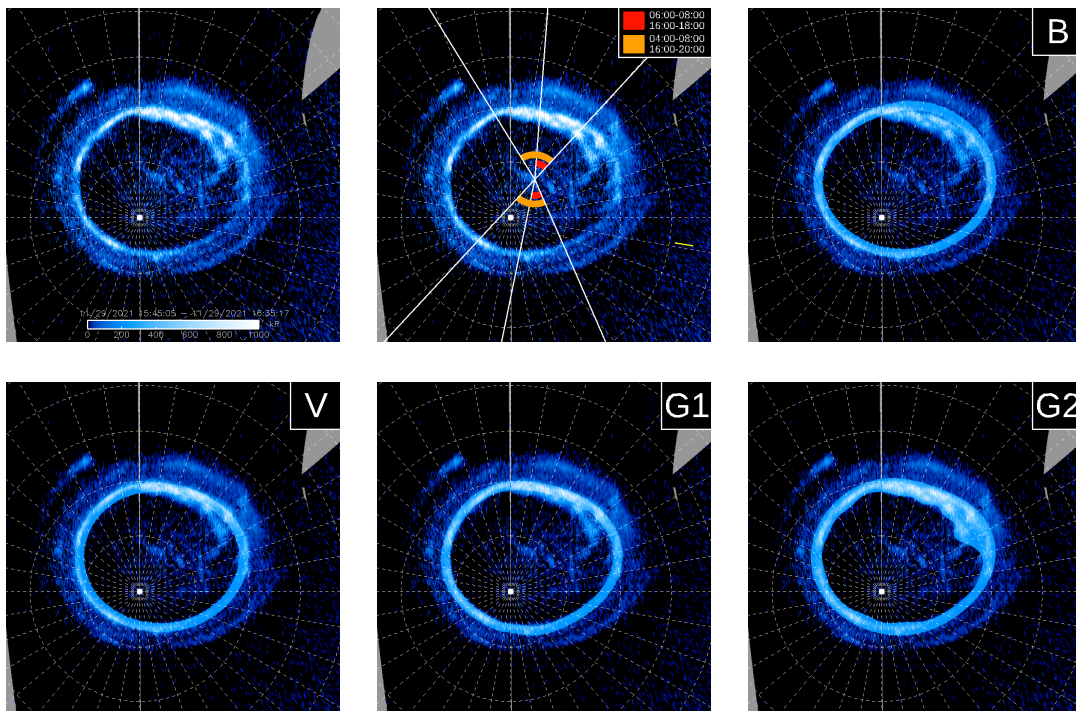
PJ37 – South



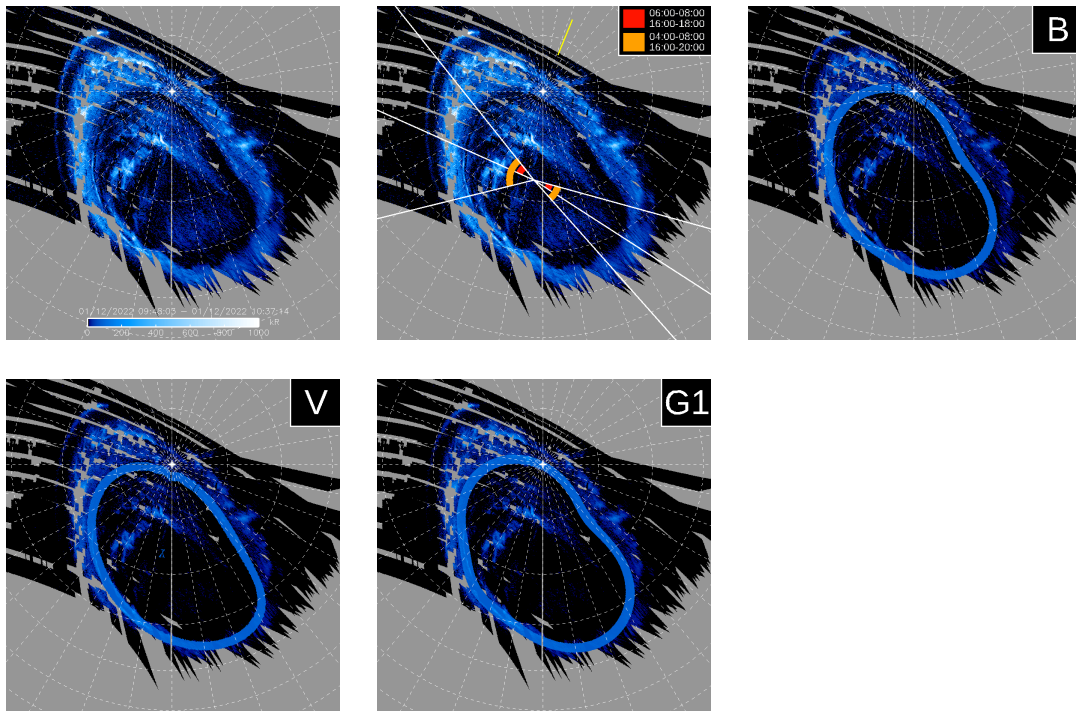
PJ38 – North



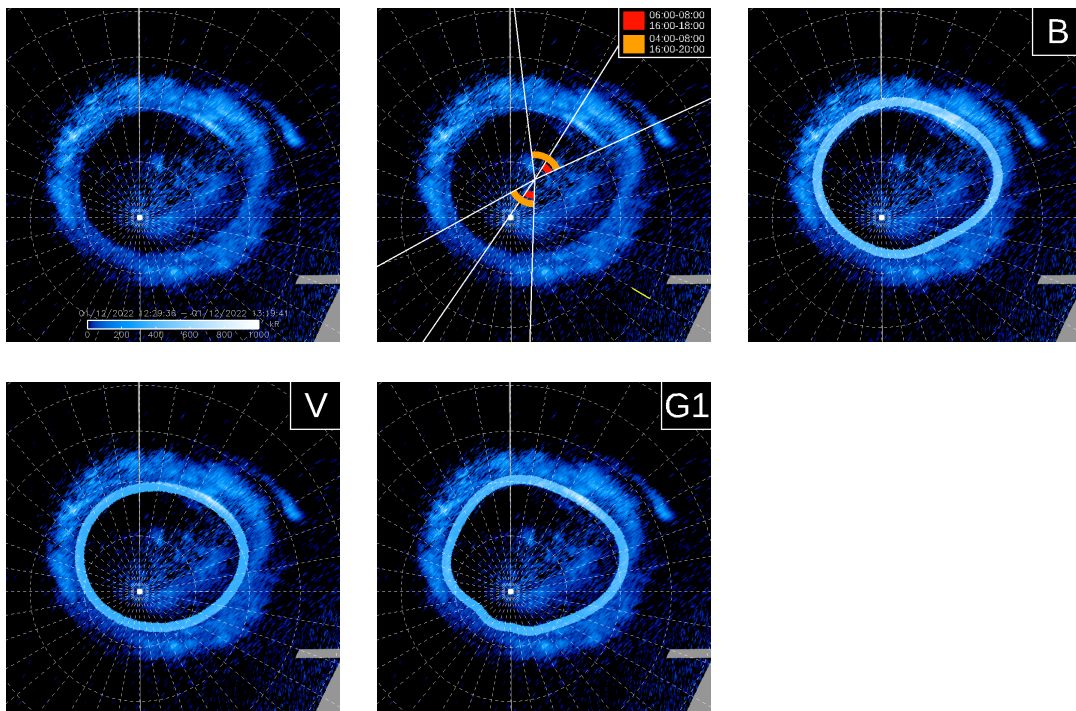
PJ38 – South



PJ39 – North



PJ39 – South



Bibliography

- [Alfvén, 1942] Alfvén, H. (1942). Existence of Electromagnetic-Hydrodynamic Waves. *Nature*, 150(3805):405–406.
- [Atreya et al., 2003] Atreya, S. K., Mahaffy, P. R., Niemann, H. B., Wong, M. H., and Owen, T. C. (2003). Composition and origin of the atmosphere of Jupiter—an update, and implications for the extrasolar giant planets. *Planetary and Space Science*, 51(2):105–112.
- [Badman et al., 2015] Badman, S. V., Branduardi-Raymont, G., Galand, M., Hess, S. L. G., Krupp, N., Lamy, L., Melin, H., and Tao, C. (2015). Auroral Processes at the Giant Planets: Energy Deposition, Emission Mechanisms, Morphology and Spectra. *Space Sci Rev*, 187(1-4):99–179.
- [Bagenal and Delamere, 2011] Bagenal, F. and Delamere, P. A. (2011). Flow of mass and energy in the magnetospheres of Jupiter and Saturn. *Journal of Geophysical Research: Space Physics*, 116(A5).
- [Bhattacharyya et al., 2018] Bhattacharyya, D., Clarke, J. T., Montgomery, J., Bonfond, B., Gérard, J.-C., and Grodent, D. (2018). Evidence for Auroral Emissions From Callisto’s Footprint in HST UV Images. *Journal of Geophysical Research: Space Physics*, 123(1):364–373.
- [Bolton et al., 2015] Bolton, S. J., Bagenal, F., Blanc, M., Cassidy, T., Chané, E., Jackman, C., Jia, X., Kotova, A., Krupp, N., Milillo, A., Plainaki, C., Smith, H. T., and Waite, H. (2015). Jupiter’s Magnetosphere: Plasma Sources and Transport. *Space Sci Rev*, 192(1):209–236.
- [Bolton et al., 2017] Bolton, S. J., Lunine, J., Stevenson, D., Connerney, J. E. P., Levin, S., Owen, T. C., Bagenal, F., Gautier, D., Ingersoll, A. P., Orton, G. S., Guillot, T., Hubbard, W., Bloxham, J., Coradini, A., Stephens, S. K., Mokashi, P., Thorne, R., and Thorpe, R. (2017). The Juno Mission. *Space Sci Rev*, 213(1):5–37.
- [Bonfond et al., 2008] Bonfond, B., Grodent, D., Gérard, J.-C., Radioti, A., Saur, J., and Jacobsen, S. (2008). UV Io footprint leading spot: A key feature for understanding the UV Io footprint multiplicity? *Geophysical Research Letters*, 35(5).
- [Bonfond et al., 2012] Bonfond, B., Grodent, D., Gérard, J.-C., Stallard, T., Clarke, J. T., Yoneda, M., Radioti, A., and Gustin, J. (2012). Auroral evidence of Io’s control over the magnetosphere of Jupiter. *Geophysical Research Letters*, 39(1).
- [Bonfond et al., 2015] Bonfond, B., Gustin, J., Gérard, J.-C., Grodent, D., Radioti, A., Palmaerts, B., Badman, S. V., Khurana, K. K., and Tao, C. (2015). The far-ultraviolet main auroral emission at Jupiter – Part 1: Dawn–dusk brightness asymmetries. *Annales Geophysicae*, 33(10):1203–1209.

- [Bonfond et al., 2020] Bonfond, B., Yao, Z., and Grodent, D. (2020). Six Pieces of Evidence Against the Corotation Enforcement Theory to Explain the Main Aurora at Jupiter. *Journal of Geophysical Research: Space Physics*, 125(11):e2020JA028152.
- [Bonfond et al., 2021] Bonfond, B., Yao, Z. H., Gladstone, G. R., Grodent, D., Gérard, J.-C., Matar, J., Palmaerts, B., Greathouse, T. K., Hue, V., Versteeg, M. H., Kammer, J. A., Giles, R. S., Tao, C., Vogt, M. F., Mura, A., Adriani, A., Mauk, B. H., Kurth, W. S., and Bolton, S. J. (2021). Are Dawn Storms Jupiter’s Auroral Substorms? *AGU Advances*, 2(1):e2020AV000275.
- [Brygoo et al., 2021] Brygoo, S., Loubeyre, P., Millot, M., Rygg, J. R., Celliers, P. M., Eggert, J. H., Jeanloz, R., and Collins, G. W. (2021). Evidence of hydrogen-helium immiscibility at Jupiter-interior conditions. *Nature*, 593(7860):517–521.
- [Clarke et al., 2004] Clarke, J., Grodent, D., Cowley, S., Bunce, E., and Connerney, J. (2004). 26 Jupiter’s Aurora. <https://www.semanticscholar.org/paper/26-Jupiter-%27-s-Aurora-Clarke-Grodent/5316fe85664ce148fbd4ab95b1d83900135e4e39>.
- [Connerney et al., 1998] Connerney, J. E. P., Acuña, M. H., Ness, N. F., and Satoh, T. (1998). New models of Jupiter’s magnetic field constrained by the Io flux tube footprint. *Journal of Geophysical Research: Space Physics*, 103(A6):11929–11939.
- [Connerney et al., 1993] Connerney, J. E. P., Baron, R., Satoh, T., and Owen, T. (1993). Images of Excited H₃⁺ at the Foot of the Io Flux Tube in Jupiter’s Atmosphere. *Science*, 262(5136):1035–1038.
- [Connerney et al., 2018] Connerney, J. E. P., Kotsiaros, S., Oliverson, R. J., Espley, J. R., Joergensen, J. L., Joergensen, P. S., Merayo, J. M. G., Herceg, M., Bloxham, J., Moore, K. M., Bolton, S. J., and Levin, S. M. (2018). A New Model of Jupiter’s Magnetic Field From Juno’s First Nine Orbits. *Geophysical Research Letters*, 45(6):2590–2596.
- [Connerney et al., 2022] Connerney, J. E. P., Timmins, S., Oliverson, R. J., Espley, J. R., Joergensen, J. L., Kotsiaros, S., Joergensen, P. S., Merayo, J. M. G., Herceg, M., Bloxham, J., Moore, K. M., Mura, A., Moirano, A., Bolton, S. J., and Levin, S. M. (2022). A New Model of Jupiter’s Magnetic Field at the Completion of Juno’s Prime Mission. *Journal of Geophysical Research: Planets*, 127(2):e2021JE007055.
- [Cowley and Bunce, 2001] Cowley, S. W. H. and Bunce, E. J. (2001). Origin of the main auroral oval in Jupiter’s coupled magnetosphere–ionosphere system. *Planetary and Space Science*, 49(10):1067–1088.
- [Cowley et al., 2003] Cowley, S. W. H., Bunce, E. J., Stallard, T. S., and Miller, S. (2003). Jupiter’s polar ionospheric flows: Theoretical interpretation. *Geophysical Research Letters*, 30(5).
- [Cowley et al., 2002] Cowley, S. W. H., Nichols, J. D., and Bunce, E. J. (2002). Distributions of current and auroral precipitation in Jupiter’s middle magnetosphere computed from steady-state Hill–Pontius angular velocity profiles: Solutions for current sheet and dipole magnetic field models. *Planetary and Space Science*, 50(7):717–734.
- [D’Amario et al., 1992] D’Amario, L. A., Bright, L. E., and Wolf, A. A. (1992). Galileo trajectory design. *Space Sci Rev*, 60(1):23–78.

- [Delamere and Bagenal, 2010] Delamere, P. and Bagenal, F. (2010). Solar wind interaction with Jupiter’s magnetosphere. *AGU Fall Meeting Abstracts*, 115:1618.
- [Dungey, 1961] Dungey, J. W. (1961). Interplanetary Magnetic Field and the Auroral Zones. *Phys. Rev. Lett.*, 6(2):47–48.
- [Ganushkina et al., 2018] Ganushkina, N. Y., Liemohn, M. W., and Dubyagin, S. (2018). Current Systems in the Earth’s Magnetosphere. *Reviews of Geophysics*, 56(2):309–332.
- [Genestreti et al., 2012] Genestreti, K., Kistler, L., and Mouikis, C. (2012). *The Role and Dynamics of Oxygen of Ionospheric Origin in Magnetopause Reconnection*. PhD thesis.
- [Gérard et al., 2016] Gérard, J. C., Bonfond, B., Grodent, D., and Radioti, A. (2016). The color ratio-intensity relation in the Jovian aurora: Hubble observations of auroral components. *Planetary and Space Science*, 131:14–23.
- [Gérard et al., 2019] Gérard, J.-C., Bonfond, B., Mauk, B. H., Gladstone, G. R., Yao, Z. H., Greathouse, T. K., Hue, V., Grodent, D., Gkouvelis, L., Kammer, J. A., Versteeg, M., Clark, G., Radioti, A., Connerney, J. E. P., Bolton, S. J., and Levin, S. M. (2019). Contemporaneous Observations of Jovian Energetic Auroral Electrons and Ultraviolet Emissions by the Juno Spacecraft. *Journal of Geophysical Research: Space Physics*, 124(11):8298–8317.
- [Grodent, 2015] Grodent, D. (2015). A Brief Review of Ultraviolet Auroral Emissions on Giant Planets. *Space Sci Rev*, 187(1):23–50.
- [Grodent et al., 2008] Grodent, D., Bonfond, B., Gérard, J.-C., Radioti, A., Gustin, J., Clarke, J. T., Nichols, J., and Connerney, J. E. P. (2008). Auroral evidence of a localized magnetic anomaly in Jupiter’s northern hemisphere. *Journal of Geophysical Research: Space Physics*, 113(A9).
- [Grodent et al., 2003] Grodent, D., Clarke, J. T., Kim, J., Waite Jr., J. H., and Cowley, S. W. H. (2003). Jupiter’s main auroral oval observed with HST-STIS. *Journal of Geophysical Research: Space Physics*, 108(A11).
- [Gurnett et al., 2000] Gurnett, D. A., Persoon, A. M., Kurth, W. S., Roux, A., and Bolton, S. J. (2000). Plasma densities in the vicinity of Callisto from Galileo plasma wave observations. *Geophysical Research Letters*, 27(13):1867–1870.
- [Gustin et al., 2012] Gustin, J., Bonfond, B., Grodent, D., and Gérard, J.-C. (2012). Conversion from HST ACS and STIS auroral counts into brightness, precipitated power, and radiated power for H2 giant planets. *Journal of Geophysical Research: Space Physics*, 117(A7).
- [Hill, 1979] Hill, T. (1979). Inertial limit on corotation. *Journal of Geophysical Research: Space Physics*, 84(A11):6554–6558.
- [Khurana et al., 2004] Khurana, K., Vasyliūnas, V., Mauk, B., Frank, L., Paterson, B., Kivelson, M., Krupp, N., Woch, J., Lagg, A., and Kurth, B. (2004). 24 - The configuration of Jupiter’s magnetosphere. *undefined*.
- [Khurana, 2001] Khurana, K. K. (2001). Influence of solar wind on Jupiter’s magnetosphere deduced from currents in the equatorial plane. *Journal of Geophysical Research: Space Physics*, 106(A11):25999–26016.

- [Khurana and Schwarzl, 2005] Khurana, K. K. and Schwarzl, H. K. (2005). Global structure of Jupiter’s magnetospheric current sheet. *Journal of Geophysical Research: Space Physics*, 110(A7).
- [Martin et al., 2020] Martin, C. J., Ray, L. C., Constable, D. A., Southwood, D. J., Lorch, C. T. S., and Felici, M. (2020). Evaluating the Ionospheric Mass Source for Jupiter’s Magnetosphere: An Ionospheric Outflow Model for the Auroral Regions. *Journal of Geophysical Research: Space Physics*, 125(7):e2019JA027727.
- [Mauk et al., 2020] Mauk, B. H., Clark, G., Gladstone, G. R., Kotsiaros, S., Adriani, A., Allegri, F., Bagenal, F., Bolton, S. J., Bonfond, B., Connerney, J. E. P., Ebert, R. W., Haggerty, D. K., Kollmann, P., Kurth, W. S., Levin, S. M., Paranicas, C. P., and Rymer, A. M. (2020). Energetic Particles and Acceleration Regions Over Jupiter’s Polar Cap and Main Aurora: A Broad Overview. *Journal of Geophysical Research: Space Physics*, 125(3):e2019JA027699.
- [Mauk et al., 2002] Mauk, B. H., Clarke, J. T., Grodent, D., Waite, J. H., Paranicas, C. P., and Williams, D. J. (2002). Transient aurora on Jupiter from injections of magnetospheric electrons. *Nature*, 415(6875):1003–1005.
- [McComas and Bagenal, 2007] McComas, D. J. and Bagenal, F. (2007). Jupiter: A fundamentally different magnetospheric interaction with the solar wind. *Geophysical Research Letters*, 34(20).
- [Militzer et al., 2016] Militzer, B., Soubiran, F., Wahl, S. M., and Hubbard, W. (2016). Understanding Jupiter’s interior. *Journal of Geophysical Research: Planets*, 121(9):1552–1572.
- [Mura et al., 2018] Mura, A., Adriani, A., Connerney, J. E. P., Bolton, S., Altieri, F., Bagenal, F., Bonfond, B., Dinelli, B. M., Gérard, J.-C., Greathouse, T., Grodent, D., Levin, S., Mauk, B., Moriconi, M. L., Saur, J., Waite, J. H., Amoroso, M., Cicchetti, A., Fabiano, F., Filacchione, G., Grassi, D., Migliorini, A., Noschese, R., Olivieri, A., Piccioni, G., Plainaki, C., Sindoni, G., Sordini, R., Tosi, F., and Turrini, D. (2018). Juno observations of spot structures and a split tail in Io-induced aurorae on Jupiter. *Science*, 361(6404):774–777.
- [Nenon et al., 2021] Nenon, Q., Clark, G., Jun, I., Kollmann, P., Liuzzo, L., Mauk, B., Nordheim, T. A., Poppe, A. R., Roussos, E., Shprits, Y. Y., Turner, D. L., and Woodfield, E. E. (2021). Open science questions and missing measurements in the radiation belts of Jupiter. 53:088.
- [Nerney et al., 2017] Nerney, E. G., Bagenal, F., and Steffl, A. J. (2017). Io plasma torus ion composition: Voyager, Galileo, and Cassini. *Journal of Geophysical Research: Space Physics*, 122(1):727–744.
- [Nichols and Cowley, 2022] Nichols, J. D. and Cowley, S. W. H. (2022). Relation of Jupiter’s Dawnside Main Emission Intensity to Magnetospheric Currents During the Juno Mission. *Journal of Geophysical Research: Space Physics*, 127(1):e2021JA030040.
- [Priest and Forbes, 1986] Priest, E. R. and Forbes, T. G. (1986). New models for fast steady state magnetic reconnection. *Journal of Geophysical Research: Space Physics*, 91(A5):5579–5588.
- [Radioti et al., 2008a] Radioti, A., Gérard, J.-C., Grodent, D., Bonfond, B., Krupp, N., and Woch, J. (2008a). Discontinuity in Jupiter’s main auroral oval. *Journal of Geophysical Research: Space Physics*, 113(A1).

- [Radioti et al., 2008b] Radioti, A., Grodent, D., Gérard, J.-C., Bonfond, B., and Clarke, J. T. (2008b). Auroral polar dawn spots: Signatures of internally driven reconnection processes at Jupiter’s magnetotail. *Geophysical Research Letters*, 35(3).
- [Radioti et al., 2011] Radioti, A., Grodent, D., Gérard, J.-C., Vogt, M. F., Lystrup, M., and Bonfond, B. (2011). Nightside reconnection at Jupiter: Auroral and magnetic field observations from 26 July 1998. *Journal of Geophysical Research: Space Physics*, 116(A3).
- [Ray et al., 2014] Ray, L. C., Achilleos, N. A., Vogt, M. F., and Yates, J. N. (2014). Local time variations in Jupiter’s magnetosphere-ionosphere coupling system. *Journal of Geophysical Research: Space Physics*, 119(6):4740–4751.
- [Schreier et al., 1993] Schreier, R., Eviatar, A., Vasyliūnas, V. M., and Richardson, J. D. (1993). Modeling the Europa Plasma Torus. *J. Geophys. Res.*, 98(A12):21231–21243.
- [Smith et al., 1979a] Smith, B. A., Soderblom, L. A., Beebe, R., Boyce, J., Briggs, G., Carr, M., Collins, S. A., Cook, A. F., Danielson, G. E., Davies, M. E., Hunt, G. E., Ingersoll, A., Johnson, T. V., Masursky, H., McCauley, J., Morrison, D., Owen, T., Sagan, C., Shoemaker, E. M., Strom, R., Suomi, V. E., and Veverka, J. (1979a). The Galilean Satellites and Jupiter: Voyager 2 Imaging Science Results. *Science*, 206(4421):927–950.
- [Smith et al., 1979b] Smith, B. A., Soderblom, L. A., Johnson, T. V., Ingersoll, A. P., Collins, S. A., Shoemaker, E. M., Hunt, G. E., Masursky, H., Carr, M. H., Davies, M. E., Cook, A. F., Boyce, J., Danielson, G. E., Owen, T., Sagan, C., Beebe, R. F., Veverka, J., Strom, R. G., McCauley, J. F., Morrison, D., Briggs, G. A., and Suomi, V. E. (1979b). The Jupiter System Through the Eyes of Voyager 1. *Science*, 204(4396):951–972.
- [Thomas and Wilson, 2004] Thomas, N. and Wilson, J. K. (2004). The Io Neutral Clouds and Plasma Torus. page 32.
- [Vasyliunas, 1983] Vasyliunas, V. M. (1983). *Physics of the Jovian Magnetosphere. 11. Plasma Distribution and Flow.*
- [Vasyliūnas and Eviatar, 2000] Vasyliūnas, V. M. and Eviatar, A. (2000). Outflow of ions from Ganymede: A reinterpretation. *Geophysical Research Letters*, 27(9):1347–1349.
- [Vogt et al., 2011] Vogt, M. F., Kivelson, M. G., Khurana, K. K., Walker, R. J., Bonfond, B., Grodent, D., and Radioti, A. (2011). Improved mapping of Jupiter’s auroral features to magnetospheric sources. *Journal of Geophysical Research: Space Physics*, 116(A3).
- [Wahl et al., 2017] Wahl, S. M., Hubbard, W. B., Militzer, B., Guillot, T., Miguel, Y., Movshovitz, N., Kaspi, Y., Helled, R., Reese, D., Galanti, E., Levin, S., Connerney, J. E., and Bolton, S. J. (2017). Comparing Jupiter interior structure models to Juno gravity measurements and the role of a dilute core. *Geophysical Research Letters*, 44(10):4649–4659.
- [Weygand et al., 2011] Weygand, J., Matthaeus, W., Dasso, S., and Kivelson, M. (2011). Correlation and Taylor scale variability in the interplanetary magnetic field fluctuations as a function of solar Wind Speed. *Journal of Geophysical Research*, 116.
- [Young, 2003] Young, R. E. (2003). The Galileo probe: How it has changed our understanding of Jupiter. *New Astronomy Reviews*, 47(1):1–51.